MOISTURE SORPTION AND SELECTED THERMODYNAMIC CHARACTERISTICS OF MORINGA (*Moringa oleifera* Lam.) SEED AND GRITS

BY

Akintunde AKINTOLA
B. Eng. Agric. Engineering (FUNAAB); M.Sc. Agric. and Env. Engineering (Ibadan)
Matric No: 166882

A Thesis in the Department of Agricultural and Environmental Engineering
Submitted to the Faculty of Technology in partial fulfilment of the requirements for the Degree of

DOCTOR OF PHILOSOPHY

of the

UNIVERSITY OF IBADAN

JULY, 2023.

CERTIFICATION

I certify that this work was carried out by Mr. A. Akintola in the Department of Agricultural and Environmental Engineering, University of Ibadan.

_____

Supervisor

A. K. Aremu

B.Sc., M.Sc., Ph.D (Ibadan), MNIAE, MNSE, MASABE, Reg. Engr. (COREN)

Professor, Department of Agricultural and Environmental Engineering,

University of Ibadan, Nigeria.

DEDICATION

To the glory of God, the success of this research is dedicated to my late father, Mr Olugbade Akintola, who passed on the 16th of May, 2002. The memory will forever linger in my heart.

ACKNOWLEDGEMENTS

My sincere appreciation goes to my HOD; Dr. M. O. Omobowale for widening my scope on this research and for his pieces of advice. I will like to express my sincere gratitude to my diligent supervisor, Prof. A. K. Aremu, for his support and encouragement towards the completion of this work. Also, to all my Lecturers and mentors, Emeritus Professor J. C. Igbeka, Professors A. Y. Sangodoyin, A. O. Raji, Y. Mijinyawa, A. I. Bamgboye, E. A. Ajav, T. A. Ewemoje, R. Akinoso, Dr Mrs O. E. Ewemoje, I am always proud to be your student. I must also appreciate the Postgraduate Coordinator and my self-made "co-supervisor", Dr. B. O. Oyefeso, for allowing me access to his office every time and his support, encouragement and corrections when necessary.

I really appreciate my mum, Mrs. F.O. Akintola for her relentless effort to ensure that her children are well educated even after our dad's demise. I cannot but appreciate my uncles and aunties and their family (Rev'd. and Pastor (Mrs) Lawoore, Mr. and Mrs. Olaewe, Mr. and Mrs. Nihinlola, Mr. and Mrs. Aderoju, Mr. and Mrs. Oni) for their love and support throughout the course of this program. To my dearest siblings, Akintayo, Akinyinka and Adesewa (Omo Akins), I love you all for the ever-steadfast support you all showed me, especially during the period that things seem to be tough financially and I also thank God for the professionals that we have all become. Also, to my wife, Engr. Titilayo Akintola, and children, Akintoye, Akindolapo and Akinbayode, I really appreciate you for standing by me even in times of trials.

My sincere appreciation goes to the management of Oyo State College of Agriculture and Technology, Igboora, most especially, the former Rector, Prof J. G. Adewale, for his words of encouragement when I wanted to quit this program due to paucity of fund. I also appreciate my Ogas in Faculty of Engineering and Technology, Engr Dr. D. Lasisi, Engr K. A. Jimoh and all my colleagues.

Finally, I appreciate my academic friends, Dr Clement Ogunlade, Dr Seyi Fadele, Dr Taiwo Ajao, Engr Oluseyi Akangbe, Engr Abolaji Ilori, Engr Ademola Adejumobi and Mr Mojeed Anifowose for their support emotionally towards the completion of this program.

ABSTRACT

Moringa seed is a raw material that needs long period of storage. This necessitates drying the seed so as to extend its shelf life. An important factor in ensuring stability of moringa seed and grits in storage is its water activity (a_w). However, there is dearth of information on the sorption characteristics of moringa seed and grits. This study was therefore, designed to investigate the sorption and some thermodynamic characteristics of moringa seed and grits during storage.

Moringa seeds and grits (particle size 106-212 μm) were kept in two packaging materials (Polypropylene [Pp] and Low-Density Poly-Ethylene [LDPE]) and stored at ambient condition for 12 days, and shelf life was predicted using Heiss-Eichner model. Sorption Isotherms (SI) of moringa seed and grits were obtained by determining the Equilibrium Moisture Content (EMC) at a temperature range of 20-40℃ and nine a_w (0.09-0.92) levels using thermostatic water bath and concentrated H_2SO_4. The sorption data were fitted into six selected models namely: Brunauer-Emmett-Teller (BET), Guggenheim-Anderson-De Boer (GAB), Hailwood-Horrobin (HH), Modified Hasley (MH), Modified Henderson (MHM) and Modified Hailwood-Horrobin (MHH) models. The performance of the models was tested using Root Mean Square Error (RMSE), co-efficient of determination (R^2) and Residual Sum of Squares (RSS). The effect of temperature on the monolayer moisture content (M_o) of the seed and grits was determined using BET, GAB and Caurie models. Clausius-Clapeyron equation was used to determine the isosteric heat (ΔH) and entropy of sorption (ΔS) of the seed and grits. Data were analysed using ANOVA at $\alpha_{0.05}$.

The predicted shelf life in Pp and LDPE were 1,852 and 1,446 days; 994 and 748 days for seed and grits, respectively. The SI curves generated were sigmoidal in shape indicating Type-II isotherm. The GAB and MHM were the best-fitted models and predicted the EMC at all temperatures with highest R^2 (0.9994, 0.9999) in adsorption and (0.9994, 0.9999) in desorption processes for seed and grits, respectively. The BET and HH models did not fit well at all temperatures with R^2 (0.6957, 0.6869); (0.8439, 0.8149) for seed and grits, respectively, while MHH fitted well with R^2 (0.9111) for grits at a temperature of 20℃ only. The GAB gave the least RMSE and RSS and it ranged 0.0775-0.2124 and 0.0060-0.0431, respectively. The M_o for the seed and grits ranged 2.9–5.9% db and 2.1–4.4% db, respectively. Hysteresis did not have significant effect on M_o for both seed and grits. The ΔH decreased as the EMC increased and it ranged 9.90-40.86 $kJmol^{-1}$ for seed and 4.75-38.71 $kJmol^{-1}$ for grits in adsorption; 10.85-45.09 $kJmol^{-1}$ for seed and 4.82-41.66 $kJmol^{-1}$ for grits in desorption. The ΔS ranged 0.03-0.124 $kJmol^{-1}K^{-1}$ for seed and 0.014-0.113 $kJmol^{-1}K^{-1}$ for grits in adsorption; 0.033-0.137 $kJmol^{-1}K^{-1}$ for seed and 0.015-0.124 $kJmol^{-1}K^{-1}$ for grits in desorption. The ΔH and ΔS increased exponentially as the EMC decreased.
Sorption isotherm of moringa seed and grits demonstrated Type-II behaviour. Moringa seed and grits stored in polypropylene had longer shelf life and less interaction with the micro-environment during storage than Low Density Polyethylene.

Keywords: Adsorption, desorption, water activity, shelf life, net isosteric heat, entropy.

Word count: 497

TABLE OF CONTENTS

LIST OF TABLES

LIST OF FIGURES

LIST OF PLATES

LIST OF APPENDICES

CHAPTER ONE

INTRODUCTION

1.1 Background to the Study

Moisture sorption isotherm indicates the quantity of water that a material imbibed or desiccated at equilibrium with an established water activity at a specific temperature (Bell and Labuza, 2000). Every bio-material (including *Moringa oleifera* Lam.) have their own specific and unique moisture sorption isotherms (Singh and Kumari, 2014). The relationship that exists between water activity and equilibrium moisture content at a constant temperature is considered a very important criterion to take cognisance of during storage of food materials and ingredients.

The moisture sorption isotherms of food and agricultural products play a significant role in the conception and implementation of preservation and storage methods. These methods include packaging, drying, mixing, and a number of other procedures that include the prediction of food stability and shelf life (Khalloufi *et al.*, 2000). Moisture sorption isotherm is of utmost importance in so many kinds of processing and product stability applications (Falade and Aworh, 2004). The precise estimation of thermodynamic energy, enthalpy, and entropy depends on the accurate calculation of equilibrium moisture contents of dried products (Ngoddy and Bakker-Arkema, 1970; Al-Mahasneh *et al.,* 2010). Moisture sorption isotherm is of utmost importance in so many kinds of processing and product stability applications (Falade and Aworh, 2004). Vishwakarma *et al.* (2011) explained that isotherm is useful in determining the level of a_w and corresponding moisture content that will reduce the rate of development of micro-organisms and help in the estimation of the nutritional value and stability of foods with respect to differences in the amount of moisture present. Singh and Kumari (2014) also reported that while designing and optimizing processes, it is essential to understand how food products adsorb or desorb moisture. For instance, during drying, to evaluate packaging issues, to simulate moisture changes that occur, to forecast shelf-life stability, to predict component mixing and many more.

Several factors affect the sorption properties of agricultural materials (Khalloufi *et al.*, 2000). These factors include its origin, composition, postharvest operations and methods used to measure the sorption characteristics.

The leaves, pods, and seeds of the moringa plant contain a range of vital phytochemicals, hence, they are highly nutritious (Aremu and Akintola, 2014). According to Rockwood *et al.* (2013), moringa contains 25 times more iron than spinach and 7 times more vitamin C than oranges. It also contains 10 times more vitamin A than carrots, 9 times more protein than yoghurt, and 15 times more potassium than bananas.

Rural women in Sudan have used moringa seeds for wastewater treatment to clear the excessively murky Nile water of bacteria because they also contain a variety of therapeutic and nutritional benefits (Njidda, 2021). Moringa oleifera exhibits excellent properties of treating water (Lea, 2010; Yin, 2011; Ghebremichael and Gebremedhin, 2011). It has therefore been used by the public as a water purifier because of its coagulant properties (Oluwalana *et al.,* 1999; Ayotunde *et al.,* 2011; Mustapha *et. al*., 2012; Musa and Njidda, 2021).

The tree's components can all be used in a variety of ways. Moringa is rich in vitamins and nutrients and is beneficial for both human and animal diet. Moringa is a useful source of medicines and helps to clean up soiled water. When using alley-cropping methods, it offers a lot of leafy material that is helpful. Every food item made from moringa has a very high nutritional value. The leaves, particularly the young shoots, young pods, flowers, roots, and in some species, even the bark, can all be consumed. According to Asaolu and Omotayo (2007), leaves are high in minerals, iron, and vitamin B and low in fats and carbs. Because the leaves appear toward the end of the dry season, when few other kinds of green leafy vegetables are available, it is very beneficial as a human food.

Around the world, every part of the moringa tree has been used effectively against varying ailments (Abdulkarim *et al.,* 2005). According to Asaolu and Omotayo (2007), the seeds are utilized for their antibacterial and anti-inflammatory characteristics to cure boils, rheumatism, gout, cramps, and sexually transmitted infections. The affected

region is treated with the roasted, ground-up, coconut oil-infused seeds. The same problems can be treated using seed oil.

River water can be cleaned quickly and easily using the seed flour (Oluwalana *et al.*, 1999). The flour sinks to the bottom of the water after mixing with the particles there. Additionally, 90–99% of the microorganisms in water are eliminated by this process. Moringa is a natural water purifier that can take the place of costly and risky chemicals like aluminium sulphate (Mangale *et al.,* 2012). Due to the varied contaminants found in different sources of water, different amounts of powder will be required. *Moringa stenopetala* seeds are superior to Moringa oleifera seeds in terms of their ability to filter water (Mangale *et al.,* 2012).

According to Adejumo and Abayomi (2012), ground and defatted moringa seeds can be used to replenish soil, fertilize crops, and augment animal feed. This enables farmers and ranchers to increase productivity and get better outcomes from their agricultural endeavors. Because moringa seeds are a good source of natural oils, they have been looked at as a possible source for biofuel components (Oliveira *et al.*, 1999). As the supply of fossil fuels continues to decline, newer extraction methods may make this even more lucrative and common (Fahey, 2005).

1.2 Problem Statement

Water activity (a_w) is a critical factor when studying qualitative losses that occur in dried biological materials such as moringa seed during storage. It influences the behaviour and quality retention of dried products. Moringa seeds and grits are usually stored and sold without a specific known optimum condition that will keep the product's quality the best during storage. Information about the sorption isotherms of moringa seeds and grits will provide the needed information so as to preserve the produce for further processing and usage in various foods, pharmaceutical and cosmetic industries.

1.3 Objectives of the Study

The broad objective of this study is to determine the effects of some storage parameters namely relative humidity and temperature on the moisture sorption characteristics of moringa seed and grits.

The specific objectives are to

i. determine the effect of relative humidity and storage period on oxidative rancidity of moringa seed oil.
ii. evaluate and model the moisture adsorption and desorption isotherms of moringa seed and grits at temperature range between 20 and 40^{o}C and a wide relative humidity range from 8.95 to 92.61%.
iii. determine the effect of temperature and hysteresis on monolayer moisture content of moringa seed and grits during storage.
iv. predict the shelf life of moringa seed and grits stored in two packaging materials.
v. determine the isosteric heat and the entropy of moisture sorption of the seeds and grits.

1.4 Justification of the Study

The processing quality of agricultural materials can be improved by experimentally evaluating the sorption characteristics (Ethmane-Kane *et al.*, 2008). The moisture sorption isotherm is a powerful tool for predicting and extending the shelf life of a product. It helps to determine the critical water activity values where physiological changes such as caking, clumping, and loss of texture occur and to predict how the product will respond to ingredient and formulation changes.

It is therefore imperative to establish the kind of interaction that exist between relative humidity (RH) and equilibrium moisture content (EMC) at a constant temperature and so as to correctly carry out drying and storage operations as well as determine the safest conditions for preserving the product. Sorption isotherms are required for obtaining this information (Alakali and Shatimehin, 2007).

1.5 Scope and Limitations

The scope of this research is to evaluate moisture adsorption and desorption isotherms of moringa seed and grits and use the data to predict the storage ability and shelf life of both the seed and grits stored in selected packaging materials so as to determine the best form in which it can be stored.

This research is limited to determination of adsorption and desorption isotherm of Moringa seed and grits at a relative humidity range of 10- 90% and temperature range of 20- 40^{0}C.

CHAPTER TWO

LITERATURE REVIEW

2.1 The Drumstick (*Moringa oleifera* Lam)

Moringa oleifera Lam. plant (Plate 2.1) originated from some parts Asia and it is the only genus in the flowering plant family Moringaceae (Fahey, 2005) It is now cultivated extensively across the tropics as shown in Figure 2.1. The tree can survive in both hot, arid lands and tropical tropics. It can also survive on less fertile soils (Anwar *et al.,* 2007). It is frequently utilized for food, medicine, as a windbreak in fields, and a variety of other things. (Oleivera, 1999; Singh and Kumari 2014). Its common names include drumstick tree, horseradish tree, *Benzolive, Kelor, Marango, Mlonge, Mulangay, Saijihan and Sajna* (Fadele *et al.,* 2018). There are 14 various varieties of moringa, all of which originate in various places (Oliveira *et al.,* 1999). The variety grown in Nigeria is the *Moringa oleifera* (Asaolu and Omotayo, 2007; Anjorin *et al.,* 2010). According to Indian Ayurvedic medicine's oral heritage, moringa prevents about 300 diseases (Fuglier, 1999).

The ancient Romans, Greeks, and Egyptians made use this fast-growing tree. As of late, it has been extensively grown and has spread over the world. Moringa can be described as one of the richest plants on earth in terms of nutritional composition. The plant is a little, attractive tree that grows quickly. During the first year of growth, it creates lengthy pods resembling drumsticks, which contain the seeds (Busani *et al.,* 2011). In Nigeria, it is widely grown in the Northern part of the country while sparsely grown in the Southern Nigeria.

Each pod of the *Moringa oleifera* Lam. can contain more than a dozen seeds and grow to a length of well over a foot. Large and round in appearance, the seeds develop inside the tree's protracted pods and brownish semi-permeable shell. The shell of the seeds produces three white wings that cut across the hull at about an angle of 120 degrees. During reproduction, the trees produce an astounding number of seed pods. The height

of a typical moringa tree is about four to six meters and has a yearly seed production capacity of between 15,000 and 25,000. The kernel is about three times the hull, and the seed is about 0.3 g averagely (Rockwood *et al.,* 2013).

In addition to having several medicinal and nutritional benefits, some Sudanese women made use of the seeds for wastewater treatment to treat the highly turbid Nile water (Njidda, 2021). It has a very good water treatment property (Lea, 2010; Yin, 2011; Ghebremichael and Gebremedhin, 2011). As a result of its coagulant qualities, it has been utilized by some people as a water purifier. (Oluwalana *et al.,* 1999; Ayotunde *et al.,* 2011; Mustapha *et al*., 2012; Musa and Njidda, 2021).

The organic features of the promising plant, *Moringa oleifera* L. may help people consume some important minerals and phytochemicals that are good for their health (Balbir, 2006). The oil found in the seed kernels, known commercially as "Ben oil" or "Behen oil," is utilized by watchmakers to lubricate and illuminate sensitive mechanisms (Fadele *et al.,* 2018) and it is widely used as a very stable, non-drying oil (Aremu and Akintola, 2016; Fu *et al.*, 2021). Moringa oil was valued by the ancient Egyptians for its ability to shield their body from the damaging effects of arid climatic conditions. Subsequently, the Greeks discovered other beneficial uses of moringa and shared these with the Romans.

Moringa seed grits, although, have a mild bitter and astringent taste; they are used for food seasoning (Ogunsina *et al.*, 2010). It has been utilized in a number of poor nations to stop protein-energy malnutrition, particularly in young children and pregnant women (Musa and Njidda, 2021). It has active ingredients with enhanced digestion and metabolism as well as antimicrobial and immune-stimulating properties (Lannaon, 2007). Also, it contains bioceutical substances that poultry birds may use instead of synthetic growth promoters and vitamins (Ghazalah and Ali, 2008).

Plate 2.1: ***Moringa oleifera*** **Lam. Plant showing the pods**

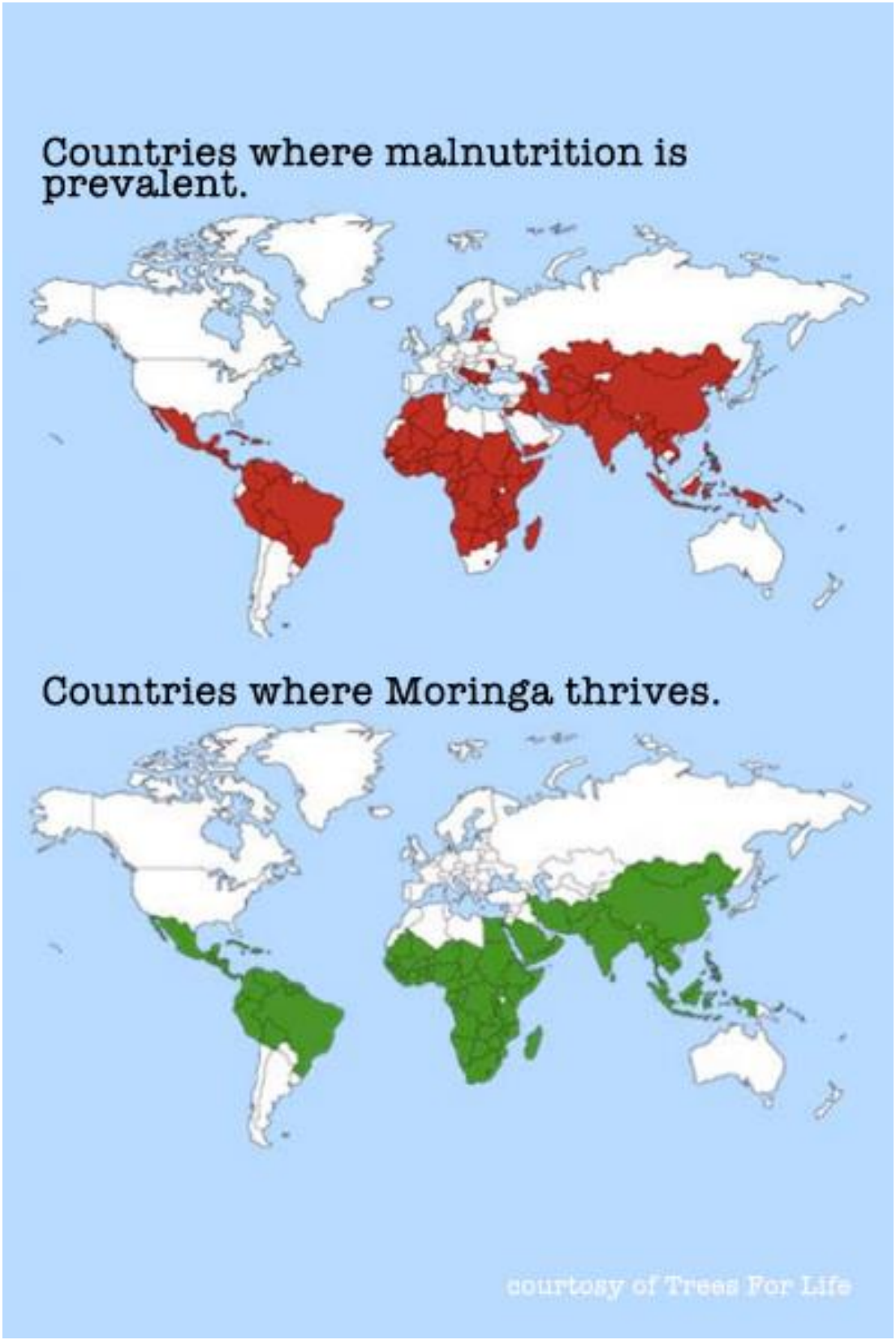

Figure 2.1: **Countries where *Moringa Oleifera* is grown (Fuglier, 1999).**

2.2 Water Activity (a_w)

Each constituent in a uniform mixture has an existing a chemical potential. (μ). This determines the extent by which the free energy increases with each additional mole of substance. (Fontana, 2007; Labuza and Altunakar, 2020). The chemical potential of water in an ideal solution can be expressed by Equation 2.1 (Schmidt 2004).

$$\mu w = \mu w° + RT ln\, a_w \quad 2.1$$

where:

$\mu_w°$ is the chemical potential of pure water in a standard state (J/ mol^{-1})

R is the universal gas constant ($JK^{-1}mol^{-1}$)

T is temperature (K)

a_w is water activity.

Considering the thermodynamic aspect, an attribute or propensity of water molecules to migrate from the liquid state to the vapour state is measured by the a_w. At constant temperature, the proportion of water's pressure value (ƥ) to pure water in a standard form ($ƥ_o$) is given by Damodaran *et al.* (2008) in Equation 2.2.

$$aw = ƥ/ƥ\, o \quad 2.2$$

Damodaran *et al.* (2008) stated that the difference between a_w and the ratio of the partial vapour pressure of water and the vapour pressure of pure water at low pressure is less than 1%, so a_w can be defined according to Equation 2.3.

$$a_w = p/p_o \quad 2.3$$

Also, a_w is equivalent to the percentage of relative humidity (% RH).

2.3 Effect of Moisture Content on Physical Properties of Moringa Seeds

According to Adejumo *et al.* (2013), as the moisture content of the seeds increased, so did their physical characteristics except porosity as shown in Table 2.1. The information provided by the study is useful for engineers and designers for effective machinery design and processing and handling of moringa seeds.

2.4 Moisture Sorption Isotherm

One of the most helpful aspects of the water activity concept is the interaction between equilibrium moisture content and relative humidity for food systems and components

at the same temperature. Sorption isotherm, which differs from one product to another, describes this relationship (Singh and Kumari, 2014). Sánchez-Torres *et al.* (2021), described sorption isotherm as the moisture adsorbed or desorbed at equilibrium by a material existing at specific water activity and a constant temperature as depicted in Figure 2.2. A typical sorption isotherm has a shape that is similar to a sigmoid (Janjai *et al.*, 2007). Aviara (2020), showed that a sorption curve which has a sigmoid shape can be broken into three regions so as to understand the meaning and usefulness of sorption isotherms as indicated in Figure 2.3. Timmermann *et al.* (2001), explained that the first region which usually occurs when water activity is less than 0.25 depicts monolayer water. It is closely related to the particular substance, most unlikely to freeze, and difficult to dry out. In this area, the water is least mobile and reacts most strongly with the solids. Even though it acts like a solid, it is nevertheless quite interchangeable. The second region where water activity falls between 0.25 and 0.75 depicts the multilayers of moisture that are adsorbed or desorbed in soluble component solutions and foods. It has a little lower mobility than bulk water. Water has a considerable plasticizing effect on solutes. The third region where water activity is greater than 0.75, indicates readily removed by drying bulk or "free" water that can be frozen. This water is conducive to enzymatic reactions and microbiological growth. (Fennema, 1996).

The adsorption isotherms are broadly categorized into six, as depicted in Figure 2.4. The most typical moisture sorption isotherms for food items are types I, II, and III. Sorption isotherms are influenced by a variety of variables, such as composition, temperature, and many more (Adeoye *et al.*, 2020).

Three different isotherm curve types: adsorption (beginning from the dry state), desorption (beginning from the wet state), and working (native state) were described by Seid and Hensel (2012). An isotherm produced by adsorption won't always be the same as an isotherm produced through desorption (Alakali and Shatimehin, 2009).

Table 2.1: **Physical properties of Moringa seeds as affected by moisture content**

	Shelled Moringa seed		
Parameters	**Sample A (6.8%)**	**Sample B (10%)**	**Sample C (15%)**
Length (mm)	8.3	8.4	8.7
Width (mm)	7.4	7.5	7.6
Thickness(mm)	6.5	6.7	7.3
Geometric mean diameter(mm)	133.1	140.7	160.1
Sphericity(mm)	16.0	16.8	18.4
Thousand seed mass (grams)	316.8	319.3	326.7
Bulk density(g/cm^3)	0.031	0.032	0.032
True density(g/cm^3)	0.221	0.262	0.632
Porosity (%)	85.9	87.7	94.9
Angle of repose(degree)	29.8	28	27.5
Coefficient of friction (%)			
Glass (%)	0.466	0.456	0.445
Sheet metal (%)	0.425	0.446	0.466
Wood (%)	0.740	0.601	0.597
Surface area(cm^2)	3.19	2.63	2.21
Specific gravity (grams)	3.986	4.932	5.402

Adejumo and Abayomi (2012).

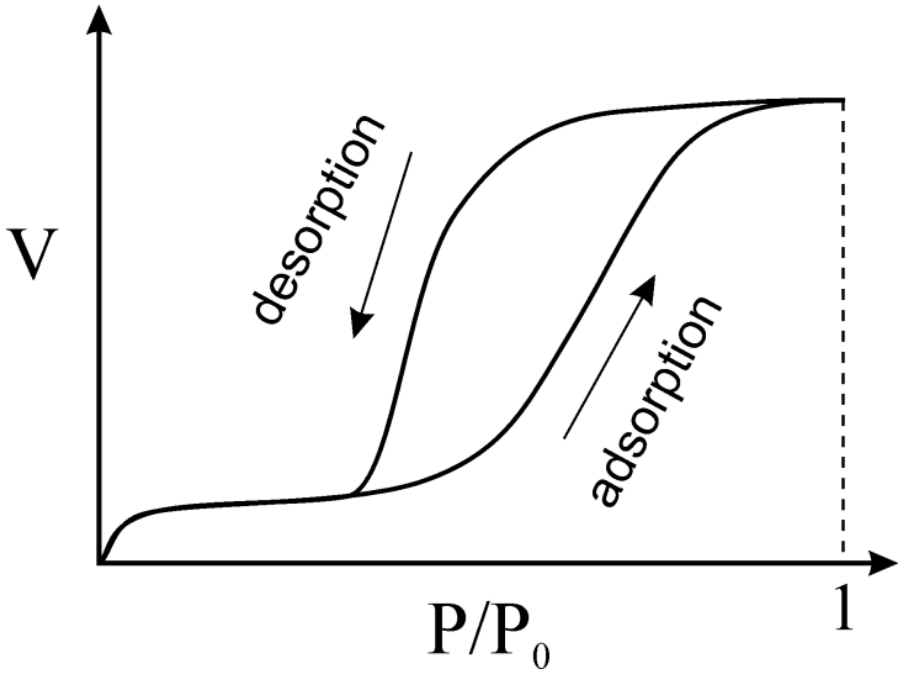

Figure 2.2: Typical sorption isotherms (Carmody *et al.*, 2007).

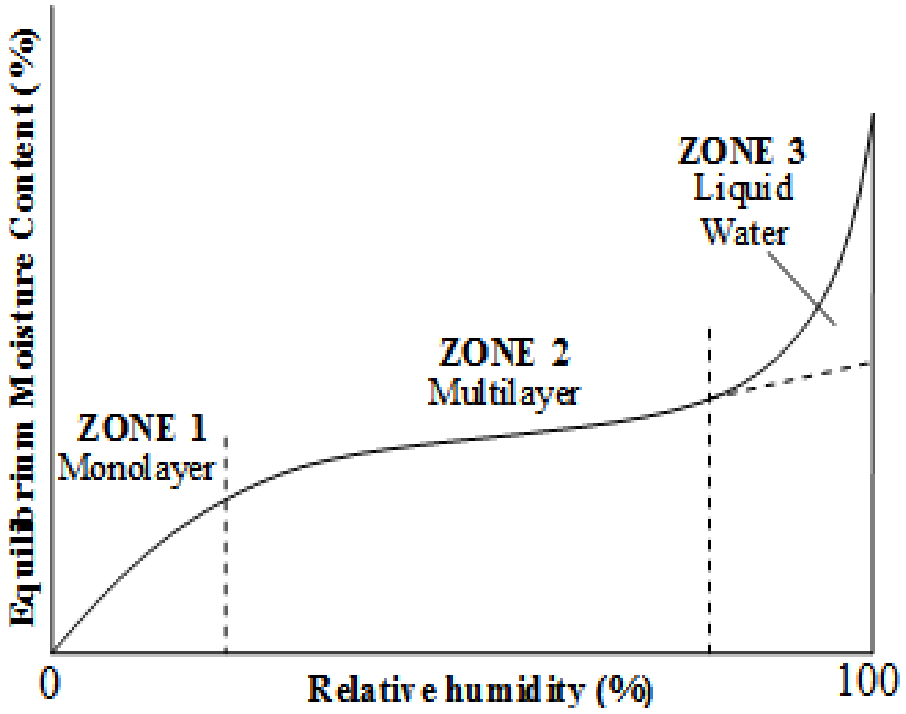

Figure 2.3: Three regions in sorption isotherm curve (Bastias, 2006).

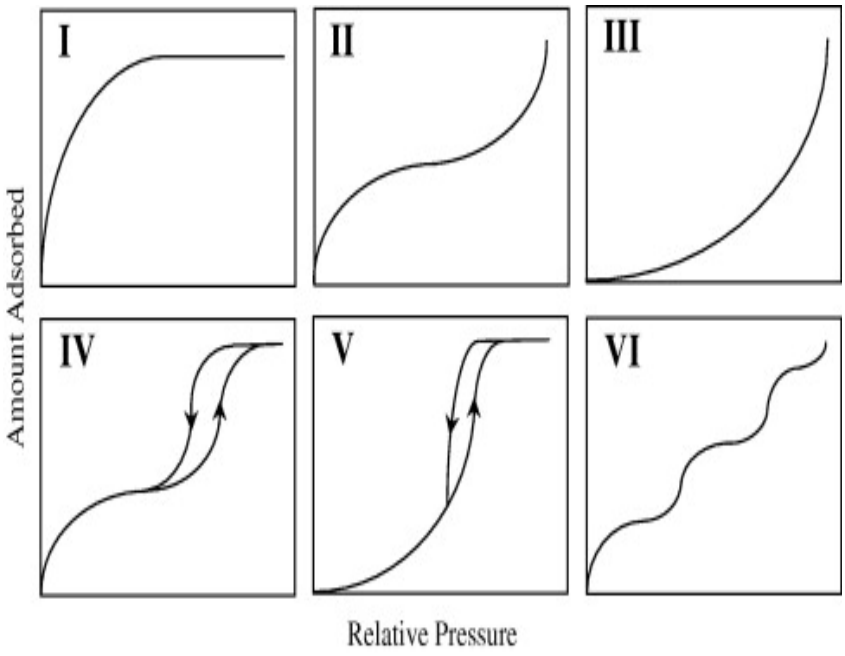

Figure 2.4: **Some categories of adsorption isotherms (Carmody *et al.*, 2007).**

2.5 Applications of Moisture Sorption Isotherm

The point at which desorption is at equilibrium is necessary to calculate the minimum possible moisture content at constant temperature because the elimination of moisture is an important phase in the drying process (Oyelade *et al.,* 2008)

Moisture sorption isotherm is of utmost importance in so many kinds of processing and product stability applications (Falade and Aworh, 2004). From a shelf-life perspective, Vishwakarma *et al.* (2011) explained that isotherm is useful in determining the level of a_w and corresponding moisture content that will reduce the rate of development of micro-organisms and help in the estimation of the nutritional value and stability of foods with respect to differences in the amount of moisture present. In terms of product development, Arslan and Togrul (2005) stated that while creating food formulation and mixtures, knowledge of isotherm helps to prevent moisture transfer between ingredients and enables the choice of constituents so as to prevent alteration of the a_w.

From a processing standpoint, Damodaran *et al.* (2008) contributed that isotherms are important while monitoring the desiccation and inhibition processes because ability of reducing moisture content is largely dependent on the relative vapour pressure.

Singh and Kumari (2014) also reported that while designing and optimizing processes, it is essential to understand how food products adsorb or desorb moisture. For instance, during drying, to evaluate packaging issues, to simulate moisture changes that occur, to forecast shelf-life stability, to predict component mixing and many more.

2.6 Characteristics of Moisture Sorption

Several factors affect the sorption properties of agricultural materials (Khalloufi *et al.,* 2000). These factors include its origin, composition, postharvest operations and methods used to measure the sorption characteristics. Polymers often absorb more moisture than sugars and soluble substances at lower water activity (Schmidt, 2004). Yet, depending on the substance, the soluble components adsorb more moisture beyond a given water activity.

The sorption isotherm for a given product coming from several origins typically varies and may only be compared with caution. Pre-treatments of a certain product may alter

the bound water, altering the capillarity (Adeoye *et al.,* 2020). Yu *et al.* (1999) studied the inhibition and desiccation of cherries and blue berries dried with different methods. It was discovered that at temperatures between 25 and 40 °C, there was no significant difference in the amount of moisture sorbed. The same report was made about blueberries. Aviara (2010) reported that pre-treatment of some food products had a significant effect on their sorption properties Palou *et al.* (1997) found out that the EMC cookies and corn snacks with different constituents such as total carbohydrate and fat during a moisture sorption experiment is different at 5% significance level. The variance in EMC could be as a result of the different sources of the materials, the temperature range, methods used for measurement, the history of products postharvest and sorption characteristics and differences in varieties and the types of models selected.

2.7 Influence of Temperature on Sorption Characteristics

Temperature is the major factor which influences the migration of water vapour, adsorbed moisture, and other gases. (Schmidt, 2004). If equilibrium relative humidity remains constant, a rise in temperature causes a decrease in the quantity of moisture adsorbed as depicted in Figure 2.5 (Aviara *et al.,* 2006).

A rise in temperature is an unfavourable situation for water sorption, according to Menkov (2000). Some sugars and other low-molecular-weight food components are an exception to this principle since they dissolve in water and have a tendency to absorb moisture at higher temperatures. When a product is stored in a closed container, temperature changes can have a substantial impact on the reactivity of microorganisms and chemicals contributing to quality degradation. (Sudathip *et al.,* 2009). Water activity rises as temperature rises at constant moisture levels (Figure 2.6). This expedites the reactions and enhances the level at which deterioration occurs (Rodriguez-Bernal *et al.,* 2015). Vishwakarma *et al.,* (2011) examined guar (*Cyamposis tetragonoloba*) equilibrium moisture contents and discovered that the grain and gum's capacity to absorb moisture decreased with increasing drying temperature. The same findings were reported for different foods (Timmermann *et al.,* 2001).

Temperature variations also have an impact on saturated salt solutions' water activity, which is used to calculate sorption isotherms Using experimental data and

thermodynamic analysis, Pagano and Mascheroni (2005) showed that the with a rise in temperature, the water activity of saturated salt solutions would decrease.

2.8 Moisture Sorption Isotherm Measurement

There are a number of techniques by which the moisture sorption isotherm of various crops has been determined by various scientists (Aviara, 2020). Gal (1975; 1981; 1983) conducted comprehensive evaluations of some techniques and reported that the most common methods of measuring sorption isotherm include the gravimetric, hygrometric, vapour pressure manometric, and a unique approach utilizing AquaLab devices.

2.8.1 Gravimetric method

Gravimetric methods of carrying out sorption experiments of agricultural and food materials, water activities, and various temperatures may be categorized into static and dynamic gravimetric method.

The static gravimetric approach includes putting the product in a controlled environment without agitating the air or product mechanically until it reaches equilibrium (stops accumulating or losing moisture, as the case may be). The limitation of this approach is that it may take several weeks for the product to achieve environmental balance, and due to the lengthy duration, mould may grow at high water activities above 0.8 on food products especially those with high moisture level. Therefore, for outcome of studies at higher water activities such as 0.8 and above, to be reliable, it is important to prevent mold growth while equilibrating. This particular moisture content is referred to as the EMC.

Dynamic gravimetric method involves agitating the air mechanically around the product or the product itself. This approach is faster but it is accompanied with some challenges of designing and implementation. The static gravimetric approach has been widely applied for gathering sorption data and claimed to be the most acceptable for obtaining complete sorption isotherms (Speiss and Wolf, 1987; Chukwu and Ajisegiri, 2011). Also, it has been suggested by various researchers as the conventional approach of obtaining the moisture sorption data of materials. Figure 2.7a and b during shows the experimental set up of gravimetric method of determining sorption isotherm. However, acids are not generally accepted because of its volatility and the dangers

involved handling. Also, concentrated acids have ability to corrode easily and emit fume that may be harmful to the crop. Using a saturated salt solution involves various types of salts so as to regulate the relative humidity within a wide range of 0–100%, whereas only one acid could be used for the same purpose at different levels of concentration.

Static gravimetric method was employed satisfactorily during the measurement of sorption characteristics of vetch seeds (Menkov, 2000), lupine (Vazquez, 2003), sunflower seeds and kernels (Santalla and Mascheroni, 2003), quinoa grains (Tolaba *et al.,* 2004), soya bean (Aviara *et al.,* 2004), red chillies (Kaleemullah and Kailappan, 2004), chickpea flour (Durakov and Menkov, 2005), black nuggets (Swami *et al.,* 2005), sorghum malt (Aviara *et al.,* 2006), parboiled rice (Ajisegiri *et al.,* 2007) and castor seeds (Ojediran *et al.,* 2014) using saturated salt solutions. The MSIs of starch powders Al-Muhtaseb *et al.* (2004), maize flour Oyelade *et al.* (2008a), and yam flour Oyelade *et al.* (2008b) were measured by employing various sulphuric acid concentrations.

2.8.2 Hygrometric method

The MSIs of agricultural materials have also frequently been obtained using electric hygrometers. Many kinds of specially constructed hygrometers are in use. The main components of the apparatus seen in Figure 2.8 are a potentiometer, sample chamber, and sensor. The sensor might make use a resin that exchanges ions, like sulphated polystyrene, or a chemical that is hygroscopic, like lithium chloride, and its conductivity would alter in accordance with the water activity of the sample above. Another option for the sensor is a humidity sensor, which relies on variations in capacitance in thin film capacitors. Electric hygrometers are simple to use and provide quick, generally accurate results Arslan and Togrul (2005). Hygrometer use is restricted by the necessity to calibrate some instruments, evaluate the time required for the sample and sensor to equilibrate, and maintain correct temperature management.

Fasina and Sokhansanj (1993) and Arslan and Togrul (2005) analyzed the MSI of alfalfa and red peppers using the hygrometric method, respectively.

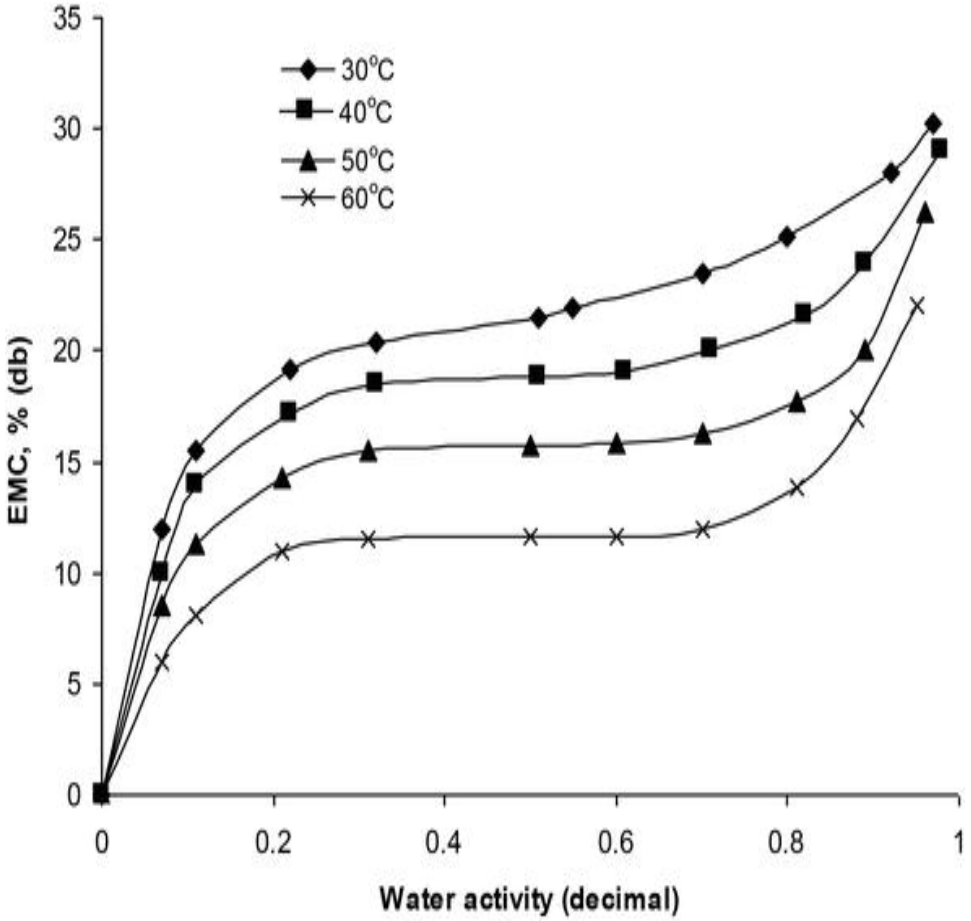

Figure 2.5: **Typical adsorption isotherms at different temperature levels (Aviara *et al.*, 2020).**

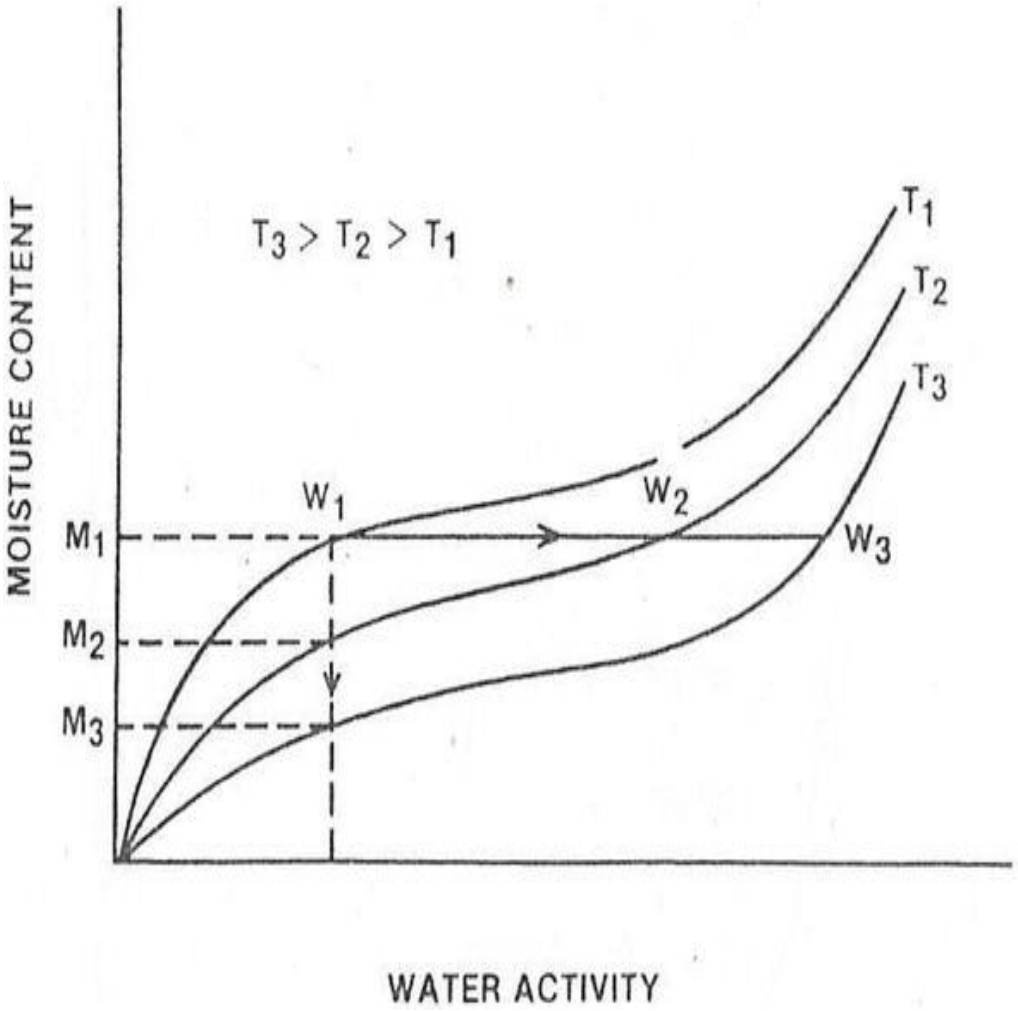

Figure 2.6: **Relationship between moisture content and water activity (Rodriguez-Bernal *et al.*, 2015)**.

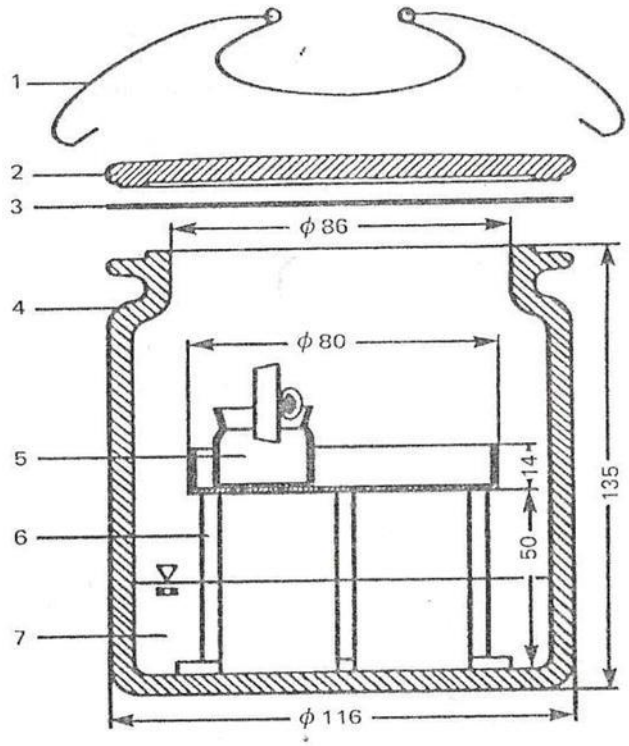

(a)

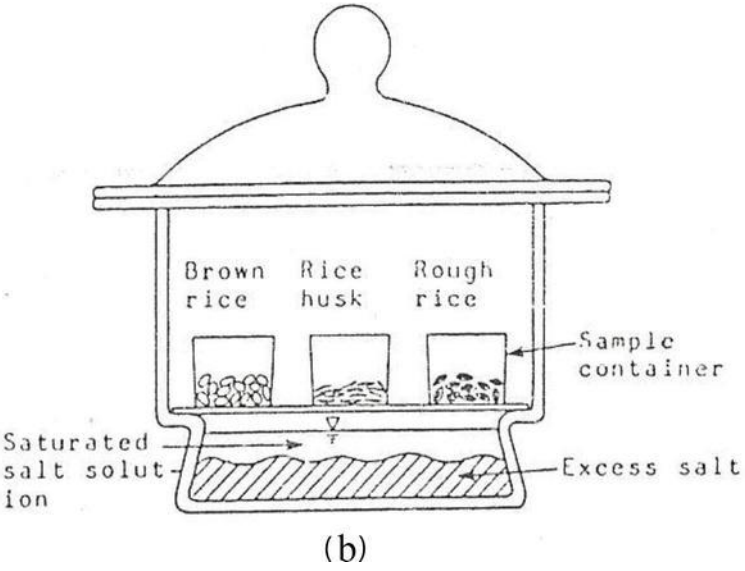

(b)

Figure 2.7a: **Dessicator containing tetra-oxo-sulphate (VI) acid**

2.7b: Desiccator containing different salt solutions. (Aviara, 2020)

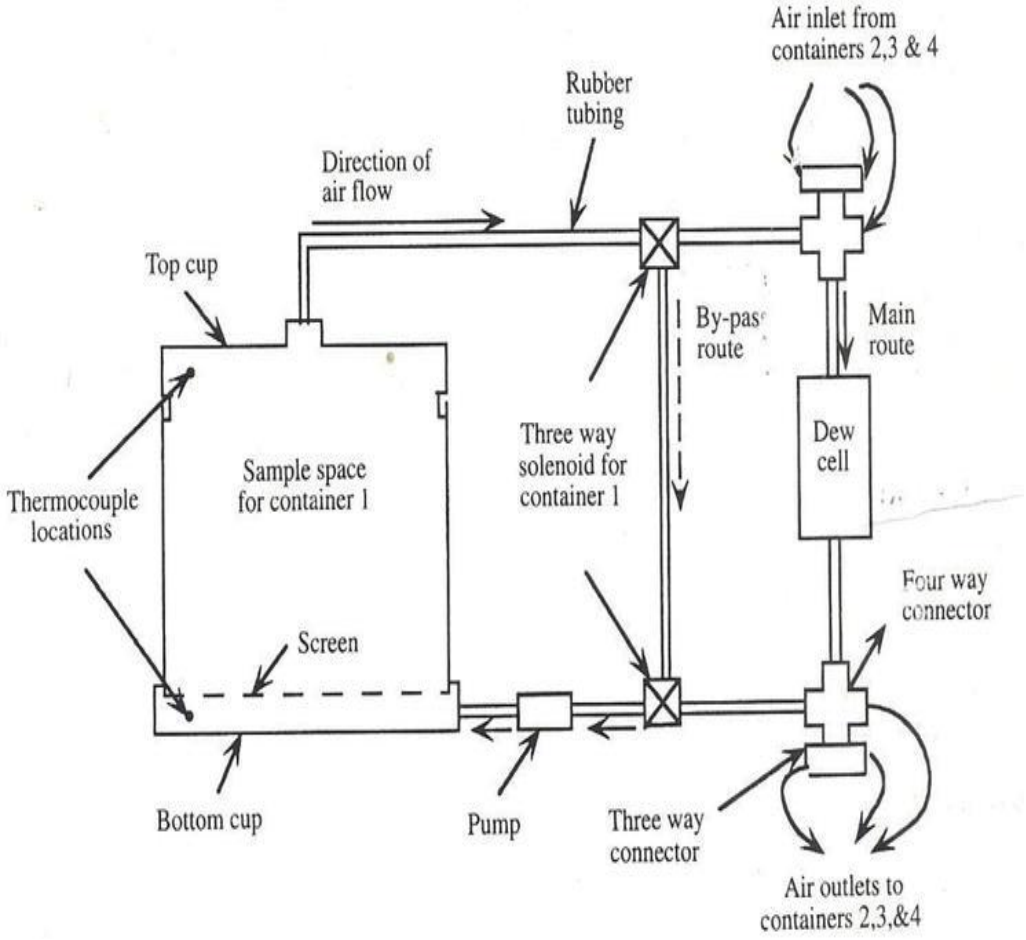

Figure 2.8: **Deteremining moisture sorption isotherm using a hygrometer (Fasina and Sokhansanj, 1993)**

2.8.3 Vapour pressure manometric method

Using the vapour pressure manometric (VPM) method, the equilibrium relative humidity of the air is measured as the relative humidity of the atmosphere, which entails bringing air to a steady temperature and moisture content so that it can reach equilibrium with the agricultural or food product. With this technique, the product's moisture content's vapour pressure is immediately detected. It is considered one of the greatest ways to determine the quality of food as a result (Labuza *et al.*, 1976; Ajibola *et al.*, 2003). The ratio of the sample's vapour pressure compared with the pure water at the same temperature is then used to determine relative humidity at equilibrium. Figures 2.9a and b, respectively, display simplified representations of the system setup and schematic diagrams of the equipment. The relative humidity at equilibrium can be determined using Equation 2.4 (Ajibola *et al.*, 2005).

$$ERH = \frac{(H_1 - H_2)\left(\frac{T_1}{T_0}\right)}{P_S} \qquad 2.4$$

where:

ERH is the equilibrium relative humidity (%)

H_1 is the micro-manometer reading with sample flask connected to the system (mm of manometric oil)

H_2 is the micro-manometer reading with desiccant flask connected to the system (mm of manometric oil)

T_1 is the temperature of the environment surrounding the water bath taken as the temperature of sample (K)

T_o is the temperature of the environment surrounding the micro-manometer (K)

P_s is the saturated vapour pressure at sample temperature (mm of manometric oil).

The MSI was obtained of sesame seed (Ajibola and Dairo, 1998), cowpea (Ajibola *et al.*, 2003) and palm kernels (Ajibola *et al.*, 2005) using the VPM approach.

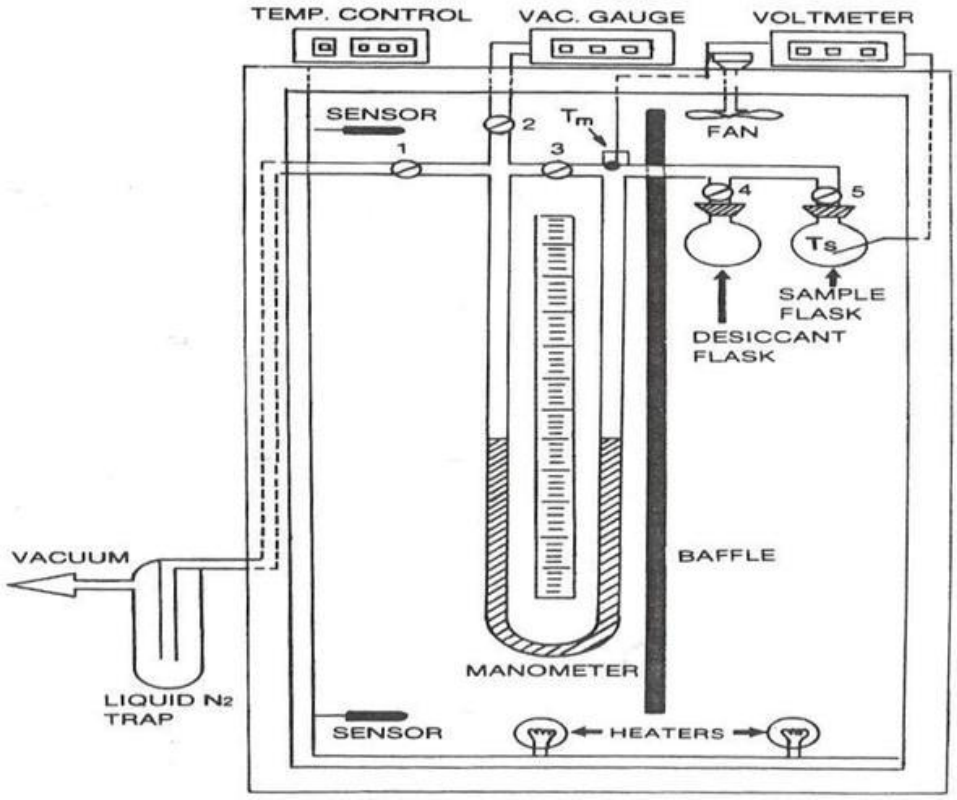

Figure 2.9a: Vapour pressure apparatus setup, (Rizvi, 1986)

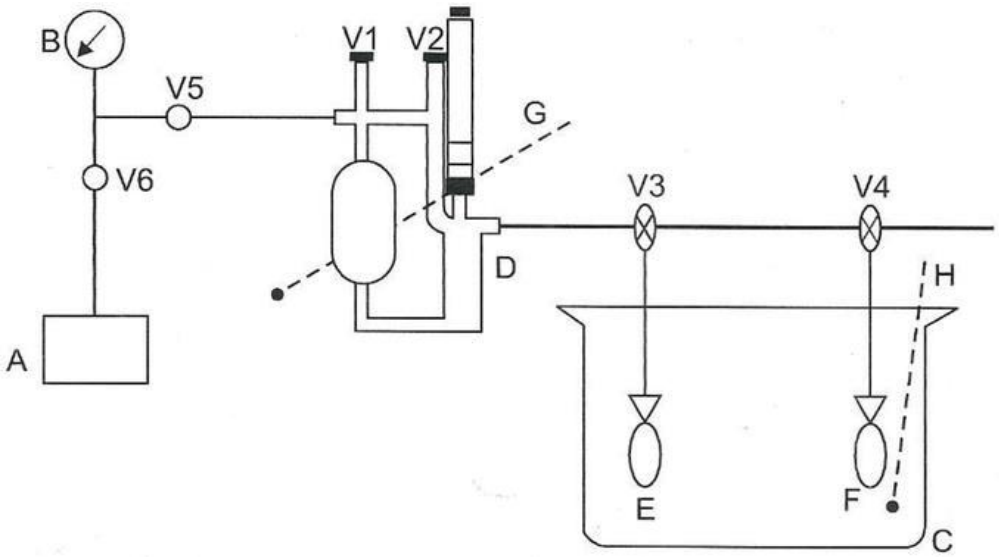

Figure 2.9b: Representation of vapour pressure apparatus setup, (Ajibola *et al.*, 2005).

2.8.4 Humidity Generating Equipment

The vast majority of issues that have been recorded by using saturated salt technique were resolved using humidity generating equipment. This equipment can easily generate sorption isotherms in short period compared to other methods due to the fact that they are designed on the basis of divided flow technology. The sample is exposed to the chosen relative humidity and the mass is determined gravimetrically. A highly sensitive and reliable digital microbalance is used to determine the weight change. The equipment is set up to cycle in an automated way through various humidity levels while maintaining a consistent humidity level until it equilibrates (Mermelstein, 2009).

The following are some common commercial based humidity generating equipment described by Mermelstein (2009): AquaSorp Isotherm Generator, IGA-Sorp, Dynamic Vapor Sorption (DVS), Hydrosorb TM 1000, Cisorp Water Sorption Analyzer, VTI and Q5000SA, SPS Moisture Sorption Analyzers, Water Vapor Sorption Analyze. For many of the listed equipment, establishing whether equilibrium has been attained involves using a method named dm/dt. This value was determined on the basis of the final mass measured. The sample mass reduces as dm/dt tends towards 0, hence, until it reached EMC (Yu, 2007).

The (DVS) equipment has been employed in various studies including Buckton and Darcy (1995), for lactose; Mackin *et al.* (2002) for some pharmaceutical solids. Yu *et al.* (2008) conducted analysis on moisture sorption characteristics of sucrose in amorphous form with the help of the DVS equipment and reported that as the relative humidity increased, the time until crystallization was caused by moisture decreased.

2.9 Isotherm Predictive Models

For determining critical moisture content as well as estimating probable changes while studying storage stability, isotherm prediction models are helpful. According to Labuza and Altunakar (2007), over 270 isotherm equations have been postulated and two or more parameter mathematical models have been employed. They are categorized as empirical, theoretical or semi-empirical models. They are all generated using mathematical models that express the interactions that occur between water activity (percentage equilibrium relative humidity) and equilibrium moisture content (EMC).

2.10 Moisture Sorption Hysteresis

Desorption EMC is the phase at which a material reaches equilibrium with the immediate environment by losing moisture at a given temperature while adsorption (EMC) occurs when the perceived dry material acquires moisture from a high humid surrounding at the time when the temperature is made constant. The isotherm curves usually indicate a noticeable gap or difference at certain equilibrium relative humidity and temperatures between desorption and adsorption EMC values. This gap or difference is termed moisture sorption hysteresis (Aviara *et al.,* 2006). Within the monolayer moisture region, a classic hysteresis loop shown in Figure 2.10 might take place, although it might start at a higher equilibrium relative humidity and go all the way down to zero equilibrium relative humidity, depending on the category as stated by Kapsalis (1987).

2.11 Influence of Temperature on Hysteresis

Temperature, being a major factor that influences sorption isotherm, definitely has a significant influence on sorption hysteresis. The width of the closed boundary along the isotherm curve is also constrained by an increase in temperature, which also results in a decrease in the overall hysteresis. (Aviara *et al.,* 2020). Chirife *et al.,* (1978) investigated how temperature affected the degree of moisture sorption hysteresis in foods. It was found out that for some foods, raising temperature reduced or completely eliminated hysteresis, whereas others saw a stable or even rise in the total hysteresis size. When the size of hysteresis diminished, it became more pronounce when the temperature becomes higher. The desorption isotherms were found to be more strongly affected by temperature than the adsorption isotherms.

There appears to be dearth of information on sorption isotherm of moringa seed. Moravec *et al.* (2008) reported on the adsorption isotherm of moringa seed at 25^{o}C while Alimi *et al.* (2018) gave information on adsorption isotherm of moringa seed at 25^{o}C and 60^{o}C only. However, there is no recorded information on that of moringa seed grits. This research was therefore designed to study the sorption isotherms and thermodynamic properties of moringa seed and seed grits at 20, 25, 30, 35 and 40 ^{o}C with a view of providing information that will be useful in the storage of the seed and grits.

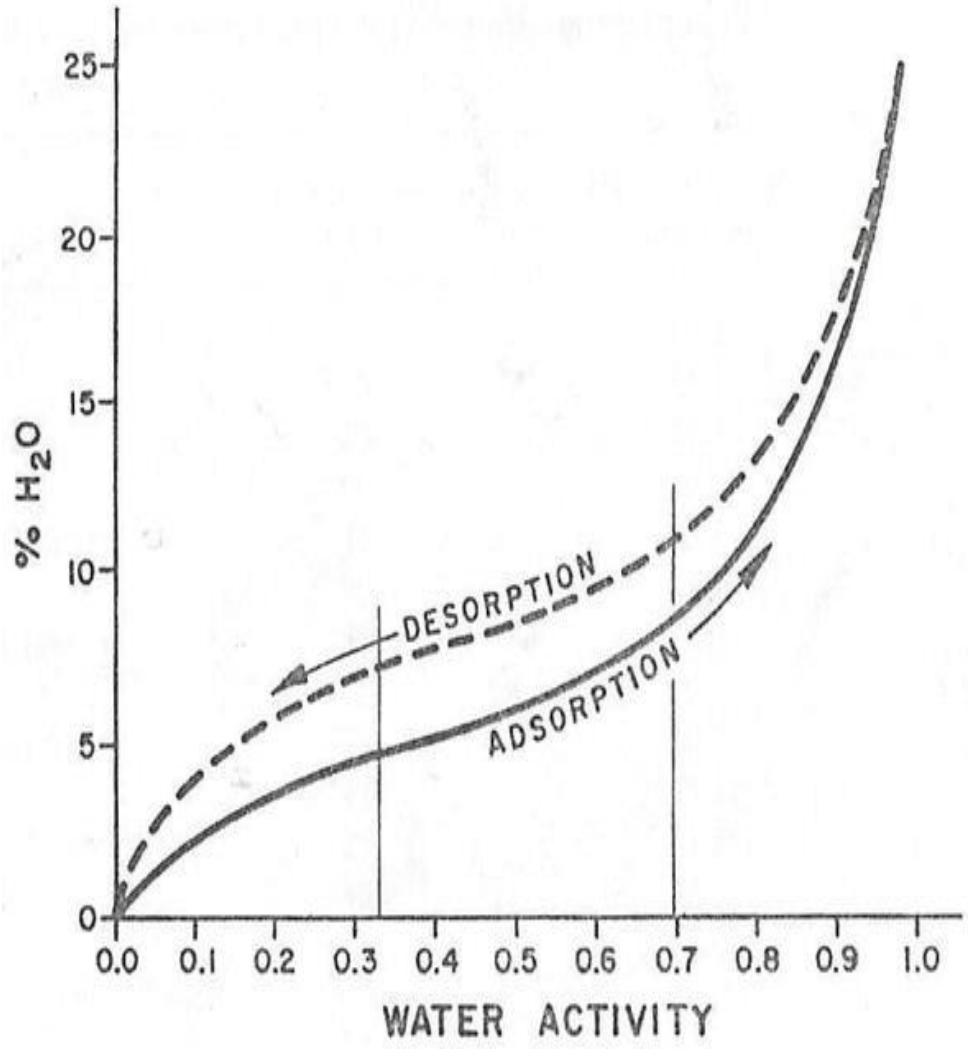

Figure 2.10: Moisture sorption hysteresis loop (Kapsalis, 1987)

CHAPTER THREE

MATERIALS AND METHODS

3.1 Sample Preparation

Matured *Moringa oleifera* Lam. Pods (Plate 3.1) were harvested from Oyo State College of Agriculture and Technology (OYSCATECH) farm, Igboora, Nigeria. The seeds (Plate 3.2), were shelled, cleaned of impurities and foreign matters from the kernels and then dried until equilibrium moisture content (2.82% dry basis) was reached. The dried kernels were ground in an electric laboratory burr mill (Gourmia GCG185 Electric Burr Coffee Grinder) to obtain the grits (particle size 106-212 μm) as shown in Plate 3.3, using the procedure described by Alakali and Satimehin (2007). The residual moisture in the grits was subsequently removed by drying it in desiccators over concentrated sulfuric acid for seven days, and it was then stored in airtight containers until further analysis were carried out (Ogunsina *et al.*, 2014).

3.2 Extraction of Oil

The ground seeds were collected in a cellulose thimble with pores in it. In an extraction chamber, the thimble was positioned in between a condenser and a flask with the solvent. The solvent dissipated and migrated to the condenser, and was transformed into liquid before trickling directly into the sample's extraction chamber (Ibrahim and Onwualu, 2005). After the conclusion of the separation procedure, the flask was emptied and evaporated in an oven, and the mass of lipid that was remaining was estimated to determine the amount of oil in the seeds.

Plate 3.1: ***Moringa oleifera*** **Lam pods**

Plate 3.2: Moringa seeds

Plate 3.3: Moringa grits

3.3 Control of Relative Humidity

Concentrated tetraoxosulphate (VI) acid (H_2SO_4) was used to create a controlled environment for the storage of moringa seed and the seed grits (Aviara, 2020). The acid was chosen as the desiccant because it equilibrates quickly unlike saturated salts that take days before equilibration. The percentage of concentrated H_2SO_4 as well as the respective water activity values at different temperature is shown in Table 3.1 as reported by Aviara, 2020. The desiccators' lids were tightly sealed and held at room temperature, the oil was removed for analysis after 30, 60, and 90 days while the control was the oil gotten immediately after extraction termed as day 1.

3.4 Measurement of the Quality Parameters of Moringa Oil

3.4.1 Saponification value

The Saponification Value (SV) was evaluated using a method described in AOAC (2010) as reported by Onilude *et al.* (2010) as shown in Equation 3.1. Two grams of the sample and 25.0 mL of potassium hydroxide (0.5 mol/L) were added to a 200 mL conical flask. It was then heated for 30 minutes, instantly cooled, and titrated with 0.5 mol/L HCl until a light pink colour appeared.

$$\text{SV (mg of KOH /g)} = \frac{(BL - EP) \times TF \times C \times K}{m} \quad 3.1$$

where:

EP is Titration volume (mL)

BL is Blank level (25 mL)

TF is Reagent (HCl) factor (1.006)

C is Concentration conversion coefficient (28.05 mg/mL)

(Potassium hydroxide in Eq.:56.11×0.5)

K is Unit conversion coefficient (1)

m is Sample size (g)

3.4.2 Iodine value

The Iodine Value was employed to measure the amount of reactive double bonds were present in the oil (IV). More double bonds and the likelihood of oxidation are indicated by a higher IV value. The iodine value as displayed in Equation 3.2 was calculated using data from the AOAC, (2010). The process involves adding 0.1 g of each of the sample to a 300 mL conical flask. 20 mL of carbon tetrachloride were added and dissolved in an ultrasonic washer. The jar was filled with 25 milliliters of Hanus

solution before being sealed. The combination was maintained in a closed room without light for 30 minutes at 20°C. With the addition of 10 mL of 15% potassium iodide and 100 mL of water, the mixture was agitated for 30 seconds. The mixture was titrated with 0.1 mol/L sodium thiosulfate to a colourless endpoint in order to determine the amount of iodine present.

$$\text{IV (mg of KOH /g)} = \frac{(BL - EP) \times TF \times C \times K}{m} \quad 3.2$$

where:

EP is Titration volume (mL)

BL is Blank level (47 mL)

TF is Titrant factor (1.006)

C is Concentration conversion coefficient (1.269 mg/mL)

(Atomic mass of Iodine: 126.9/100)

K is Unit conversion coefficient (1)

m is Sample size (g)

3.4.3 Peroxide value

The level of oil deterioration was evaluated using the peroxide value. A rancid taste and odour can be noticed when the peroxide value falls to a range of 20 and 40 Meq/Kg (Barakat and Ghazal, 2016). The peroxide value was determined using Equation 3.3 AOAC, (2010). The process involved putting 5 g of the sample to a conical flask with a stopper. The sample was thoroughly dissolved by adding 30 milliliters of solvent and giving it a gentle shake. After adding 0.5 mL of saturated potassium iodide, the flask was closed and gently shaken for a minute. The flask was kept at room temperature in a dark area. 30 mL of pure water was then added and the container was sealed. The mixture was then titrated with sodium thiosulfate at a concentration of 0.01 mol/L until a light-yellow colour appeared, which was used to calculate the peroxide value.

$$\text{PV (Meq/Kg)} = \frac{(EP - BL) \times TF \times R}{m} \quad 3.3$$

where:

EP is Titration volume (mL)

BL is Blank level (0.0 mL)

TF is Reagent factor (1.006)

R is Constant (10)

m is Sample size (g)

3.4.4 Acid value

The percentage free fatty acid measured as oleic acid was used to determine the Acid Value (AV). 5 g of oil sample were accurately weighed in a dish, then poured to a conical flask and reweighed to determine an exact mass of the oil used. 50 ml of a small amount of phenolphthalein and a hot neutral alcohol were added, and the mixture was vigorously agitated. The solution was titrated with 0.5 M sodium hydroxide (NaOH) solution while being continuously shaken until it turned pink. Using the amount of 0.5 M alkali used as described in Equation 3.4, the amount of acid present was calculated, and the result was termed the acid value (Onilude *et al.*, 2010).

$$\text{Acid value} = \frac{V_{NaOH} \times 5.61}{W} \qquad 3.4$$

where:

V_{NaOH} is the volume of sodium hydroxide titrant used (mL)

W is the weight of the fatty oil being examined (g)

3.5 Moisture Content Determination

Moisture contents of moringa seed and grits was determined using AOAC (2010). Cans were cleaned and dried in an oven for 1 hour at 100^{o}C and then placed in a desiccator for 40 minutes to cool down and weighed as W_1. One gram each of moringa seed grits was weighed into separate cans as W_2 and placed inside the oven at a temperature of 130^{o}C. The samples' weights were kept under observation until same values were obtained repeatedly as W_3. Each measurement was taken in triplicate. The moisture content was derived from Equation 3.5 reported by Raji and Oyefeso (2017) and Oyefeso *et al*. (2021)

$$\text{Moisture Content (dry basis)} = \frac{W_2 - W_3}{W_3 - W_1} \times 100\% \qquad 3.5$$

where:

W_1 = Initial weight of empty moisture can (g)

W_2 = Initial weight of sample and can (g)

W_3 = Final weight of can and sample (g)

Table 3.1: **Concentrated H_2SO_4 and corresponding water activity values**

Percent H_2SO_4	Temperature (^oC)				
	20	25	30	35	40
15.00	0.9237	0.9241	0.9245	0.9253	0.9261
25.00	0.8218	0.8218	0.8252	0.8285	0.8317
35.00	0.6607	0.6651	0.6693	0.6773	0.6846
40.00	0.5599	0.5656	0.5711	0.5816	0.5914
45.00	0.4524	0.4589	0.4653	0.4775	0.4891
50.00	0.3442	0.3509	0.3574	0.3702	0.3827
55.00	0.2440	0.2505	0.2563	0.2685	0.2807
60.00	0.1573	0.1625	0.1677	0.1781	0.1887
65.00	0.0895	0.0933	0.0972	0.1052	0.1135

Rizvi, (1986); Bell and Labuza (2000) as reported by Aviara, (2020).

3.6 Evaluation of the Moisture Sorption Isotherms

Static gravimetric method using concentrated tetraoxosulphate (IV) acid (H_2SO_4) was deployed to study the moisture adsorption and desorption of moringa seed and grits. Equilibrium moisture content was determined for both adsorption and desorption processes at five temperature levels (20, 25, 30, 35 and 40 ^oC) and nine water activity levels (0.09, 0.15, 0.24, 0.34, 0.45, 0.56, 0.66, 0.82 and 0.92) using concentrated tetraoxosulphate (IV) acid (H_2SO_4) shown in Table 3.1 to obtain constant water activities at the temperature levels.

Thirty grams each of moringa seed and grits (Plate 3.4) was kept in separate petri dishes and the dishes were kept inside glass desiccator (Plate 3.5) containing 350 ml of the concentrated acid. The desiccator was placed in a thermostatic water bath (Plate 3.6) which had been regulated to the chosen temperature and the samples were allowed to reach equilibrium. The samples were weighed every six hours until uniform weight was attained thereby obtaining the equilibrium moisture content at the specified conditions. Equilibrium moisture content was determined in dry basis through the known initial moisture content and the difference in weight (Chukwu and Ajisegiri, 2011; Ade *et al.*, 2016; Adeoye *et al.*, 2020). The experiment was conducted three times, and the average value was determined and documented.

The isotherm curves were obtained by plotting moisture content of the equilibrated samples against the water activity (Appendix A). The same samples used for adsorption experiments were used for desorption at the same temperatures, this was to obtain the boundary called hysteresis between the adsorption and desorption curves (Oyelade *et al.*, 2008). The adsorption and desorption data were fitted into three sorption models that factored temperature as a parameter and another three that did not consider temperature as a parameter. Table 3.2 shows the mathematical expressions of each of the selected models.

Plate 3.4: Moringa grits weighed on the weighing scale.

Plate 3.5: Glass desiccator.

Plate 3.6: Thermostatic water bath

Table 3.2: Established sorption models used to evaluate EMC-a_w relationship

Model Name	Mathematical equation
BET	$M = \frac{M_o C a_w}{(1-a_w)[1+(C-1)a_w]}$
GAB	$M = \frac{ABCa_w}{[1-Ba_w][1-Ba_w+BCa_w]}$
Hailwood-Horrobin	$M = \left(\frac{A}{a_w} + B - Ca_w\right)^{-1}$
Modified Henderson	$M = \left[\frac{-ln(1-a_w)}{A[T+B]}\right]^{1/C}$
Modified Halsey	$M = \left[\frac{-lna_w}{exp(A+BT)}\right]^{-1/C}$
Modified Hailwood-Horrobin	$M = \left(T\left(\frac{A}{a_w} + B\right) - \frac{C}{T^n}a_w\right)^{-1}$

where:

a_w is the decimal equivalent of equilibrium relative humidity

M is the equilibrium moisture content in % (db)

M_o is monolayer moisture content in % (db)

T is the temperature in °C

A, B, C are sorption isotherm constants specific to each equation

T^n is the absolute temperature.

3.6.1 Model Parameter Evaluation Procedures

3.6.1.1 Brunauer-Emmett-Teller (BET)

The BET equation is the most widely used moisture sorption isotherm model because it provides a very good fit to sorption data around the region of $a_w < 0.45$ (Chirife and Iglesias, 1978; Alamri *et al.,* 2018). The BET equation defining EMC with respect to a_w is shown in Equation 3.6:

$$M = \frac{M_o C a_w}{(1-a_w)[1+(C-1)a_w]} \quad 3.6$$

where:

M is the equilibrium moisture content (% db)

M_o is the monolayer moisture content (%, db)

a_w is water activity ranging from 0.01-0.45

C is the energy constant associated with net isosteric heat of sorption.

Solving Equation 3.6 yields a simpler, linear form as shown in Equation 3.7.

$$\frac{a_w}{(1-a_w)M} = \frac{1}{M_o C} + \frac{a_w(C-1)}{M_o C} \quad 3.7$$

A plot of $\frac{a_w}{(1-a_w)M}$ against a_w at the chosen temperature within the range of a_w shown in appendix B gives the slope as $\frac{(C-1)}{M_o C}$ and intercept as $\frac{1}{M_o C}$. From the slopes of the graph at different temperatures, the defined parameters in Equation 3.6 were obtained.

3.6.1.2 Guggenheim-Anderson-De Boer (GAB)

GAB equation was derived by Guggenheim, Anderson and de Boer and it contains three parameters (Etim *et al.,* 2011). It is as expressed in terms of EMC with respect to a_w in Equation 3.8.

$$M = \frac{M_o C k a_w}{(1-k a_w)[1-k a_w+C k a_w]} \quad 3.8$$

where:

M is equilibrium moisture content (% db)

M_o is monolayer moisture content (%, db)

C and k are sorption constants of the GAB model

a_w is water activity of the entire range.

Equation 3.8 was rewritten as a second order polynomial expression to give Equation 3.9.

$$\frac{a_w}{M} = \propto {a_w}^2 + \beta a_w + \gamma \qquad 3.9$$

where:

$$\propto = \frac{K}{M_o}\left(\frac{1}{C} - 1\right) \qquad 3.9a$$

$$\beta = \frac{1}{M_o}\left(1 - \frac{2}{C}\right) \qquad 3.9b$$

$$\gamma = \frac{1}{M_o C k} \qquad 3.9c$$

Equation 3.9 was solved by plotting a_w/M versus a_w at a constant temperature as shown in Appendix C and plotting a two-parameter polynomial curve to evaluate coefficients and the constant in Equation 3.9.

3.6.1.3 Hailwood-Horrobin Model

The Hailwood-Horrobin model shown in Table 3.2 and GAB model are mathematically comparable and after algebraic modifications, it can be represented as shown in Equation 3.10.

$$\frac{a_w}{M} = C{a_w}^2 + Ba_w + A \qquad 3.10$$

The non-linear regression method utilizes the values of C, B, and A as initial model parameters for the evaluation of the mode and are obtained by plotting a_w/M versus a_w and a second-order polynomial of each temperature is fitted to the graph**.**

3.6.1.4 Modified Henderson Model

Modified Henderson model presented in Table 3.2 was transformed to yield an expression given in Equation 3.11.

$$1 - exp[-A[T + B]M^C] \qquad 3.11$$

Equation 3.11 was then linearized by logarithmic transformation as presented in Equations 3.12 to 3.15.

$$1 - a_w = exp[-A[T + B]M^C] \quad 3.12$$

$$ln(1 - a_w) = -A[T + B]M^C \quad 3.13$$

$$-ln(1 - a_w) = A[T + B]M^C \quad 3.14$$

$$ln[-ln(1 - a_w)] = ln\big[A[T + B]\big] + ClnM \quad 3.15$$

Using Equation 3.15, a straight line with a slope of C and an intercept on the y-axis of $ln\big[A[T + B]\big]$ is generated by plotting $ln[-ln(1 - a_w)]$ versus lnM at each temperature as presented in Appendix D. Intercept on the y-axis was used to find the parameters related to temperature as shown in Equation 3.16.

Therefore,

$$\exp(b_1) = A[T + B] = AT + AB \quad 3.16$$

When exp(b_1) is plotted against T, a straight line is generated with a_2=A as the slope and b_2=AB as the intercept on the y-axis. The average of C=C, A, and B was used as the model's initial parameter estimate in the nonlinear regression procedure.

3.6.1.5 Modified Halsey Model

Modified Halsey model presented in Table 3.2, can be rewritten by algebraic modifications to yield Equation 3.17.

$$a_w = exp[-exp(A + BT)M^{-C}] \quad 3.17$$

Linearizing Equation 3.17 by logarithmic transformation yields Equation 3.18 to 3.20.

$$ln\ a_w = -exp(A + BT)M^{-C} \quad 3.18$$

$$-ln\ a_w = exp(A + BT)M^{-C} \quad 3.19$$

Therefore,

$$ln[-ln\ a_w] = (A + BT) - ClnM \quad 3.20$$

Using Equation 3.20, a straight line with a slope of (-C) and an intercept on the y-axis of $(A + BT)$ is generated by plotting $ln[-ln\ a_w]$against lnM at each temperature as shown in Appendix E. The initial values for parameter estimate for the model in the nonlinear regression analysis were the average of C as C and the values for A and B.

3.6.1.6 Modified Hailwood-Horrobin Model

Modified Hailwood-Horrobin model presented in Table 3.2, can be rewritten algebraically to give Equation 3.21 below:

$$\frac{a_w}{M} = {\varphi_w}^2 + \mu a_w + \omega \quad 3.21$$

Plotting $\frac{a_w}{M}$ against a_w and a second-order polynomial of each temperature is fitted to the graph to give the following functions:

$$\varphi = \frac{C}{T^n}; \mu = BT; \omega = TA$$

In order to evaluate the model, a nonlinear regression analysis was performed using the average values of A, B, and C as initial parameter estimates.

3.6.2 Validation of the Sorption Isotherm Models

Statistical measures such as the root mean square error (RMSE), co-efficient of determination (R2), mean relative error (MRE), and residual sum of squares (RSS) were used to assess the statistical validity of the fit to the models as shown in Equations 3.22, 3.23, 3.24 and 3.25 respectively.

$$RMSE = \sqrt{\frac{\sum\left(M_e - M_p\right)^2}{N}} \quad 3.22$$

$$R^2 = \frac{\sum\left(M_e - M_p\right)^2}{\sum M_e^2 \sum M_p^2} \quad 3.23$$

$$MRE = \frac{100}{N}\sum\frac{M_e - M_p}{M_e} \quad 3.24$$

$$RSS = \frac{\sum\left(M_e - M_p\right)^2}{N} \quad 3.25$$

where:

M_e is the experimental EMC

M_p is the predicted EMC

N is the number of experimental data.

The R^2 values closest to 1, and RMSE and RSS values closest to 0, depicts a better fit. Values of MRE below 10% shows a suitable fit for practical reasons (Sudathip *et al.*, 2009).

3.7 Effect of Temperature and Hysteresis on Monolayer Moisture Content.

3.7.1 Monolayer Moisture Content

The monolayer moisture content (M_o) of moringa seed and grits was evaluated at 20, 25, 30, 35 and 40 ^oC temperature levels for both adsorption and desorption isotherms by applying BET, GAB and Caurie's equations.

3.7.1.1 Caurie equation

The M_o was calculated for the whole span of water activities using Caurie's equation as shown in Equation 3.26.

$$ln\left(\frac{1}{M}\right) = -ln(M_oC) + \left(\frac{2C}{M_o}\right) ln\frac{(1-a_w)}{a_w} \quad 3.26$$

where:

M is equilibrium moisture content (% db)

M_o is monolayer moisture content (%, db)

a_w water activity

C is Caurie's constant.

Rearranging Equation 3.26 gives Equation 3.27.

$$ln\left(\frac{(1-a_w)}{a_w}\right) = ln\left(\frac{1}{M}\right)\left(\frac{M_o}{2C}\right) + ln(M_oC)\left(\frac{M_o}{2C}\right) \quad 3.27$$

A graph of $ln\frac{(1-a_w)}{a_w}$ was plotted against $ln\left(\frac{1}{M}\right)$ as shown in Appendix F. The values of the slope $\left(\frac{M_o}{2C}\right)$ and intercept $ln(M_oC)\left(\frac{M_o}{2C}\right)$ were obtained and solved to estimate the monolayer moisture content.

3.8 Determination of Water Vapour Transmission Rate and Permeability Coefficient

According to ASTM E 96, permeability coefficient and Water Vapour Transmission Rate (WVTR) of two different packaging materials (Polypropylene (Pp) and low-density polyethylene (LDPE)) were determined through gravimetric method (Robertson, 2013; Slamet *et al.*, 2020 and Pantidol and Norio, 2022). The packaging samples were prepared by placing ten grams of silica gels into each packaging material and placed in a desiccator, while another set of packaging material served as control. The thickness of each material was measured using an analogue vernier calliper, while

surface areas were calculated by measuring the dimensions of the packaging materials with a measuring tape.

The study was carried out at ambient temperature with average storage conditions of 29 ^{o}C temperature and at 80% relative humidity. Inside the desiccator, an Elitech RC-4 data logger was installed to keep track of the relative humidity and temperature. The packaging material samples were weighed constantly at intervals of two days for twelve days (Yaptenco *et al.*, 2017).

Mean weight gain by the two packaging materials (Pp and LDPE) as well as those that were not in desiccation, throughout the twelve days of monitoring at average temperature of 29 ^{o}C and relative humidity of 80% were documented. Weight gains in the control samples were subtracted from weight gains in Pp and LDPE with the weight plotted against time and the slope determined the WVTR and permeability coefficient (P) using the expression given by Pantidol and Norio (2022) in Equations 3.30 and 3.31 respectively.

$$WVTR = \frac{Q}{tA} \quad 3.30$$

$$P = \frac{WVTR\ (X)}{\Delta p} \quad 3.31$$

where:
Q/t is the slope (g H_2O/day)
A is the surface area (m^2)
X is the thickness (m)
Δp is the partial pressure change (mmHg)
where:
$\Delta p = p_o - p_i$
P_o is saturated vapour pressure of pure water (mmHg)
RH is storage relative humidity (%)

3.9 Shelf-Life Determination

The shelf life of both the seeds and grits at different storage temperatures and water activities were determined in this study. The packaging materials were filled with 30 g each of moringa seed and grits with initial moisture content of 12.2 and 10.25 g H_2O/100 g dry solids, respectively. The filled packaging materials were closed tightly to avoid any air space and were placed in a thermostatic water bath at 25℃ and water activity range of 0.5 to 0.8. The shelf life (t) in days was calculated using equation 3.32 according to Labuza, (1984), Anandito *et al.* (2017) and Gichau *et al.* (2019).

$$ln\frac{(M_i-M_e)}{(M_c-M_e)}=\frac{PAP_o}{Xmb}t \quad 3.32$$

where;

t is time (days)

M_i is initial moisture content (% dry basis)

M_c is critical moisture content (% dry basis)

M_e is moisture content during storage (% dry basis)

P is coefficient of permeability ($gH_2O\ m^2\ day^{-1}\ mmHg^{-1)}$

Po is water vapour pressure at saturation (25°C) (mmHg)

X is the thickness of the packaging material (mm)

A is surface area (m^2)

m is product weight (g)

b is slope

3.10 Determination of Isosteric Heat and Entropy of Sorption

The sorption isotherm values were used to estimate the isosteric heat of sorption. The approach was based on the Clausius-Clapeyron equation, which is frequently used to assess how temperature impacts isotherms. The technique works for a large range of temperatures and is characterized by its simplicity and reliability (Phomkong *et al.*, 2006). Clausius- Clapeyron equation is as given in Equation 3.33 (Yazdani *et al.*, 2006).

$$\frac{d(lna_w)}{d\left(\frac{1}{T}\right)}=-\left(\frac{q_{st}}{R}\right) \quad 3.33$$

where q_{st} is the isosteric heat of sorption (KJ/mol) which was calculated using Equation 3.34.

$$q_{st}=Q_s-\Delta H_{vap} \quad 3.34$$

where:

a_w is the water activity

q_{st} is the net isosteric heat of sorption (kJ mol^{-1})

ΔH_{vap} is the heat of vaporisation (kJ mol^{-1} water)

R is the universal gas constant (kJ $mol^{-1}\ K^{-1}$)

T is absolute temperature (K).

The q_{st} was calculated using the slope gotten from the plot of $ln(a_w)$ and $1/T$ at constant moisture.

CHAPTER FOUR

RESULTS AND DISCUSSION

4.1 Some Chemical Characteristics of Moringa Oil

Table 4.1 describes the influence of storage duration of 30, 60, and 90 days and relative humidity on some chemical properties namely, Acid Value (AV), Peroxide Value (PV), Iodine Value (IV) and Saponification Value (SV) of moringa seed oil. The parameters determined increased as relative humidity rises and falls just below the maximum standard already set for edible oils by FAO/WHO (2009) with the exception of the Iodine value, because it reduces as relative humidity increased. This confirms unequivocally the stability of moringa oil when stored at a wide range of environmental conditions for a long period. These result support earlier researches by Farooq *et al.* (2006) on characterization of *Moringa oleifera* seed oil from drought and irrigated regions of Punjab, Pakistan and Rahman *et al.* (2009) on physicochemical properties of *Moringa oleifera* Lam. seed oil of the indigenous-cultivar of Bangladesh.

4.1.1 Acid value

The AV presented in Figure 4.1, increased in a linear manner as relative humidity increase and during the whole period of storage. It ranged from 2.47 to 3.44 mg of KOH/g with the highest value recorded after 60 and 90 days of storage at 94% relative humidity. This implies that there is more free fatty acid in moringa oil at a very high humidity than lower ones. This suggests that the acid value of moringa oil may not exceed the maximum 4.0 mg of KOH/g FAO/WHO standard for edible oil when kept for a longer period because constant values were recorded after 60 and 90 days at higher relative humidity levels. This result agrees with the reports of Karima *et al.*, 2021 and Fu *et al.*, 2021 on chemical composition and properties of moringa seed oil.

Table 4.1: Some chemical characteristics of Moringa oil during storage

	RH %	11	23	43	57	70	80	94
	Days							
Acid value (mg of KOH/g)	0	2.47	2.62	2.66	2.73	2.77	2.92	2.92
	30	2.62	2.66	2.69	2.77	2.81	2.95	3.07
	60	2.73	2.84	2.92	2.99	3.14	3.33	3.44
	90	2.73	2.84	2.95	2.99	3.14	3.33	3.44
Peroxide value (Meq/Kg)	0	1.01	1.01	1.01	1.14	1.21	1.21	1.21
	30	1.01	1.01	1.01	1.01	1.07	1.21	1.21
	60	1.01	1.01	1.07	1.14	1.21	1.21	1.21
	90	1.07	1.14	1.21	1.21	1.21	1.21	1.21
Iodine value (g/100g)	0	71.92	70.64	69.36	68.51	66.81	64.26	62.98
	30	69.79	69.36	68.09	66.81	65.96	64.68	62.55
	60	68.94	68.09	67.24	66.38	64.68	63.83	61.28
	90	68.94	68.51	67.66	66.81	66.81	65.53	63.83
Saponification value (mg of KOH/g)	0	174.48	174.95	176.83	177.78	181.07	182.01	183.89
	30	174.48	175.89	177.30	177.78	180.60	182.01	183.89
	60	173.07	174.95	176.83	177.78	180.60	182.48	183.89
	90	172.13	174.01	175.42	177.30	180.13	182.48	184.36

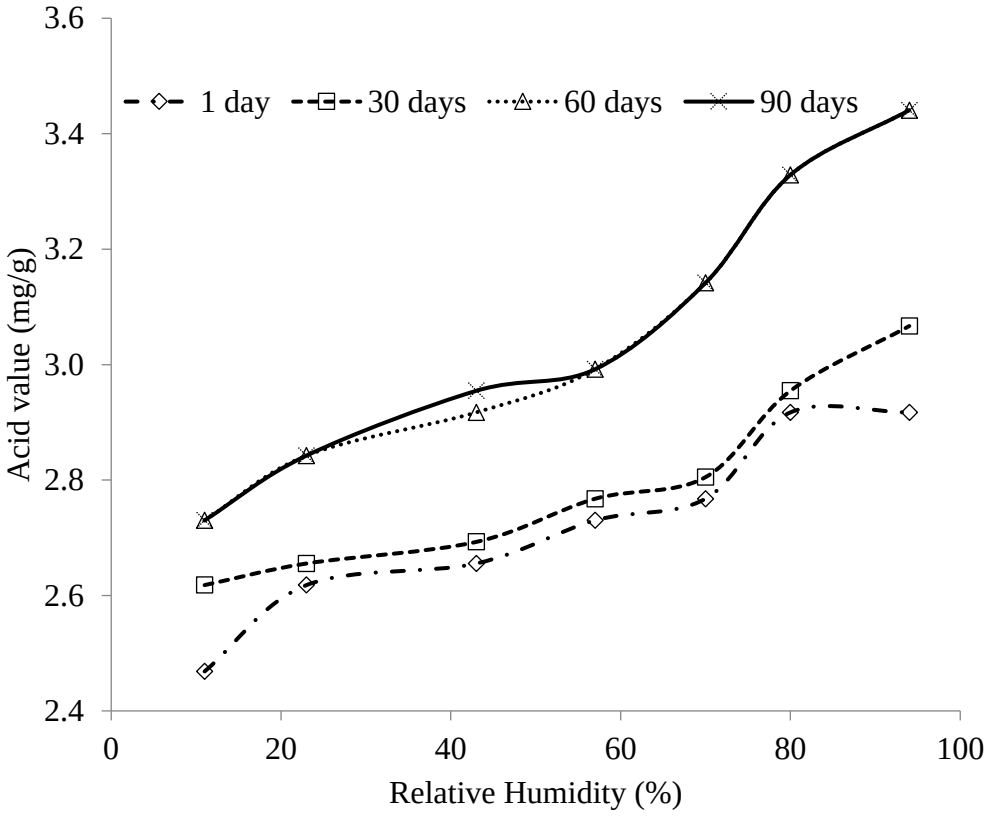

Figure 4.1: Acid value of moringa oil

4.1.2 Peroxide value

Moringa seed oil's peroxide value was determined to range from 1.01 to 1.21 Meq/Kg, this is remarkably minute when considering the standard already set by FAO/WHO (2009) as the requirement for consumable oil, which is 4 Meq/Kg. The peroxide values of the oil increased slightly as relative humidity increase from 11 and 94% and it remained constant at 1.21 Meq/Kg after storing for 60 and 90 days as shown in Figure 4.2. This demonstrates that it has an oxygen concentration below the FAO/WHO criterion of 4.0Meq/Kg, which is used to observe the development of rancidity. Its stability and shelf life are increased by the decreased peroxide level, which makes it less likely to grow rancid Rahman *et al.* (2009). This finding agrees with the report of Manzoor *et al.* (2007) on physicochemical characterization of *Moringa concanensis* seed and seed oil and Athikomkulchai *et al.,* (2021) on *Moringa oleifera* seed oil formulation, physical stability and chemical constituents for enhancing skin hydration and antioxidant activity.

4.1.3 Iodine value

According to Figure 4.3, the iodine value (IV) of moringa seed oil ranged from 61.28 to 71.92 g/100 g of oil, with the maximum value being at 11% RH, this is in order with several earlier investigations (Leone *et al.,* 2016). Between 80 and 106 g/100 g is the FAO/WHO recommended iodine content for edible oil. Even though the values are within acceptable standard of consumable oil, the IV consistently decreases as storage time and relative humidity increase. This is consistent with Ogunsina *et al.* (2014) and Chalh *et al.,* (2021). The amount of unsaturated acid and the oil's non-drying qualities can both be determined by an oil's iodine value. The liquidity increases with increasing unsaturation level, thereby increasing the iodine value.

4.1.4 Saponification value

According to Figure 4.4, the greatest value for moringa seed oil's saponification ranged from 173.09 to 183.89 mg KOH/g oil at 94% relative humidity. The results for each sample fall within the range of the FAO/WHO (2009) recommended acceptable limit for consumable oil (Dinesha *et al.* 2018). The oil's fatty acid composition and the soap that can be made from it are both revealed by the saponification values. Low fatty acid concentration in the oil is suggested by a high saponification value. This shows that it is unlikely for rancidity to happen when the product is being stored.

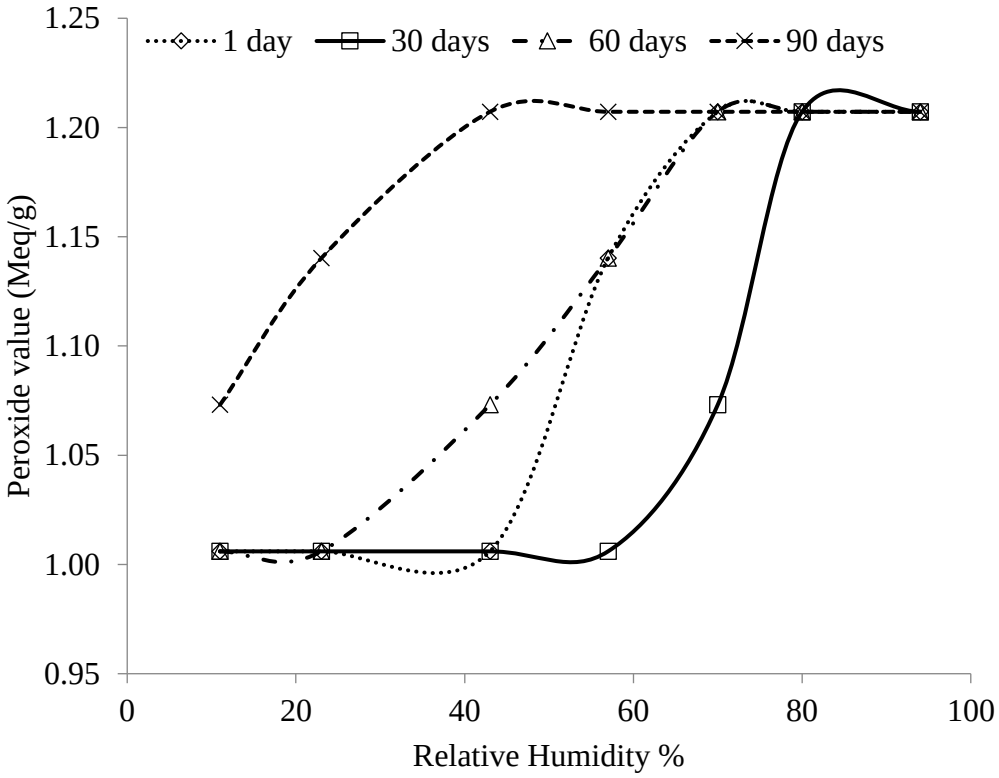

Figure 4.2: Peroxide value of moringa oil

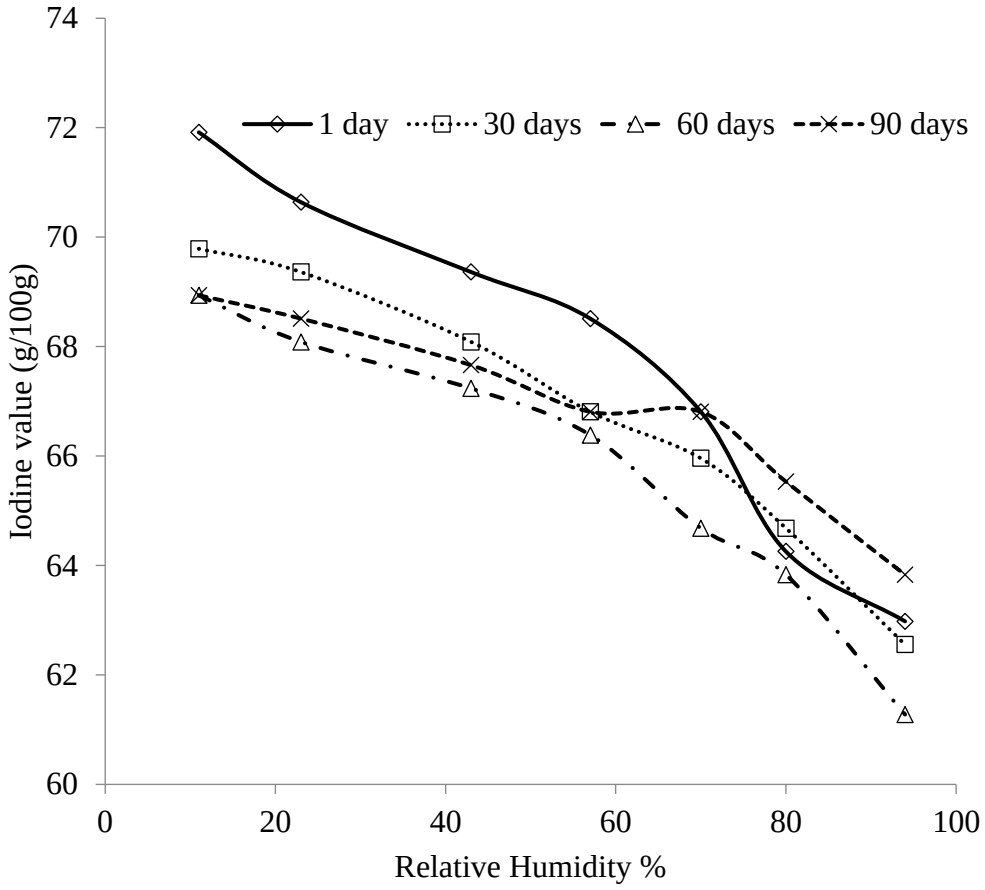

Figure 4.3: Iodine value of moringa oil

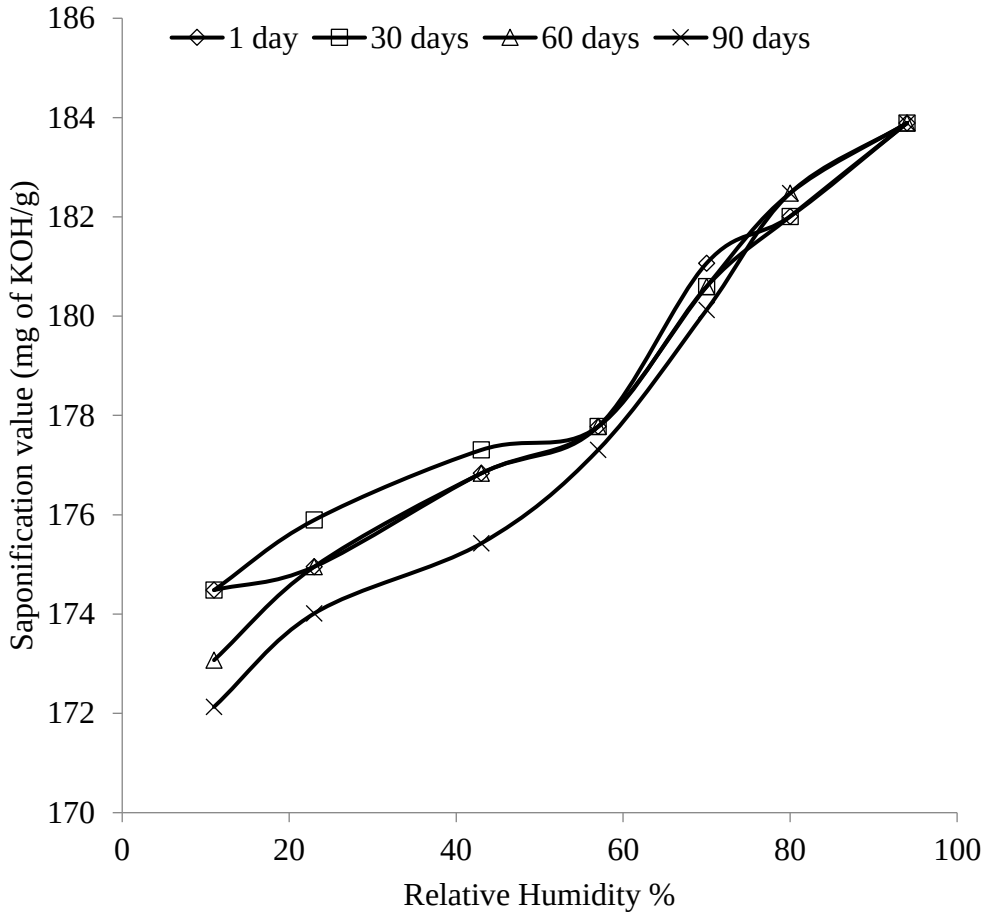

Figure 4.4: Saponification value of moringa oil

4.2 Moisture Sorption Isotherms of Moringa Seed and Grits

The quantity of moisture adsorbed and desorbed reflects the value of the equilibrium moisture content (EMC) of the seed and grits and it depends on the water activity and temperature. The EMC of the seed and grits at various water activities (a_w) at which moisture sorption isotherm experiments were carried out are presented in Tables 4.2 to 4.5. It was observed that as water activity increases, the EMC increases. Conversely, as temperature increases, the EMC reduces. This is expected because EMC is largely dependent on water activity and temperature. Similar trends for many seeds have been reported (Menkov, 2000; Vazquez, 2003: Santalla and Mascheroni, 2003: Tolaba *et al.,* 2004: Aviara *et al.,* 2004: Tarigan *et al.,* 2006; Akanbi *et al.,* 2006 and Yan *et al.,* 2008). These EMC values obtained were used to plot the adsorption and desorption isotherm of moringa seed and grits at different temperatures as shown in Figures 4.5 to 4.8 respectively. With an increase in a_w, the EMC increased for each of the temperature levels considered. This can be explained by the higher active state of water molecules at higher temperature thus the attractive forces between them decreasing (Yan *et al.,* 2008). This corroborated the reports given by Vazquez, 2003, Kaleemullah and Kailappan, 2004 Swami *et al.,* 2005, Aviara *et al.,* 2006, and castor seeds Ojediran *et al*., 2014.

The sorption isotherm for both moringa seed and grits indicated a sigmoidal form that is typical of most biological materials, supporting Type II according to the BET classification (Aviara, 2020). However, moringa grits adsorbs and desorbs less amount of moisture than moringa seed. This could be because moringa grits has been broken down into smaller particles thereby reducing the bound water and increasing the surface water. At lower activity levels, they absorb relatively little water, but at higher relative humidity levels, they absorb more. For items with a high oil content, this is consistent with Kumar *et al.* (2005). There is evidence that a product's composition, processing method, temperature, and relative humidity all affect its ability to absorbs moisture. (Vishwakarma *et al.*, 2011; Ojediran *et al*., 2014).

Table 4.2: Adsorption equilibrium moisture content for moringa seed

Water activity (A_w)	Equilibrium moisture content (EMC, % dry basis)				
	20°C	25°C	30°C	35°C	40°C
0.0895	4.85	4.13	3.58	3.16	2.85
0.1573	5.25	4.54	3.98	3.55	3.28
0.244	5.90	5.23	4.65	4.22	3.94
0.3442	6.54	5.84	5.22	4.81	4.50
0.4524	7.50	6.88	6.25	5.80	5.55
0.5599	8.45	7.71	7.14	6.74	6.47
0.6607	9.58	8.86	8.27	7.82	7.51
0.8218	10.88	10.22	9.66	9.48	9.14
0.9237	12.26	11.60	11.00	10.66	10.36

Table 4.3: Desorption equilibrium moisture content for moringa seed

Water activity A_w	Equilibrium moisture content (EMC, % dry basis)				
	20°C	25°C	30°C	35°C	40°C
0.0895	4.92	4.20	3.61	3.21	2.96
0.1573	5.28	4.55	4.05	3.69	3.37
0.244	5.94	5.26	4.78	4.36	4.05
0.3442	6.69	6.00	5.48	5.05	4.75
0.4524	7.62	6.91	6.40	6.00	5.68
0.5599	8.42	7.75	7.22	6.81	6.53
0.6607	9.72	9.02	8.43	8.01	7.72
0.8218	10.96	10.56	9.77	9.35	9.25
0.9237	12.39	11.89	11.16	10.75	10.55

Table 4.4: Adsorption equilibrium moisture content for moringa grits

Water activity (A_w)	Equilibrium moisture content (EMC, % dry basis)				
	20°C	25°C	30°C	35°C	40°C
0.0895	2.90	2.58	2.48	2.36	2.32
0.1573	3.50	3.13	2.87	2.73	2.64
0.244	4.09	3.67	3.16	2.94	2.87
0.3442	4.65	4.37	3.73	3.49	3.42
0.4524	5.24	4.93	4.53	4.18	3.92
0.5599	5.85	5.64	5.25	4.75	4.68
0.6607	6.46	6.38	5.92	5.65	5.26
0.8218	7.28	7.42	6.95	6.87	6.06
0.9237	8.30	8.36	8.22	8.11	7.55

Table 4.5: Desorption equilibrium moisture content for moringa grits

Water activity (A_w)	Equilibrium moisture content (EMC, % dry basis)				
	20°C	25°C	30°C	35°C	40°C
0.0895	2.87	2.54	2.45	2.33	2.29
0.1573	3.45	3.09	2.83	2.68	2.60
0.244	4.06	3.63	3.13	2.90	2.73
0.3442	4.62	4.30	3.66	3.44	3.30
0.4524	5.19	4.84	4.47	4.12	3.86
0.5599	5.80	5.60	5.16	4.66	4.45
0.6607	6.38	6.25	5.84	5.44	5.04
0.8218	7.15	7.18	6.88	6.75	5.95
0.9237	8.22	8.15	8.06	7.93	7.41

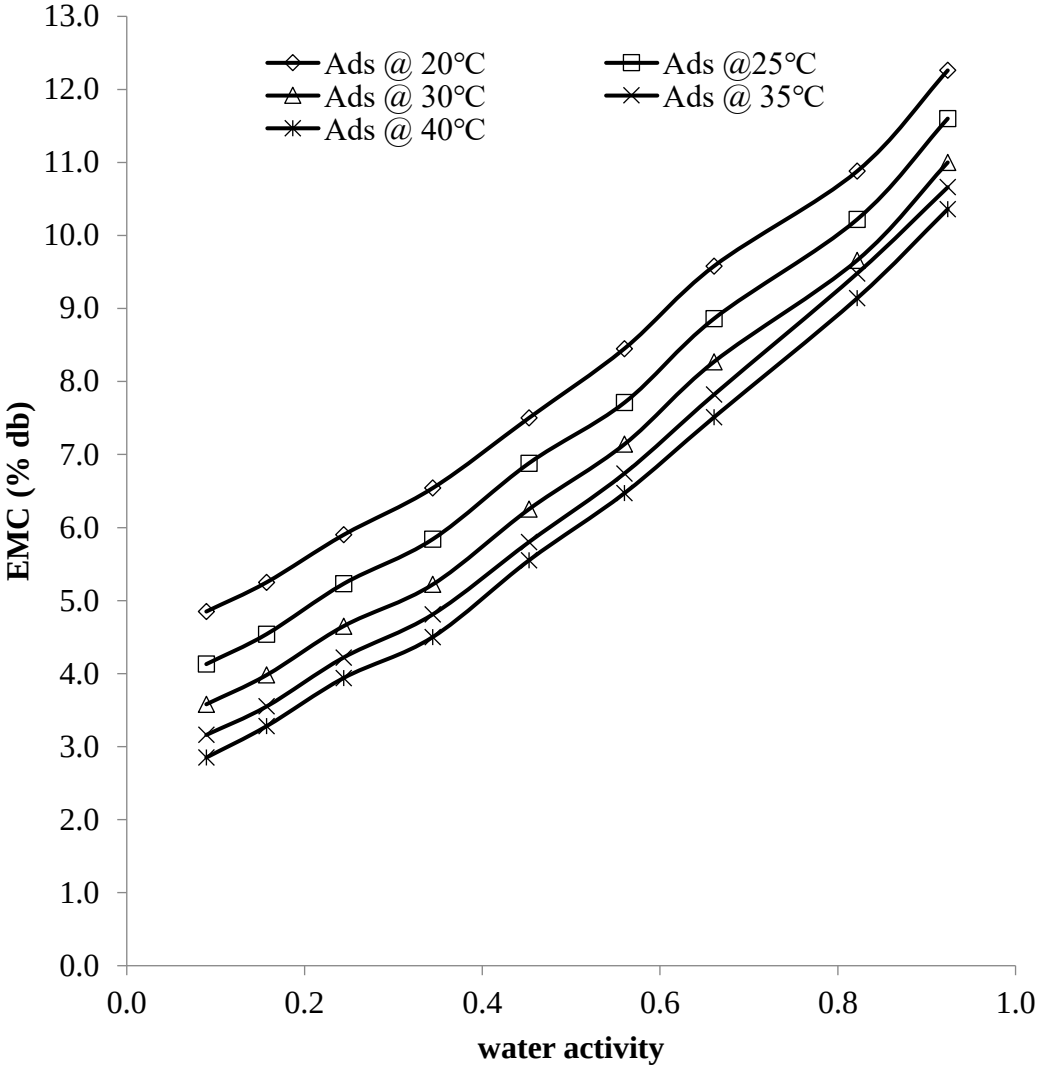

Figure 4.5: Adsorption isotherm of moringa seed

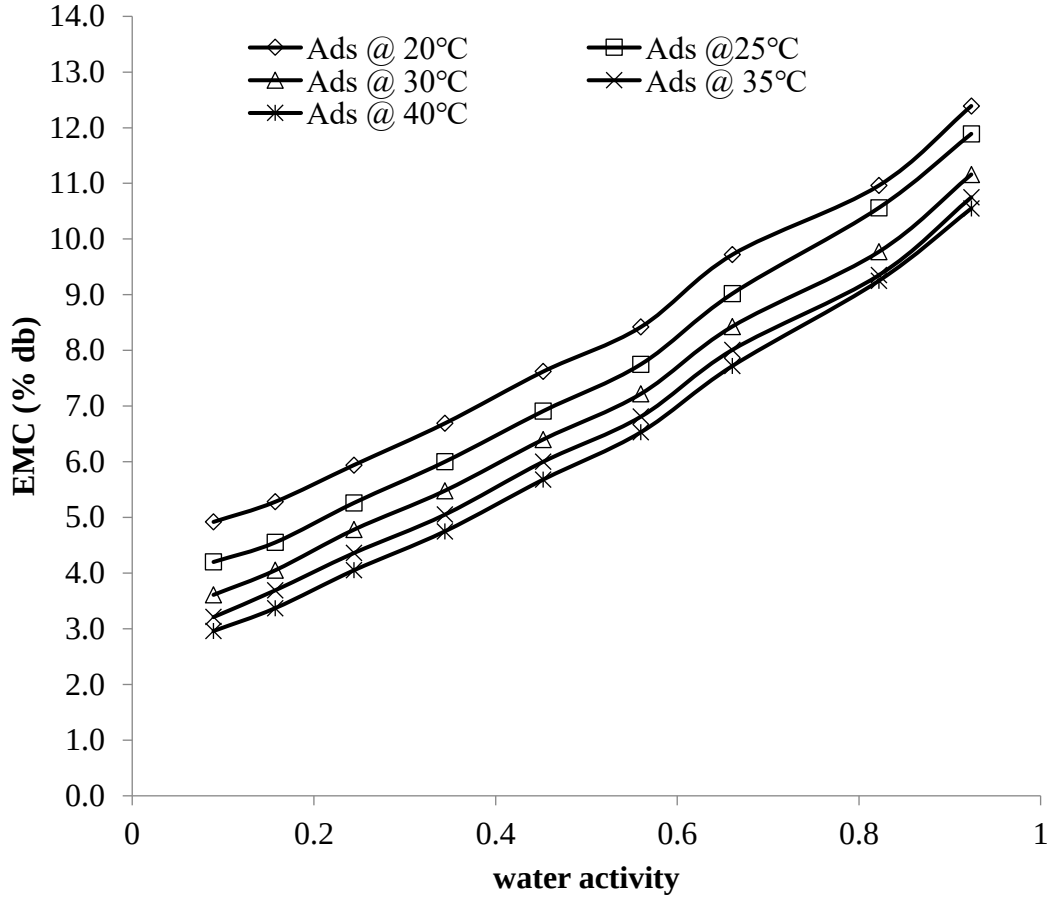

Figure 4.6: Desorption isotherm of moringa seed

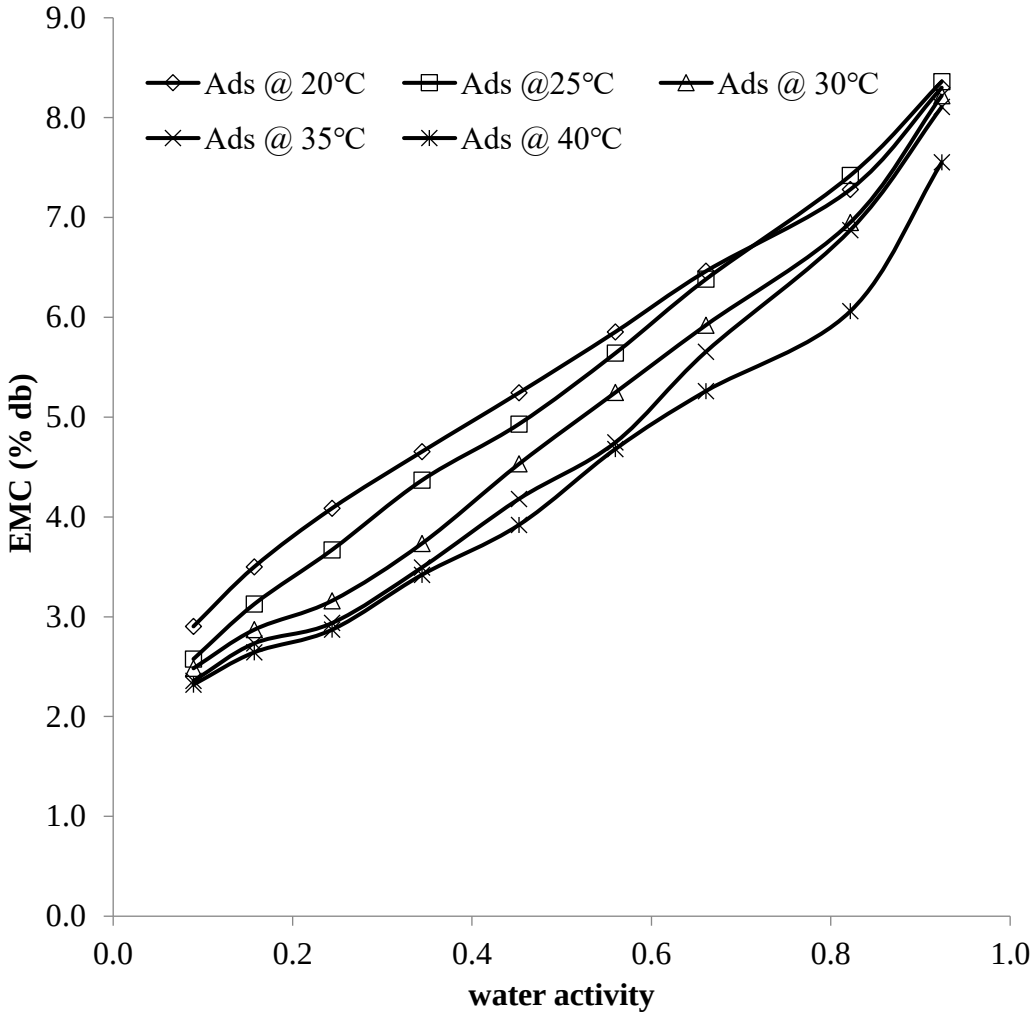

Figure 4.7: Adsorption isotherm of moringa seed grits

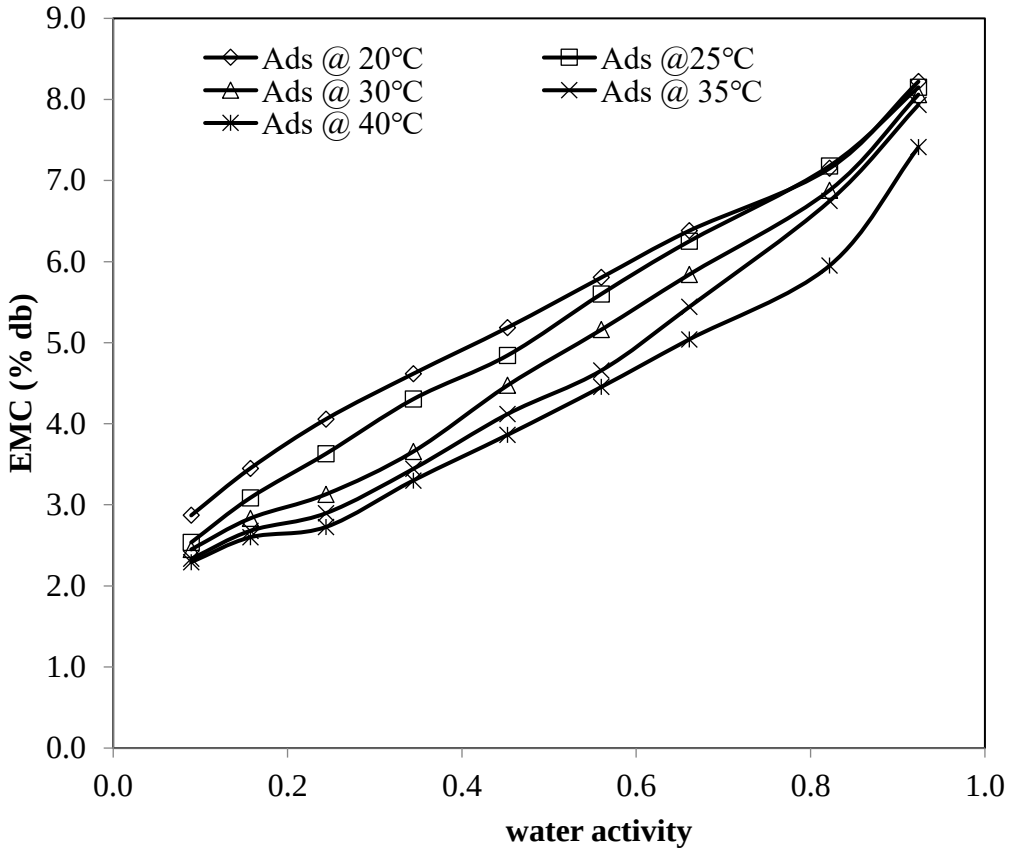

Figure 4.8: Desorption isotherm of moringa seed grits

4.3 Hysteresis Loop

The quantity of moisture taken up by moringa seed during adsorption (Table 4.2) was comparatively higher than the quantity of moisture released during desorption process (Table 4.3) while the quantity of moisture taken up during adsorption by moringa grits (Table 4.4) was comparatively lower than the quantity of moisture desorbed during desorption process (Table 4.5). The quantity progressively decreased at each subsequent lower temperature. Oyelade *et al.* (2008) noted that food products subjected to repeated adsorption and desorption processes through a number of cycles (minimal hysteresis) are believed to be more stable, otherwise, as they are less prone to operational contamination and less vulnerable to excessive heat known to affect nutritive value (Fontana, 2007). According to Yan *et al.* (2008), hysteresis has been associated with the nature and condition of food ingredients, reflecting the possibility for structural and conformational rearrangements. The narrow ends of surface pores gather and hold moisture internally below the water activity where the water should have been released as it exits the capillaries of biomaterials during moisture desorption. According to Raji and Ojediran (2011), the swelling of polymeric materials during moisture adsorption can also cause hysteresis. Pure water would dissolve solutes present in the material during adsorption and the dissolution of solutes increased the surface tension, resulting in lower water activity at given moisture content. The hysteresis loops between adsorption and desorption processes for both moringa seed and grits at each temperature are shown in Figures 4.9 to 4.13 and Figures 4.14 to 4.18 respectively. Hysteresis started in both moringa seed and grits at an a_w over 0.2 for 20°C, although, it started below an a_w of 0.2 for 40°C. The hysteresis' termination proceeded in the same manner. The termination point extends as temperature increases. The hysteresis loop ended at roughly the same a_w for all temperatures in the greater range of a_w. This shows that as the temperature rises, the range of moisture sorption hysteresis in moringa seed and grits also increases. The size of the loop is higher at 40°C than at 20°C, showing that the overall hysteresis increases with temperature, as shown in Figures 4.9 to 4.18. This agrees with the report given by Oyelade *et al.,* (2008), Moreira *et al.,* (2010) Koc *et al.* (2010), Rodriguez-Bernal *et al.,* (2015), Aviara *et al.,* (2016) and Mohammad *et al.,* (2021).

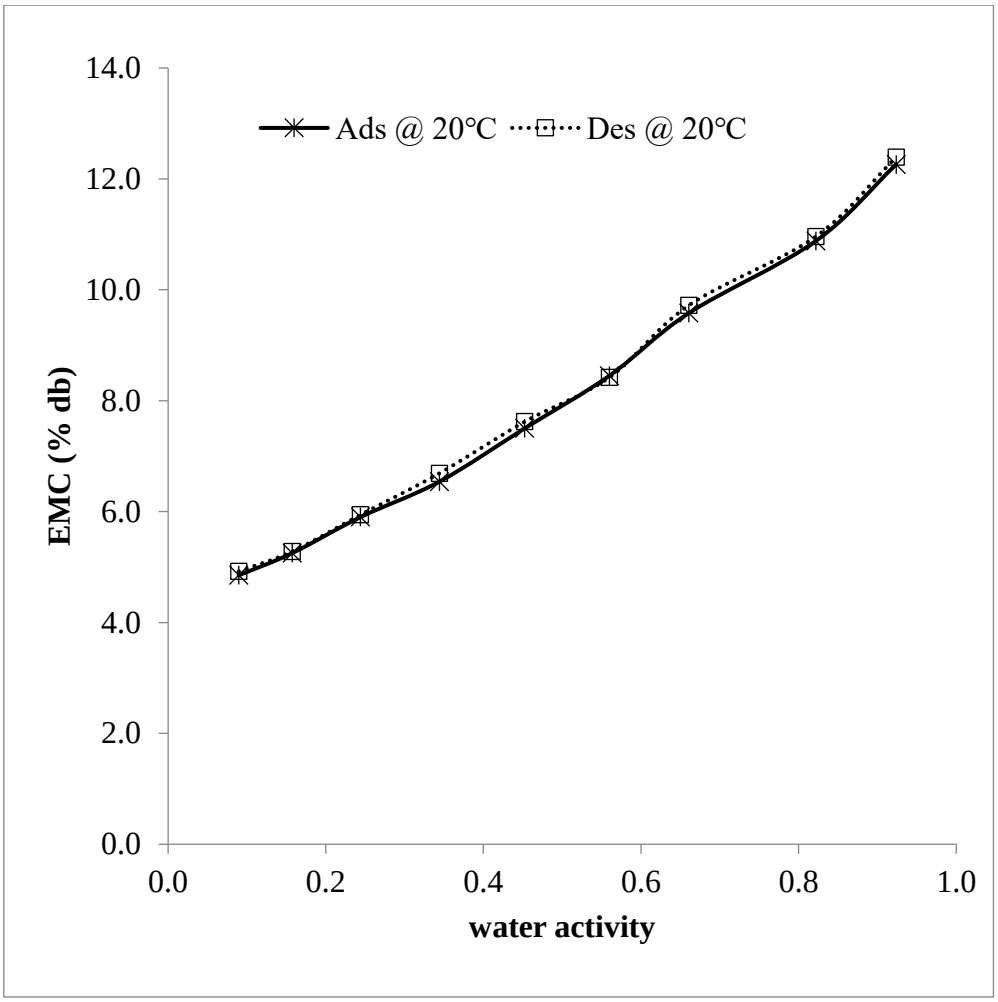

Figure 4.9: Hysteresis loop for moringa seed at 20°C

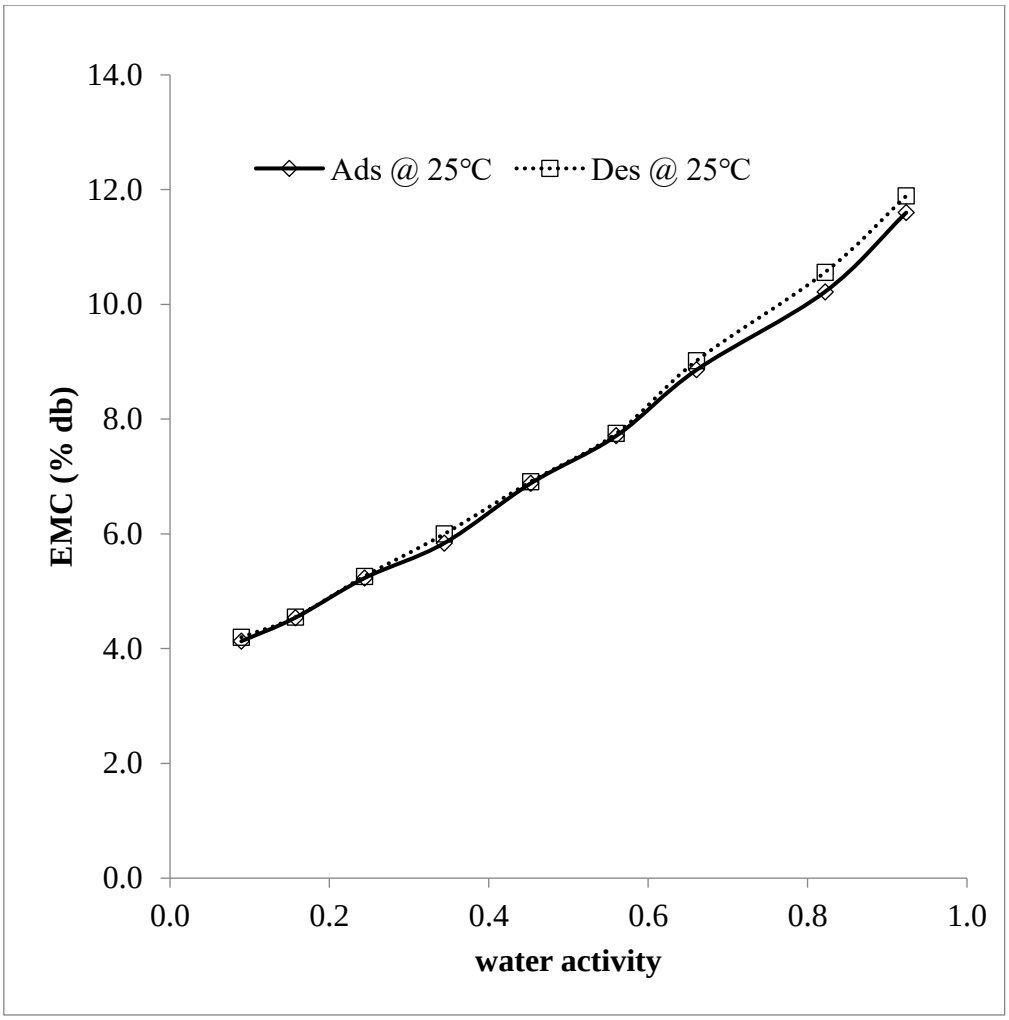

Figure 4.10: Hysteresis loop for moringa seed at 25°C

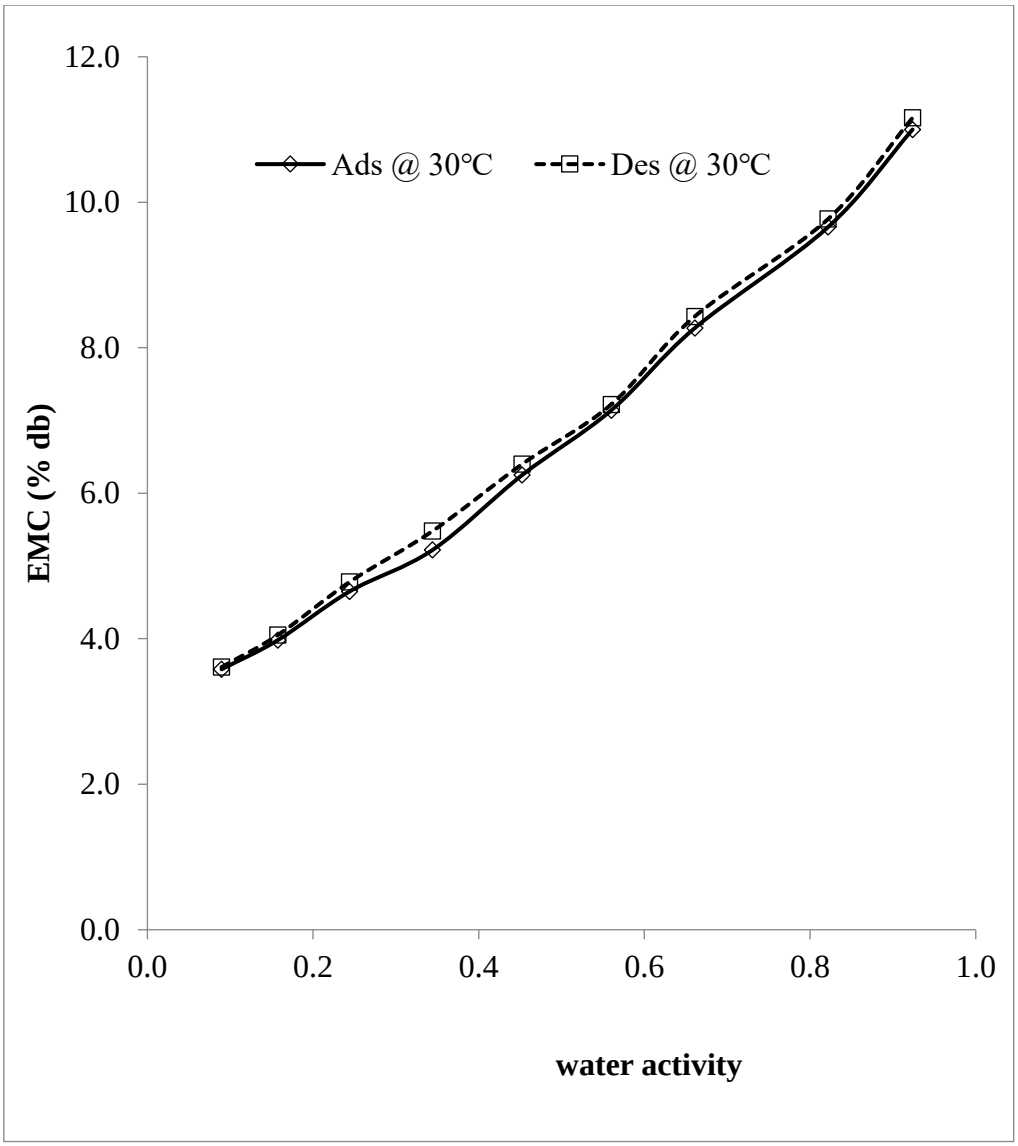

Figure 4.11: Hysteresis loop for moringa seed at 30°C

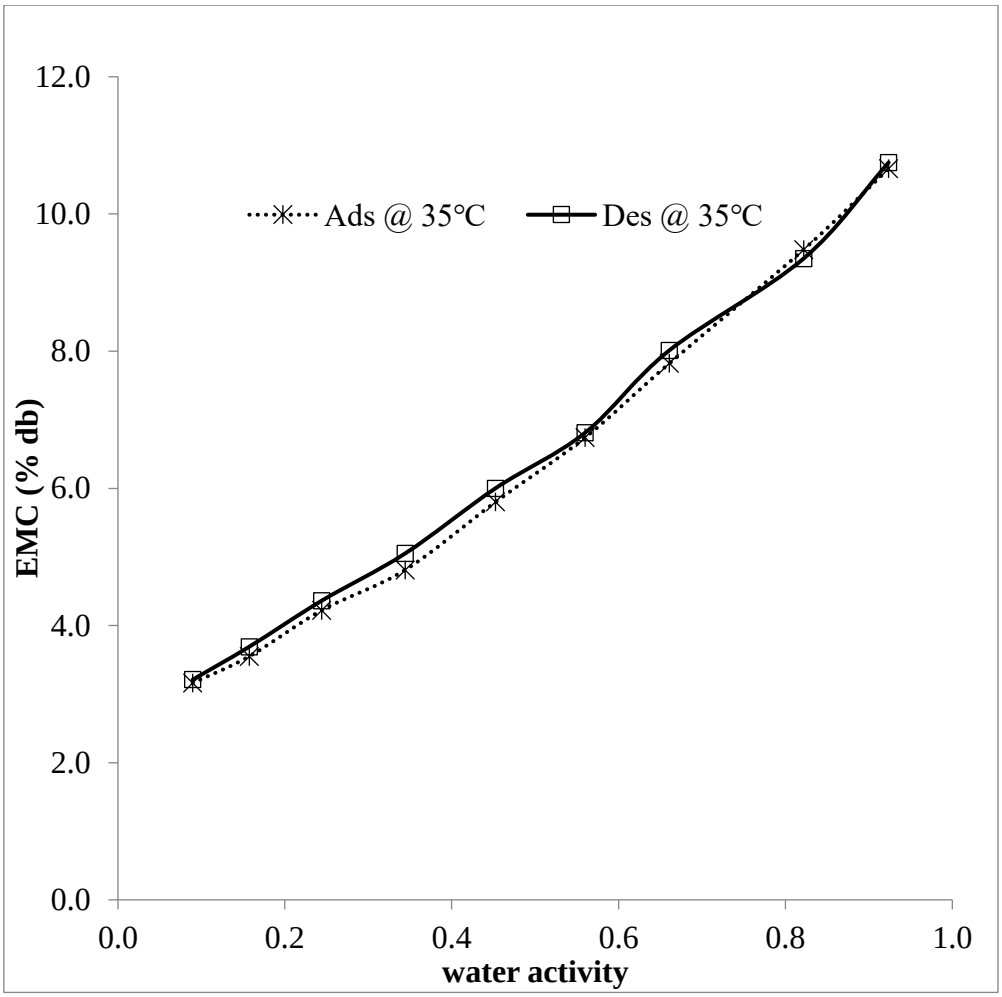

Figure 4.12: Hysteresis loop for moringa seed at 35°C

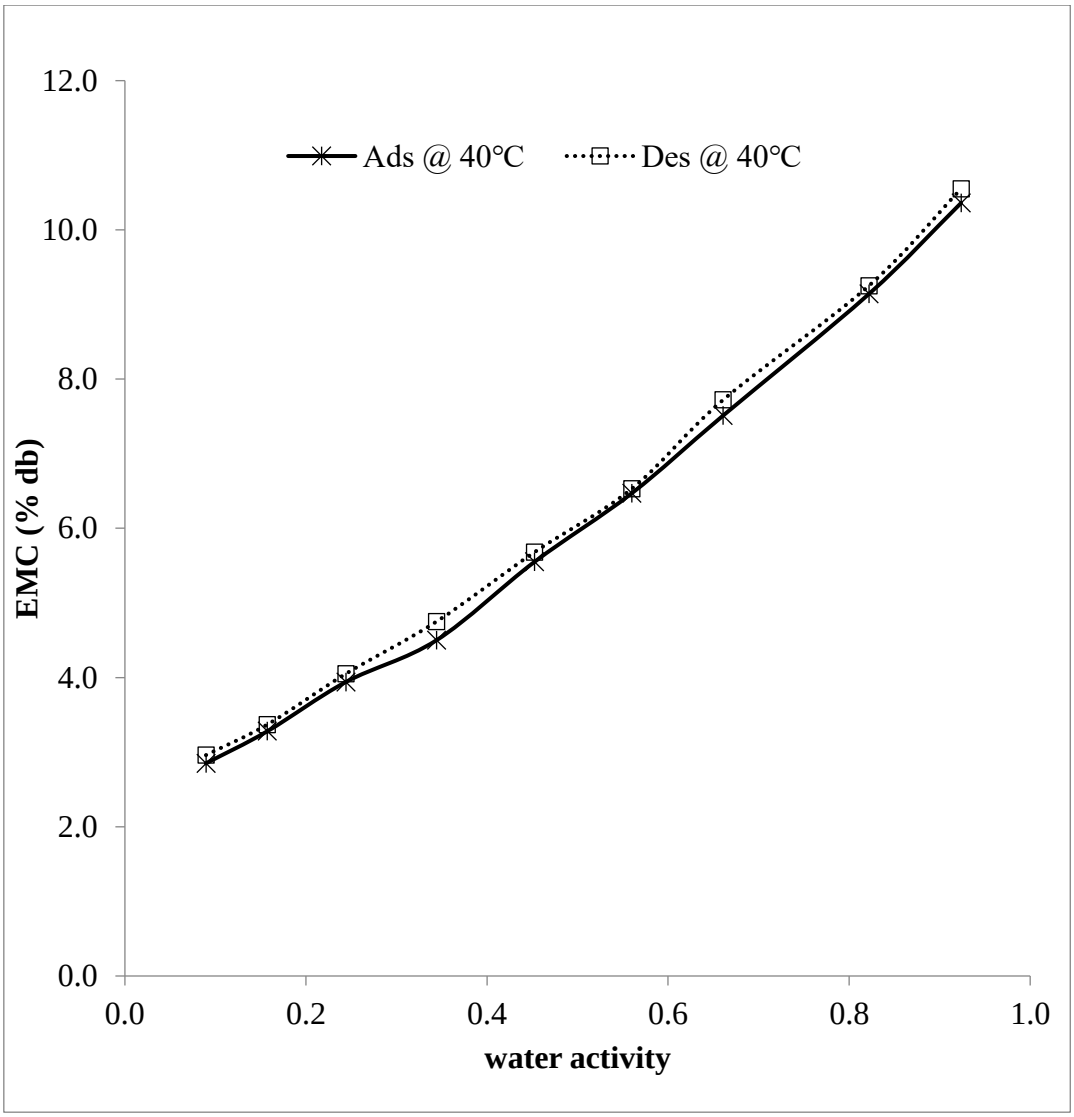

Figure 4.13: Hysteresis loop for moringa seed at 40°C

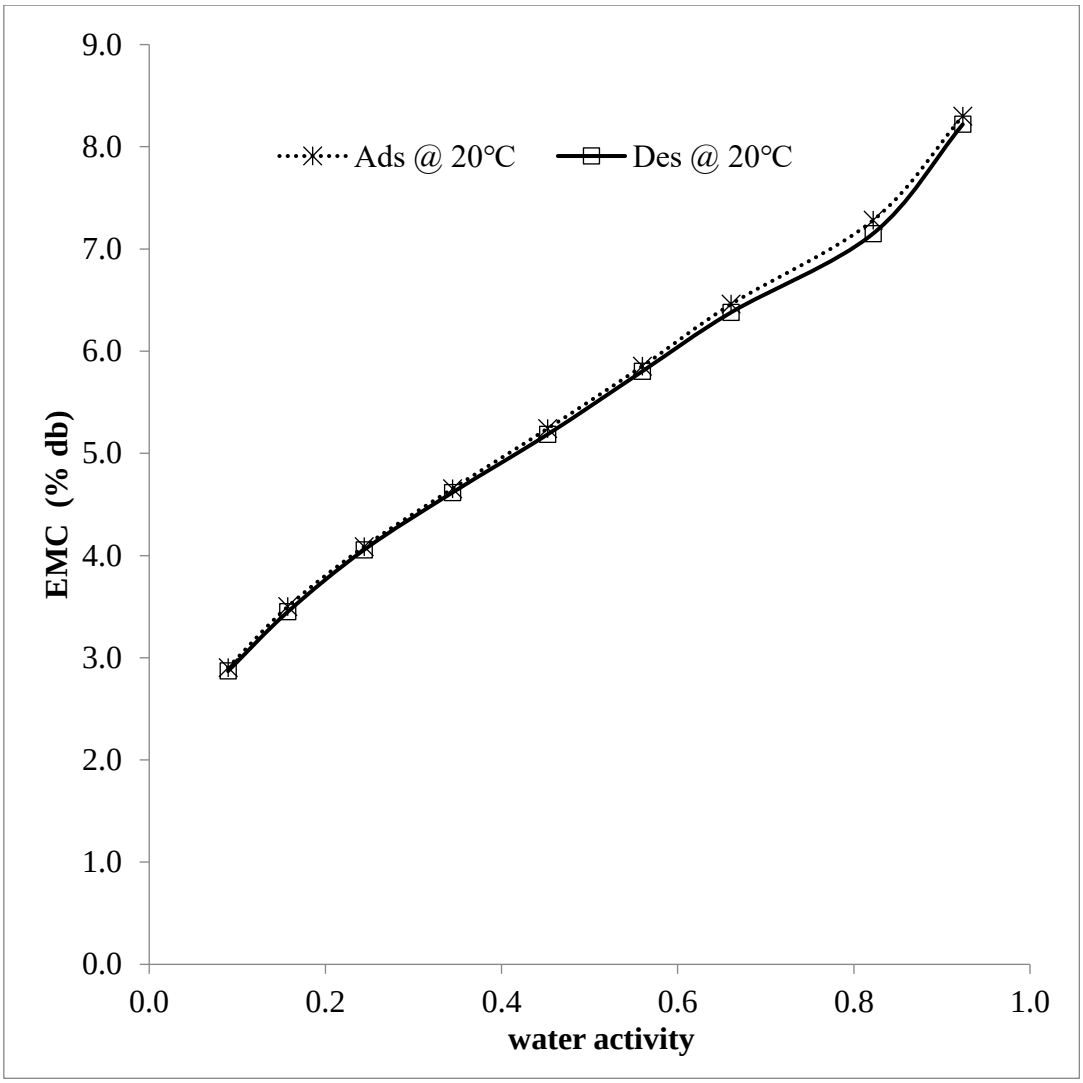

Figure 4.14: Hysteresis loop for moringa grits at 20°C

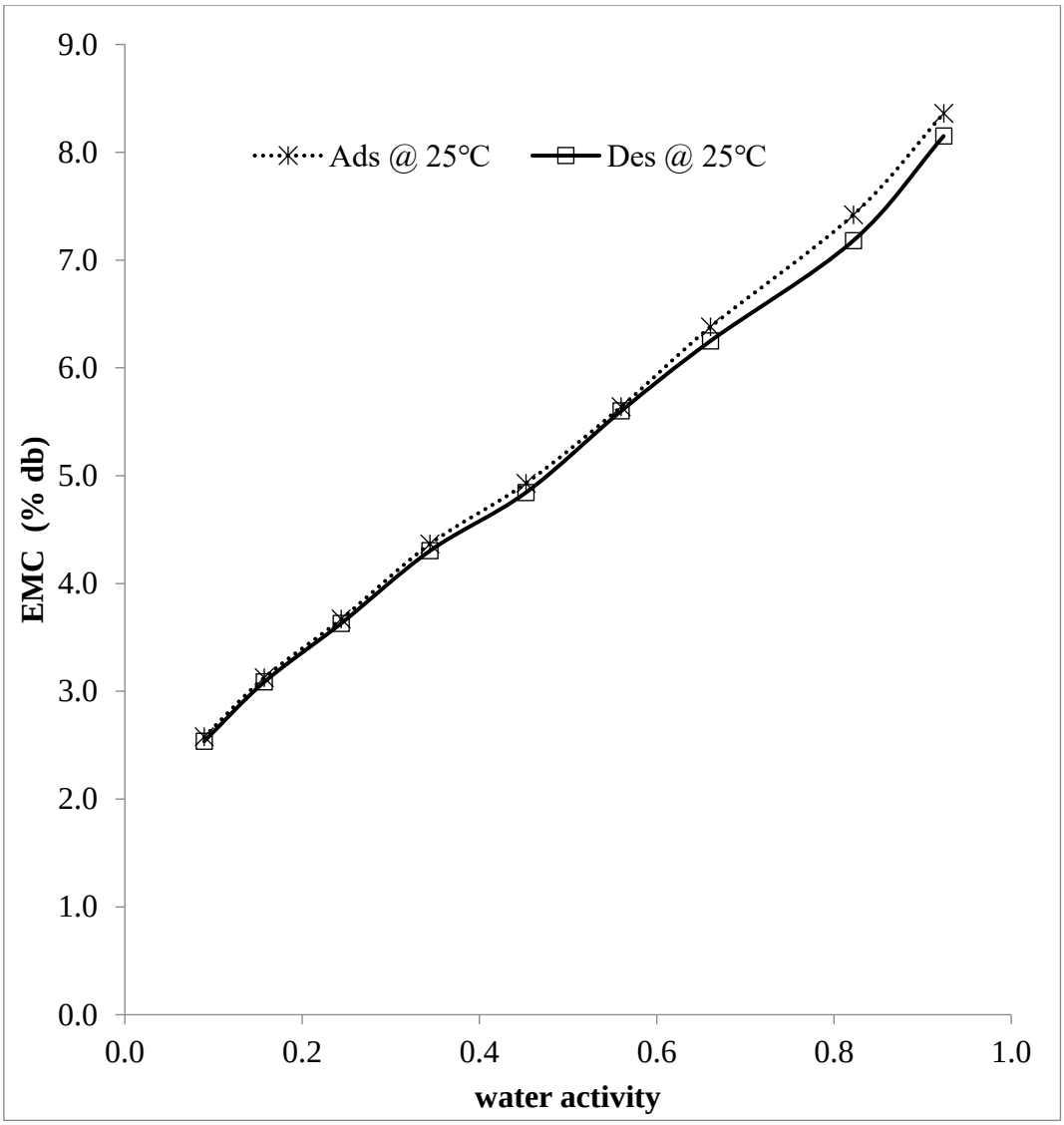

Figure 4.15: Hysteresis loop for moringa grits at 25°C

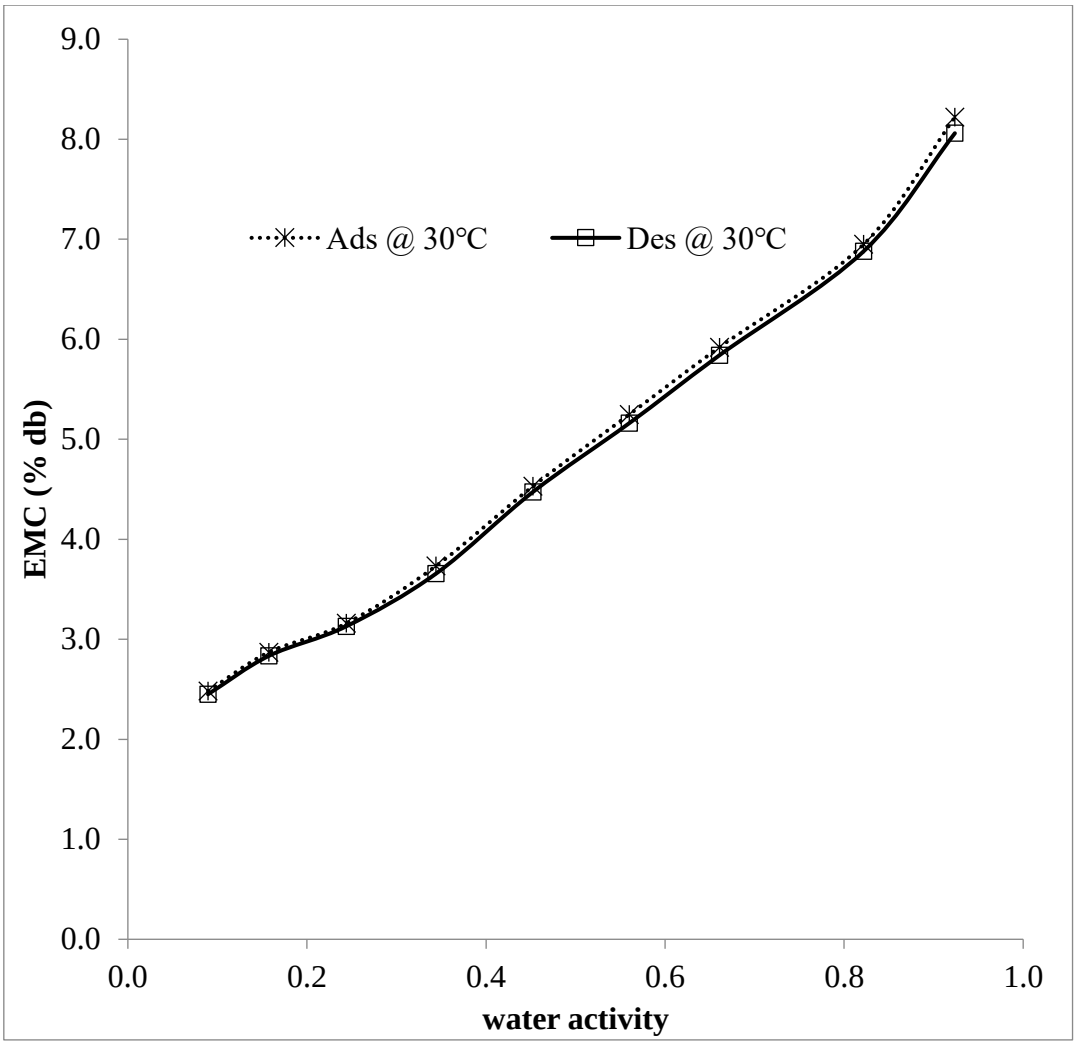

Figure 4.16: Hysteresis loop for moringa grits at 30°C

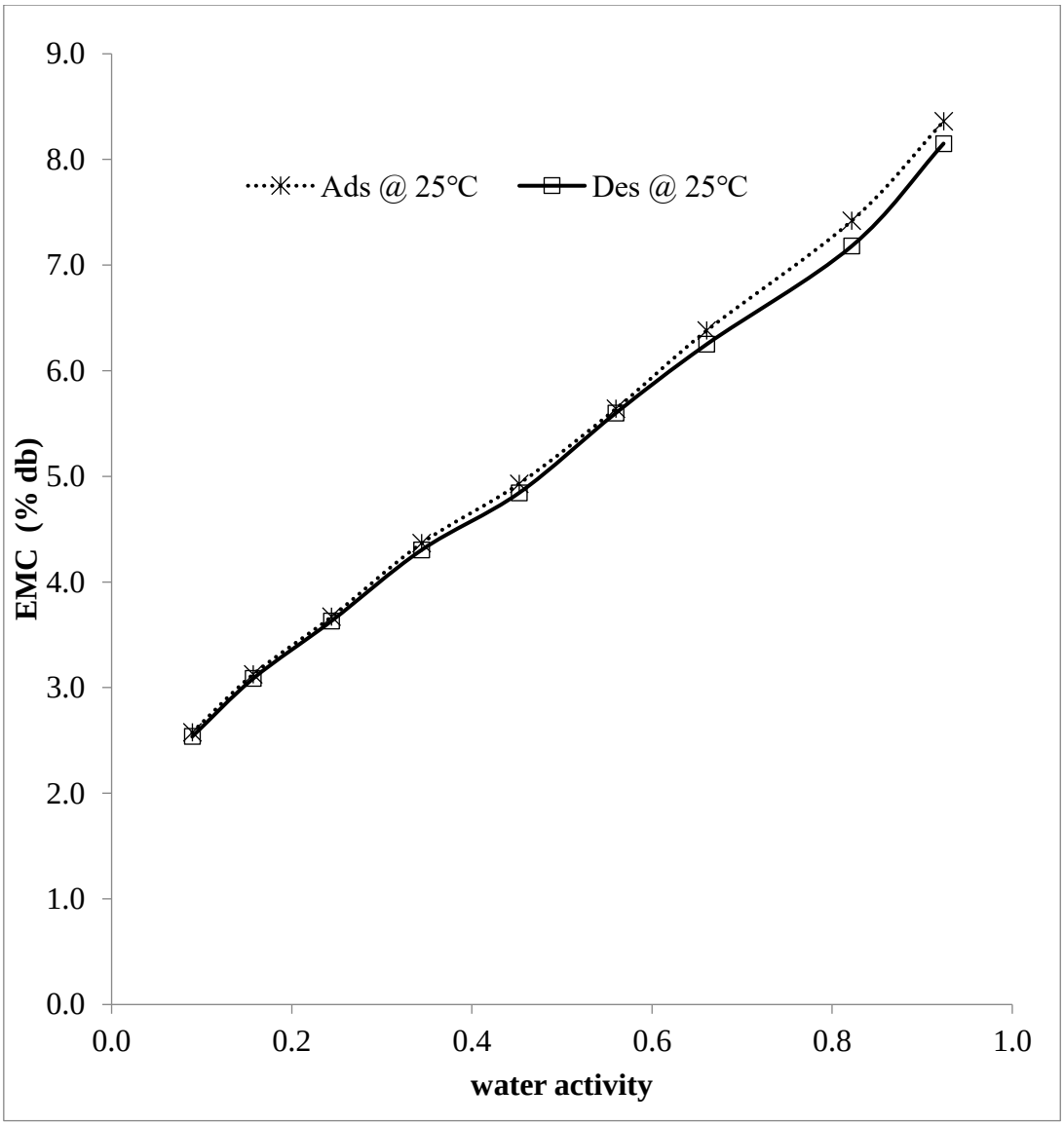

Figure 4.17: Hysteresis loop for moringa grits at 35ºC

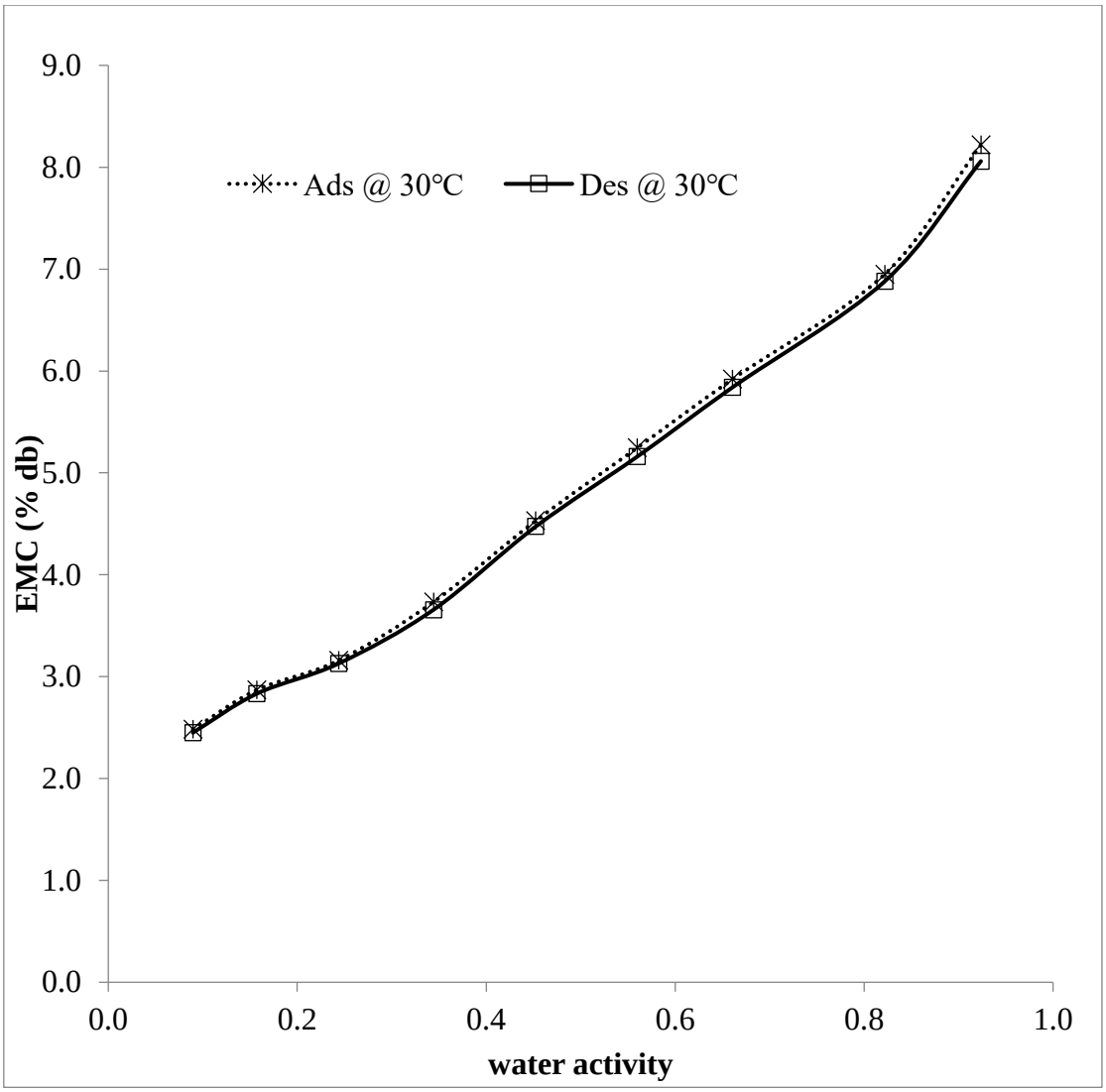

Figure 4.18: Hysteresis loop for moringa grits at 40ºC

4.4 Sorption Parameters of moringa seed and grits

The parameters for the sorption models through which the desorption and adsorption EMCs were taken as dependent variables were estimated for both moringa seed and grits, respectively. The sorption isotherm parameters of the moringa seed stored at various temperatures based on the BET, GAB, Hailwood-Horobin, modified Henderson, modified Hasley and modified Hailwood-Horobin models are shown in Tables 4.6 to 4.17 while the sorption parameters for the six selected models of moringa grits are shown in Tables 4.18 to 4.29. Using the GAB, BET, Hailwood-Horobin and modified Hailwood-Horobin sorption models, quadratic relationships between the water activity and the equilibrium moisture content were established at various storage temperatures, whereas linear relationships were established for the modified Henderson and modified Hasley sorption models. The magnitude of the a_w/M increased as storage temperature increase until it reached 0.6 a_w before it started reducing for the GAB and Hailwood-Horobin models. Also, the BET model showed that the magnitude of the $a_w/(1-a_w)$ M continually increase as storage temperature and a_w increase. It is possible that the variations in the variable interaction that were discovered are a result of how the models were designed for the sorption isotherm description. A similar result to that of moringa seed was reported by Moravec *et al.* (2008) on sorption isotherm for moringa seed at 25^{o}C. Reports by Ajibola and Dairo (1998), Menkov (2000), Aviara and Ajibola (2002), Ade *et al.* (2016), Adeoye *et al.* (2020) corroborate the findings of this study while results similar to those reported in this study for moringa grits were reported by Oyelade *et al.* (2008) and Muhammad *et al.* (2021) corroborate the findings of this research.

The sorption parameters obtained in Tables 4.6 to 4.29 were fitted into each of the six models at various water activities to derive the (EMC) for each model. The relationship between predicted EMC for the sorption models and experimental EMC at each temperature for the seed and grits is shown in Appendix G. The predicted EMC for GAB model was closest to the experimental EMC at all temperature levels for moringa seed while modified Henderson model was closest for moringa grits. However, the predicted EMC for BET model gave the least prediction. This could be as a result of its reported inaccuracy when water activity is greater than 0.45 (Alamri *et al.*, 2018).

4.5 Validation of Sorption Data

The observations of the model validation and calibration are presented in Tables 4.6 to 4.17 for moringa seed and Tables 4.18 to 4.29 for grits. All the six models except BET and Hailwood-Horrobin models could be used to predict the sorption characteristics of moringa seed and grits with coefficient of determination (R^2) values well above 90%. The GAB model was the best-fitted model for the seed and most accurately predicted the EMC at all temperatures with highest R^2 (0.9994) both in adsorption and desorption processes. This was followed closely by modified Henderson model and modified Hailwood-Horrobin model having least root mean square error (RMSE) values. The values of R^2 reduced as temperature increased. This result supports a study by Santalla and Mascheroni (2003) and Sahu *et al.,* (2018) who reported that the GAB model provided the greatest fit to the data gotten experimentally on sorption isotherm of sunflower seeds and kernels and chironji kernels, respectively. Modified Henderson model performed best and most accurately predicted the EMC at all temperatures for the grits with R^2 (0.9999) both in adsorption and desorption processes. This is closely followed by modified Hasley and GAB model with least RMSE values. The BET model did not fit well at all temperatures with highest R^2 value (0.6957) for seed and (0.6869) for grits. Also, Hailwood-Horrobin model did not fit very well but performed better than BET model with R^2 value (0.8439) for seed and (0.8149) for grits. This did not agree with the study of Boquet *et al.* (1979) who stated that the Hailwood-Horrobin model extraordinarily fits the experimental data for the majority of food products as reported by Aviara (2020). Modified Hailwood-Horrobin model fitted well with R^2 (0.9111) for grits at a temperature of 20^{o}C only. This is further supported by the variations in the RSS and MRE values derived from the evaluation of the six models. This indicates that the GAB, modified Henderson and modified Hasley models would be accurate to demonstrate the sorption characteristics of both moringa seed and grits over the entire range of water activity considered. It was also observed that the models better predicted the EMC for moringa seed and grits at lower temperatures. This clearly shows that temperature had an effect on moisture adsorption and desorption. This supports the study by Gichau *et al.,* (2020) and Tavares *et al.,* (2021).

Table 4.6: Brunauer-Emmett-Teller model adsorption parameters for moringa seed

Parameters	20℃	25℃	30℃	35℃	40℃
C	2190952	205151	231.006	97.106	55.365
Mo	4.293	3.787	3.392	3.088	2.892
R^2	0.6957	0.7149	0.7313	0.7480	0.7576
RMSE	0.2033	0.0981	0.0758	0.0720	0.0864
MRE	0.9541	0.2089	0.5542	1.0427	1.6822
RSS	0.0413	0.0096	0.0058	0.0052	0.0075

Table 4.7: Brunauer-Emmett-Teller model desorption parameters for moringa seed

Parameters	20℃	25℃	30℃	35℃	40℃
C	489369	217807	133.579	76.394	56.847
Mo	4.354	3.829	3.521	3.224	2.986
R^2	0.6957	0.7197	0.7272	0.7407	0.7550
RMSE	0.1880	0.1111	0.1018	0.0864	0.0891
MRE	0.8826	0.5542	0.8530	1.3525	1.6868
RSS	0.0354	0.0124	0.0104	0.0075	0.0079

Table 4.8: Guggenheim-Anderson-De Boer model adsorption parameters for moringa seed

Parameters	20℃	25℃	30℃	35℃	40℃
C	55.046	37.525	27.768	19.814	15.059
K	0.582	0.604	0.624	0.646	0.653
Mo	5.818	5.288	4.831	4.509	4.340
R^2	0.9994	0.9993	0.9991	0.9991	0.9991
RMSE	0.2064	0.1974	0.2077	0.2072	0.1946
MRE	0.2031	0.1427	0.1032	0.0107	0.0277
RSS	0.0426	0.0389	0.0431	0.0429	0.0379

Table 4.9: Guggenheim-Anderson-De Boer model desorption parameters for moringa seed

Parameters	20℃	25℃	30℃	35℃	40℃
C	55.648	37.727	26.879	20.445	15.963
K	0.581	0.616	0.614	0.630	0.650
Mo	5.876	5.303	5.004	4.677	4.428
R^2	0.9994	0.9993	0.9994	0.9993	0.9992
RMSE	0.2124	0.2034	0.1817	0.1760	0.1826
MRE	0.1419	0.1998	0.0648	0.0030	0.0550
RSS	0.0451	0.0414	0.0330	0.0310	0.0333

Table 4.10: Hailwood Horrobin model adsorption parameters for moringa seed

Parameters	20℃	25℃	30℃	35℃	40℃
A	0.0066	0.0094	0.0126	0.0167	0.0215
B	0.1607	0.1757	0.1916	0.206	0.2125
C	-0.0943	-0.1091	-0.1256	-0.1439	-0.1536
R^2	08860	08745	0.8620	0.8469	0.8439
RMSE	0.1698	0.1857	0.1307	0.1329	0.1238
MRE	1.23	0.5456	1.2547	0.8895	0.4707
RSS	0.0288	0.0345	0.0171	0.0177	0.0153

Table 4.11: Hailwood Horrobin model desorption parameters for moringa seed

Parameters	20℃	25℃	30℃	35℃	40℃
A	0.0065	0.0091	0.0127	0.0165	0.0204
B	0.1591	0.176	0.1842	0.1958	0.2069
C	-0.0931	-0.1117	-0.1184	-0.132	-0.1476
R^2	0.8865	0.8671	0.8691	0.8606	0.8477
RMSE	0.1165	0.1828	0.1282	0.1092	0.1195
MRE	0.5673	0.9384	1.3071	0.3733	0.4907
RSS	0.0136	0.0334	0.0164	0.0119	0.0143

Table 4.12: Modified Henderson model adsorption parameters for moringa seed

Parameters	20℃	25℃	30℃	35℃	40℃
A	0.0007	0.0011	0.0016	0.0025	0.0032
B	6.4581	6.4312	6.2641	6.1452	6.0845
C	3.2846	2.9296	2.5278	2.3742	2.4769
R^2	0.9990	0.9990	0.9989	0.9979	0.9969
RMSE	0.5271	0.4745	0.4232	0.3736	0.3468
MRE	6.384	6.2033	6.0089	5.2515	4.9668
RSS	0.2778	0.2251	0.1791	0.1396	0.1203

Table 4.13: Modified Henderson model desorption parameters for moringa seed

Parameters	20℃	25℃	30℃	35℃	40℃
A	0.0006	0.0018	0.0024	0.0030	0.0038
B	6.4545	6.4268	6.2875	6.1874	6.1047
C	3.2936	2.7185	2.5334	2.3991	2.4709
R^2	0.9989	0.9989	0.9992	0.9979	0.9976
RMSE	0.5457	0.5144	0.4784	0.3920	0.3701
MRE	6.5429	6.6394	6.6759	5.5180	5.2676
RSS	0.2978	0.2642	0.2289	0.1537	0.1370

Table 4.14: Modified Hasley model adsorption parameters for moringa seed

Parameters	20℃	25℃	30℃	35℃	40℃
A	8.8931	8.9024	8.9048	8.9108	8.9163
B	-0.1419	-0.1406	-0.1395	-0.1361	-0.1322
R^2	0.9885	0.9885	0.9853	0.9814	0.9782
RMSE	0.1279	0.1554	0.1115	0.1093	0.1145
MRE	0.5880	0.4603	0.8486	0.3048	0.6752
RSS	0.0164	0.0241	0.0124	0.0120	0.0131

Table 4.15: Modified Hasley model desorption parameters for moringa seed

Parameters	20℃	25℃	30℃	35℃	40℃
A	8.7545	8.822	8.8662	8.8835	8.889
B	-0.1346	-0.1345	-0.1321	-0.1308	-0.1284
R^2	0.9917	0.9885	0.9851	0.9824	0.9795
RMSE	0.1409	0.1404	0.1055	0.1069	0.1056
MRE	0.4437	0.0201	0.2316	0.4766	0.0712
RSS	0.0198	0.0197	0.0111	0.0143	0.0111

Table 4.16: Modified Hailwood Horrobin model adsorption parameters for moringa seed

Parameters	20℃	25℃	30℃	35℃	40℃
A	0.0003	0.0004	0.0004	0.0005	0.0005
B	0.0008	0.0007	0.0006	0.0006	0.0005
C	-0.0943	-0.1091	-0.1256	-0.1439	-0.1536
R^2	0.8171	0.8342	0.8161	0.8200	0.8117
RMSE	0.1196	0.1259	0.1050	0.1340	0.1002
MRE	0.4062	0.7595	0.8486	0.0137	0.4234
RSS	0.0143	0.0158	0.0110	0.0180	0.0100

Table 4.17: Modified Hailwood Horrobin model desorption parameters for moringa seed

Parameters	20℃	25℃	30℃	35℃	40℃
A	0.0003	0.0004	0.0004	0.0005	0.0005
B	0.0008	0.0007	0.0006	0.0006	0.0005
C	-0.0931	-0.1117	-0.1184	-0.132	-0.1476
R^2	0.8195	0.8261	0.8280	0.8457	0.8219
RMSE	0.1263	0.3292	0.1169	0.0975	0.0589
MRE	0.1195	1.4999	0.5291	0.0625	0.0448
RSS	0.0160	0.1084	0.0137	0.0095	0.0035

Table 4.18: Brunauer-Emmett-Teller model adsorption parameters for moringa grits

Parameters	20℃	25℃	30℃	35℃	40℃
C	99.976	56.336	33.65	32.795	71.824
Mo	3.03	2.823	2.441	2.2	2.064
R^2	0.6870	0.7101	0.7450	0.7704	0.7646
RMSE	0.1637	0.1362	0.0453	0.0521	0.0776
MRE	1.2735	1.7532	0.8867	0.3391	0.5192
RSS	0.0268	0.0185	0.0021	0.0027	0.006

Table 4.19: Brunauer-Emmett-Teller model desorption parameters for moringa grits

Parameters	20℃	25℃	30℃	35℃	40℃
C	95.838	57.991	38.57	32.863	79.335
Mo	3.007	2.776	2.405	2.168	2.011
R^2	06869	0.7062	0.7432	0.7704	0.7705
RMSE	0.1658	0.1409	0.0443	0.0568	0.0738
MRE	1.2075	1.7545	0.8145	1.1066	0.5221
RSS	0.0275	0.0199	0.002	0.0033	0.0054

Table 4.20: Guggenheim-Anderson-De Boer model adsorption parameters for moringa grits

Parameters	20℃	25℃	30℃	35℃	40℃
C	32.384	22.525	25.223	28.406	32.975
K	0.527	0.57	0.643	0.695	0.683
Mo	4.38	4.145	3.432	2.977	2.792
R^2	0.9998	0.9997	0.9990	0.9993	0.9990
RMSE	0.0775	0.0927	0.1589	0.1339	0.1492
MRE	0.0094	0.0257	0.1406	0.1894	0.1307
RSS	0.0060	0.0086	0.0252	0.018	0.0223

Table 4.21: Guggenheim-Anderson-De Boer model desorption parameters for moringa grits

Parameters	20℃	25℃	30℃	35℃	40℃
C	32.244	22.649	25.161	30.136	40.178
K	0.524	0.558	0.641	0.696	0.700
Mo	4.346	4.12	3.393	2.899	2.621
R^2	0.9998	0.9997	0.9990	0.9995	0.9991
RMSE	0.0874	0.095	0.1562	0.1122	0.1308
MRE	0.0222	0.0926	0.1778	0.1229	0.2052
RSS	0.0076	0.0090	0.0244	0.0126	0.0171

Table 4.22: Hailwood Horrobin model adsorption parameters for moringa grits

Parameters	20℃	25℃	30℃	35℃	40℃
A	0.014	0.0191	0.019	0.0173	0.0177
B	0.2113	0.2196	0.2666	0.3163	0.3303
C	-0.1139	-0.1318	-0.18	-0.2315	-0.2329
R^2	0.9111	0.8927	0.8530	0.8149	0.8321
RMSE	0.7081	0.7729	0.6887	0.6685	0.599
MRE	13.71	14.22	12.70	12.06	12.51
RSS	0.5014	0.5973	0.4743	0.4469	0.3588

Table 4.23: Hailwood Horrobin model desorption parameters for moringa grits

Parameters	20℃	25℃	30℃	35℃	40℃
A	0.0142	0.0196	0.0193	0.0168	0.0159
B	0.213	0.22	0.2703	0.325	0.3542
C	-0.114	-0.1289	-0.1823	-0.2373	-0.254
R^2	0.9117	0.8989	0.8538	0.8143	0.8207
RMSE	0.7161	0.7186	0.6286	0.6475	0.497
MRE	14.11	13.75	12.13	12.47	10.48
RSS	0.5128	0.5164	0.3951	0.4192	0.2472

Table 4.24: Modified Henderson model adsorption parameters for moringa grits

Parameters	20℃	25℃	30℃	35℃	40℃
A	0.0009	0.0011	0.0016	0.0025	0.0032
B	6.5728	6.4312	6.2641	6.1452	6.0845
C	3.1231	2.6852	2.5278	2.3742	2.4769
R^2	0.9999	0.9997	0.9989	0.9979	0.9980
RMSE	0.2612	0.2280	0.2294	0.2502	0.2574
MRE	4.6490	4.1550	4.4311	5.0146	5.5451
RSS	0.0682	0.0519	0.0526	0.0626	0.0663

Table 4.25: Modified Henderson model desorption parameters for moringa grits

Parameters	20℃	25℃	30℃	35℃	40℃
A	0.001	0.0018	0.0024	0.003	0.0038
B	6.5365	6.4268	6.2875	6.1874	6.1047
C	3.1272	2.7185	2.5334	2.3991	2.4709
R^2	0.9999	0.9997	0.9989	0.9979	0.9976
RMSE	0.2650	0.8062	0.2644	0.2599	0.2584
MRE	4.7723	5.0997	5.1969	5.3296	5.7156
RSS	0.0702	0.6499	0.0699	0.0675	0.0667

Table 4.26: Modified Hasley model adsorption parameters for moringa grits

Parameters	20℃	25℃	30℃	35℃	40℃
A	5.605	5.218	4.954	4.741	4.526
B	-0.675	-0.646	-0.619	-0.587	-0.555
C	3.0508	2.6525	2.5804	2.5019	2.6536
R^2	0.9854	0.9795	0.9851	0.9883	0.9913
RMSE	0.6542	0.7042	0.6161	0.6077	0.4602
MRE	12.92	13.07	11.32	10.68	10.36
RSS	0.4279	0.4959	0.3796	0.693	0.3118

Table 4.27: Modified Hasley model desorption parameters for moringa grits

Parameters	20℃	25℃	30℃	35℃	40℃
A	5.6139	5.243	5.015	4.866	4.695
B	-0.687	-0.668	-0.635	-0.602	0.584
C	3.0528	2.6787	2.5852	2.5312	2.6653
R^2	0.9854	0.9792	0.9847	0.9894	0.9930
RMSE	0.6909	0.706	0.5711	0.5819	0.3887
MRE	13.53	13.22	10.77	11.03	9.93
RSS	0.4774	0.4984	0.3261	0.3386	0.2511

Table 4.28: Modified Hailwood Horrobin model adsorption parameters for moringa grits

Parameters	20℃	25℃	30℃	35℃	40℃
A	0.0261	0.0244	0.0245	0.0281	0.0295
B	0.2813	0.2223	0.2814	0.3924	0.4014
C	-0.1553	-0.1843	-0.203	-0.2513	-0.2661
R^2	0.9111	0.8834	0.8501	0.7509	0.7577
RMSE	0.6647	0.7352	0.6402	0.6495	0.4470
MRE	12.98	13.43	11.68	11.13	10.47
RSS	0.4418	0.5404	0.4099	0.4219	0.2998

Table 4.29: Modified Hailwood Horrobin model desorption parameters for moringa grits

Parameters	20℃	25℃	30℃	35℃	40℃
A	0.0264	0.0249	0.025	0.0288	0.0305
B	0.282	0.2229	0.2868	0.3988	0.4112
C	-0.1557	-0.1851	-0.2082	-0.2551	-0.2674
R^2	0.9110	0.8896	0.8087	0.7542	0.7424
RMSE	0.7073	0.7292	0.6191	0.6199	0.4352
MRE	13.82	13.63	11.74	11.69	10.13
RSS	0.5002	0.5317	0.3833	0.3843	0.2894

4.6 Monolayer Moisture Content

The monolayer moisture contents (M_o) were calculated using BET, GAB and Caurie models at different temperature levels for moringa seed and grits are presented in Tables 4.30 and 4.31, respectively. There was significant decrease in monolayer moisture content of both moringa seed and grits as temperature increased in both sorption processes. It has been stated that the decrease in the monolayer moisture content with increase in temperature is due to the reduction in the number of active sites brought on by the chemical and physical changes brought about by temperature (McMinn and Magee, 2003). For moringa seed, similar reports were given by Siripatrawan and Jantawat (2006), Oluwamukomi (2009), Eim *et al.* (2011) Fadeyibi *et al.* (2012), Maleki-Majd *et al.* (2014). For moringa grits, Oyelade *et al.* (2008), Moreira (2001), Koc *et al.* (2010), Rodriguez-Bernal *et al.* (2015), Mohammad *et al.* (2021) and Akintola *et al.*, (2022) gave similar reports. GAB and Caurie monolayer values were very close and more than the BET values. Timmermann *et al.*, (2001) also reported a similar finding. This could be because the BET model is better able to predict the monolayer moisture content of dry materials because it is more closely related to moisture sorption at the immediate layer, while GAB and Caurie models are with moisture sorption at the multilayer region, making them more suitable for predicting the monolayer moisture content of low to high moisture foods (Maleki-Majd *et al.*, 2014).

Variations in monolayer moisture content of moringa seed and grits with temperatures during sorption isotherms are reported in Figures 4.19 to 4.22. It was noticed that adsorption monolayer moisture values were more than the corresponding desorption values at the same temperatures and relative humidities. The ANOVA results showing the effects of hysteresis on the monolayer moisture content during adsorption and desorption for BET, GAB and Caurie models in seed and grits are shown in Appendix H. One way ANOVA showed that there were no remarkable differences between adsorption and desorption M_o at $p \leq 0.05$ for both seed and grits. This means that hysteresis had not occurred before monolayer moisture content was attained. The (M_o) predicted using the three selected models varied linearly with temperature for both sorption processes. Suitable regression models that could be reliably used to predict the M_o of moringa seed and grits at various temperature levels are as shown in Tables 4.32 and 4.33, respectively.

Table 4.30: Monolayer moisture content of moringa seed

	Adsorption			Desorption		
	BET	GAB	Caurie	BET	GAB	Caurie
T (^oC)	M_o	M_o	M_o	M_o	M_o	M_o
20	4.293	5.818	5.622	4.354	5.876	5.684
25	3.787	5.288	5.086	3.829	5.303	5.105
30	3.392	4.831	4.655	3.521	5.004	4.851
35	3.088	4.509	4.336	3.224	4.677	4.448
40	2.892	4.35	4.154	2.986	4.428	4.125

Table 4.31: Monolayer moisture content of moringa seed grits

	Adsorption			Desorption		
	BET	GAB	Caurie	BET	GAB	Caurie
T (^oC)	M_o	M_o	M_o	M_o	M_o	M_o
20	3.030	4.380	4.240	3.007	4.346	4.215
25	2.823	4.145	4.086	2.776	4.120	4.054
30	2.441	3.432	3.606	2.405	3.393	3.424
35	2.200	2.977	2.851	2.168	2.899	2.833
40	2.064	2.792	2.630	2.011	2.621	2.545

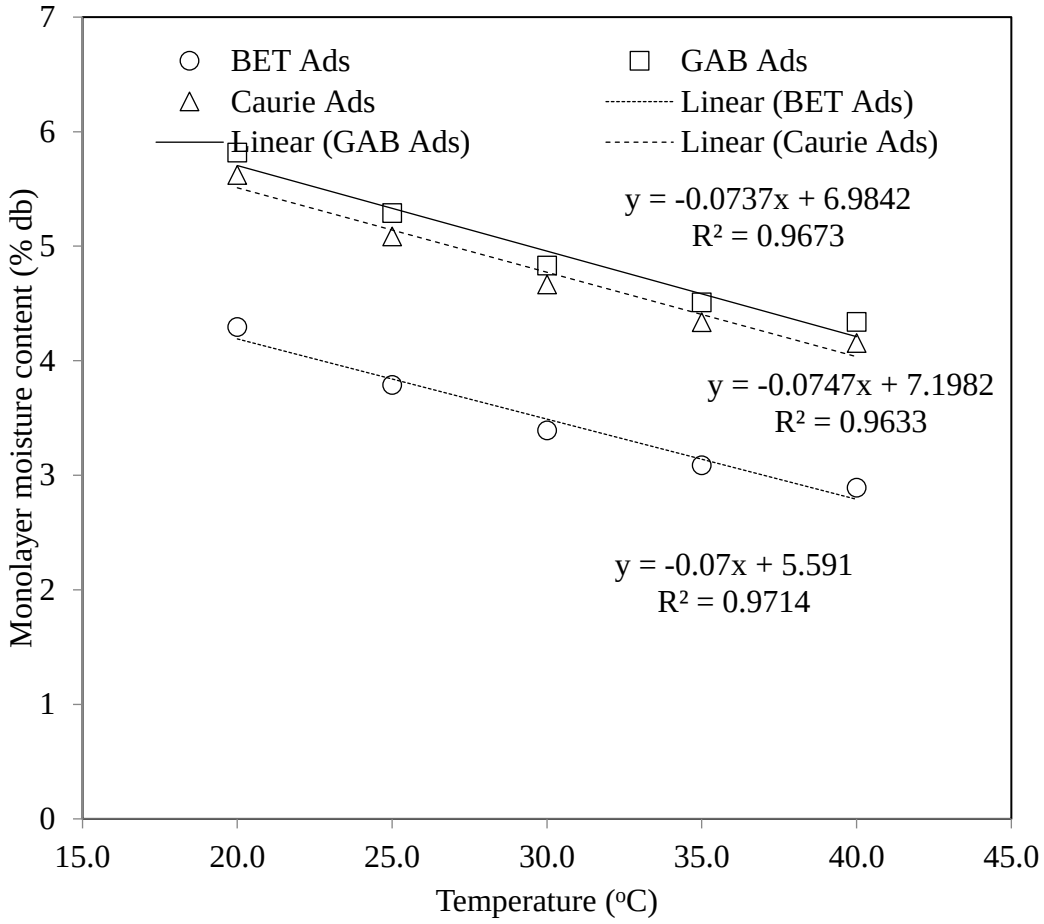

Figure 4.19: Adsorption monolayer moisture content of moringa seed

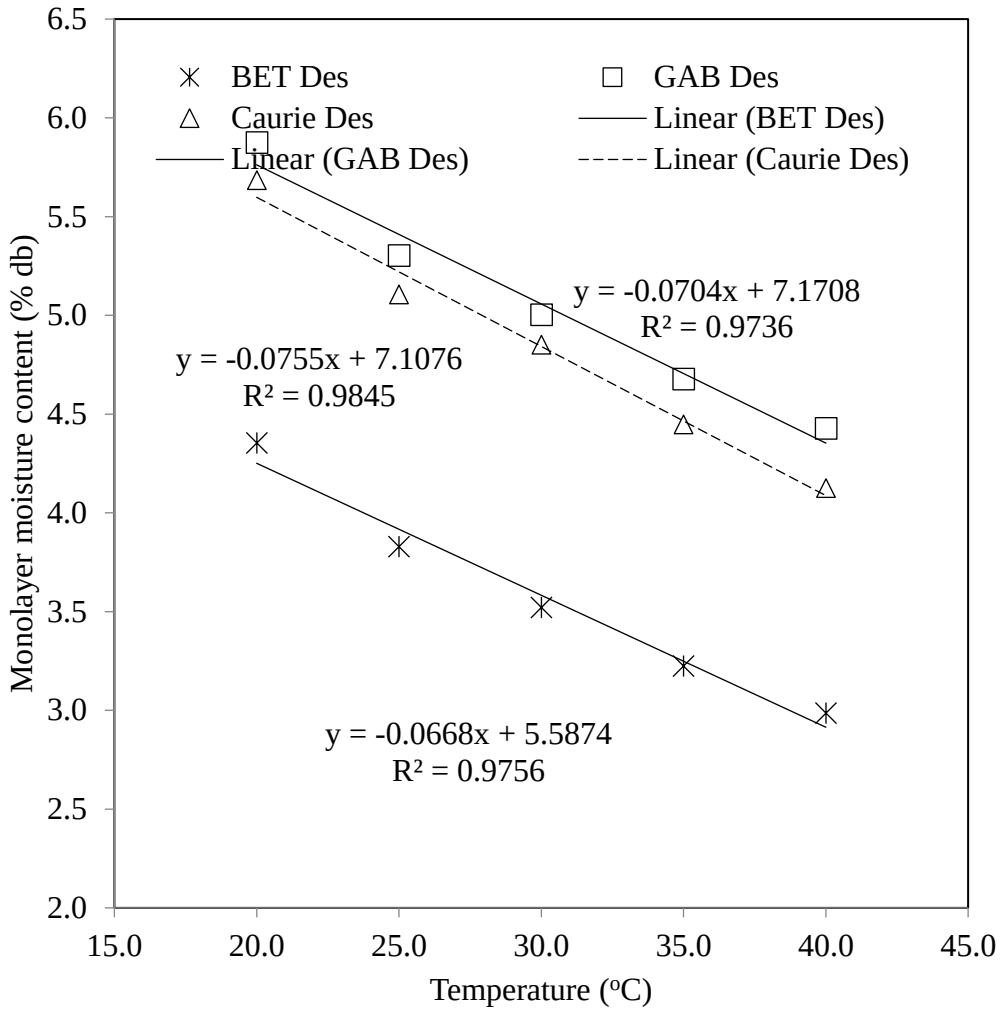

Figure 4.20: Desorption monolayer moisture content of moringa seed

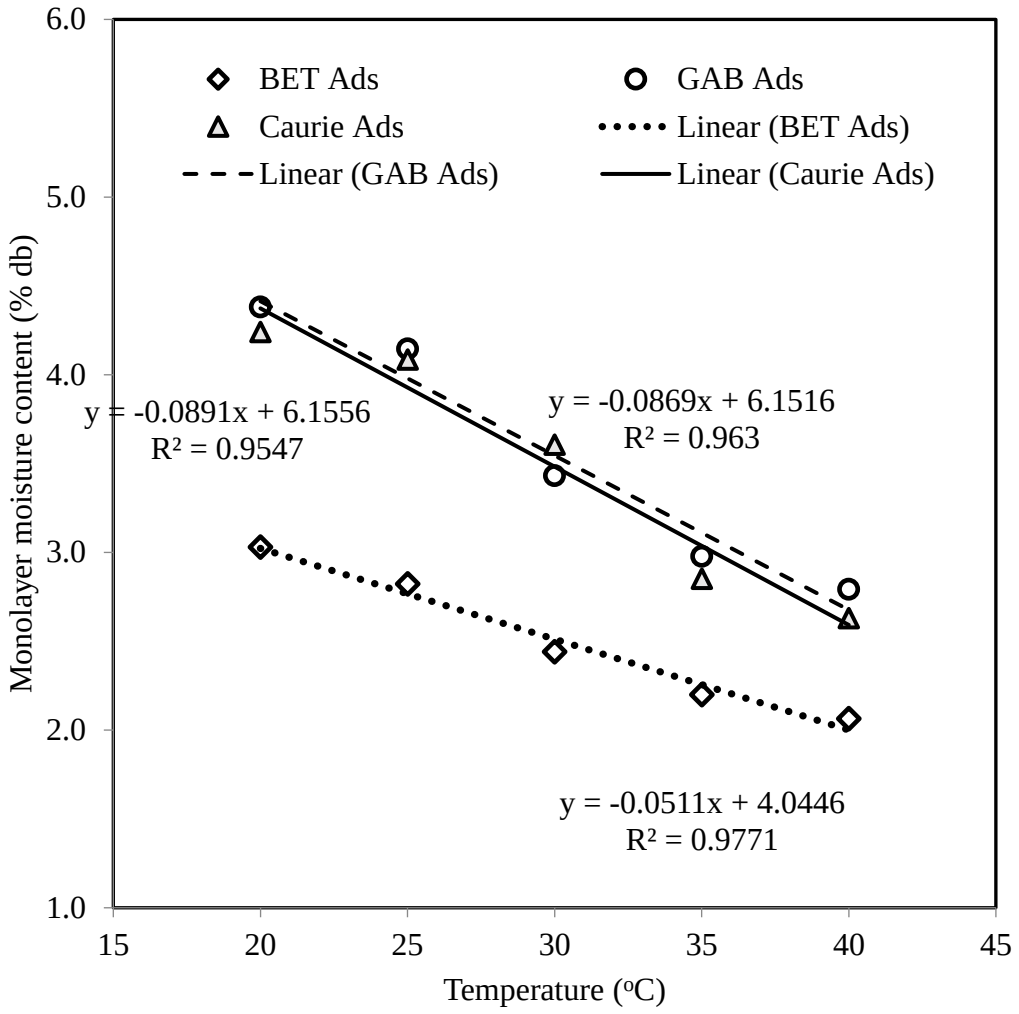

Figure 4.21: Adsorption monolayer moisture content of moringa seed grits.

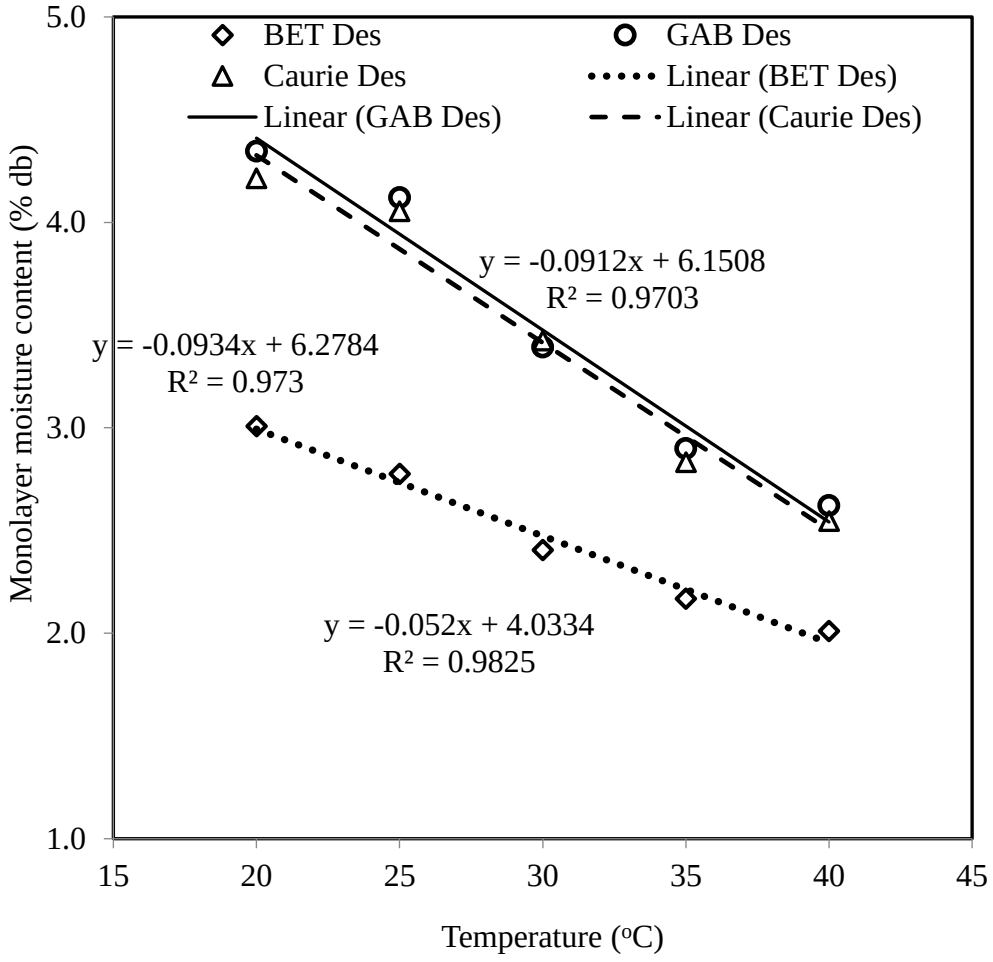

Figure 4.22: **Desorption monolayer moisture content of moringa seed grits**

Table 4.32: Relationship between M_o and temperature for moringa seed.

Models	Adsorption	Desorption
BET	Mo= -0.07T + 5.591 R^2 = 0.9714	Mo = -0.0668T + 5.5874 R^2 = 0.9756
GAB	Mo = -0.0747T + 7.1982 R^2 = 0.9633	Mo= -0.0704T + 7.1708 R^2 = 0.9736
Caurie	Mo = -0.0737T + 6.9842 R^2 = 0.9673	Mo = -0.0668T + 5.5874 R^2 = 0.9756

Table 4.33: Relationship between M_o and temperature of moringa grits

Models	Adsorption	Desorption
BET	M_o= -0.0511T + 4.0446 R^2 = 0.9771	M_o = -0.052T + 4.0334 R^2 = 0.9825
GAB	M_o = -0.0869T + 6.1516 R^2 = 0.963	M_o = -0.0934T + 6.2784 R^2 = 0.973
Caurie	M_o = -0.0891T + 6.1556 R^2 = 0.9547	M_o = -0.0912T + 6.1508 R^2 = 0.9703

4.7 Water Vapour Transmission Rate and Permeability Coefficient

The water vapour transmission rate (WVTR) and permeability coefficient of the two packaging materials [low density polyethylene (LDPE) and Polypropylene (Pp)] is presented in Table 4.34. The mean weight gain by the two packaging materials and the control throughout the 12 days of weighing at average relative humidity and storage temperature of 80% and 29^{o}C, respectively is presented in Figure 4.23. The study reveals that LDPE had a larger weight increase from 0.06 to 0.3g within 12 days of storage because of fewer barrier qualities. This agrees with Kenawi *et al.* (2015) and Ojo *et al.,* (2021) who explained that LDPE materials have higher WVTR than other packaging materials. On the other hand, the weight of Pp increased from 0.04g to 0.18g gaining less amount of weight. The thickness of the polypropylene material is responsible for its low water vapour transmission rate. Consequently, from the permeability coefficient, LDPE is more permeable with a value of 0.4271g mm/m^2 day mmHg when used for packaging; this was expected since it has no protection layer and it is also a very thin material.

4.8 Shelf-Life Determination

The shelf life of moringa seed and grits was predicted using the values of initial moisture content (M_i), determined critical moisture content (M_c), water vapour transmission rate (WVTR) and permeability coefficient (P) of each packaging material estimated in Table 4.34, the shelf life of moringa seed when stored in the two packaging materials are presented in Tables 4.35 and 4.36 while the shelf life of the grits is presented in Tables 4.37 and 4.38. Low Density Polyethylene (LDPE) had the shorter shelf life (994 and 748 days) for the seed and grits between the two packaging materials because of its high WVTR and permeability; it has a greater capacity to allow the passage of moisture through it. On the other hand, because Polypropylene (Pp) material contain more barriers to prevent moisture absorption and because of its smaller surface area, it had the longer shelf life (1,852 and 1,446 days) for both seed and grits, respectively. This agrees with previous studies carried out by Pua *et al.,* (2008), Koc *et al.,* (2010) and Karthik *et al.,* (2013). The grits had a shorter shelf life than the seed because the grits has been broken down into smaller particles and the intermolecular forces have been reduced thereby causing more interaction with the micro environment (Ogunsina *et al.,* 2010).

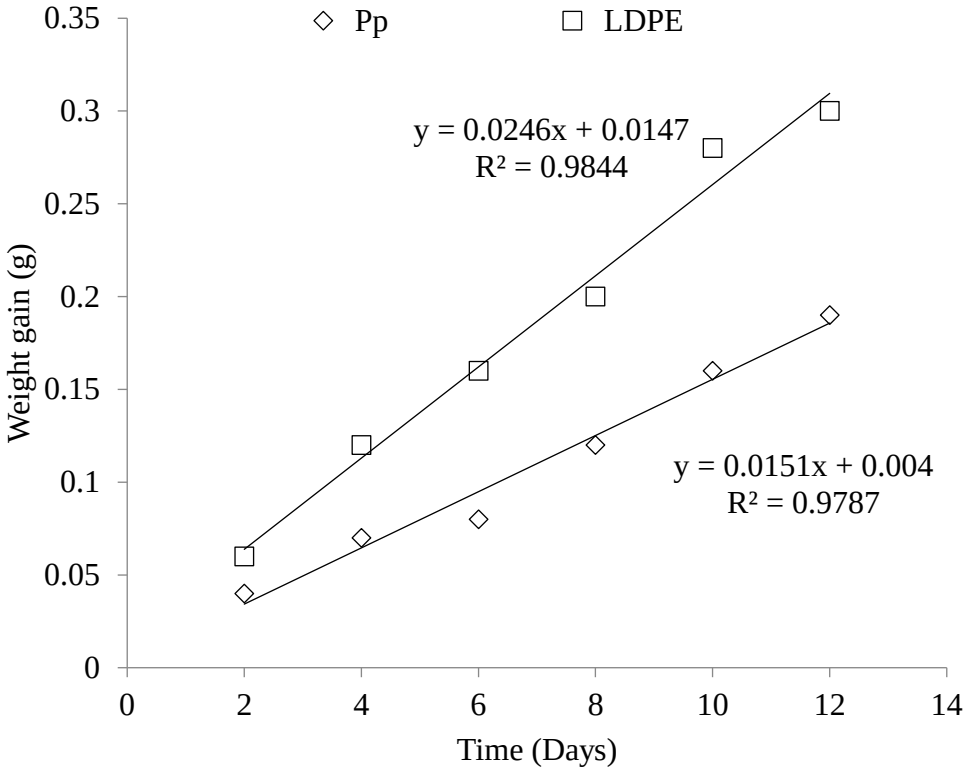

Figure 4.23: Weight gain in different packaging materials.

Table 4.34: WVTR and Permeability Coefficient of the Packaging Materials

	Polypropylene (Pp)	Low Density Polyethylene (LDPE)
Q/t (g H_2O/day)	0.0151	0.0246
Surface Area (m^2)	0.00986	0.0024
WVTR (g H_2O/day m^2)	1.53	10.25
Δp (29^oC at 80%) mmHg	24	24
P (g mm/m^2 day mmHg)	0.1275	0.4271

Table 4.35: Predicted shelf life of moringa seed stored in Polypropylene material

a_w	Mi (%db)	Me (%db)	Mc (%db)	P (gH_2O m^2/day/mmHg)	A (m^2)	Po (mm Hg)	X (mm)	m (g)	b	t (days)
0.5	12.20	6.88	10.91	0.1275	0.00986	24	0.2	30	8.89	489
0.6	12.20	7.71	10.91	0.1275	0.00986	24	0.2	30	8.89	596
0.7	12.20	8.86	10.91	0.1275	0.00986	24	0.2	30	8.89	859
0.8	12.20	10.22	10.91	0.1275	0.00986	24	0.2	30	8.89	1852

Table 4.26: Predicted shelf life of moringa seed stored in low density polyethylene material

a_w	Mi (%db)	Me (%db)	Mc (%db)	P (gH_2O m^2/day/mmHg)	A (m^2)	Po (mm Hg)	X (mm)	m (g)	b	t (days)
0.5	12.20	6.88	11.01	0.4271	0.0024	24	0.1	30	8.89	274
0.6	12.20	7.71	11.01	0.4271	0.0024	24	0.1	30	8.89	333
0.7	12.20	8.86	11.01	0.4271	0.0024	24	0.1	30	8.89	477
0.8	12.20	10.22	11.01	0.4271	0.0024	24	0.1	30	8.89	994

Table 4.37: Predicted shelf life of moringa grits stored in Polypropylene material

a_w	Mi (%db)	Me (%db)	Mc (%db)	P (gH_2O m^2/day/mmHg)	A (m^2)	Po (mm Hg)	X (mm)	m (g)	b	t (days)
0.5	10.25	4.93	8.38	0.1275	0.00986	24	0.2	30	6.74	580
0.6	10.25	5.64	8.38	0.1275	0.00986	24	0.2	30	6.74	696
0.7	10.25	6.38	8.38	0.1275	0.00986	24	0.2	30	6.74	883
0.8	10.25	7.42	8.38	0.1275	0.00986	24	0.2	30	6.74	1446

Table 4.38: Predicted shelf life of moringa grits stored in low density polyethylene material

a_w	Mi (%db)	Me (%db)	Mc (%db)	P (gH_2O m^2/day/mmHg)	A (m^2)	Po (mm Hg)	X (mm)	m (g)	b	t (days)
0.5	10.25	4.93	8.559	0.4271	0.0024	24	0.1	30	6.74	314
0.6	10.25	5.64	8.559	0.4271	0.0024	24	0.1	30	6.74	376
0.7	10.25	6.38	8.559	0.4271	0.0024	24	0.1	30	6.74	472
0.8	10.25	7.42	8.559	0.4271	0.0024	24	0.1	30	6.74	748

4.9 Isosteric Heat and Entropy of Sorption.

The heat required for both adsorption and desorption processes were determined at specific moisture content of both moringa seed and grits using the Clausius–Clapeyron equation. The values of net isosteric heat (ΔH) were estimated from the slope of the plots between natural log of water activity (ln a_w) and inverse of temperature (1/T) for seed and grits for equilibrium moisture contents varying between 3% and 7% db. As can be observed in Tables 4.39 and 4.40, the net isosteric heat decreased from 38.71 and 41.66 KJ/mol for 3% EMC to 4.75 and 4.82 KJ/mol for 7% EMC in adsorption and desorption processes, respectively for the grits and 40.8 and 45.09 KJ/mol for 3% EMC to 9.9 and 10.85 KJ/mol for 7% EMC in adsorption and desorption processes, respectively for the seed. This shows that more energy is required to remove a mole of moisture from the seed than the grits due to its smaller particle sizes. This finding suggests that the substrate and water molecules have a higher binding energy than the water molecules do when they are in a liquid state. Choudhury *et al.* (2011) reported the exact same findings. Also, it requires more energy to remove moisture in desorption process than in adsorption process. The entropy of sorption also decreased from 0.113 and 0.124 KJ/mol K for 3% EMC to 0.014 and 0.015 KJ/mol for 7% EMC in adsorption and desorption processes, respectively for the grits and 0.124 and 0.137 KJ/mol K for 3% EMC to 0.03 and 0.033 KJ/mol K for 7% EMC in adsorption and desorption processes, respectively for the seed. The isosteric heat of sorption is high when there is little moisture present; as water content rises, it becomes less intense. At low water levels, the isosteric heat of desorption may increase because water is strongly bonded to the substrate, which corresponds to a high interaction energy. The active sites are occupied as the water content rises, and sorption occurs on the less active sites as a result, producing a low heat of sorption. This agrees with previous studies by Lamharrar *et al.,* (2007) and Bahloul et al., (2008). This phenomenon can explain the difference between the water content of the adsorption and desorption isotherms for a given water activity in addition to the difference between the heat of adsorption and desorption (Al-Muhtaseb *et al.,* 2002).

The regression models to predict the net isosteric heat of sorption (q_{st}) and entropy of sorption (ΔS) of moringa seed and grits at a given equilibrium moisture content are presented in Tables 4.41 and 4.42, respectively.

Table 4.39: Isosteric heat and entropy of sorption of moringa seed

EMC (% db)	Isosteric heat of sorption (KJ/mol)		Entropy of sorption (KJ/mol K)	
	Adsorption	Desorption	Adsorption	Desorption
3.00	40.86	45.09	0.124	0.137
4.00	24.75	25.1	0.074	0.075
5.00	16.41	17.23	0.049	0.051
6.00	10.85	10.97	0.032	0.032
7.00	9.9	10.85	0.03	0.033

Table 4.40: Isosteric heat and entropy of sorption of moringa seed grits

EMC (% db)	Isosteric heat of sorption (KJ/mol)		Entropy of sorption (KJ/mol K)	
	Adsorption	Desorption	Adsorption	Desorption
3.00	38.71	41.66	0.113	0.124
4.00	29.44	32.07	0.088	0.094
5.00	15.95	17.74	0.047	0.053
6.00	12.60	12.84	0.038	0.039
7.00	4.75	4.82	0.014	0.015

Table 4.41: Predictive regression models for net isosteric heat of sorption and entropy of sorption of moringa seed

	Net isosteric heat of sorption (KJ/mol)	Entropy of sorption (KJ/mol K)
Adsorption	q_{st} = -0.2633M^3 + 6.3143M^2 - 50.08M + 141.28 R² = 0.999	ΔS = -0.0008M^3 + 0.0199M^2 - 0.157M + 0.4377 R² = 0.9986
Desorption	q_{st} = -0.4983M^3 + 13.419M^2 - 121.17M + 377.56 R² = 0.996	ΔS = -0.0015M^3 + 0.0409M^2 - 0.3715M + 1.1599 R² = 0.9957

Table 4.42: Predictive regression models for net isosteric heat of sorption and entropy of sorption of moringa seed grits

	Net isosteric heat of sorption (q_{st}) (KJ/mol)	Entropy of sorption (ΔS) (KJ/mol K)
Adsorption	q_{st} = -0.0233M^3 + 1.2771M^2 - 19.418M + 86.514 R² = 0.9838	ΔS = 8E-05M^3 + 0.0012M^2 - 0.0431M + 0.2309 R² = 0.9797
Desorption	q_{st} = 0.135M^3 - 1.1271M^2 - 8.6036M + 74.352 R² = 0.9885	ΔS = 8E-05M^3 + 0.0015M^2 - 0.0492M + 0.2566 R² = 0.9895

CHAPTER FIVE
SUMMARY, CONCLUSIONS AND RECOMMENDATIONS

5.1 Summary

Moringa seed and grits demonstrated a capability of holding a small amount of water at low to moderate water activity. Equilibrium moisture contents of both products were dependent on both temperature and relative humidity of the environment. The experimental isotherm for both seed and grits demonstrated Type-II behaviour. GAB model was the best-fitted model for seed while Modified Henderson model was the best-fitted model for grits. Monolayer moisture content decreased with increase in temperature in both adsorption and desorption while hysteresis did not have significant effect on the monolayer moisture content of both moringa seed and grits. Net isosteric heat and entropy of sorption increased exponentially as equilibrium moisture content decreased.

5.2 Conclusions

The following conclusions were drawn from the result of the study:

i. Moringa oil is stable during storage in a wide range of humidity. Therefore, the probability of the grits getting rancid is very minimal. Even though, relative humidity had an impact on the oil, the quality attributes were still within the acceptable standard.
ii. Equilibrium moisture contents of both products were dependent on both relative humidity and temperature of the environment. This resulted in the movement of the isotherm curves from left to right as the temperature increased from 20 to 40 ^{o}C**.** The experimental isotherm for both seed and grits demonstrated Type-II behaviour, which is typically present in dry, oily materials. Moringa seed and grits showed the ability to hold a little amount of water at low to moderate water activity and the opposite at higher water activity. GAB equation was the best-fitted model for seed while Modified Henderson model was the best-fitted model for grits among the six sorption models selected.

iii. When the temperature increased, the monolayer moisture content decreased in both adsorption and desorption for the three models which showed that temperature affected monolayer moisture content significantly while moisture sorption hysteresis did not have a remarkable effect on the monolayer moisture content of both moringa seed and grits.

iv. Based on calculated WVTR values and permeability coefficients of packaging materials, polypropylene material was found to be more suitable than low density polyethylene material in storing both moringa seed and grits. Moringa seed tends to have a longer predicted shelf life than moringa grits when stored in a polypropylene packaging material.

v. Net isosteric heat and entropy of sorption determined by Clausius Clapeyron equation increased exponentially as equilibrium moisture content decreased. However, both parameters were higher in desorption process than in adsorption process for both products. It takes higher energy to break the forces in desorption process than in adsorption process. Hence, the reason for higher net isosteric heat and entropy of sorption in desorption process than in adsorption process.

5.3 Recommendations

Based on the findings in this study, the following are recommended:

i. Moringa seed and grits should be packaged in polypropylene material for longer shelf life and effective marketing in supermarkets.

ii. The use of more non-reactive packaging materials should be tested and probably develop a biopolymer packaging material could be developed with the determined WVTR as basis. This will help to minimize the effect of non-biodegradability of most packaging materials.

iii. The quality degradation of the seed and grits within the period of acceptable shelf life should be studied so as to ensure that the nutritive value does not depreciate within this period.

5.4 Contributions to Knowledge

This study contributed the following to knowledge:

i. Moisture sorption isotherm pattern of moringa seed and grit was discovered.

ii. Optimal conditions for moringa seed and grits during storage was established.

iii. Effects of size reduction on storage stability and moisture sorption of moringa was established.
iv. Important thermodynamic characteristics that affect moringa seed processing and storage was established.
v. Shelf life of moringa seed and grits during storage under various conditions was provided.

References

Abdulkarim S. M., Lai, O. M., Long, K, Ghazali, H. M. and Muhammad, S. K. S. 2005. Some physico-chemical properties of Moringa oleifera seed oil extracted using solvent and aqueous enzymatic methods. *Journal of Food Chemistry* 93:253–263

Ade, A. R., Adetayo, S. A., Arowora, K. A., Ajav, E. A. and Raji, O. A. 2016. Moisture sorption isotherms of Mesquite seed (*Prosopis africana*). *Agricultural Engineering International: CIGR Journal* 18(3):273-281.

Adejumo, B. A. and Abayomi, D. A. 2012. Effect of moisture content on some physical properties of *Moringa oleifera* seed. *Journal of Agriculture and Veterinary Science* 1: 12-21.

Adejumo, B. A., Adamu, T. S., and Inaede, S. G. 2013. Effect of moisture content on the yield and characteristics of oil from *Moringa oleifera* seeds. *International Journal of Academic Research* 4 (4): 160-170.

Adeoye, B. K., Adeniran, A. D., Oladejo, C. J. and Opawuyi H. T. 2020. Sorption isotherm of corn chips made from blends of corn flour and bambara groundnut nut flour. *American Journal of Chemical Engineering* 8 (3): 70-75.

Ajibola, O. O., Abodurin, V. K. and Aviara, N. A. 2005. Moisture sorption equilibrium and thermodynamic properties of palm kernel. *International Agrophysics* 19:273-283.

Ajibola, O. O., Ajetumobi, O. E. and Aviara, N. A. 2003. Sorption equilibrium and thermodynamic properties of cowpea. *Journal of Food Engineering* 58: 317-324.

Ajibola, O. O., Dairo, O. U. 1998. The relationships between equilibrium relative humidity and moisture content of sesame seed using the vapour manometric method. *Ife Journal of Science and Technology* 8(1): 61-67.

Ajisegiri, E. S. A., Sopade, P. A. and Chukwu, O. 2007. Moisture sorption study of locally parboiled rice. *Australian Journal of Technology* 11(2):86-90.

Akanbi, C. T., Ojo, A. and Adeyemi, R. S. 2006. Drying characteristics and sorption isotherm of tomato slices. *Journal of Food Engineering* 73: 157–163.

Akintola, A., Ogunlade, C. A. and Aremu, A. K. 2022. Effect of storage period and relative humidity on the quality of moringa oil. *Croatian Journal of Food Science and Technology* 14(1): 74-81.

Akintola, A., Oyefeso, B. O. and Aremu, A. K. 2022. Effect of temperature and hysteresis on monolayer moisture content of moringa seed grit during storage. *Proceedings of 22nd international conference and 42nd annual general meetings of the Nigerian Institution of Agricultural Engineers* 22: 444-451.

Alakali, J. S. and Satimehin, A. A. 2007. Moisture adsorption characteristics of bambara groundnut (*Vigna subterranea*) powders. Agricultural Engineering International: *the CIGR Ejournal*. Manuscript FP 07 005. Vol. IX. Pp 1-17.

Alakali, J. S. and Satimehin, A. A. 2009. Moisture adsorption characteristics of ginger (*Zingiber officinale*) powders. Agricultural Engineering International: *the CIGR Ejournal*. Manuscript 1286. Vol. XI. Pp 1-19.

Alimi, B. A., Tesfay, S. Z., Oke, M. O. and Workneh, T. S. 2018. Moisture sorption isotherm of moringa seed at two different temperatures. *In Proceedings of International conference on managing quality in chains*. Eds.: U. L. Opara and E. W. Hoffman; pages 191-196.

Al-Mahasneh, M. A., Al-Udatt, M. H., Yang, W., and Rababeh, T. M. 2010. Moisture sorption thermodynamics of fractionated sesame hulls (*Sesamum Indicum* L.). *Journal of Food Process Engineering* 33(5): 802–819.

Al-Muhtaseb, A. H., Magee, T. R. A. McMinn and W. A. M. 2004. Water sorption isotherms of starch powders. Part I: Mathematical description of experimental data. *Journal of Food Engineering* 61: 297-307.

Al-Muhtaseb, A. H., McMinn, W. A. M. and Magee, T. R. A. 2002. Moisture sorption isotherm characteristics of food products: a review. *Food and Bioproducts Processing* 80(2): 118-128.

Anandito, R., Sodiq, H. and Siswanti-Purnamayati, L. 2017. Shelf-life determination of fish koya using critical moisture content approach. *Proceedings of the Pakistan Academy Sciences*: Life and Environmental Sciences, 54(3):201-206.

Anjorin, T. S., Ikokoh, P. and Okolo, S. 2010. Mineral composition of *Moringa oleifera* leaves, pods and seeds from two regions in Abuja, Nigeria. *International Journal of Agriculture* 12: 431–434.

Anwar, F., Gilani, A. H., Latif, S. and Ashraf, M. 2007. Moringa oleifera: A food plant with multiple medicinal uses. *Journal of Phytotherapy Researc*h. 21, 17–25.

AOAC (Association of Official Analytical Chemists). 2010. Official Method of Analysis of AOAC International. 17th ed. Association of Official Analytical Chemists Inc. Horwitz, Willium, 2,200 - 2237.

Aremu, A. K. and Akintola, A. 2016. Drying kinetics of *Moringa oleifera* seeds. *Journal of Life Sciences and Technology* 4 (1):7-10.

Aremu, A.K. and Akintola, A. 2014. Effects of some drying methods on nutritional characteristics of *Moringa Oleifera* seeds. *International Conference on Biotechnology and Environment Management* 75 (12): 66-72.

Arslan, N. and Togrul. H. 2005. Moisture sorption isotherms for crushed chillies. *Journal of Biosystems Engineering* 90 (1): 47-61.

Asaolu, M. F. and Omotayo, F. O. 2007. Phytochemical, nutritive and anti-nutritive composition of leaves of *Moringa oleifera*. *Phytochemistry and pharmacology III* 48(2): 339-344.

Athikomkulchai, S., Jantrawut, P., Tadtong, S., Tunit, P., Chittasupho, C. and Sommano, S.R., 2020. *Moringa oleifera* seed oil formulation, physical stability and chemical constituents for enhancing skin hydration and antioxidant activity. *Cosmetics* 8(2): 1-18.

Aviara, N. A. 2020. Moisture sorption isotherms and isotherm model performance evaluation for food and agricultural products. Intech Open: Pp 1-33.

Aviara, N. A. and Ajibola, O. O. 2002. Thermodynamics of moisture sorption in melon seed and cassava. *Journal of Food Engineering* 55(2): 107-113.

Aviara, N. A. Drying characteristics and storage stability of chemically modified cassava (*Manihot esculenta* Crantz), maize (*Zea mays* Linn.) and Sorghum (Sorghum bicolor L. Moench) starches [PhD dissertation]. Ibadan: University of Ibadan; 2010. 285pp

Aviara, N. A., Adedeji, M. A, Ajibola, O. O. and Aregbesola, O. A. 2006. Moisture sorption isotherms of sorghum malt at 40 and 50 °C. *Journal of Stored Products Research* 42:290-301.

Aviara, N. A., Oni, S. A. and Ajibola, O. O. 2004. Sorption equilibrium and thermodynamic characteristics of soya bean. *Journal of Biosystems Engineering* 87 (2):179-190.

Ayotunde, E. O., Adebanjo, O. T. and Fagbenro, O. A. 2011. Toxicity of aqueous extract of *Moringa oleifera* seed powder to Nile tilapia (*Oreochromis niloticus*) fingerlings. *International Research Journal of Agricultural Science* 1:142–150.

Bahloul, N., Kechaou, N. and Boudhrioua, N. 2008. Moisture desorption-adsorption isotherms and isosteric heats of sorption of Tunisian olive leaves (*Olea europaea* L.). *Industrial Crops and Products* 28(2): 162-176.

Balbir, M. 2006. Moringa for cattle fodder and plant growth. Tree for life available at www.treeforlife.org. Assesses on 14th May, 2019.

Barakat, H. and Ghazal, G. A. 2016. Physico-chemical properties of *Moringa oleifera* seeds and their edible oil cultivated at different regions in Egypt. *Food and Nutrition Sciences* 7: 472-484.

Bastias, M. V. 2006. Evaluation of wood sorption models for high temperatures. Laval University. 38 – 44.

Bell, L. N. and Labuza, T. P. 2000. Moisture sorption: Practical aspects of isotherm measurement and use (2nd Edition). American Association of Cereal Chemists, Inc. St. Paul, MN. Pp 1-23.

Boquet, R., Iglesias, H. A. and Chirife, J. 1979. Equations for fitting water sorption isotherms of foods, Part III: Evaluation of various three-parameter models. *Journal of Food Technology* 14:527-534.

Brunauer, S., Deming, W. E., Teller E. and Deming, L. S. 1940. On a theory of van der walls adsorption of gases. *American Chemical Society Journal* 62:1723-1732.

Busani, M., Voster, M., Patrick, J. M. and Amold, H. 2011. Nutritional characterization of moringa leaves. *African Journal of Biotechnology* 10: 12925-12933.

Carmody, O., Kokot, S., Xi, Y. and Frost, R. 2007. Surface characterization of selected sorbent materials for common hydrocarbon fuels. *Journal of Surface Science* 601(9):2066-2076.

Chirife, J. and Iglesias, H. A. 1978. Equations for fitting water sorption isotherms of food: Part 1-A review. *Journal of Food Technology* 13:159-174.

Choudhury, D., Sharma, G. D. and Sahu, J. K. 2011. Moisture sorption isotherms, heat of sorption and properties of sorbed water of raw bamboo (*Dendrocalamus longispathus*) shoots. *Industrial Crops and Products* 33(1): 211-216.

Chukwu, O. and Ajisegiri, E. S. A. 2011. Moisture-sorption isotherms of Bambara nut and Tiger nut. *International Journal of Postharvest Technology and Innovation* 2 (2) :211–219.

Damodaran S., Fennema O. R. and Parkin K. L. 2008. Water and ice. Food Chemistry (4th edition). Boca Raton, FL: CRC Press. Pp 17-82.

Dinesha, B. L., Ramachandra, C. T., Nidoni, U., Sankalpa, K. and Naik, N. 2018. Effect of extraction methods on physicochemical, nutritional, antinutritional, antioxidant and antimicrobial activity of Moringa (Moringa oleifera Lam.) seed kernel oil. *Journal of Applied and Natural Science* 10(1): 287–295.

Eim, V., Simal, S., Femenia, A. and Rossello, C. 2011. Moisture sorption isotherms and thermodynamic properties of carrot. *International Journal of Food Engineering* 7(3): 1-16.

Ethmane-Kane, C. S., Mimet, A., Lamharrar, A. I. and Kouhilal, M., A. 2008. Moisture sorption isotherms and thermodynamic properties of tow mints: *Mentha pulegium* and *Mentha rotundifolia.* 11:2, 181 – 195.

Fadele, O. K., Akintola, A., Oyefeso, B. O. and Aremu, A. K. 2018. Effect of moisture content, operation and design parameters on separation efficiency of moringa seed shelling machine: Optimisation approach. In: *Proceedings of International Commission of Agriculture and Biosystems Engineering, 12th CIGR Section VI International Symposium (Post Harvest Technology and Bioprocess Engineering),* IITA, Ibadan, Nigeria. Pages 213- 223.

Fadeyibi, A., Usaini, M. S., Osunde, Z. D., Balami, A. A. and Idah, P. A. 2012. Evaluating monolayer moisture content of rubber seed using BET and GAB sorption equations. *International Journal of Farming and Allied Sciences* 1(3): 72-76.

Fahey, J. W. 2005. *Moringa oleifera*: A review of the medical evidence for its nutritional, therapeutic and prophylactic properties. *Trees for Life Journal* 1: 5-12.

Falade, K. O. and Aworh, O.C. 2004. Adsorption isotherms of osmo-oven dried African star apple (*Chrysophyllum albidum*) and African mango (*Irvingia gabonensis*) slices. *European Food Research and Technology* 218: 278-283.

FAO/WHO (2009). Report of the 21st session of the Codex Alimentarius Committee on fats and oils. Kola Kinabalu, Malaysia, 16 – 20 February 2009.

Farooq, A., Umer R. and Syeda, N. Z. 2006. Characterization of *Moringa oleifera* seed oil from drought and irrigated regions of Punjab, Pakistan. *Grasas Y Aceites* 57(2): 160–168.

Fasina, O. O. and Sokhansanj, S. 1993. Equilibrium moisture relations and heat of sorption of alfalfa pellets. *Journal of Agricultural Engineering Research* 56:51-63.

Fennema, O. R. 1996. Water and ice. Food Chemistry (3rd edition). New York: Marcel Dekker, Inc. Chapter 2: pp 18-50.

Fontana A. J. J. (2007). Measurement of water activity, moisture sorption isotherms, and moisture content of foods. Water activity in Foods: Fundamentals and applications. Ames, IA: Blackwell Publishing and IFT Press. Chapter 6: pp 155-171.

Fu, X., Hou, L., Su, J., Hou, Y., Zhu, P., Xu, J. and Zhang, K. 2021. Physicochemical and thermal characteristics of *Moringa oleifera* seed oil. *Advanced Composites and Hybrid Materials* 4(3):685–695.

Fuglier, L. J. 1999. The Miracle Tree: *Moringa oleifera*, Natural Nutrition for the Tropics. Church World Service, Dakkar, Senegal, pp. 68.

Gal S. (1975). Recent advances in techniques for the determination of sorption isotherm. In: Duckworth RB, editor. Water Relations of Foods. London: Academic Press; pp. 135-155

Gal S. (1981). Recent developments in techniques for obtaining complete sorption isotherms. In: Rockland LB, Stewart GF, editors. Water Activity: Influence on Food Quality. New York: Academic Press; p. 89

Gal S. (1983). The need for and practical applications of sorption data. In: Jowitt R, Escher F, Hallstrom B, Meffert HFT, Speiss WEL, Vos G, editors. Physical Properties of Foods. New York: Applied Science Publishers; pp. 13-25

Ghazalah, A. A. and Ali, A. M. 2008. Rosemary leaves as a dietary supplement for growth in broiler chickens. *International Poultry Science* 7: 234-239.

Ghebremichael, K. and Gebremedhin N. A. G. 2011. Performance of *Moringa oleifera* as a bio-sorbent for chromium removal, *Water Science Technology* 62: 1106–1111.

Gichau, A. W., Makokha, A. and Okoth, J. K. 2019. Moisture sorption isotherm and shelf-life prediction of complementary food based on amaranth–sorghum grains. *Journal of Food Science and Technology* 57(3):962-970.

Ibrahim, A. and Onwualu, A. P. 2005. Technologies for Extraction of Oil from oil-bearing agricultural products. *Journal of Agricultural Engineering and Technology* 13(1): 58- 70.

Igbeka, J. C. 1982. Simulation of moisture movement during drying of starchy food products – Cassava. *Journal of Food Technology* 17:27-36.

Janjai, S., Mahayothee, B., Tohsing, K., Bala, B. K., Müller, J. and Haewsungcharern, M. 2007. Moisture sorption isotherms and heat of sorption of mango (*Magnifera indica* L.). *International Agricultural Engineering Journal* 16(3-4): 159-168.

Kaleemullah, S. and Kailappan, R. 2004. Moisture sorption isotherms of red chillies. *Journal of Biosystems Engineering* 88(1): 95-105.

Karima, G., Abdellah, C., Leila, R., Kamel, M. and Soltania, T. 2021. Chemical Composition and profile characterisation of *Moringa oleifera* seed oil. *South African Journal of Botany* 137(2): 475-482.

Karthik, P. and Anandharamakrishnan, C. 2013. Microencapsulation of Docosahexaenoic Acid by Spray-Freeze-Drying Method and Comparison of Its Stability with Spray-Drying and Freeze-Drying Methods. *Food Bioprocess Technology* 6: 2780–2790.

Kenawi, M., Zaghlul, M. M. A. and Abdel-Hameed, S. 2015. Effect of packaging materials and storage conditions on the moisture sorption isotherm of solar dried table egg powder. *Journal of Material Science* 32: 67-72.

Kapsalis, J. G. 1987. Influences of hysteresis and temperature on moisture sorption isotherms. In: Rockland LB, Beuchat LR, editors. Water Activity: Theory and Applications to Food. New York: Marcel Dekker Inc; pp. 173-213.

Khalloufi, S., Ratti, C. and Giasson, J. 2000. Water activity of freeze-dried mushrooms and berries. *Canadian Journal of Agricultural Engineering* 42(1): 51-56.

Koc, B., Ertekin, F. K., Balkir P. and Yilmazer M. S. 2010. Moisture sorption isotherms and storage stability of spray-dried yogurt powder. *Journal of Drying Technology* 28(6): 816–822. doi:10.1080/07373937.2010.485083

Kumar, A. J., Patel A. A., Patil, G. R. and Singh, R. R. 2005. Effect of temperature on moisture desorption isotherms of kheer. *Journal of Food Science and Technology* 38 (3), 303-310.

Labuza, T. P. and Altunakar, B. 2020. Water activity prediction and moisture sorption isotherms. Water activity in foods: fundamentals and applications, 61-205.

Labuza, T. P. and Altunakar B. 2007. Water Activity Prediction and Moisture Sorption Isotherms. Water activity in Foods: Fundamentals and applications. Ames, IA: Blackwell Publishing and IFT Press. Chapter 5: Pp 109-154.

Labuza, T. P., Lee R. Y., Tatini, S. R., Acott, K., McCall W. and Flink J. 1976. Water activity determination: A collaborative study of different methods. *Journal of Food Science* 41:910-917.

Lamharrar, A., Kouhila, M. and Idlimam, A. 2007. Thermodynamic properties and moisture sorption isotherms of Artemisia herba alba. *Revue des Energies Renouvelables*, 10(3): 311-320.

Lannaon, W. J. (2007). Herbal Plants as Source of Antibiotics for Broilers. *Agriculture Magazine*, 11(2): 55.

Lea M., 2010. Bioremediation of turbidity surface water using seed extract from *Moringa oleifera* Lam. (Drumstick) tree, *Curr. Protoc. Microbiol* 16:1–14.

Leone, A., Schiraldi, A., Battezzati, A., Spada, A., Bertoli, S. and Aristil, J. 2016. *Moringa oleifera* seeds and oil: Characteristics and uses for human health. *International Journal of Molecular Science* 17(12): 2141.

Maleki-Majd, K., Ansari, S., Farahnaky, A. and Karparvarfard, S. H. 2014. Thermodynamic properties of water sorption isotherms of grape seed. *International Agrophysics* 28(1): 63-71.

Mangale S. M., Raut P. D., Jadhav A. S., and Chonde S. G. 2012. Study of *Moringa oleifera* (Drumstick) seed as natural Absorbent and Antimicrobial agent for River water treatment. *Journal of Natural Production Plant Resour*ce 2 (1):89-100

Manzoor, M., Bhanger M. I., Iqbal, T. and Anwar, F. 2007. Physic-o-chemical characterization of *Moringa concanensis* seed and seed oil. *Journal of America Oil Chemical Society* 84: 413–419.

Menkov, N. D. 2000. Moisture sorption isotherms of vetch seeds at four temperatures. *Journal of Agricultural Engineering Research* 76:373-380.

Meter Group Inc. AquaLab water activity meter. In: Operator' s Manual for Series 4. Hopkins Court, Pullman, WA, USA: Meter Group Inc. 2018, pp 2-3.

Moravec, C. M., Laca, E. A. and Bradford, K. J. 2008. Water relations of drumstick tree seed (*Moringa oleifera*): imbibition, desiccation, and sorption isotherms. *Journal of Seed Science and Technology* 36: 311-324.

Moreira, R. G. 2001. Impingement drying of foods using hot air and superheated steam. *Journal of Food Engineering* 49:291-295.

Musa, J. and Njidda, A. A. 2021. Chemical composition, anti-nutritive substances, amino acid profile and mineral composition of *Moringa oleifera* seeds subjected to different boiling duration. *Nigerian Journal of Animal Science and Technology* 4 (1):43 – 52.

Mustapha, H. B., Suleyman, A. M. and Jonan, C. A. 2012. Kinetics of water disinfection with Moringa seed extract, *Journal of Environment and Earth Science* 2(7): 224-231.

Ngoddy, P. O. and Bakker-Arkema, F.W. 1970. A generalized theory of sorption phenomena in biological materials (Part I: The isotherm equation). *Transactions of ASAE* 13(5):612-617.

Ogunsina, B. S., Radha, C., Bhatnagar, A. S., Indira, T. N., Gopala-Krishna, A. G. and Debnath, S. 2014. Quality characteristics and stability of *Moringa oleifera* seed oil of Indian origin. *Journal of Food Science and Technology* 51: 503-510.

Ogunsina, B. S., Radha, C. and Singh, R. S. G. 2010. Physicochemical and functional properties of full-fat and defatted *Moringa oleifera* kernel flour. *International Journal of Food Science and Technology* 45: 2433–2439.

Ojediran, J. O., Aviara N. A. and Raji, A. O. 2014. Moisture sorption properties of castor seeds. *Agricultural Engineering Today* 38(1):38-44.

Ojo, O. G., Adewumi, B. A., Adebowale, A. R., and Shittu, T. A. 2021. Effect of packaging materials on the colour, foaming properties and shelf life of foam-mat-dried starch–albumen powder. *Journal of Packaging Technology and Research* 5: 69 - 77.

Oliveira, J. T., Vasconcelos, K. M., Silveia, S. B., Morira, R. A. and Cavada, B. S. 1999. Compositional and nutritional attributes of seeds from the multipurpose tree: *Moringa oleifera* Lamarck. *Journal of Science, Food and Agriculture* 79 (6): 815-20.

Oluwalana, S. A., Bolaji, G. A., Bankole, W., Alegbeleye, O. and Martins, O. 1999. Domestic water purification using *Moringa oleifera* Lam. *Nigerian Journal of Forestry* 1-2: 28-32.

Oluwamukomi, M. O. 2009. Adsorption isotherm modeling of soy-melon-enriched and un-enriched gari using GAB equation. *African Journal of Food Science* 3(5): 117-124.

Onilude, A. A., Wakil, S. M. and Igbinadolor, R. O. 2010. Effect of varying relative humidity on the rancidity of cashew (*Anacardium occidentale* L.) kernel oil by lipolytic organisms. *African Journal of Biotechnology* 9(31): 4890-4896.

Oyefeso, B. O., Akintola, A., Ogunlade, C. A., Afolabi, M. G., Odeniyi, O. M. and Fadele, O.K. 2021. Influence of moisture content and speed on cutting force and energy of Tannia cormels: a response surface approach. *Research in Agricultural Engineering* 67(3): 123-130.

Oyelade, O. J., Igbeka, J. C. and Tunde-Akintunde, T. Y. 2008. Predictive equilibrium moisture content equations for yam (*Dioscorea rotundata*, Poir) flour and hysteresis phenomena under practical storage conditions. *Journal of Food Engineering* 87:229-235.

Oyelade, O. J., Igbeka, J. C., Tunde-Akintunde, T. Y., Raji, O. Y. and Oke, M. O. 2008. Modelling moisture sorption isotherms for maize flour. *Journal of Stored Products Research* 44:179-185.

Palou, E., Argaiz, A. and Lopez-Malo, A. 1997. Effect of temperature on the moisture sorption isotherms of some cookies and corn snacks. *Journal of Food Engineering* 31:85-93.

Patindol, J. C. and Norio, R. C. 2022. Moisture sorption isotherm and shelf-life estimation of blue butterfly pea (*Clitoria ternatea* linn.) powder using GAB model. *International Journal of Multidisciplinary Research and Development* 9(4): 80-90.

Phomkong, W. G., Driscoll, H. and Srzednicki, R. 2006. Desorption isotherms for stone fruit. *Drying Technology* 24: 201-210.

Pua, C. K., Tan, C. P., Hamid, N. S. A., Rahman, R. A., Rusul, G. and Mirhosseini, H. 2008. Storage Stability of Jackfruit (*Artocarpus heterophyllus*) Powder Packaged in Aluminium Laminated Polyethylene and Metallized co-Extruded Biaxially Oriented Polypropylene during Storage. *Journal of Food Engineering* 89: 419–428.

Rahman, I. M. M., Begum, Z. A., Nazimuddin, M., Barua, S., Hasegawa, H. and Rahman, M. A. 2009. Physicochemical properties of *Moringa oleifera* Lam. seed oil of the indigenous-cultivar of Bangladesh. *Journal of Food Lipids* 16: 540–553.

Raji, A. O. and Oyefeso, B. O. 2017. Elasticity of cocoyam cormel as influenced by moisture content and loading orientation when in transit and storage. *Agricultural Engineering International: CIGR Journal* 19:193-199.

Rizvi, S. S. H. (1986). Thermodynamic properties of food in dehydration. In: Rao MA, Rizvi SSH, editors. Engineering Properties of Foods. New York: Marcel Dekker Inc; pp. 133-214.

Robertson G. L. (2013). Food packaging principles and practice, CRC Press Taylor and Francis group. Chapter 4: pp 98-128.

Rockwood, J. L., Casamatta, D. A. and Anderson, B. G. 2013. Potential uses of *Moringa oleifera* and an examination of antibiotic efficacy conferred by *Moringa oleifera* seed and leaf extracts using crude extraction techniques available to underserved indigenous populations. *International Journal of Phytotherapy Research* 3: 61-71.

Rodriguez-Bernal, J. M., Pascual-Pineda, L. A., Bonilla, E., Lizarazo-Morales, C., Flores-Andrade, E., Quintanilla-Carvajal, M. X. and Gutierrez-Lopez, G., 2015. Moisture adsorption isotherms of the borojo fruit (*Borojoa patinoi*. Cuatrecasas) and gum arabic powders. *Journal of Food and Bioproducts Processing* 94: 187–198.

Sahu, S. N., Sahu, J. K., Tiwari, A., Baitharu, I. Kariali, E. and Naik, S. N. 2018. Moisture sorption isotherms and thermodynamic properties of sorbed water of chironji (*Buchanania lanzan* Spreng.) kernels at different storage conditions. *Journal of Food Measurement and Characteristics* 12(4): 2626–2635.

Saini, R. K., Keum, Y. S. and Sivanesan, I. 2016. Phytochemicals of *Moringa oleifera*: A review of their nutritional, therapeutic and industrial significance. *Journal of Biotechnology* 6: 203-217.

Sánchez-Torres, E. A., Benedito, J., Abril, B., García-Pérez, J. V. and Bon, J. 2021. Water desorption isotherms of pork liver and thermodynamic properties. *Journal of Food Science and Technology* 49 (1):111-115.

Santalla, E. M. and Mascheroni, R. H. 2003. Equilibrium moisture characteristics of high oleic sunflower seeds and kernels. *Drying Technology* 21:147-163.

Schmidt, S. J. 2004. Water and Solids Mobility in Foods. *Advances in Food and Nutrition Research* 48: 45-67.

Seid, R. M. and Hensel, O. 2012. Experimental evaluation of sorption isotherms of chili pepper: an Ethiopian variety, Mareko Fana (*Capsicum annum* L.). *Agricultural Engineering International: CIGR E-Journal* 14(4):163–172.

Singh, A. K. and Kumari, N. 2014. Moisture sorption isotherm characteristics of ground flaxseed. *Journal of Food Process Technology* 5: 319-328.

Siripatrawan, U. and Jantawat, P. 2006. Determination of moisture sorption isotherms of Jasmine rice crackers using BET and GAB models. *Food Science and Technology International* 12(6): 459-465.

Slamet, A., Hartanto, R. and Praseptiangga, D. 2020. Moisture sorption isotherm and shelf life of pumpkin and arrowroot starch-based instant porridge. *Proceedings of AIP conference and exhibition on powder technology*. 070002-1-070002-6.

Speiss, W. E. L. and Wolf, W. 1987. Critical evaluation of methods to determine moisture sorption isotherms. In: Rockland LB, Beuchat LR, editors. Water Activity: Theory and Applications to Foods. New York: Marcel Dekker Inc; pp. 215-233

Sudathip, I., Pimpen, P. and Woatthichai, N. 2009. Moisture sorption of Thai red curry powder. *International Journal of Science Technology* 3(03): 486 –497.

Swami, S. B., Maiti, B. and Das, S. K. 2005. Moisture sorption isotherms of black gram nuggets (Bori) at varied temperatures. *Journal of Food Engineering* 67(4):477-482.

Tarigan, E., Yamsaengsung, R., Prateepchaikul, G., Tekasakul, P. and Sirichote, A. 2006. Sorption isotherms of shelled and unshelled kernels of candle nuts. *Journal of Food Engineering* 75: 447–452.

Tavares, L. and Noreña, C. P. Z. 2021. Characterization of the physicochemical, structural and thermodynamic properties of encapsulated garlic extract in multilayer wall materials. *Powder Technology* 37(8): 388–399.

Timmermann, E. O., Iglesias, H. A. and Chirife, J. 2001. Water sorption isotherms of foods and foodstuffs: BET or GAB parameters. *Journal of Food Engineering* 48, 19-31.

Tolaba, M. P., Pollio M. L., Enrique N. and Peltzer, M. 2004. Grain sorption equilibria of quinoa grains. *Journal of Food Engineering* 61:365-371.

Tsami, E., Drouzas, A. E. and Krokida, M. K. 1999. Effect of drying method on the sorption characteristics of model fruit powders. *Journal of Food Engineering* 38:381-392.

Vazquez, G., Moreira, R. and Chenlo, F. 2003. Sorption isotherms of lupine at different temperatures. *Journal of Food Engineering* 60:449-452.

Vishwakarma, R. K., Nanda, S. K. and Shivhare, U. S. 2011. Moisture adsorption isotherms of guar (*Cyamposis tetragonoloba*) grain and guar gum splits. *Food Science and Technology* 44: 969-975.

Yan, Z., Oliveira, F. A. R. and Sousa-Gallagher, M. J. 2008. Sorption isotherms and moisture sorption hysteresis of intermediate moisture content banana. *Journal of Food Engineering* 86: 342–348.

Yaptenco, K. F., Pangan, R. S., Duque J. A. C. and Pardua, S. N. 2017. Moisture sorption isotherms and shelf-life prediction for whole dried sandfish (Holothuria scabra). *Agricultural Engineering International: The CIGR E-journal* 19(2): 176-186.

Yazdani, M., P. Ghobadi, P. and Sazandehchi, M. A. 2006. Moisture sorption isotherms and isosteric heat for pistachio. *European Food Research Technology* 223: 577-584.

Yin, C. Y. 2011. Emerging usage of plant-based coagulants for water and wastewater treatment. *Journal of Processing and Biochemistry* 45:1437–1444.

Yu, L., Jayas, D. S. and Mazza, G. 1999. Moisture sorption of characteristics of freeze-dried, osmo-dried and osmo-air-dried cherries, and blueberries. *Transactions of ASAE* 42(1):141-147.

APPENDIX A: Adsorption and desorption isotherms

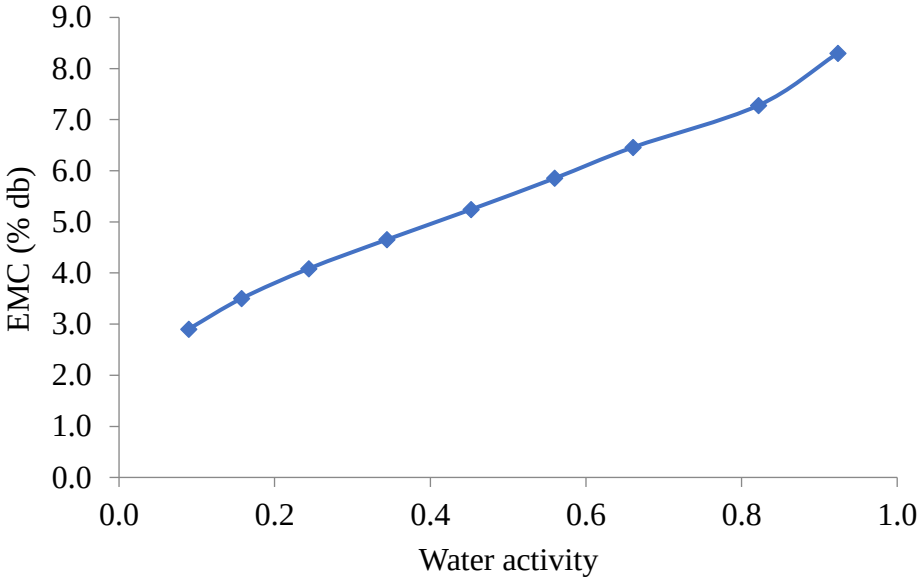

Figure A1: Moringa seed grits adsorption at 20^{o}C

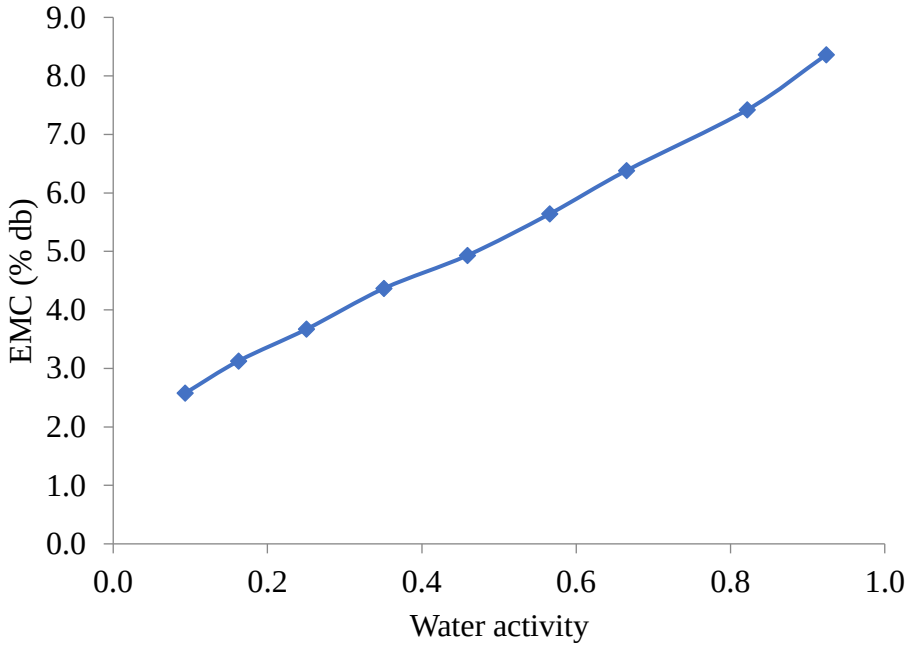

Figure A2: Moringa seed grits adsorption at 25^{o}C

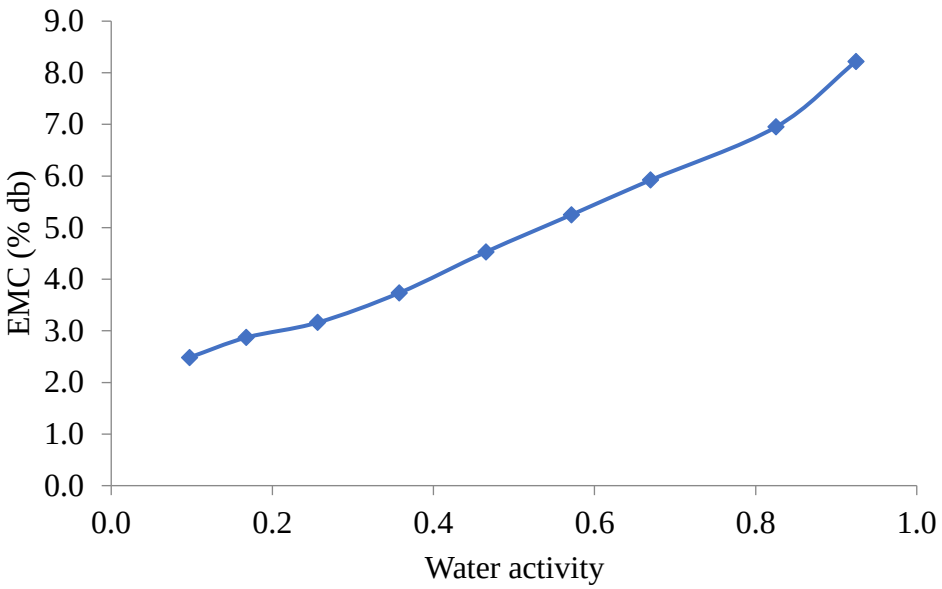

Figure A3: Moringa seed grits adsorption at 30^{o}C

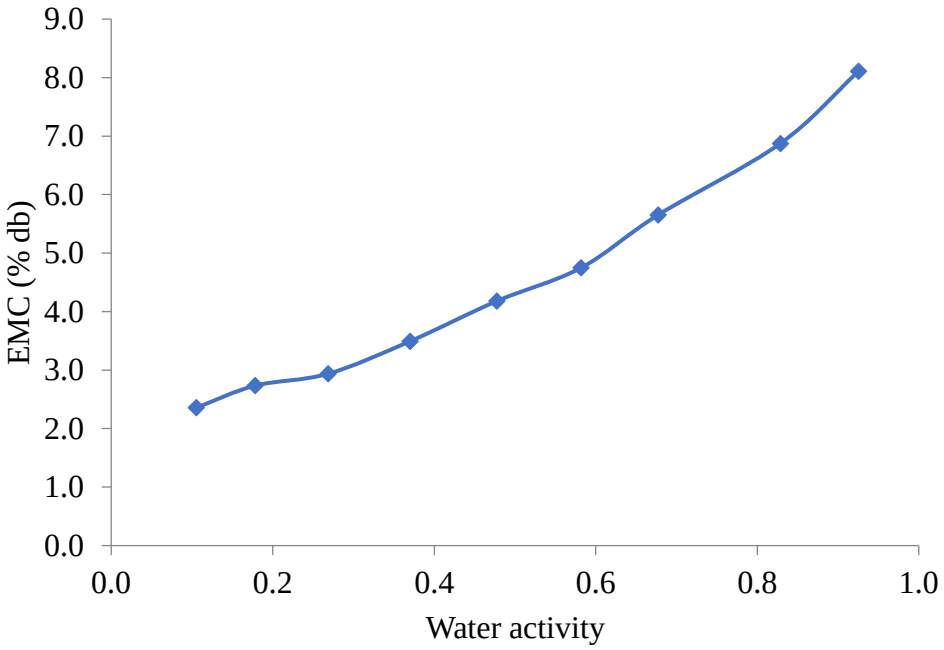

Figure A4: Moringa seed grits adsorption at 35^{o}C

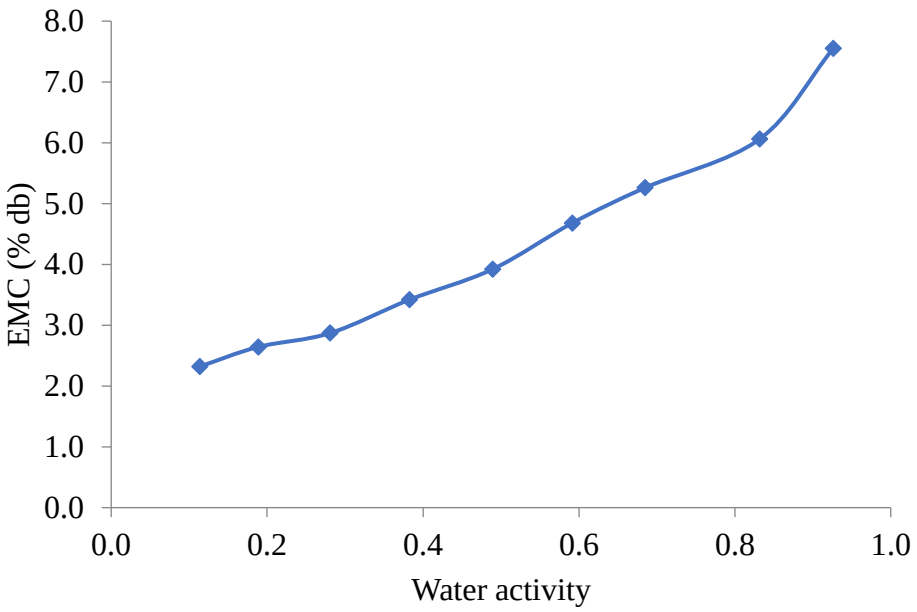

Figure A5: Moringa seed grits adsorption at 40^{o}C

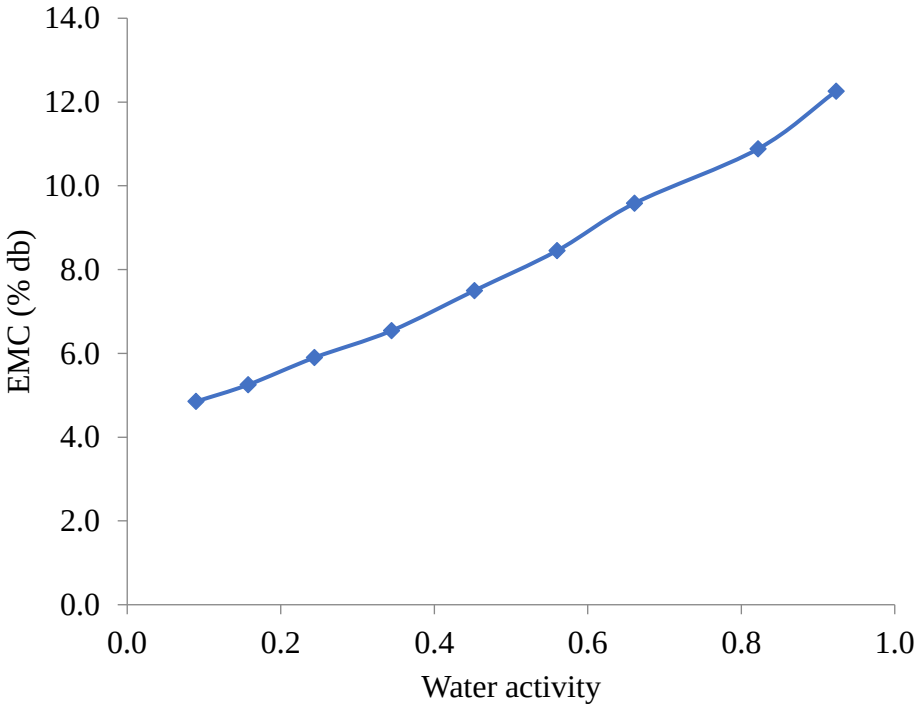

Figure A6: Moringa seed adsorption at 20^{o}C

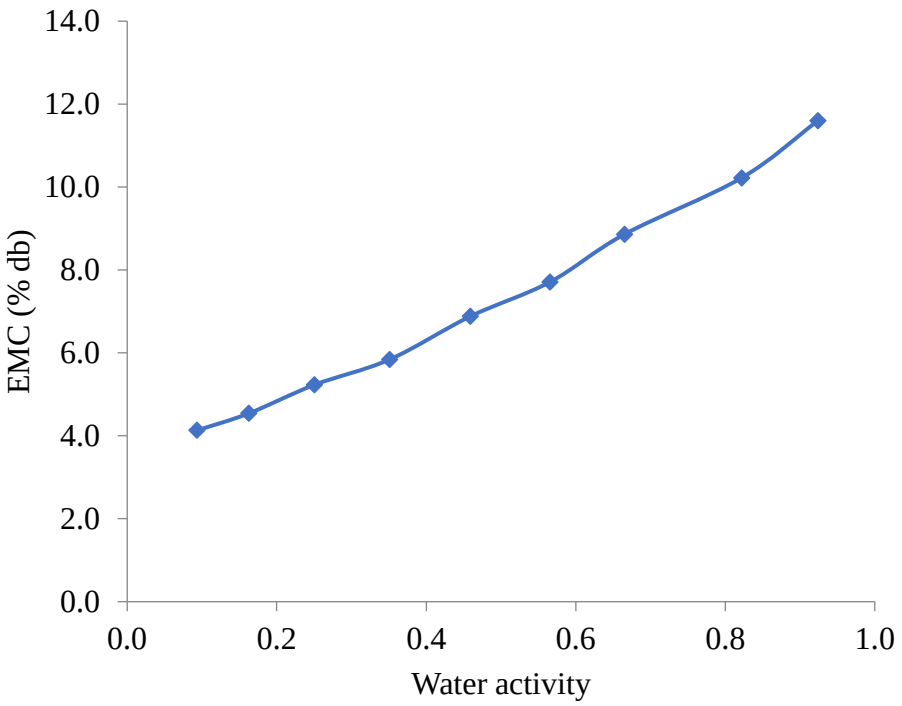

Figure A7: Moringa seed adsorption at 25^{o}C

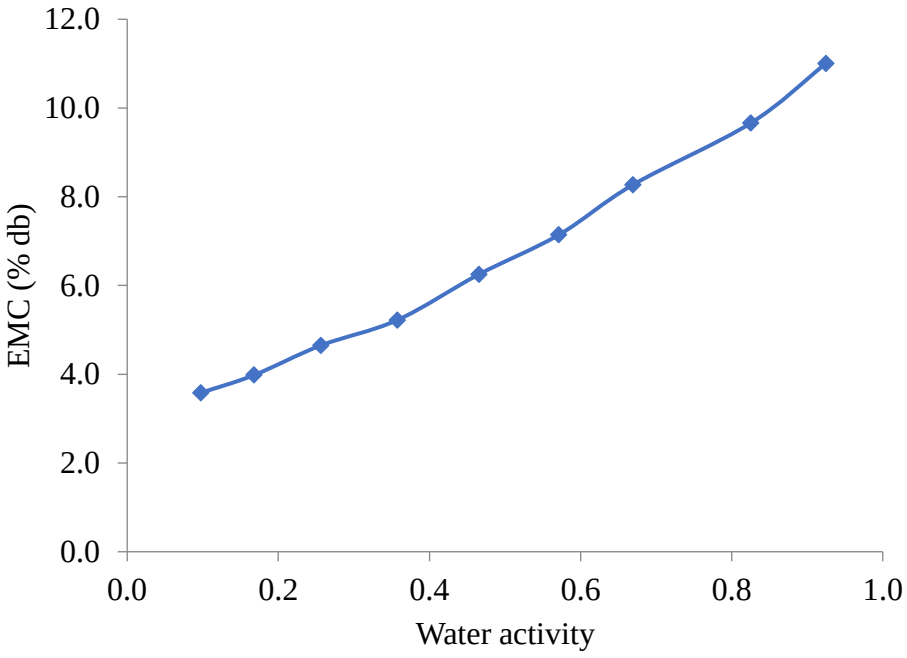

Figure A8: Moringa seed adsorption at 30^{o}C

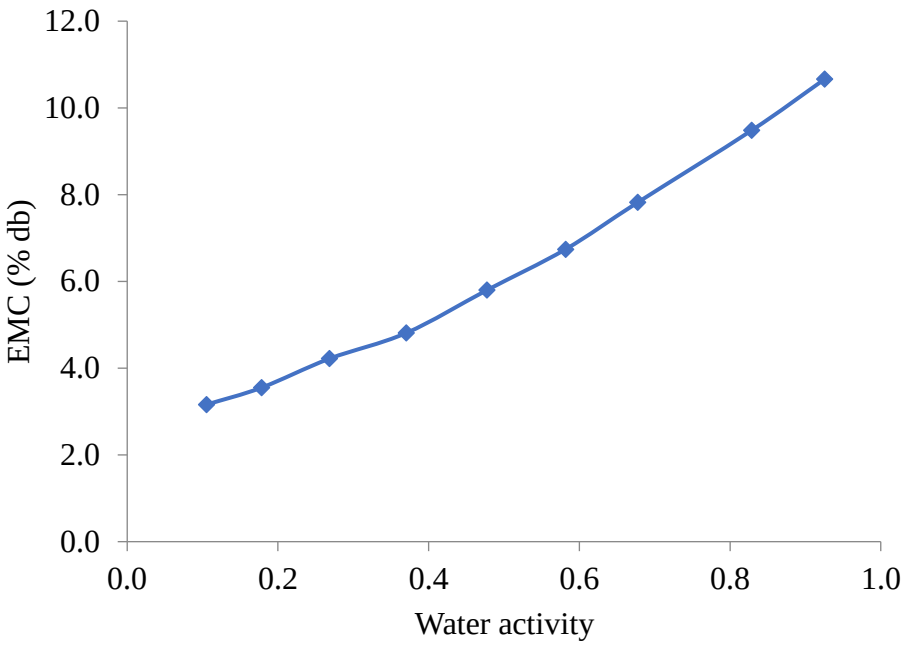

Figure A9: Moringa seed adsorption at 35^{o}C

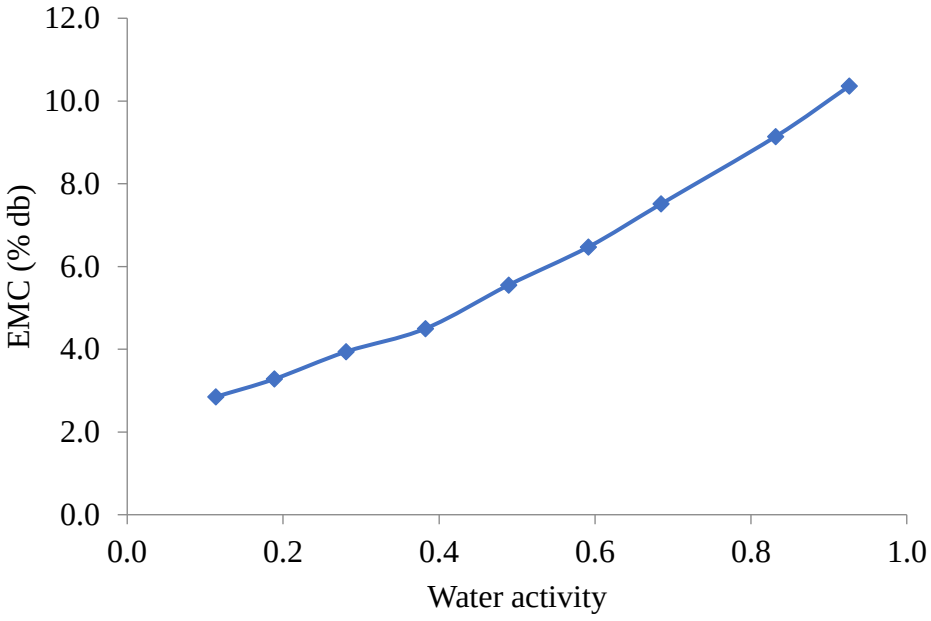

Figure A10: Moringa seed adsorption at 40^{o}C

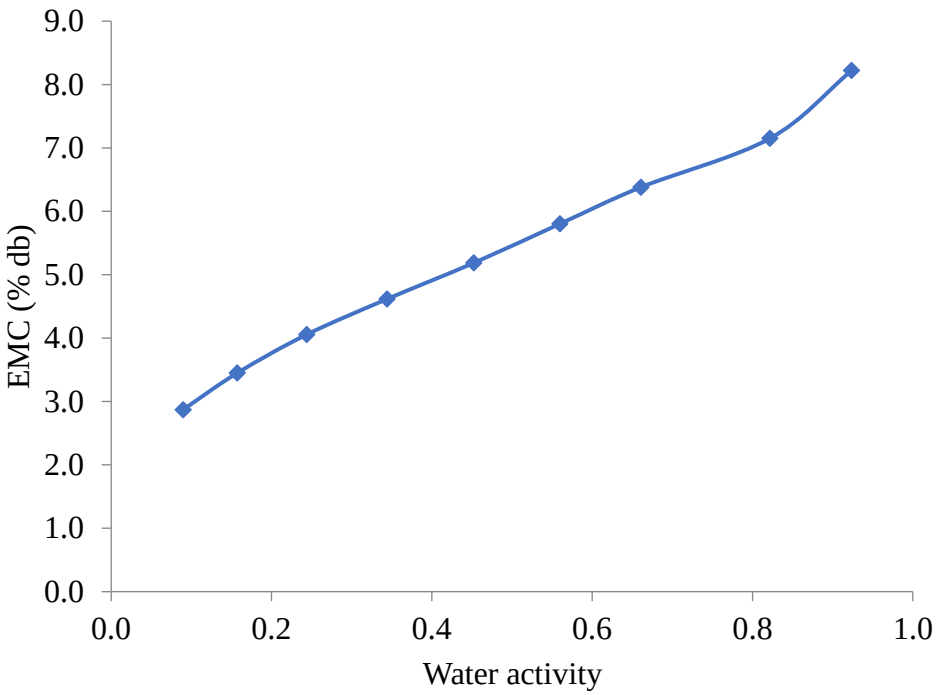

Figure A11: Moringa seed grits desorption at 20^{o}C

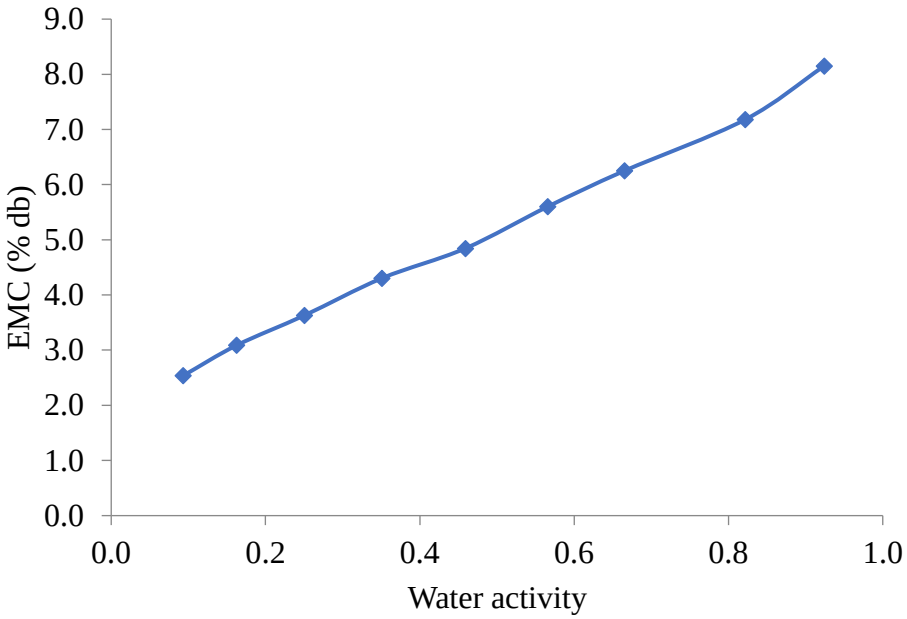

Figure A12: Moringa seed grits desorption at 25^{o}C

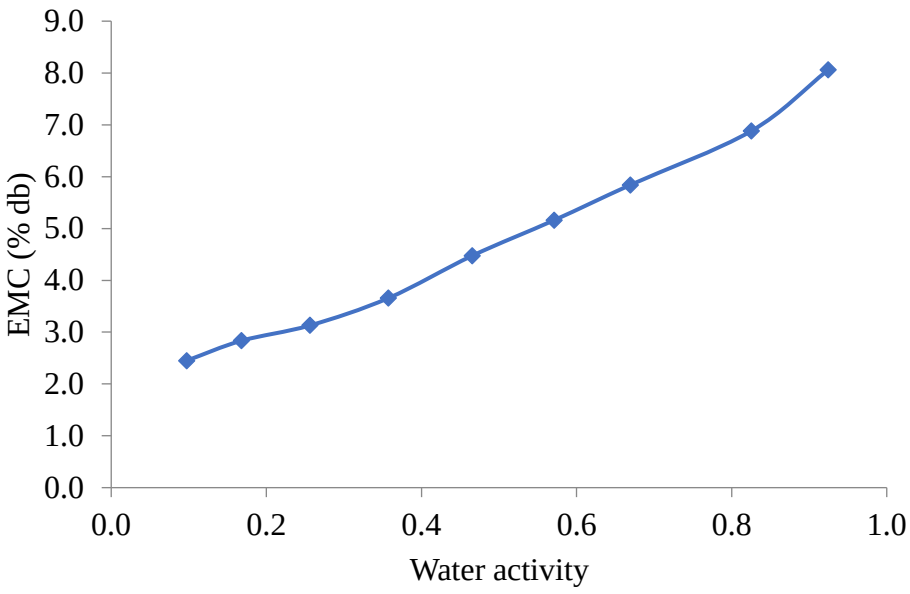

Figure A13: Moringa seed grits desorption at 30^{o}C

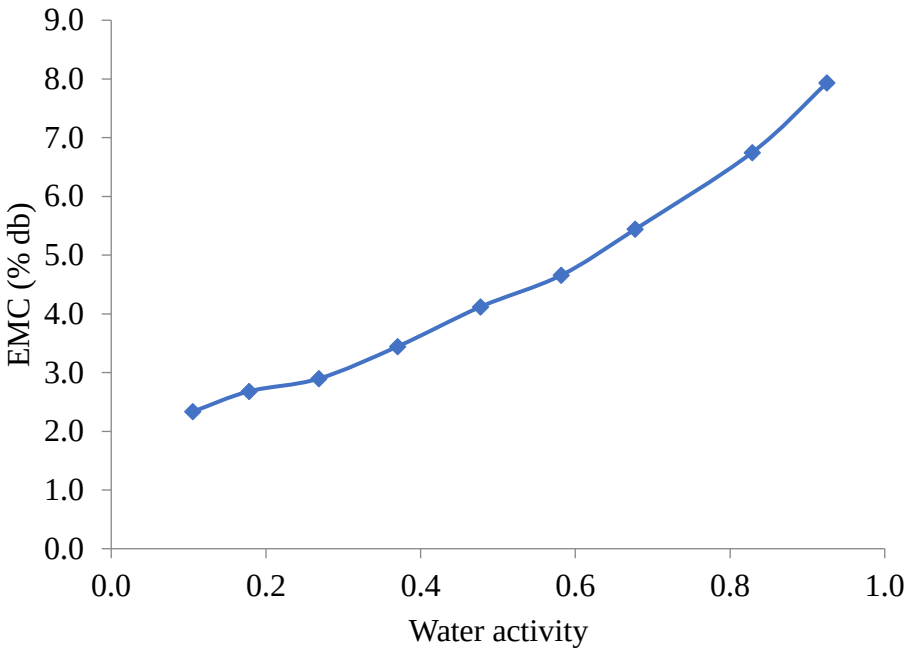

Figure A14: Moringa seed grits desorption at 35^{o}C

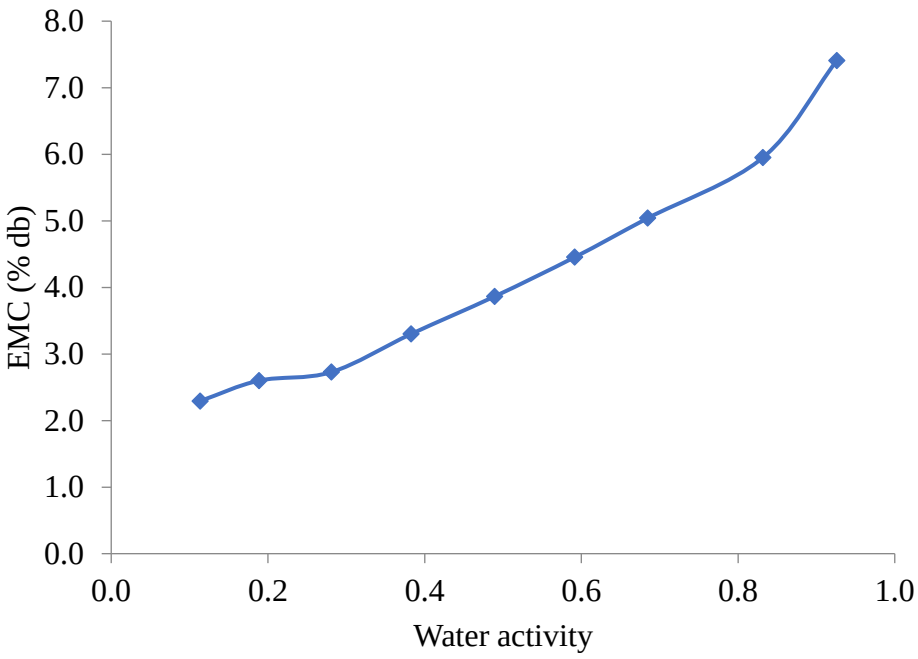

Figure A15: Moringa seed grits desorption at 40^{o}C

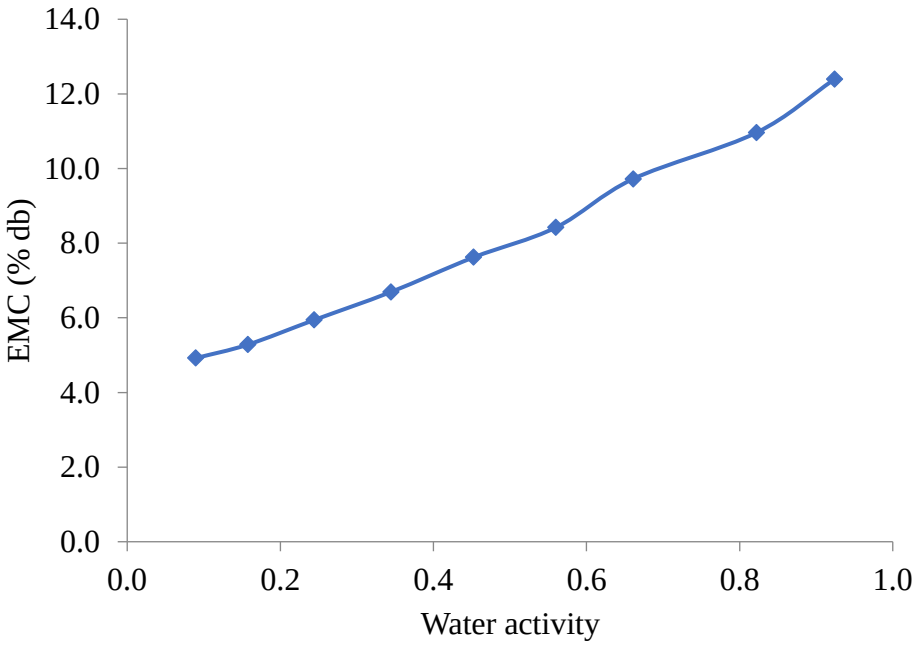

Figure A16: Moringa seed desorption at 20^{o}C

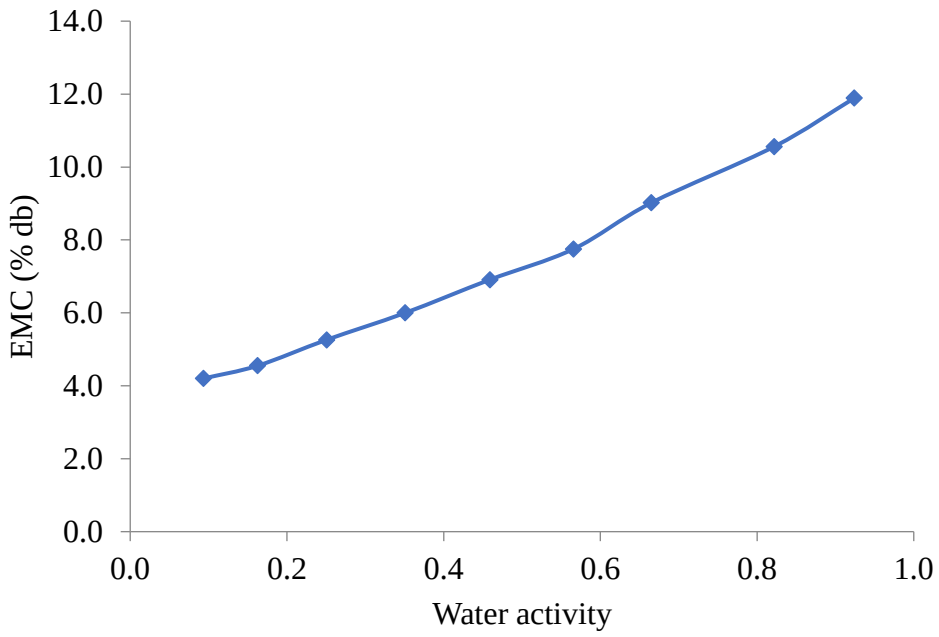

Figure A17: Moringa seed desorption at 25^{o}C

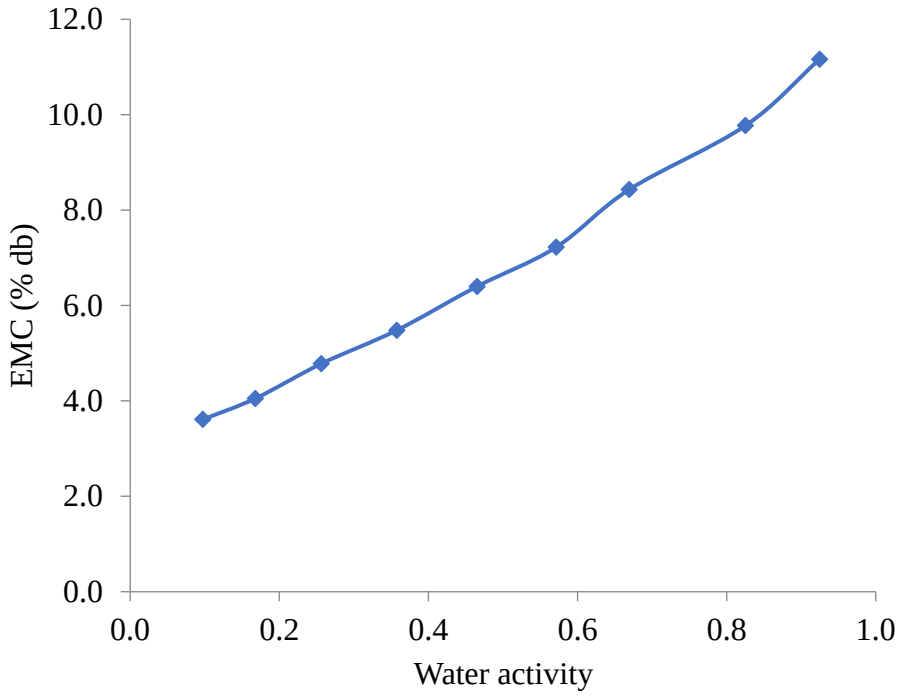

Figure A18: Moringa seed desorption at 30^{o}C

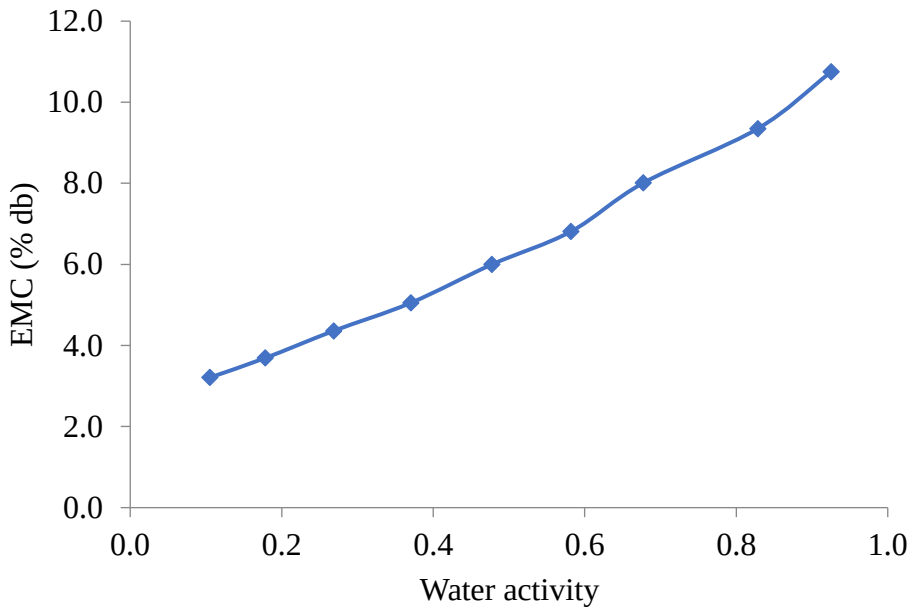

Figure A19: Moringa seed desorption at 35^{o}C

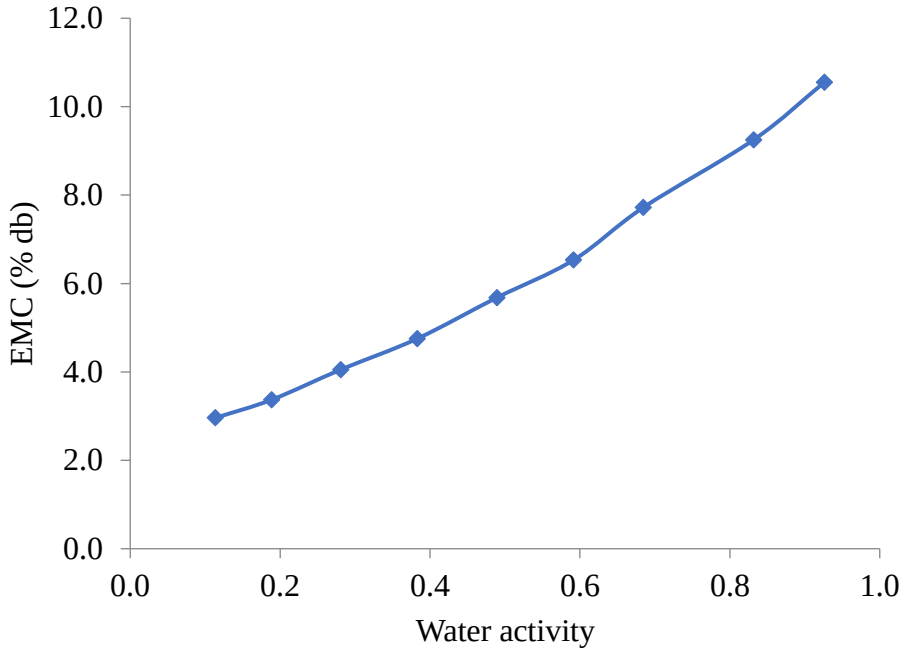

Figure A20: Moringa seed desorption at 40^{o}C

APPENDIX B: BET isotherm plots

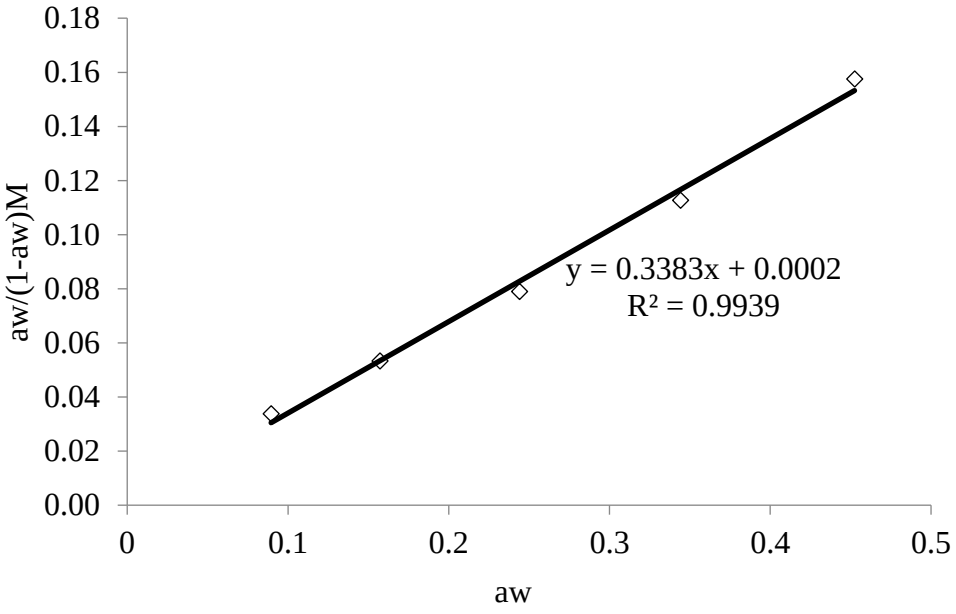

Figure B1: Moringa seed grits adsorption with BET model at 20^{o}C

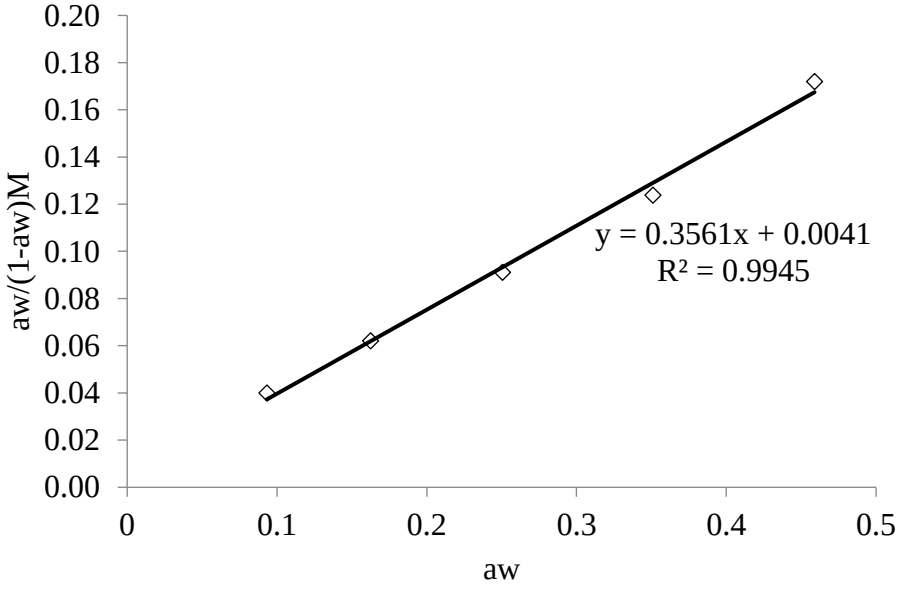

Figure B2: Moringa seed grits adsorption with BET model at 25^{o}C

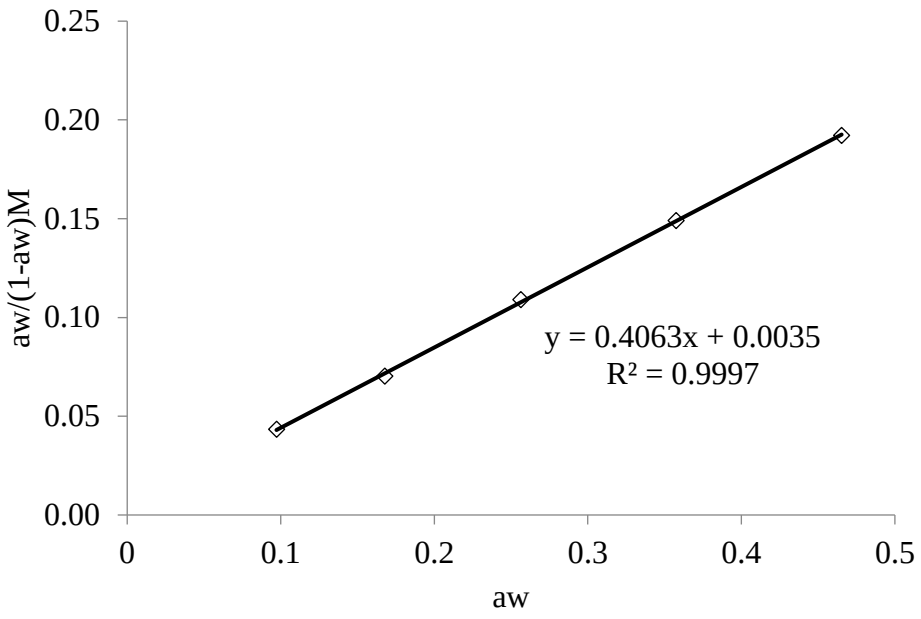

Figure B3: Moringa seed grits adsorption with BET model at 30^{o}C

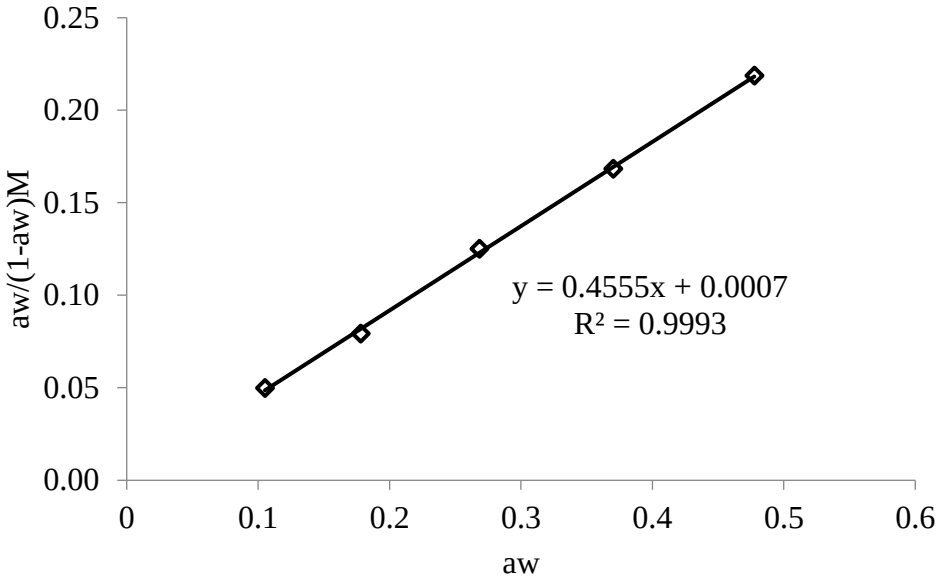

Figure B4: Moringa seed grits adsorption with BET model at 35^{o}C

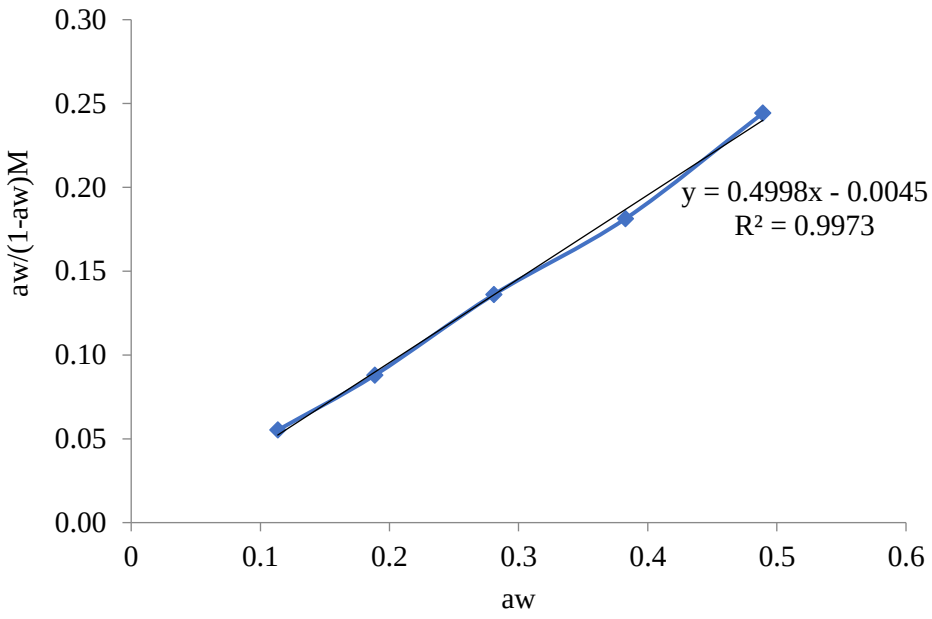

Figure B5: Moringa seed grits adsorption with BET model at 40^{o}C

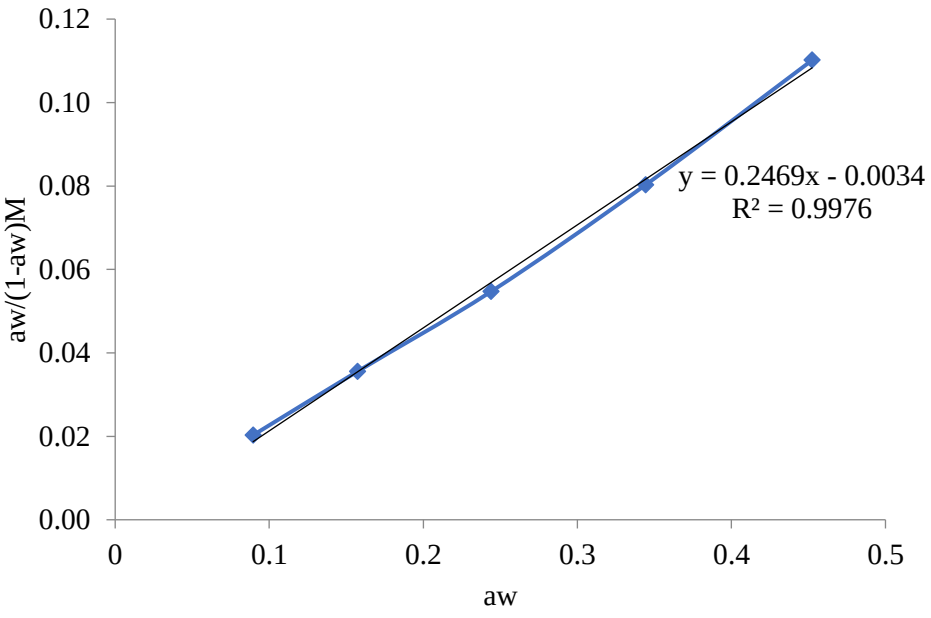

Figure B6: Moringa seed adsorption with BET model at 20^{o}C

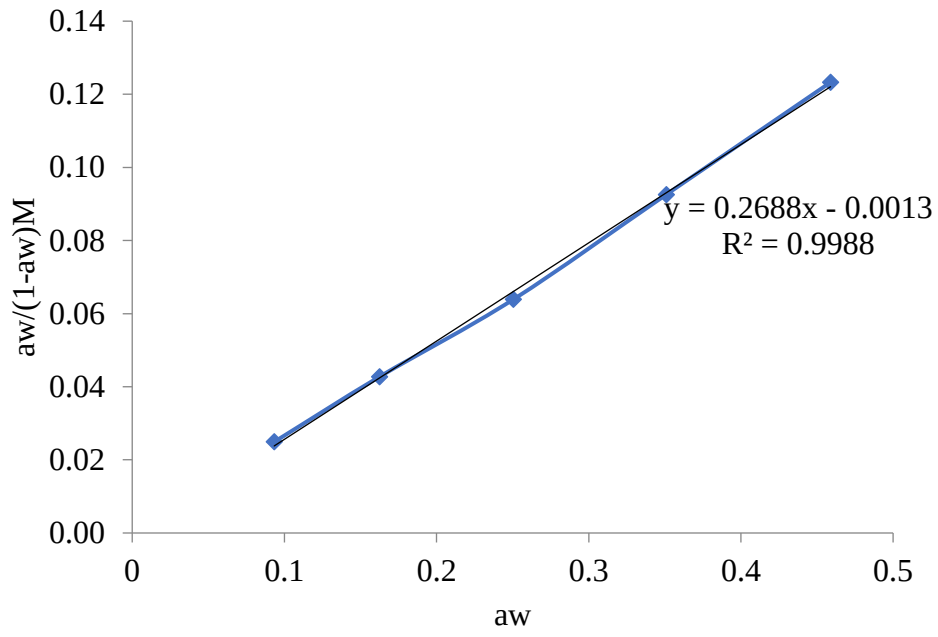

Figure B7: Moringa seed adsorption with BET model at 25°C

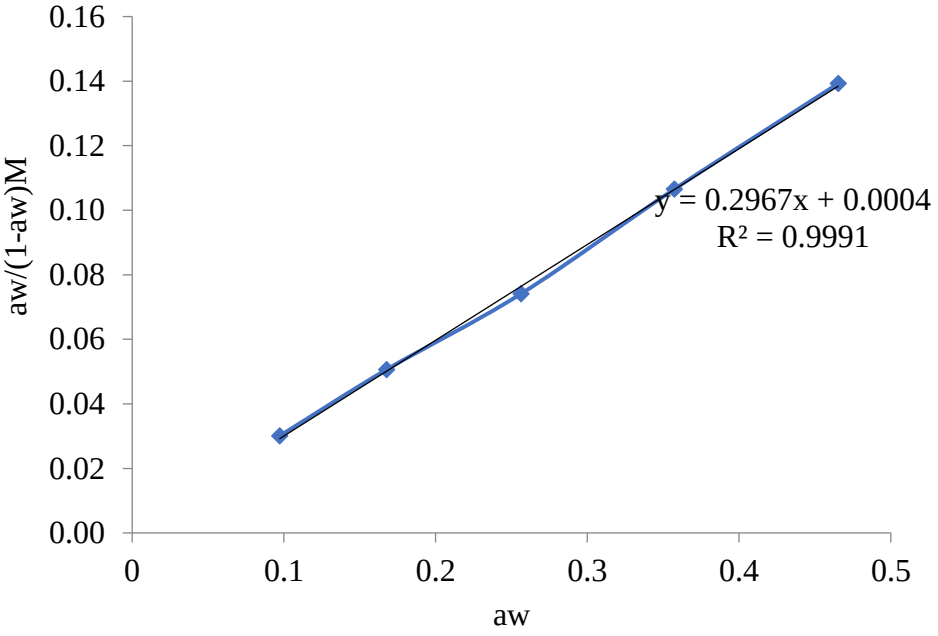

Figure B8: Moringa seed adsorption with BET model at 30°C

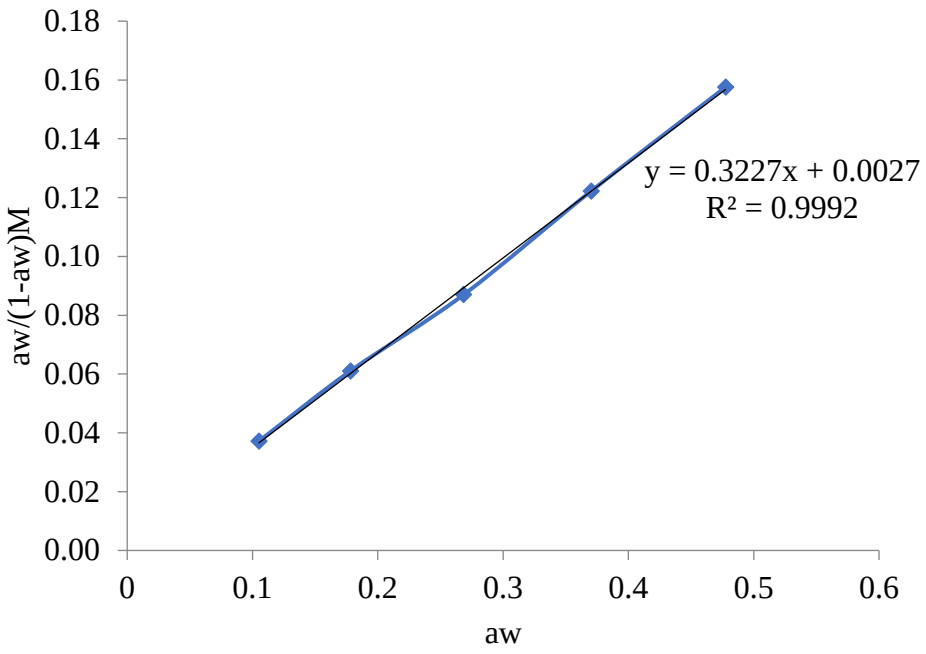

Figure B9: Moringa seed adsorption with BET model at 35^{o}C

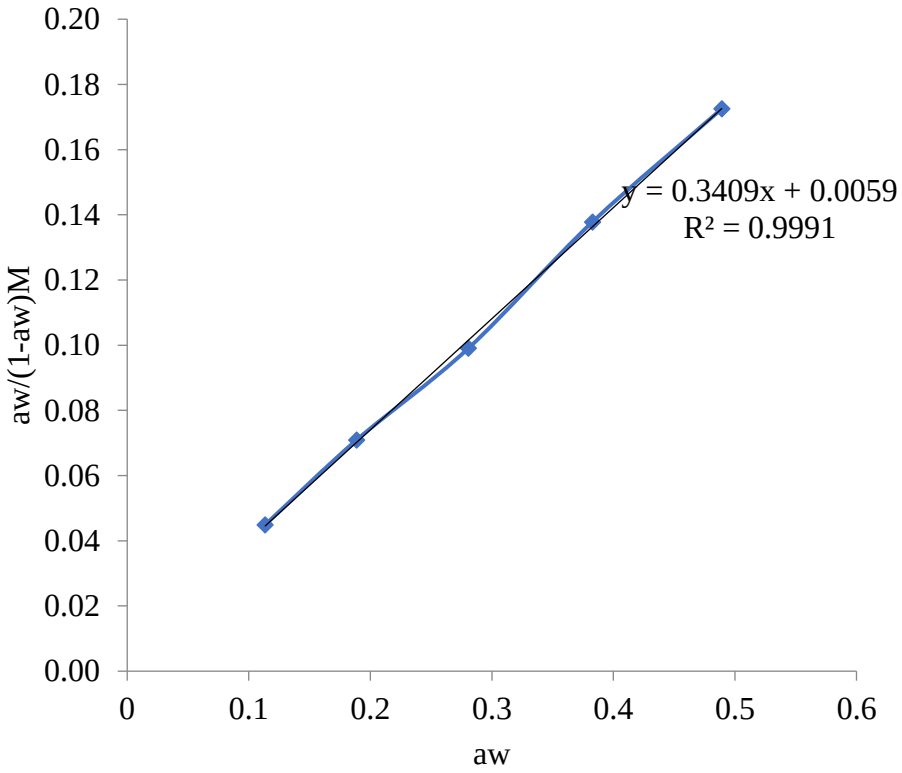

Figure B10: Moringa seed adsorption with BET model at 40^{o}C

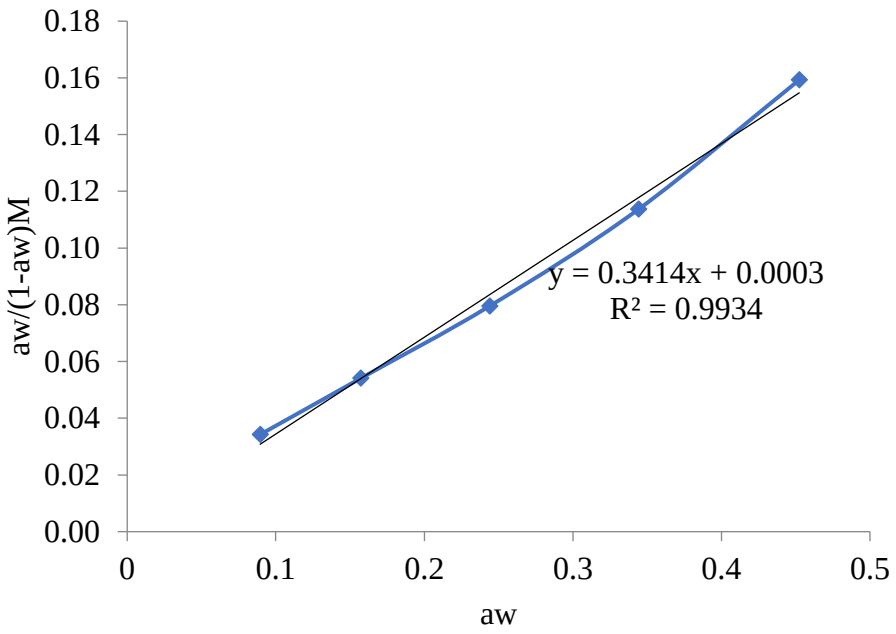

Figure B11: Moringa seed grits desorption with BET model at 20°C

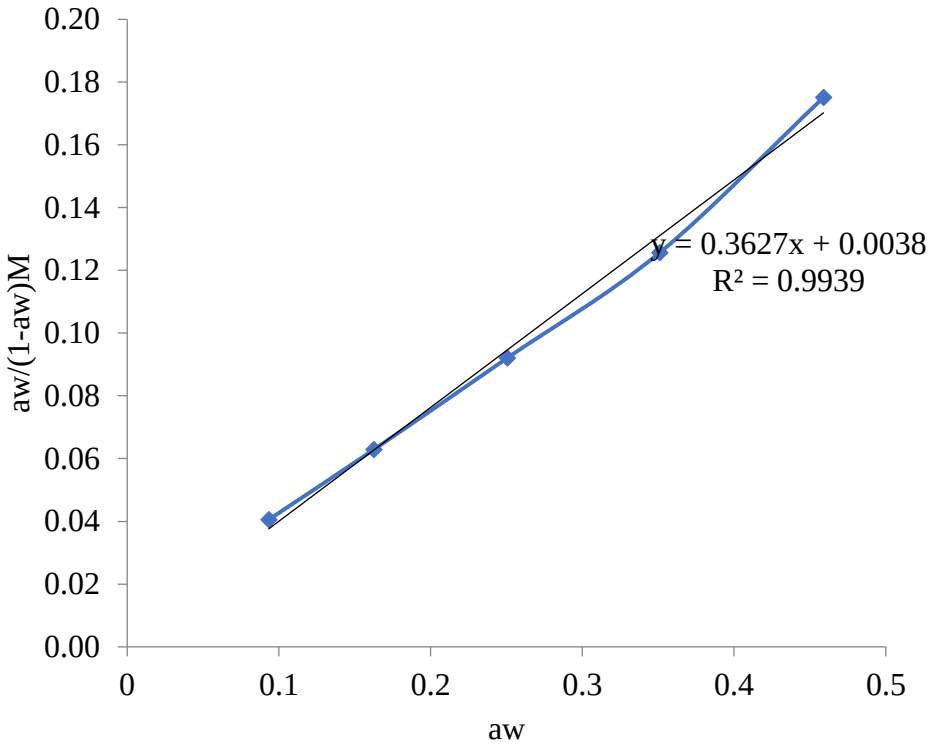

Figure B12: Moringa seed grits desorption with BET model at 25°C

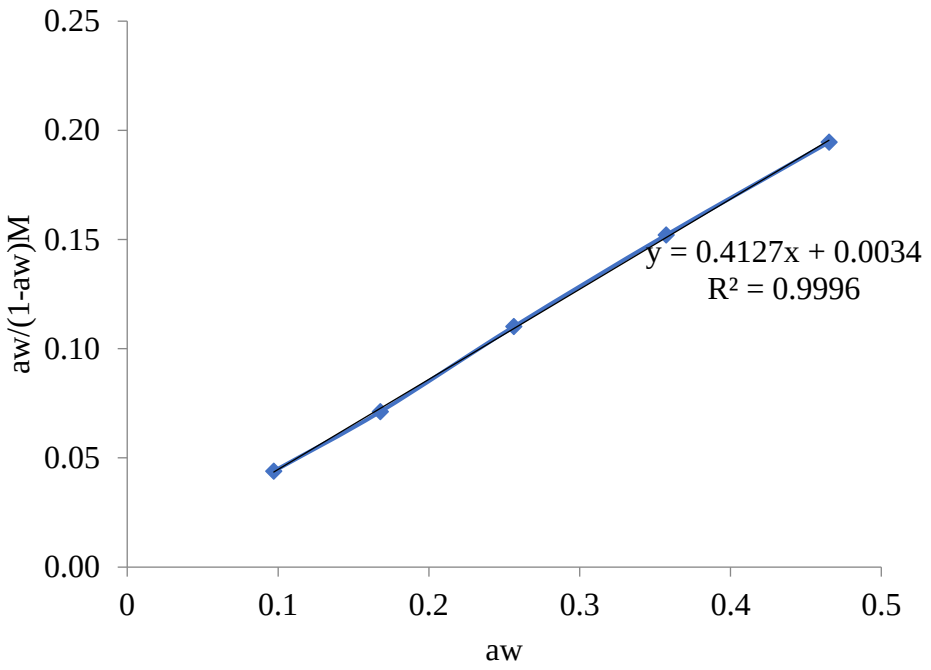

Figure B13: Moringa seed grits desorption with BET model at 30°C

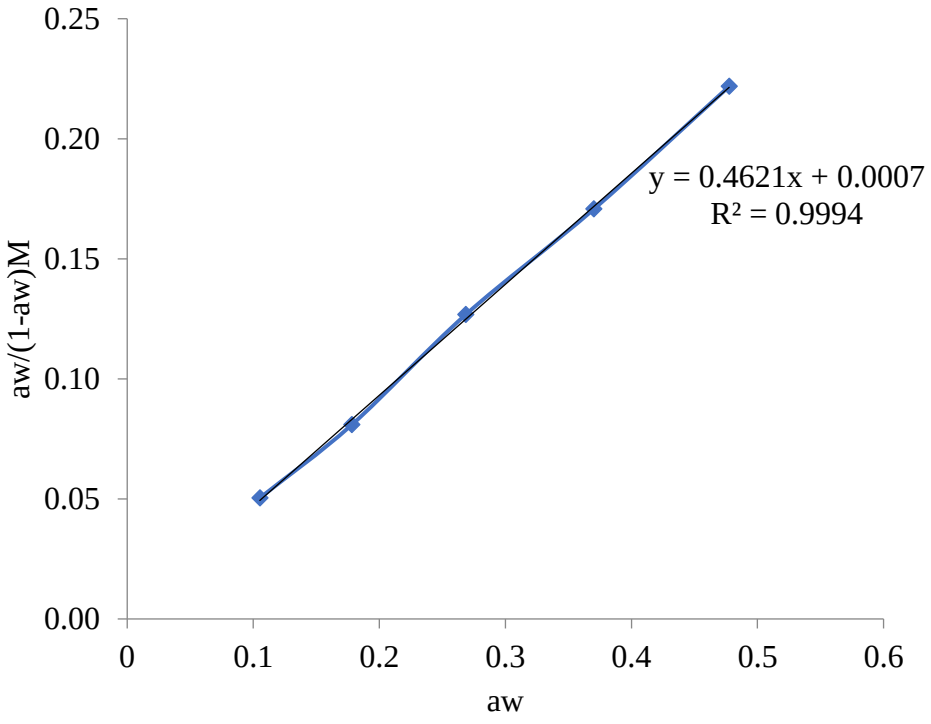

Figure B14: Moringa seed grits desorption with BET model at 35°C

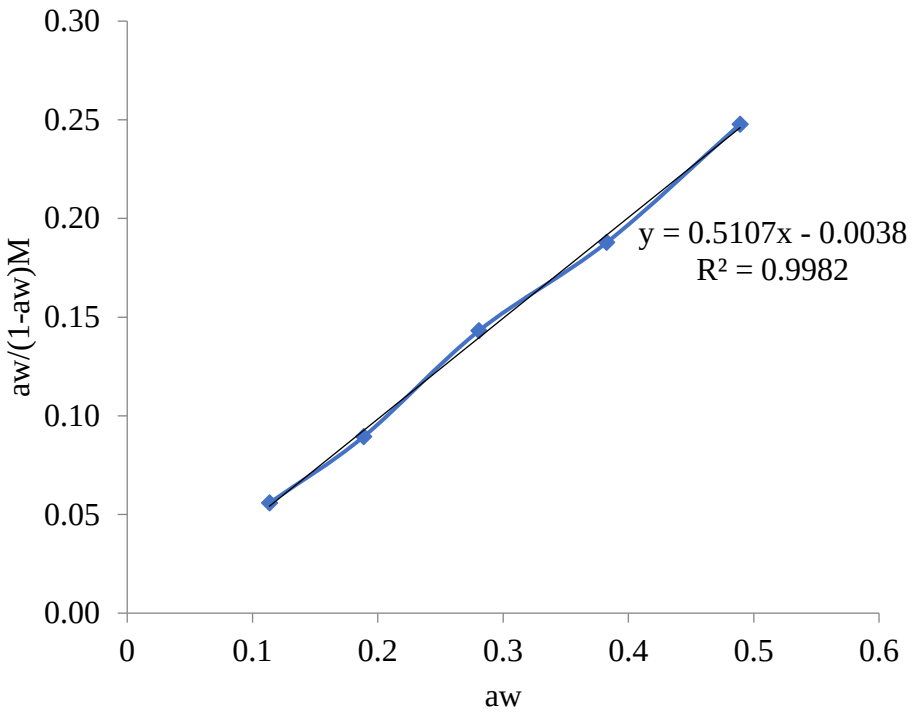

Figure B15: Moringa seed grits desorption with BET model at 40°C

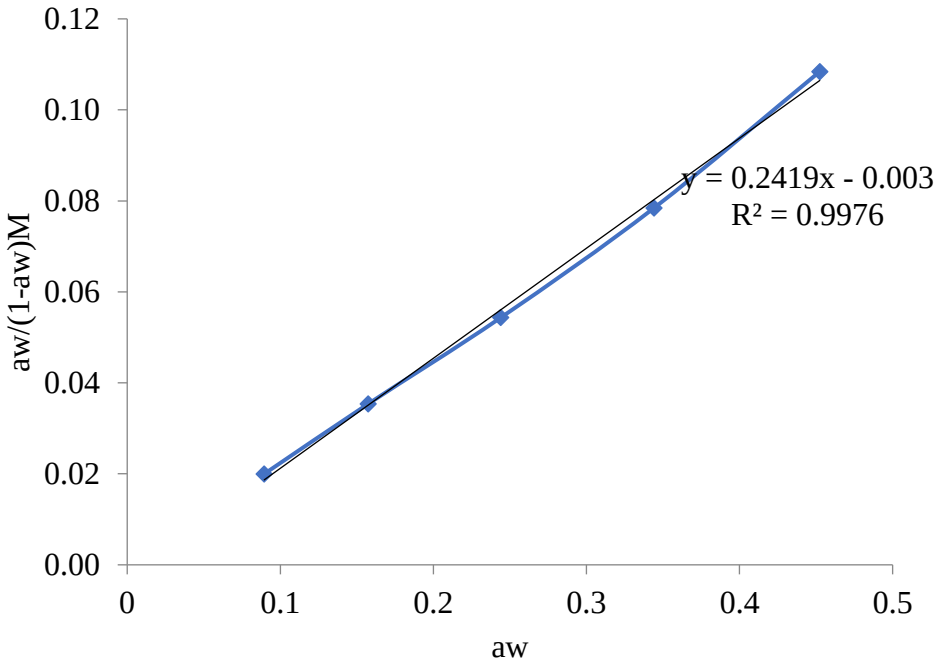

Figure B16: Moringa seed desorption with BET model at 20°C

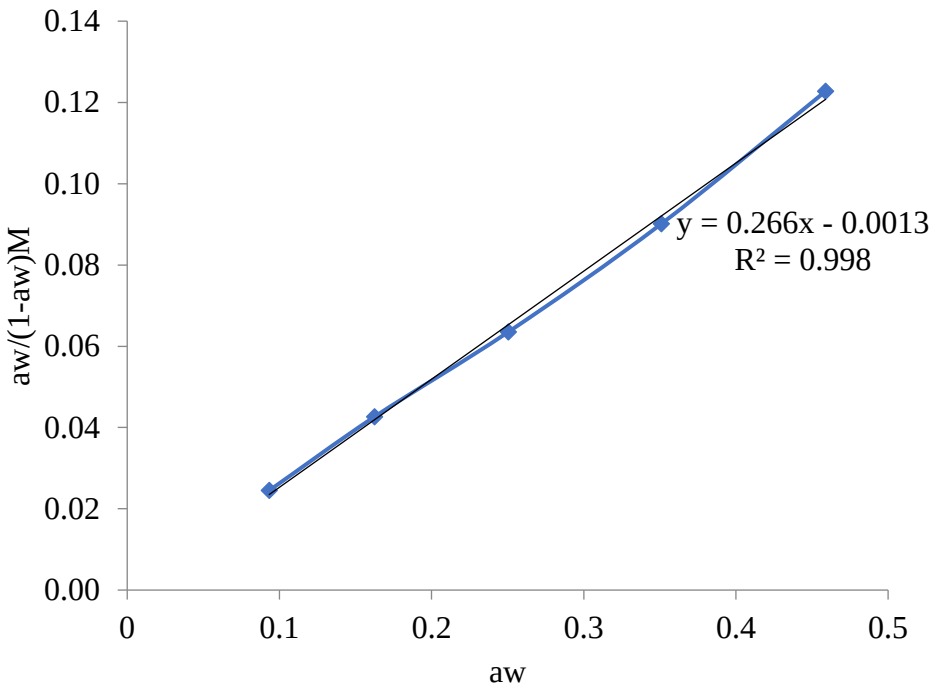

Figure B17: Moringa seed desorption with BET model at 25°C

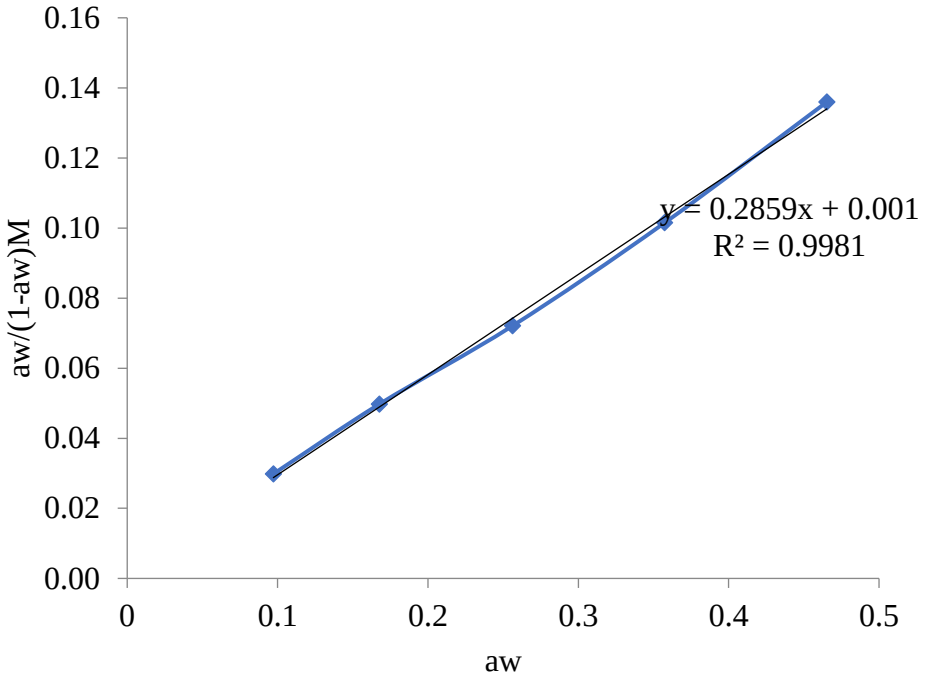

Figure B18: Moringa seed desorption with BET model at 30°C

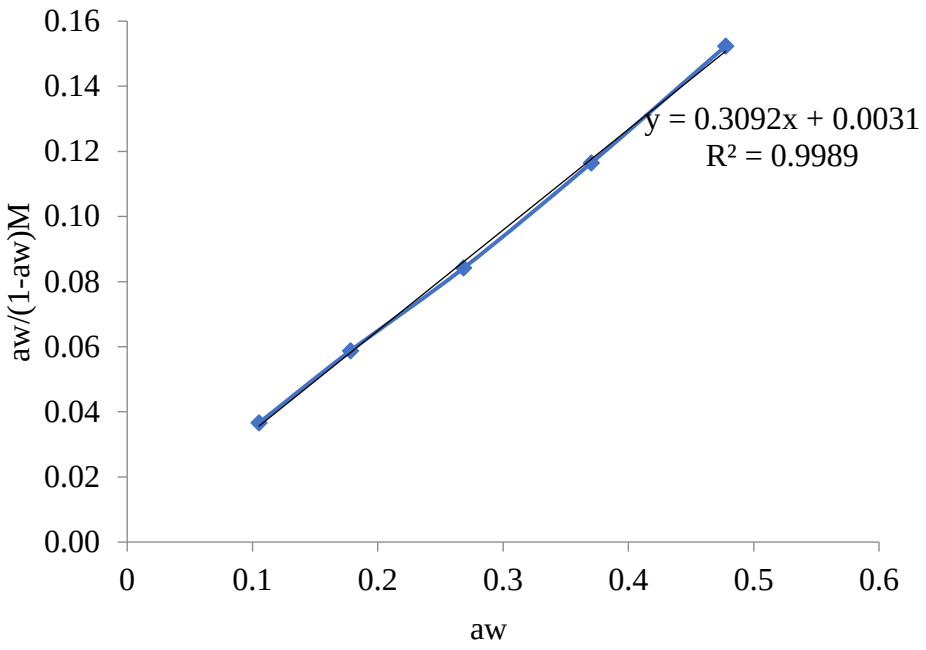

Figure B19: Moringa seed desorption with BET model at 35°C

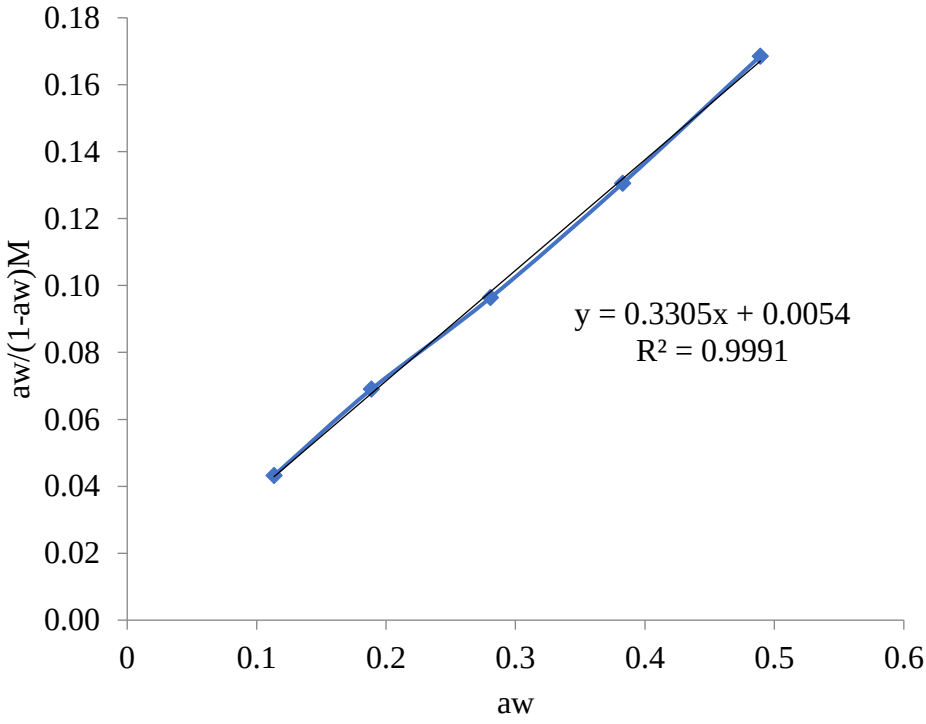

Figure B20: Moringa seed desorption with BET model at 40°C

APPENDIX C: GAB isotherm plots

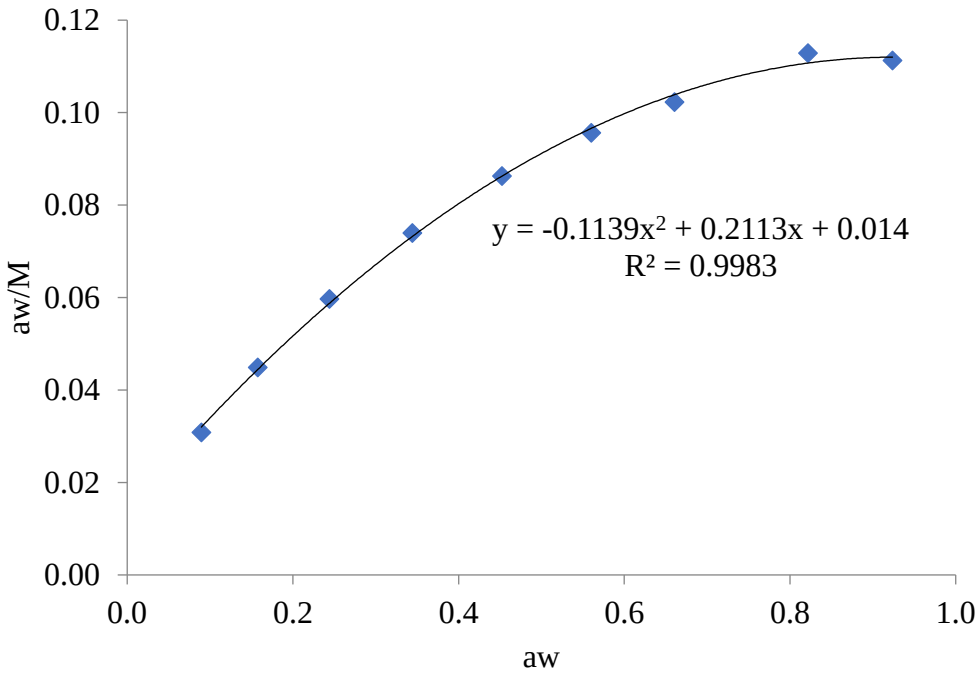

Figure C1: Moringa seed grits adsorption with GAB model at 20ºC

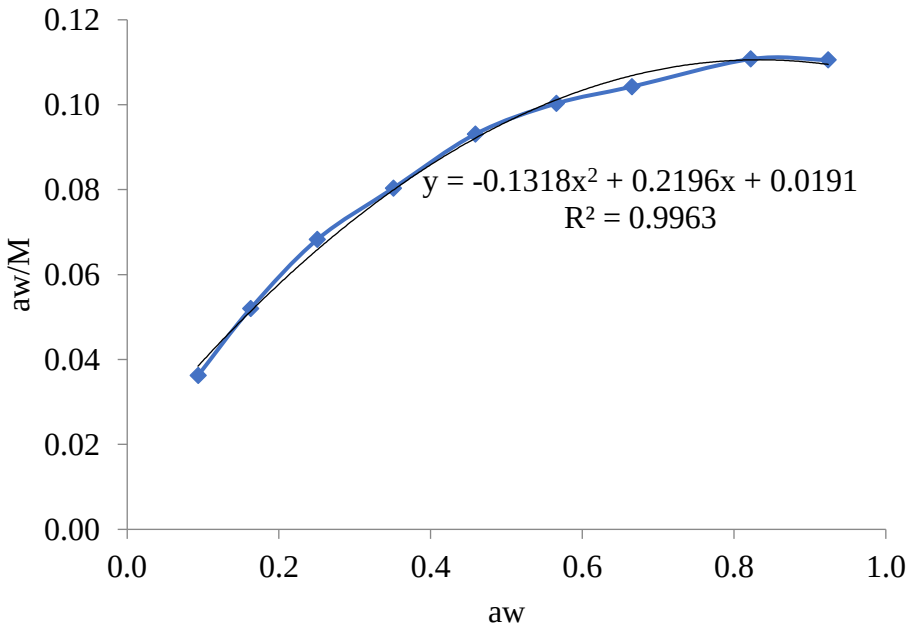

Figure C2: Moringa seed grits adsorption with GAB model at 25ºC

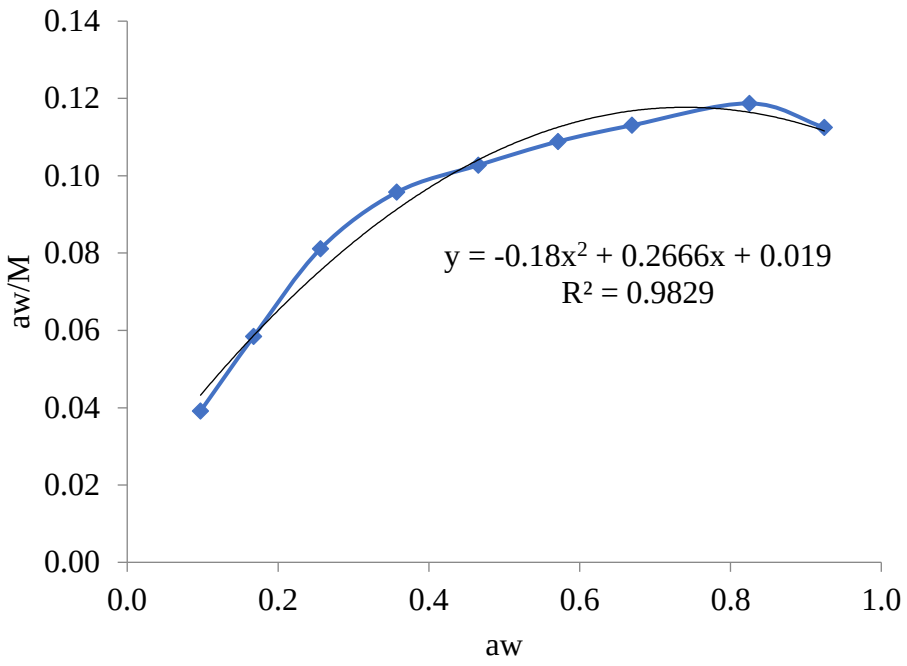

Figure C3: Moringa seed grits adsorption with GAB model at 30°C

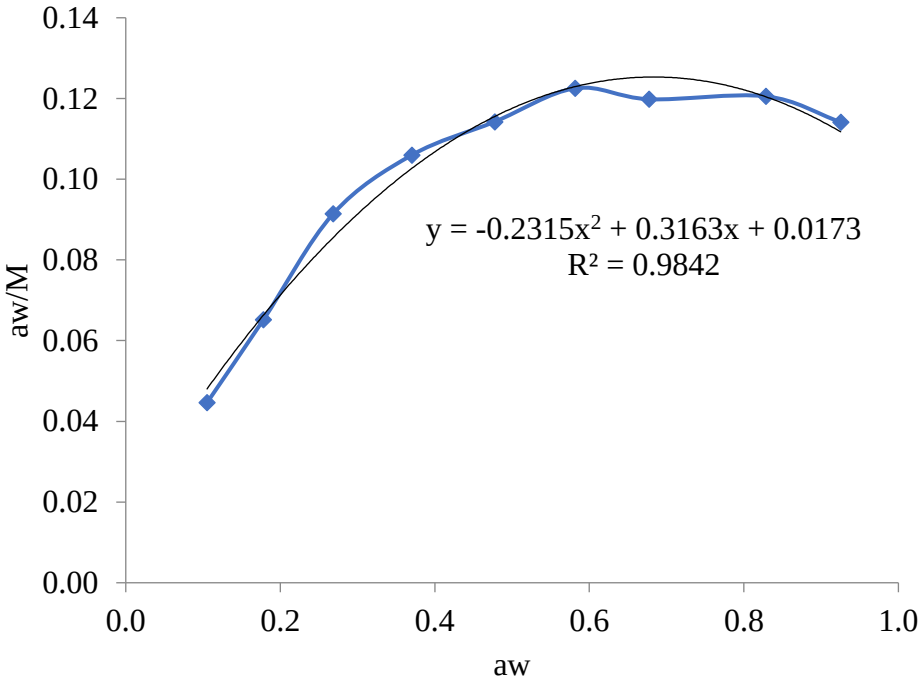

Figure C4: Moringa seed grits adsorption with GAB model at 35°C

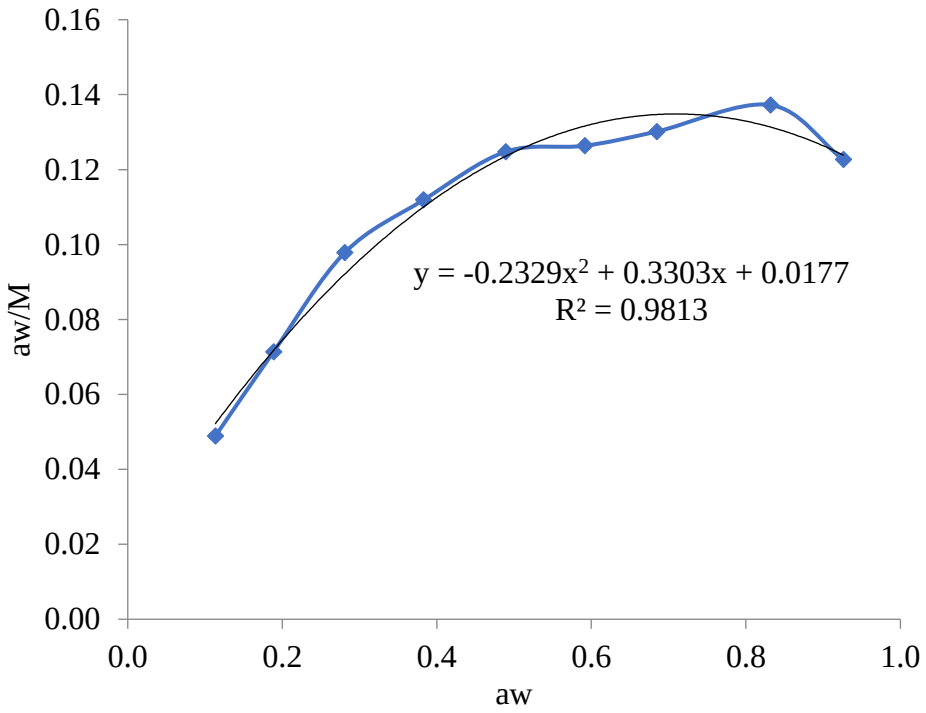

Figure C5: Moringa seed grits adsorption with GAB model at 40°C

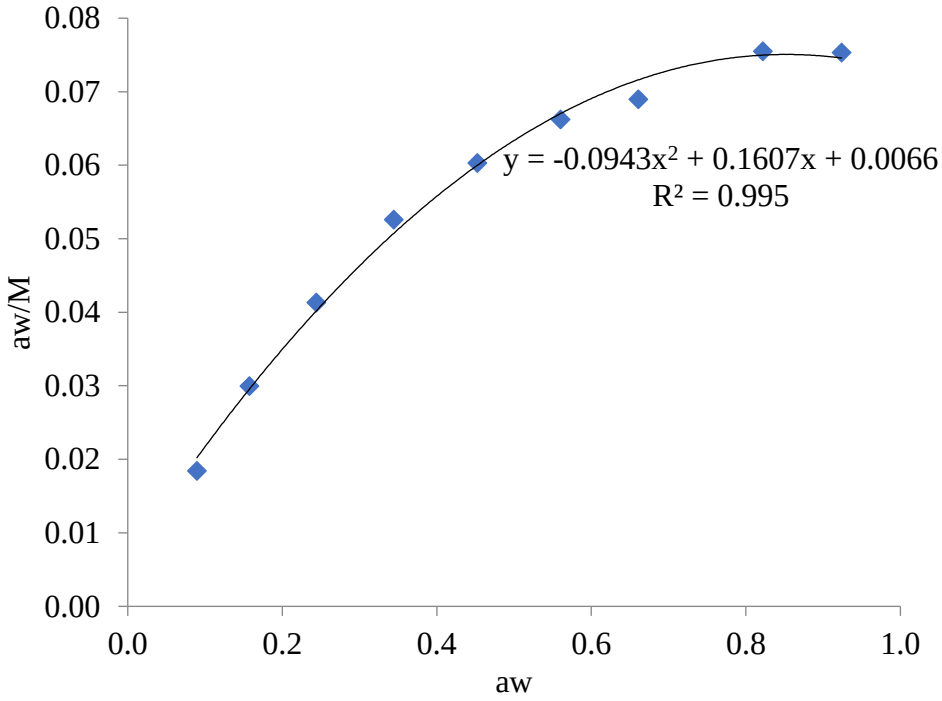

Figure C6: Moringa seed adsorption with GAB model at 20°C

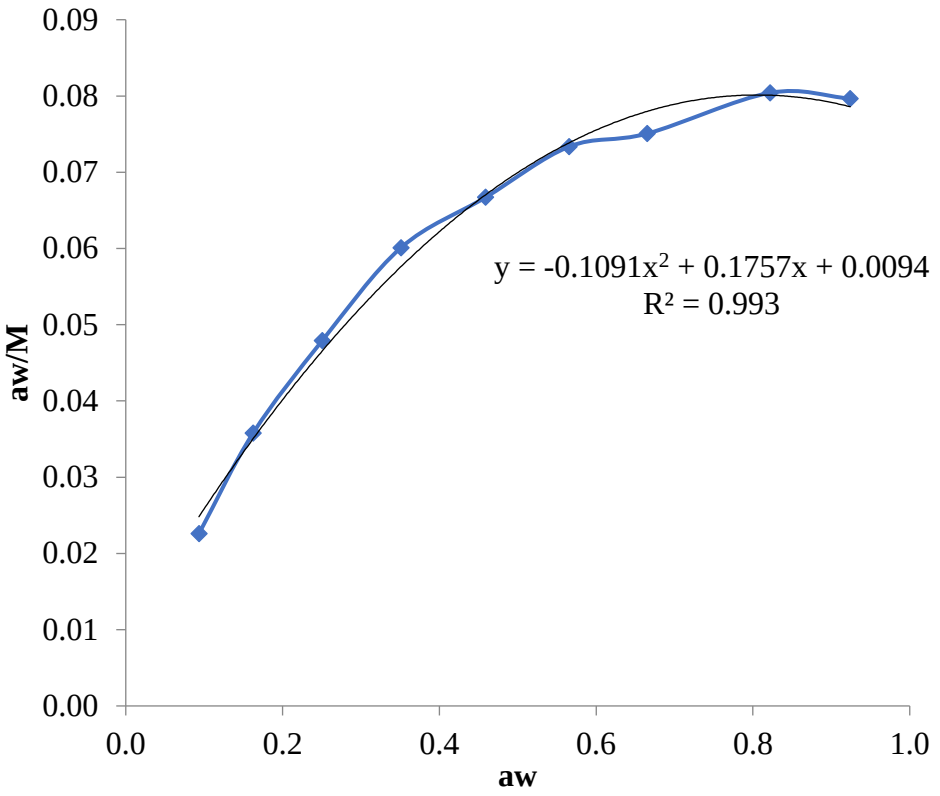

Figure C7: Moringa seed adsorption with GAB model at 25ºC

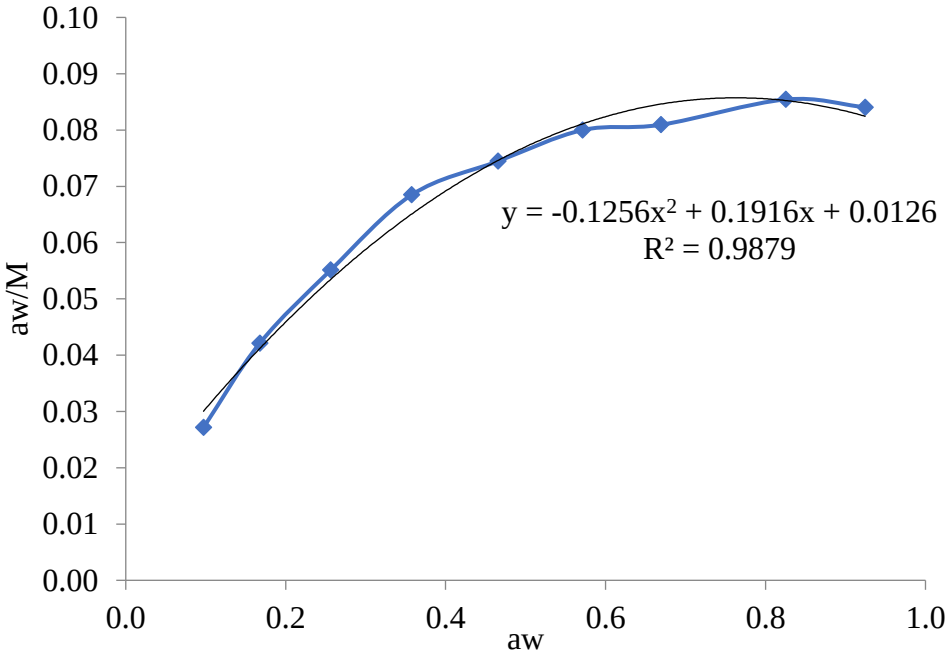

Figure C8: Moringa seed adsorption with GAB model at 30ºC

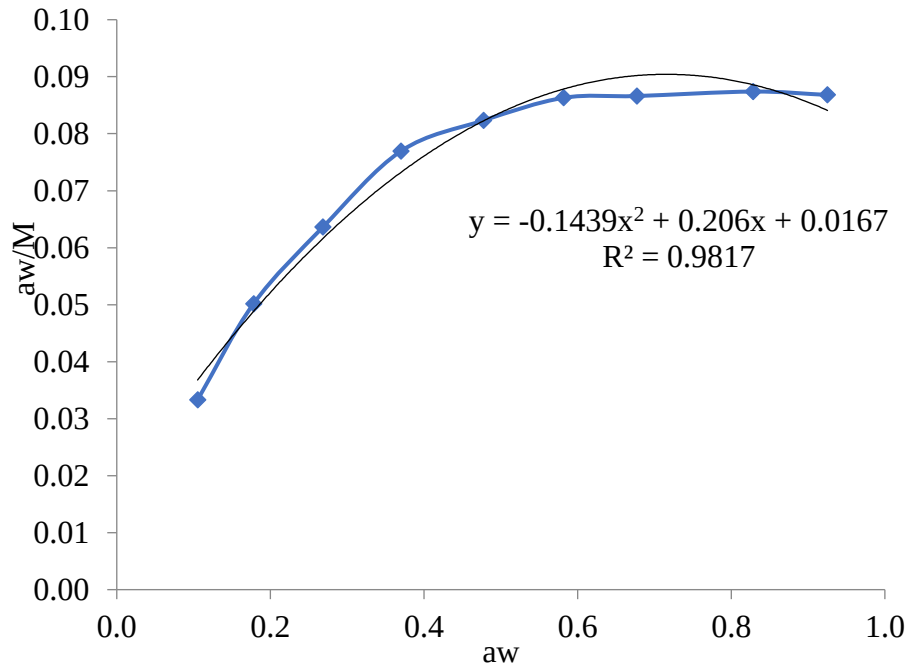

Figure C9: Moringa seed adsorption with GAB model at 35ºC

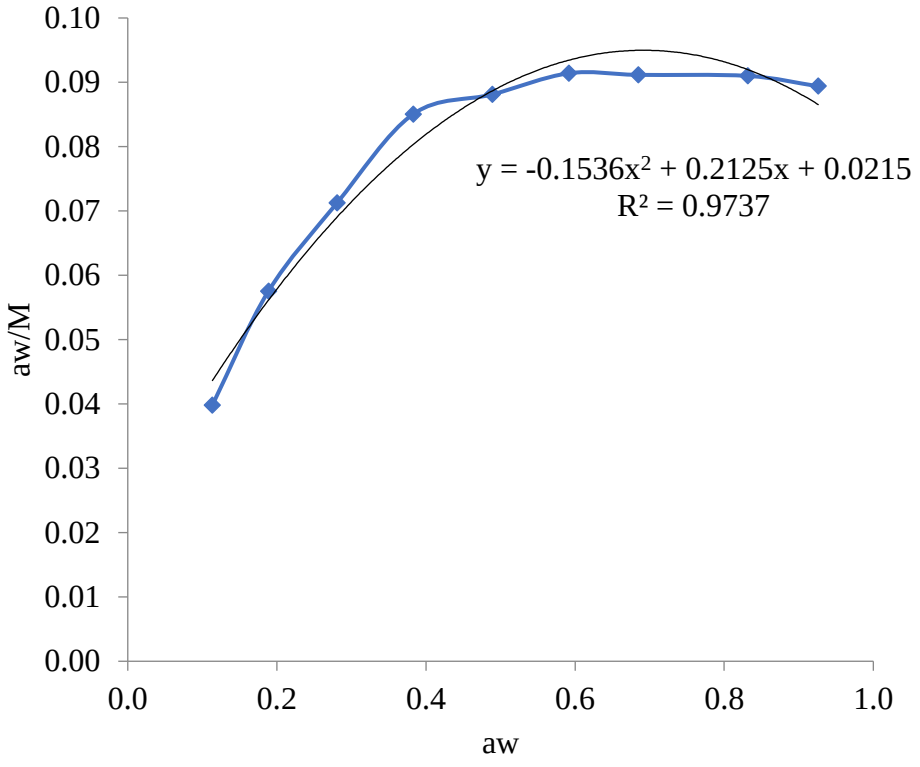

Figure C10: Moringa seed adsorption with GAB model at 40ºC

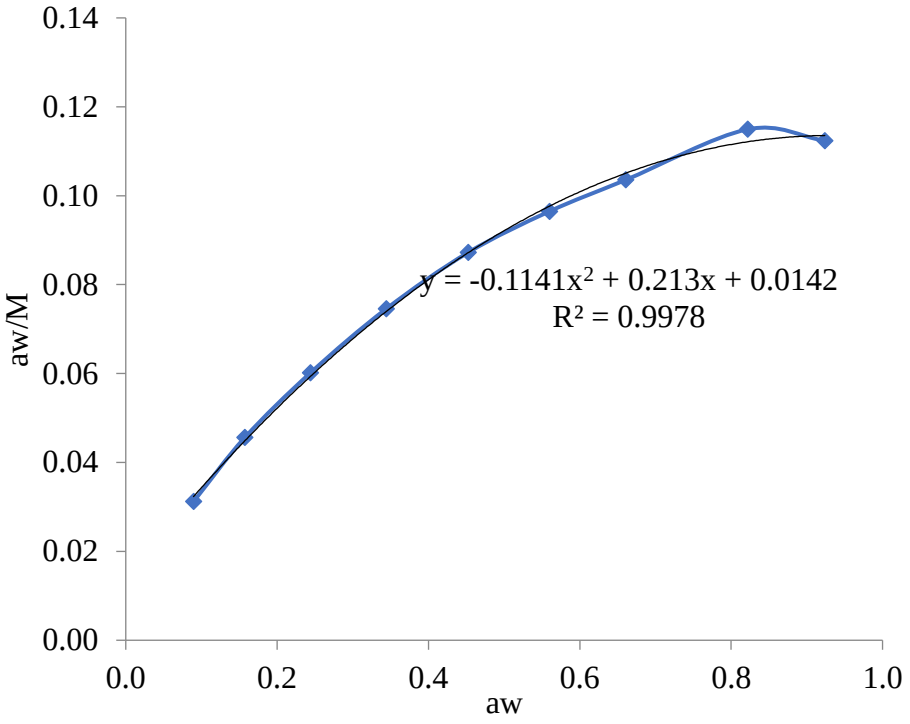

Figure C11: Moringa seed grits desorption with GAB model at 20°C

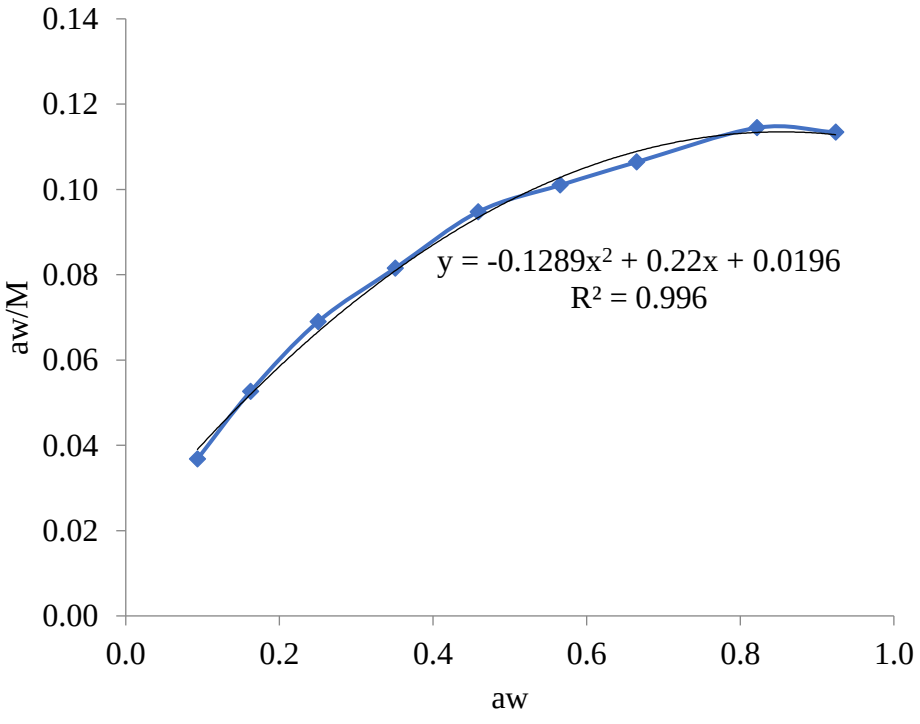

Figure C12: Moringa seed grits desorption with GAB model at 25°C

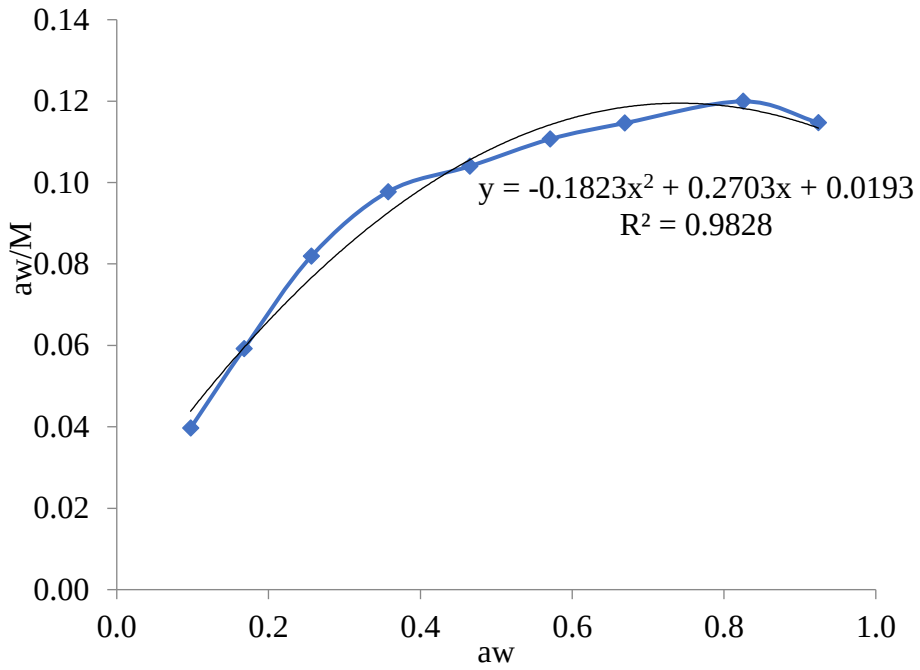

Figure C13: Moringa seed grits desorption with GAB model at 30ºC

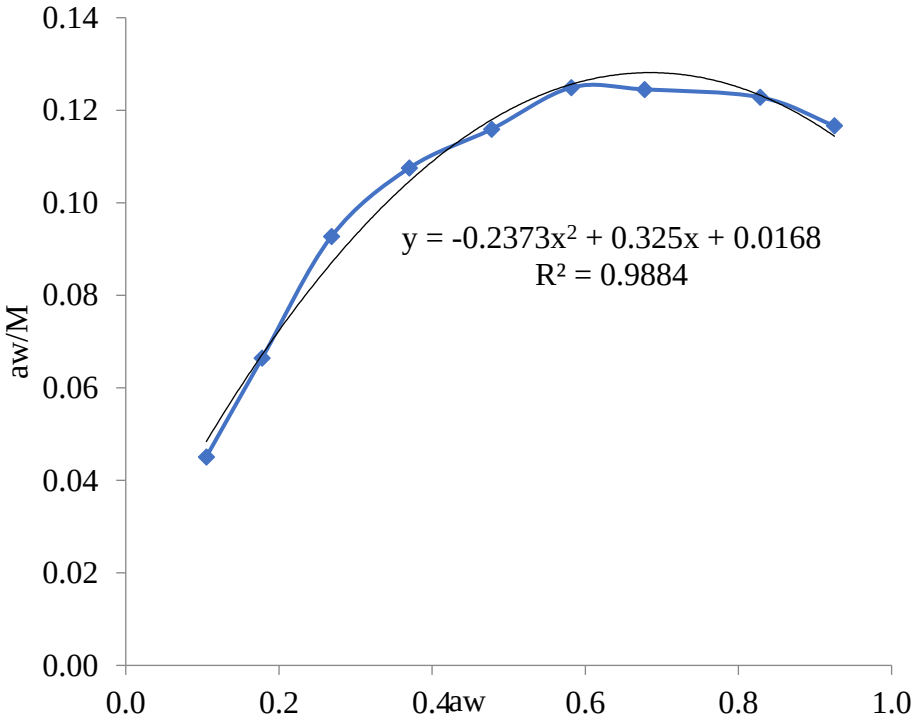

Figure C14: Moringa seed grits desorption with GAB model at 35ºC

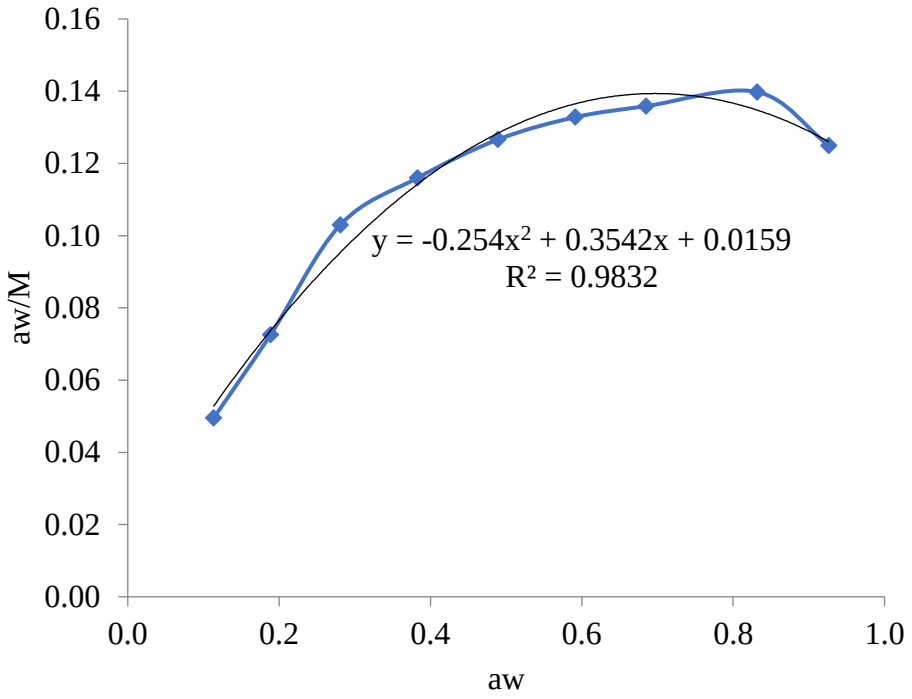

Figure C15: Moringa seed grits desorption with GAB model at 40°C

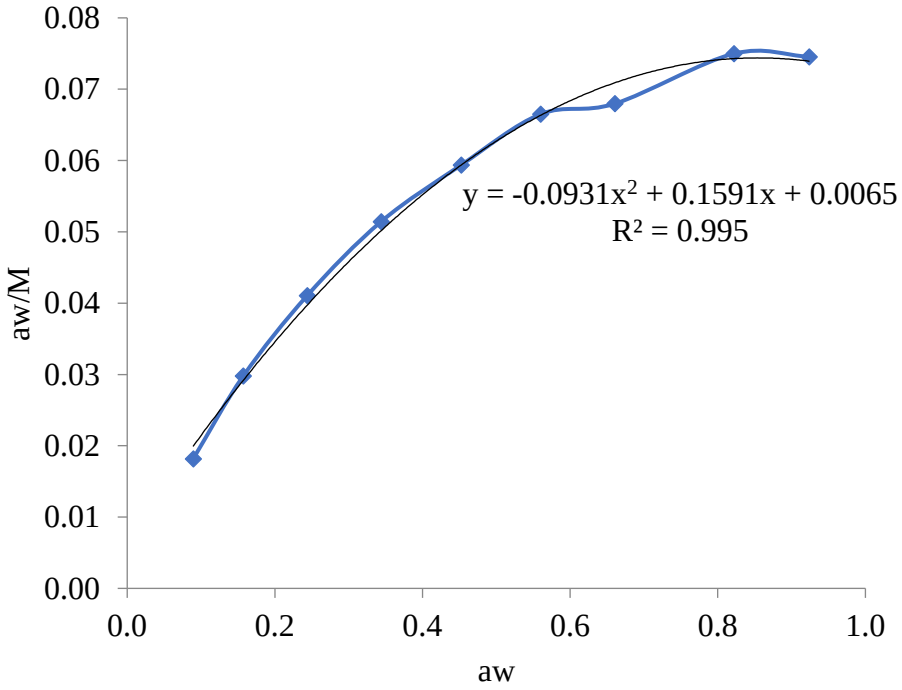

Figure C16: Moringa seed desorption with GAB model at 20°C

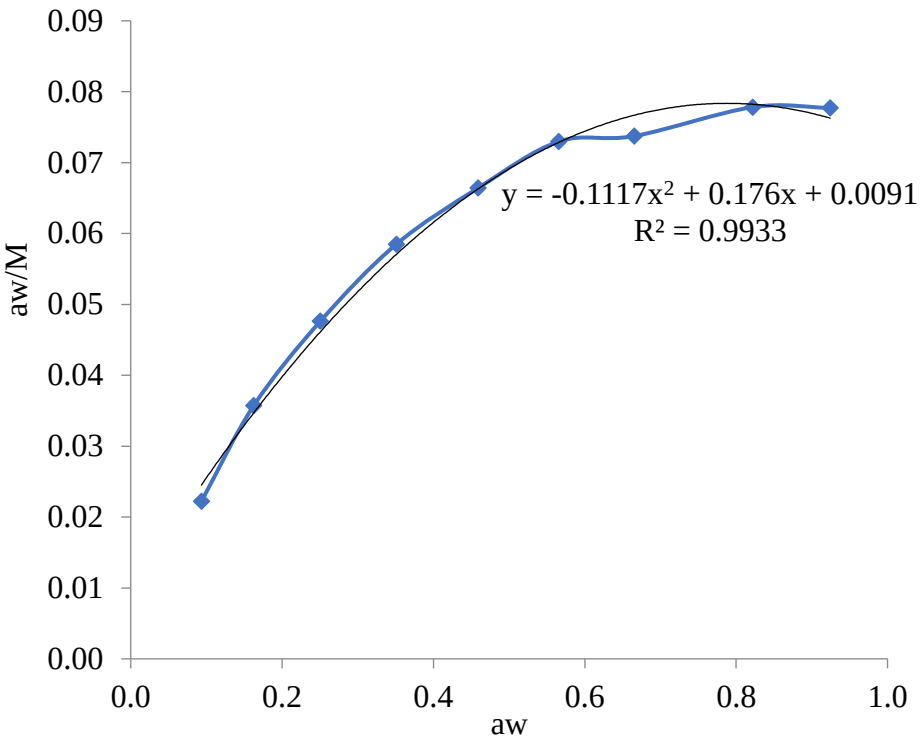

Figure C17: Moringa seed desorption with GAB model at 25ºC

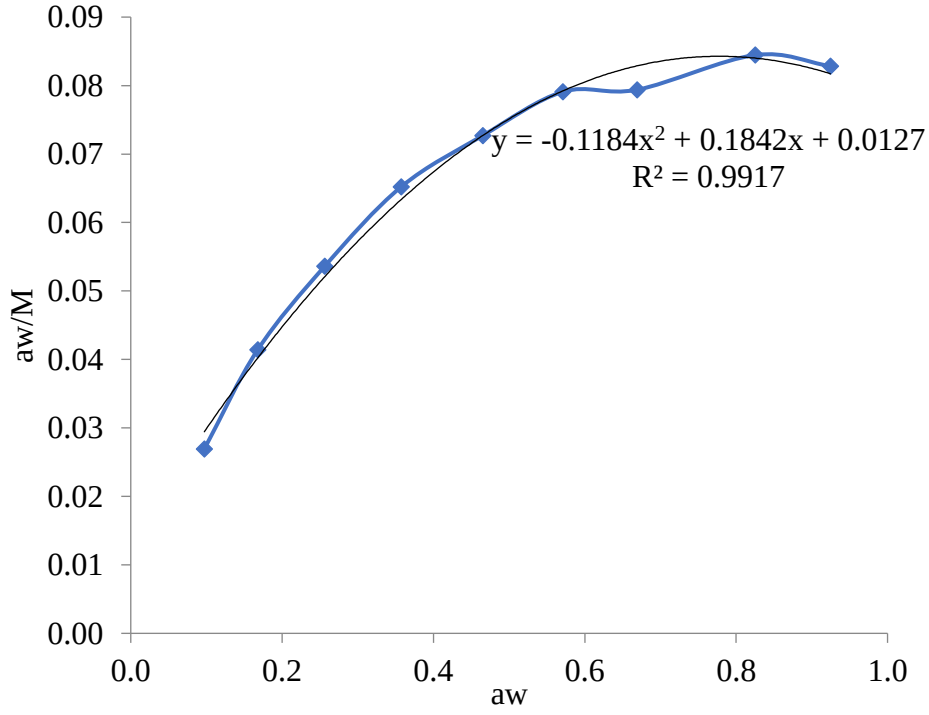

Figure C18: Moringa seed desorption with GAB model at 30ºC

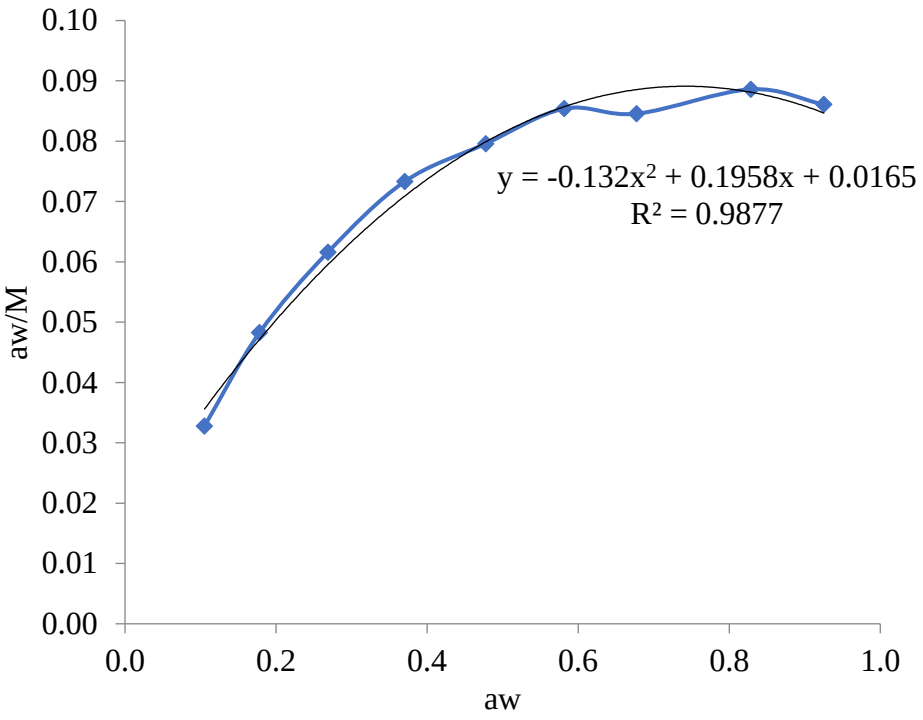

Figure C19: Moringa seed desorption with GAB model at 35ºC

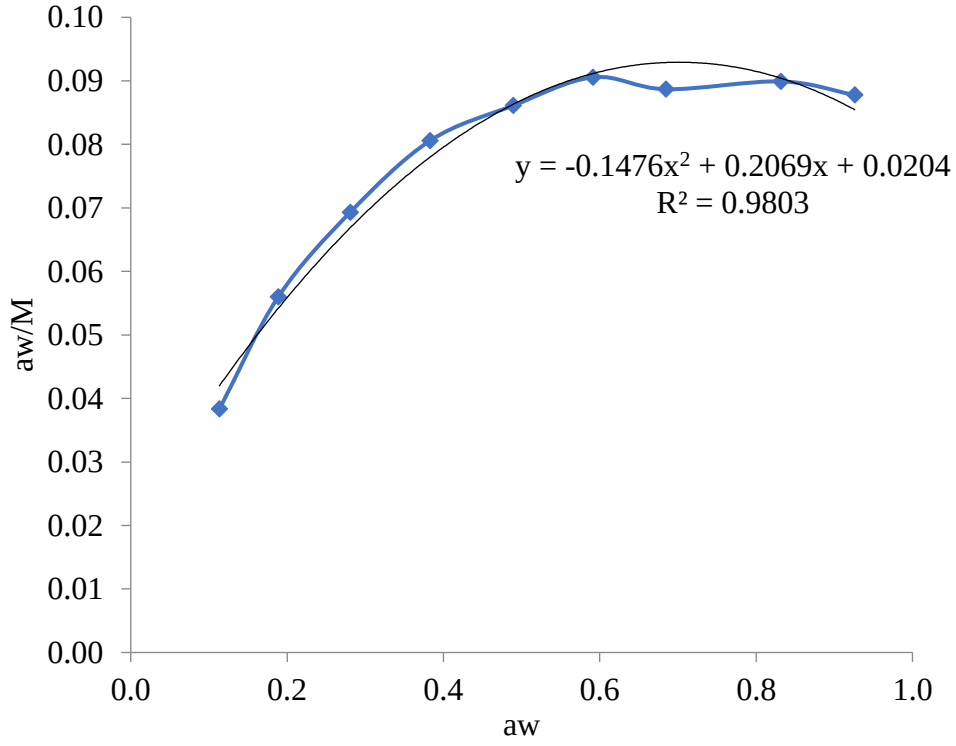

Figure C20: Moringa seed desorption with GAB model at 40ºC

APPENDIX D: Modified Henderson plots.

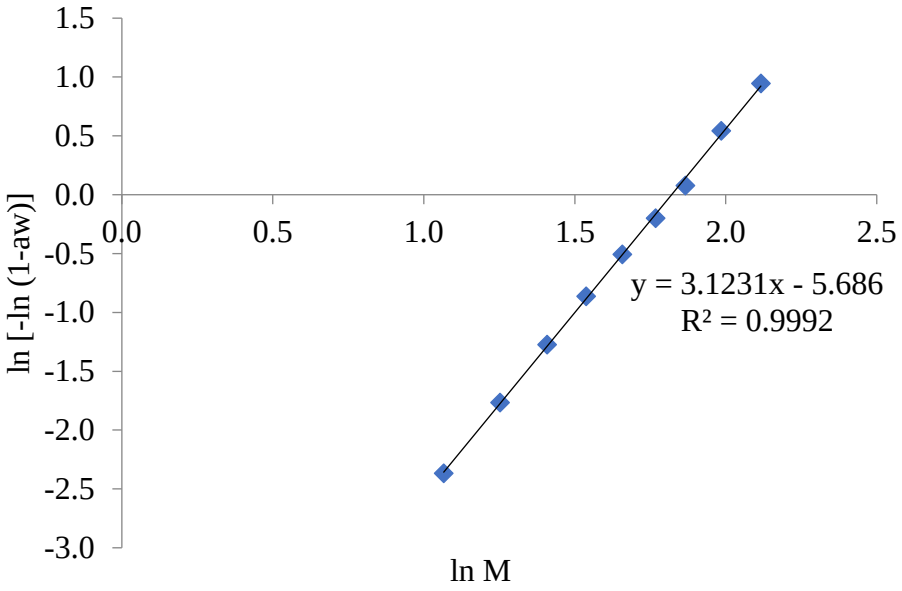

Figure D1: Moringa grits adsorption with modified Henderson model at 20°C

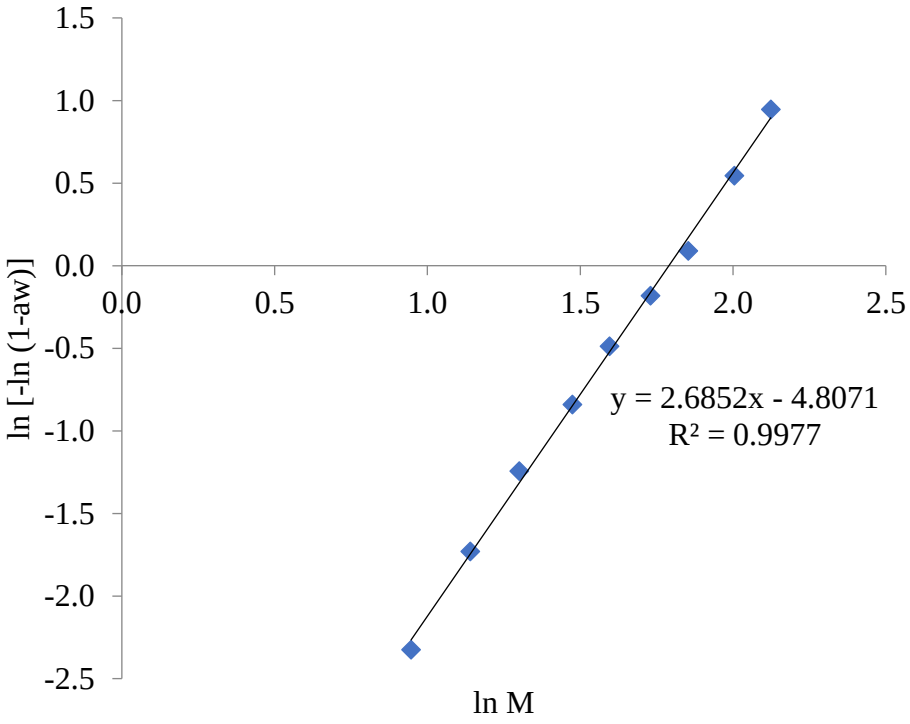

Figure D2: Moringa grits adsorption with modified Henderson model at 25°C

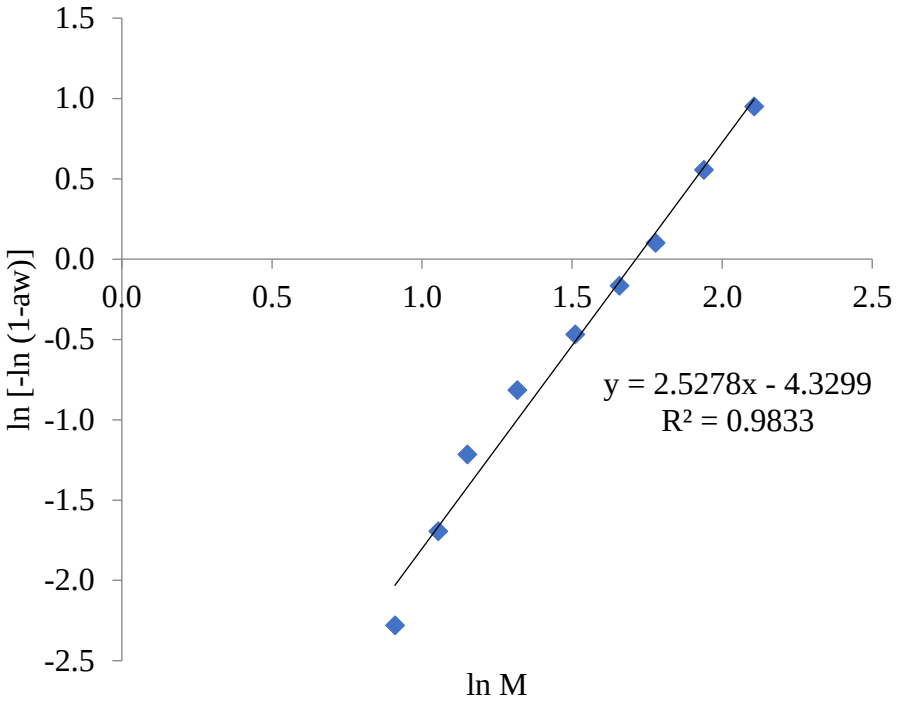

Figure D3: Moringa grits adsorption with modified Henderson model at 30°C

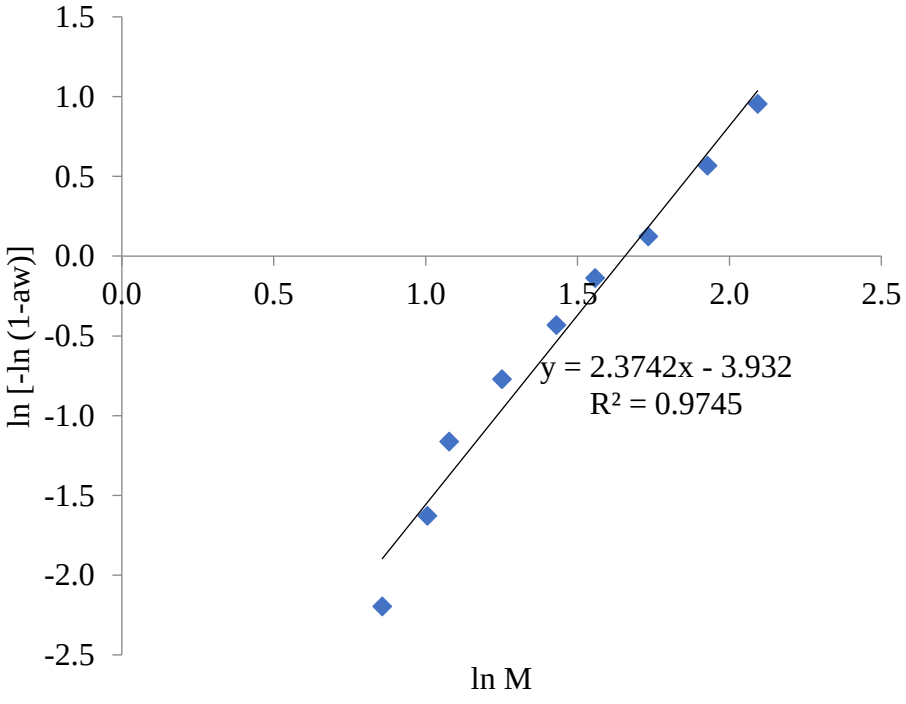

Figure D4: Moringa grits adsorption with modified Henderson model at 35°C

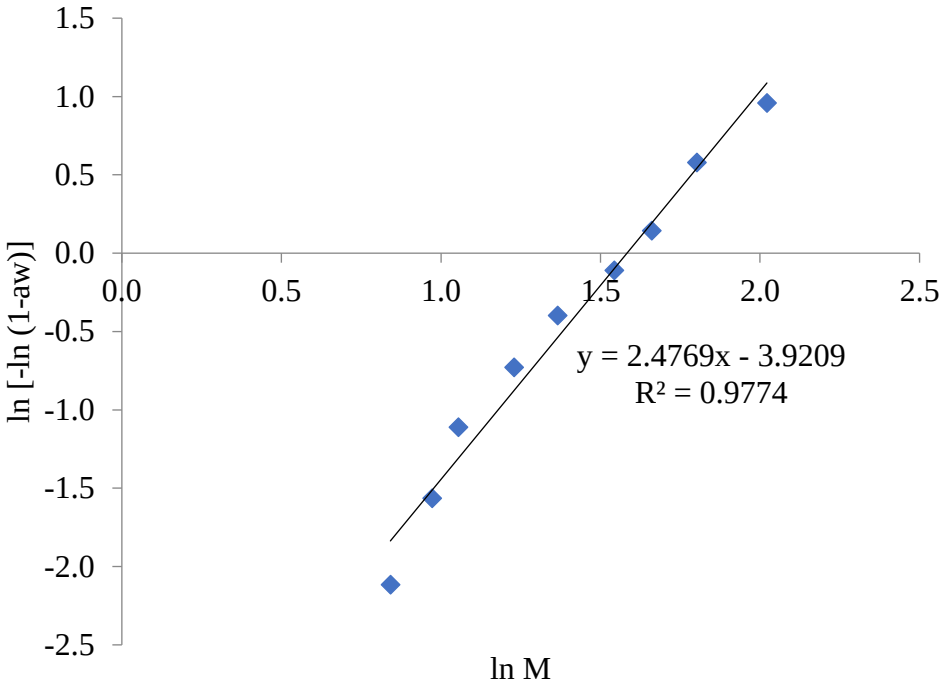

Figure D5: Moringa grits adsorption with modified Henderson model at 40^{o}C

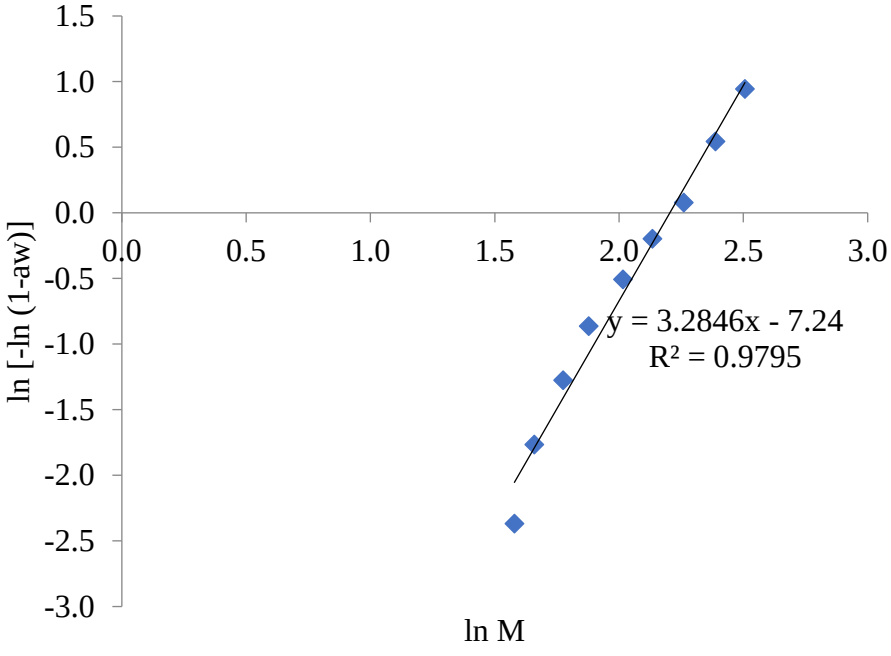

Figure D6: Moringa seed adsorption with modified Henderson model at 20^{o}C

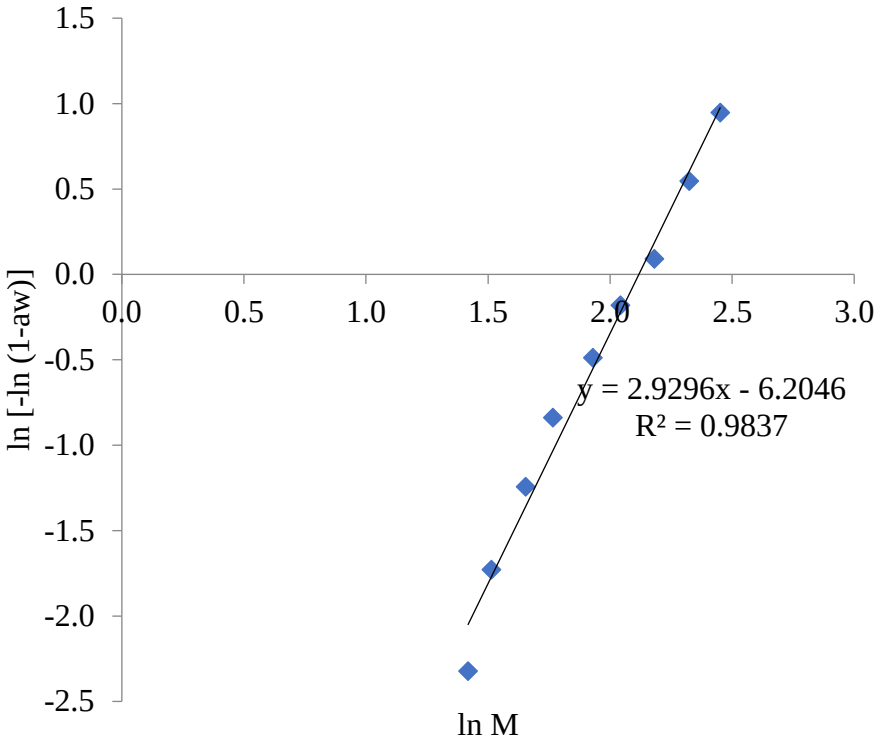

Figure D7: Moringa seed adsorption with modified Henderson model at 25°C

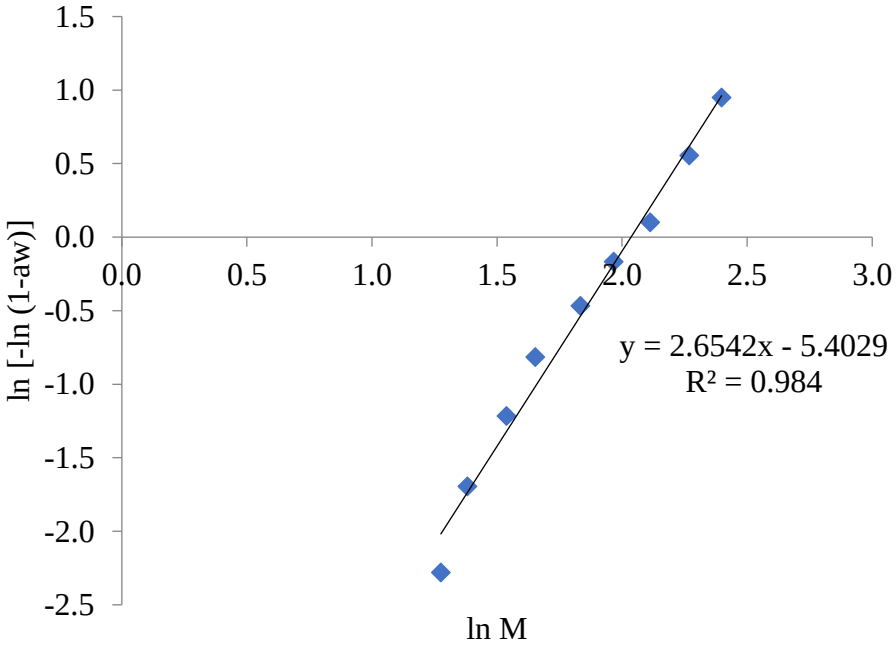

Figure D8: Moringa seed adsorption with modified Henderson model at 30°C

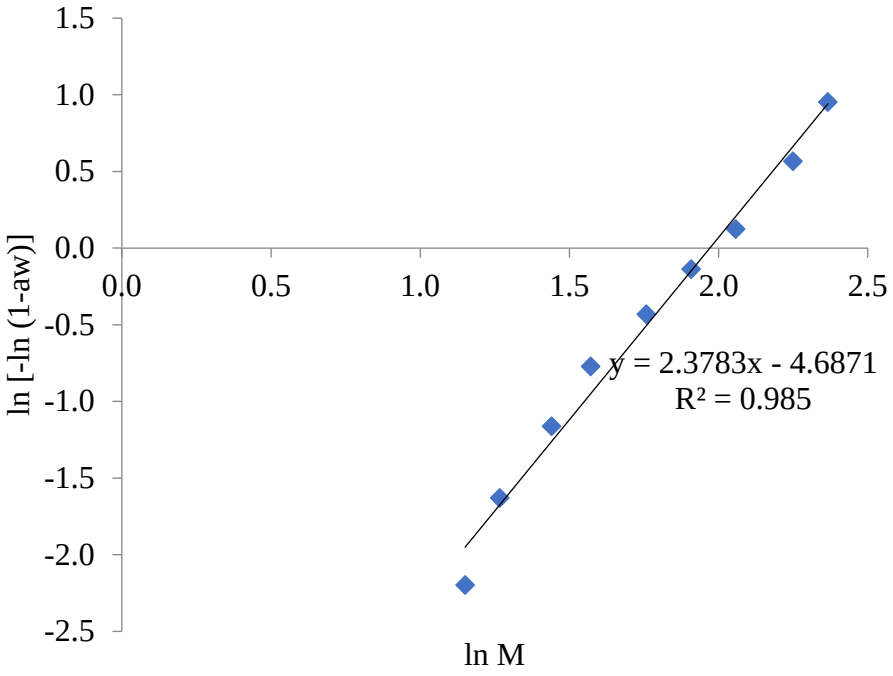

Figure D9: Moringa seed adsorption with modified Henderson model at 35^{o}C

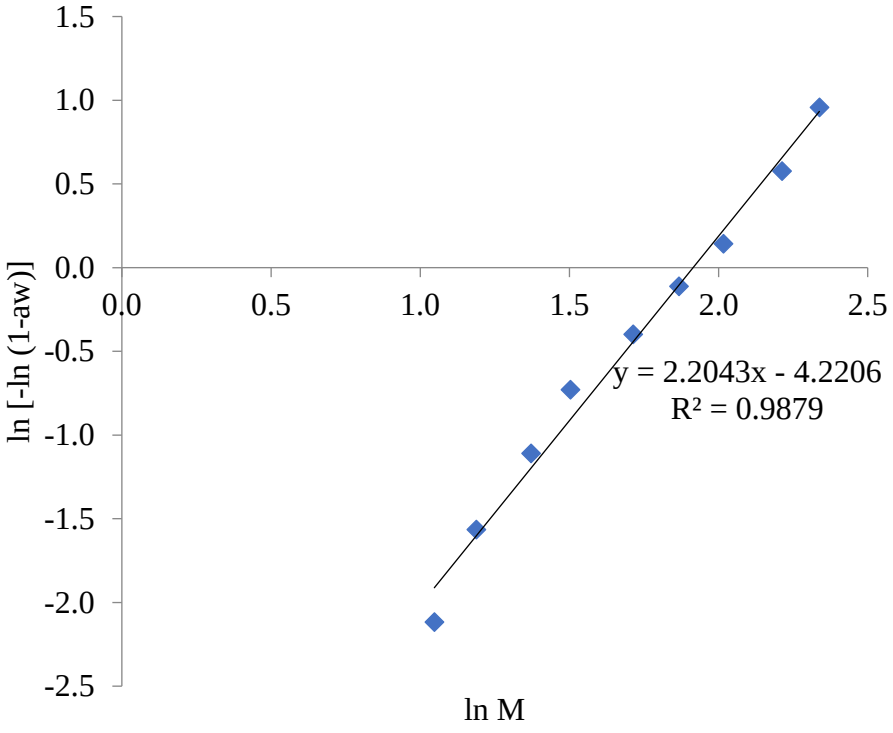

Figure D10: Moringa seed adsorption with modified Henderson model at 40^{o}C

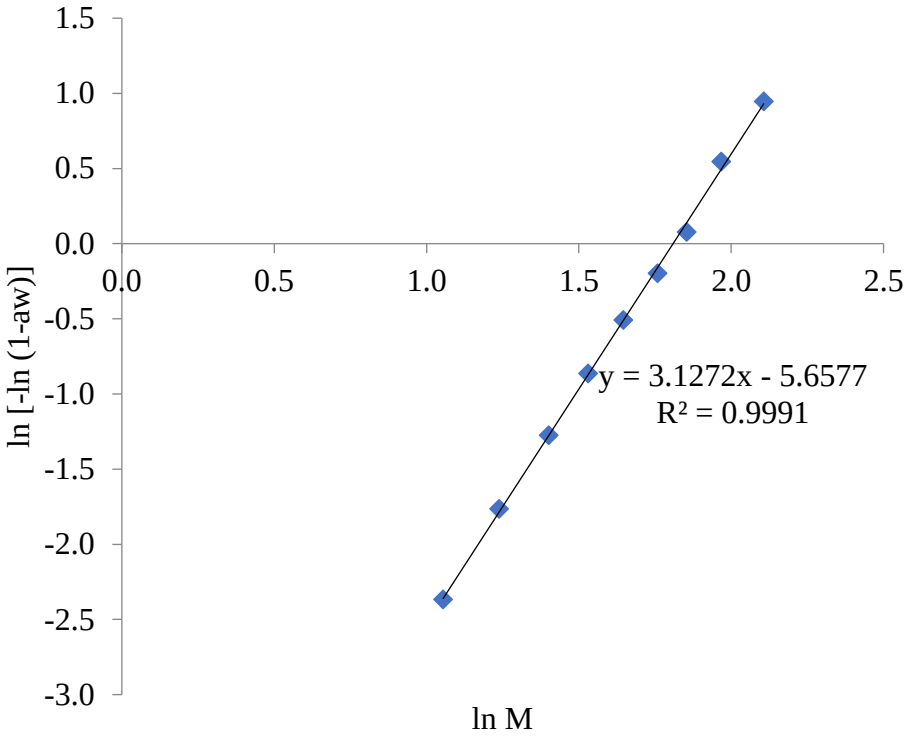

Figure D11: Moringa grits desorption with modified Henderson model at 20°C

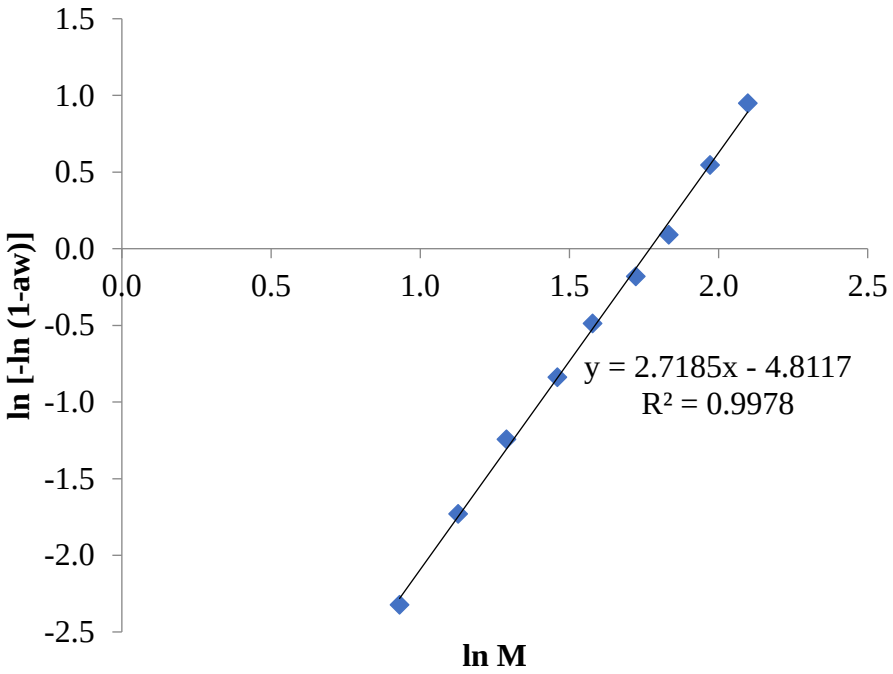

Figure D12: Moringa grits desorption with modified Henderson model at 25°C

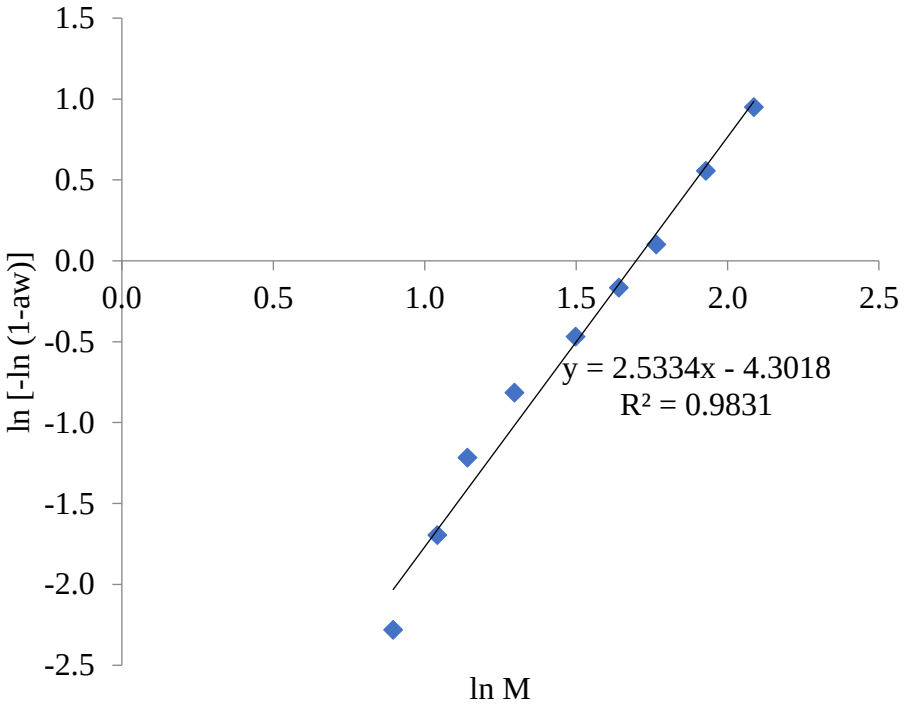

Figure D13: Moringa grits desorption with modified Henderson model at 30ºC

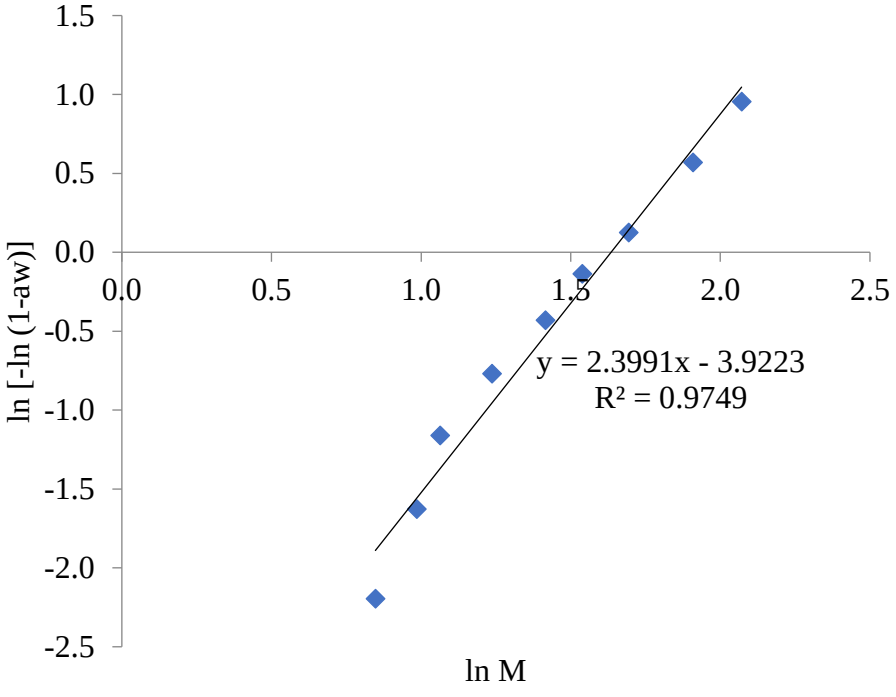

Figure D14: Moringa grits desorption with modified Henderson model at 35ºC

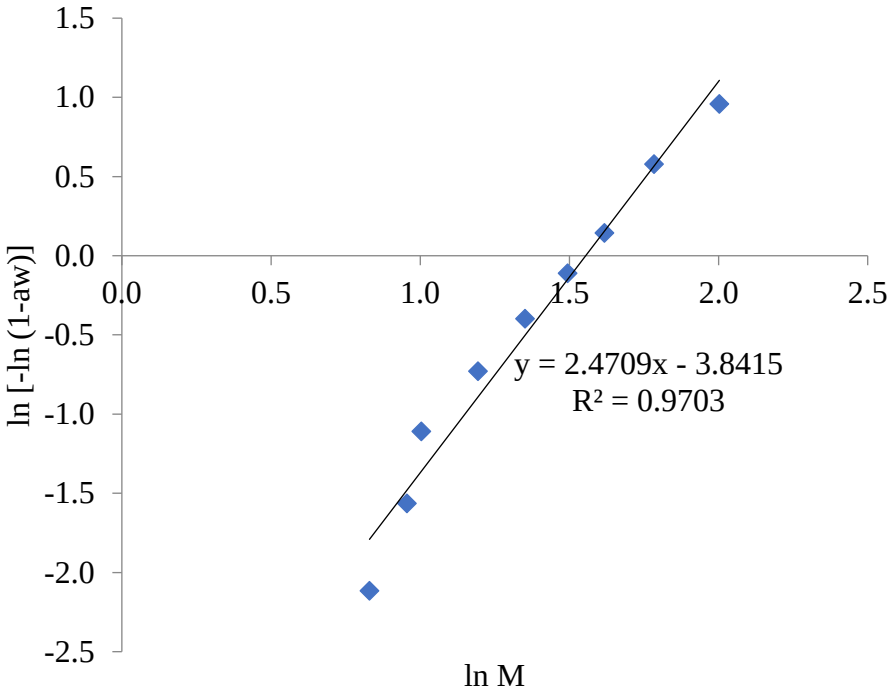

Figure D15: Moringa grits desorption with modified Henderson model at 40°C

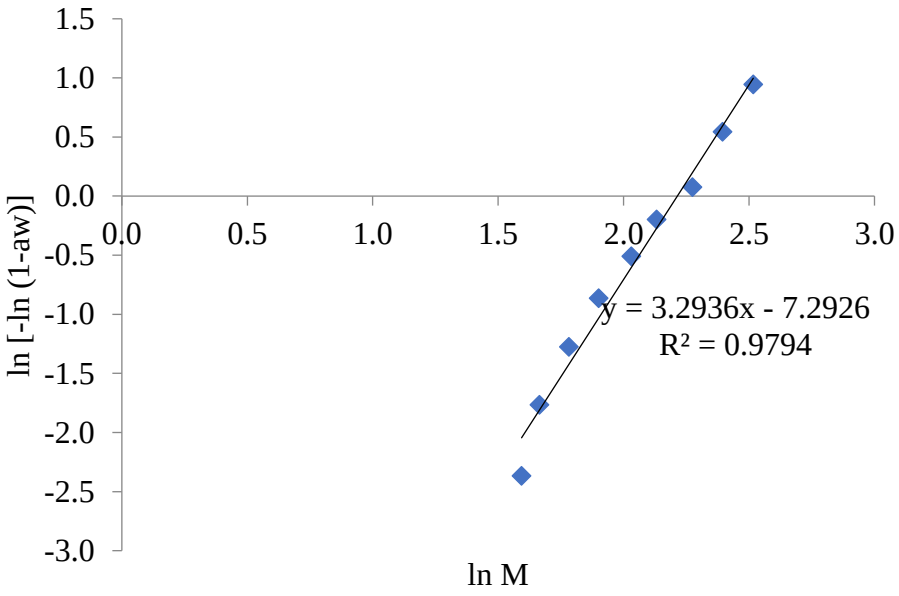

Figure D16: Moringa seed desorption with modified Henderson model at 20°C

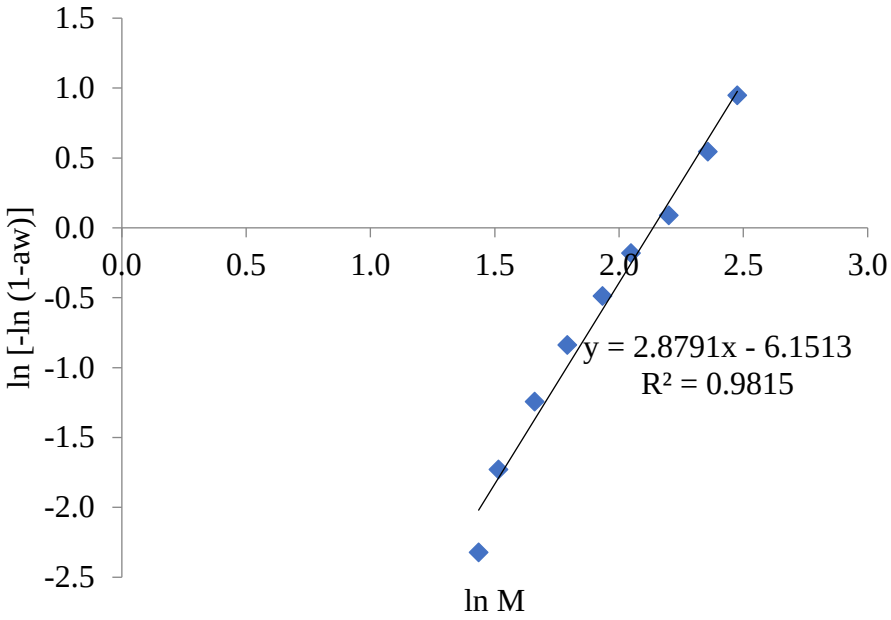

Figure D17: Moringa seed desorption with modified Henderson model at 25ºC

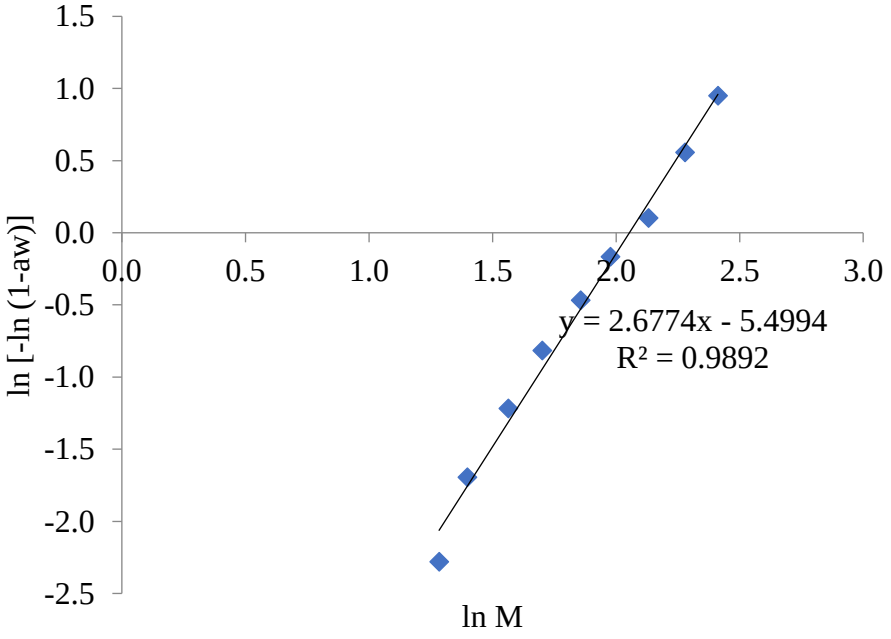

Figure D18: Moringa seed desorption with modified Henderson model at 30ºC

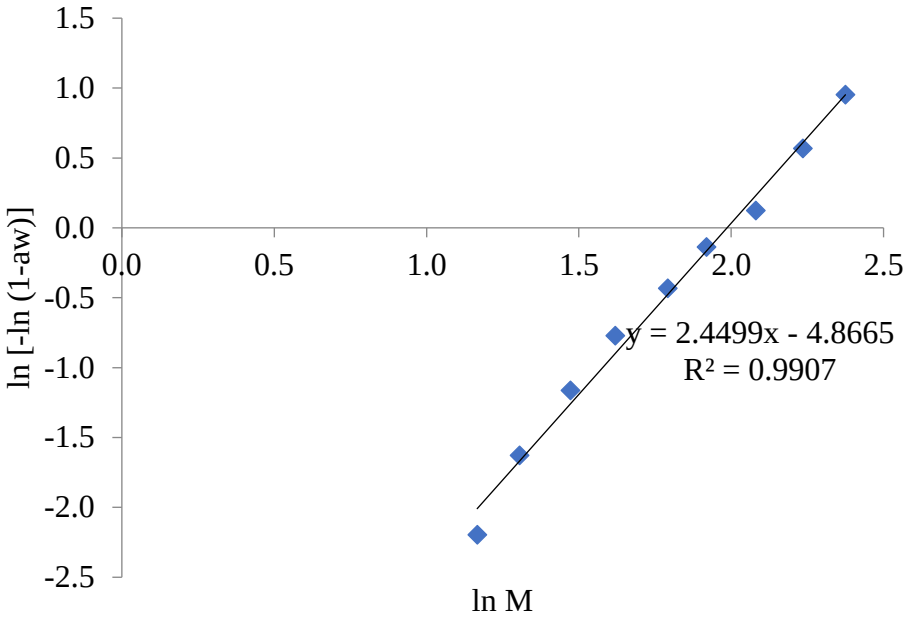

Figure D19: Moringa seed desorption with modified Henderson model at 35ºC

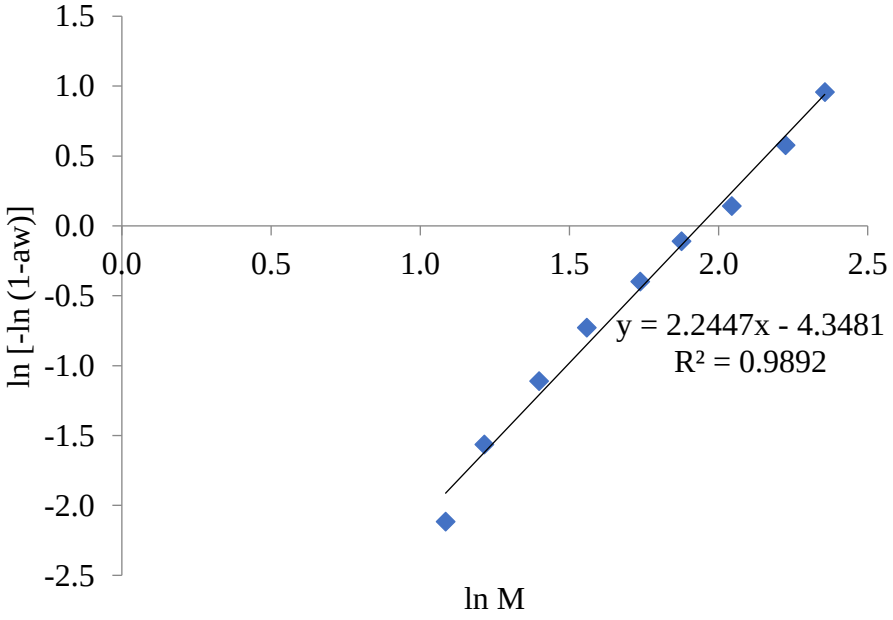

Figure D20: Moringa seed desorption with modified Henderson model at 40ºC

APPENDIX E: Modified Hasley model fittings

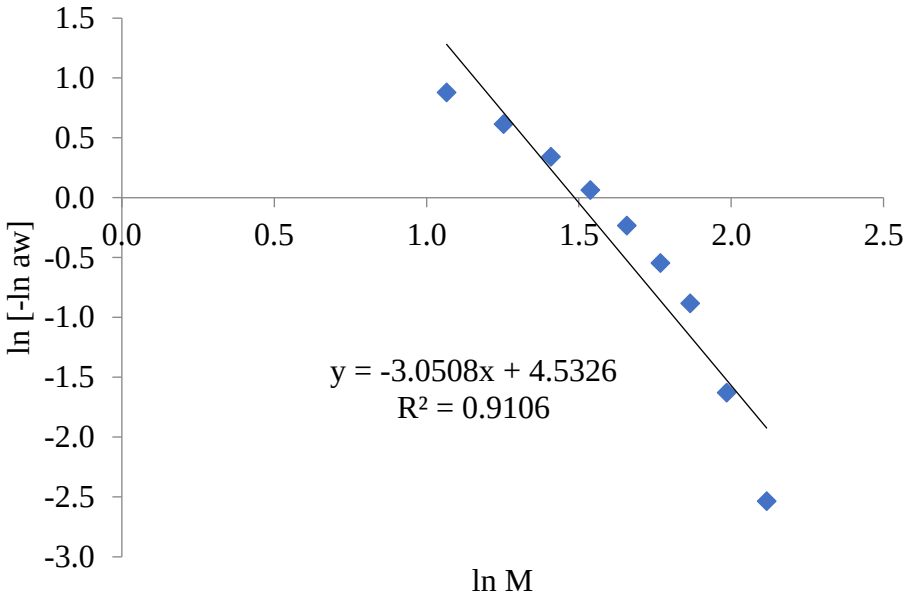

Figure E1: Moringa grits adsorption with modified Hasley model at 20°C

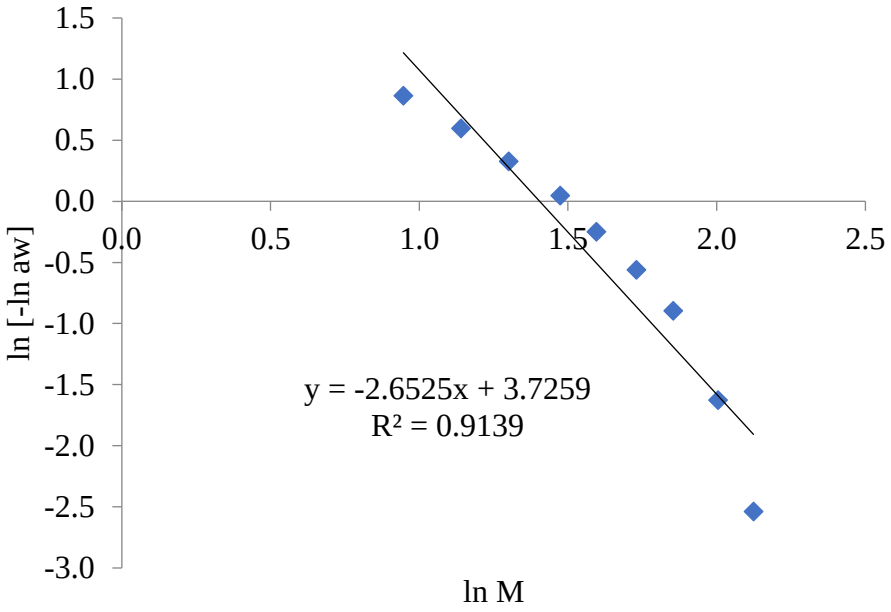

Figure E2: Moringa grits adsorption with modified Hasley model at 25°C

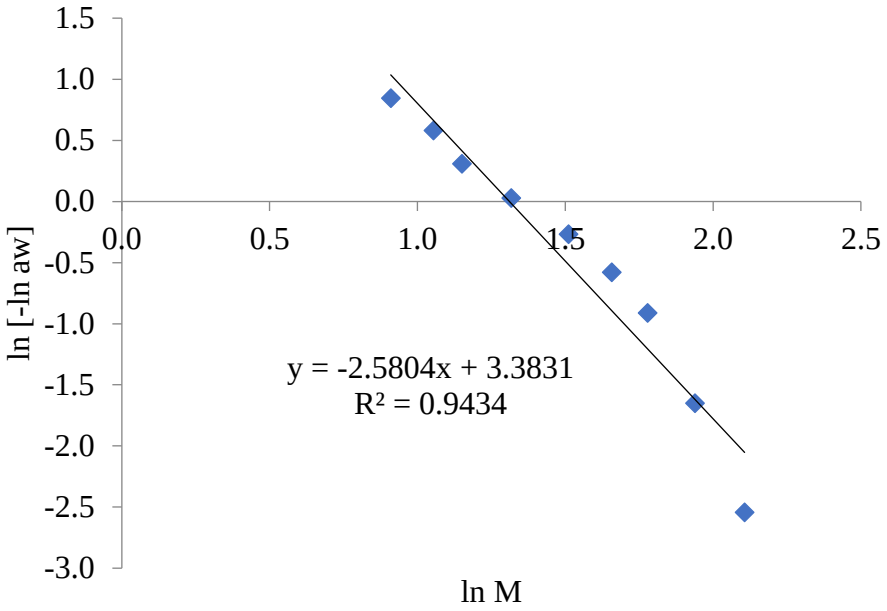

Figure E3: Moringa grits adsorption with modified Hasley model at 30°C

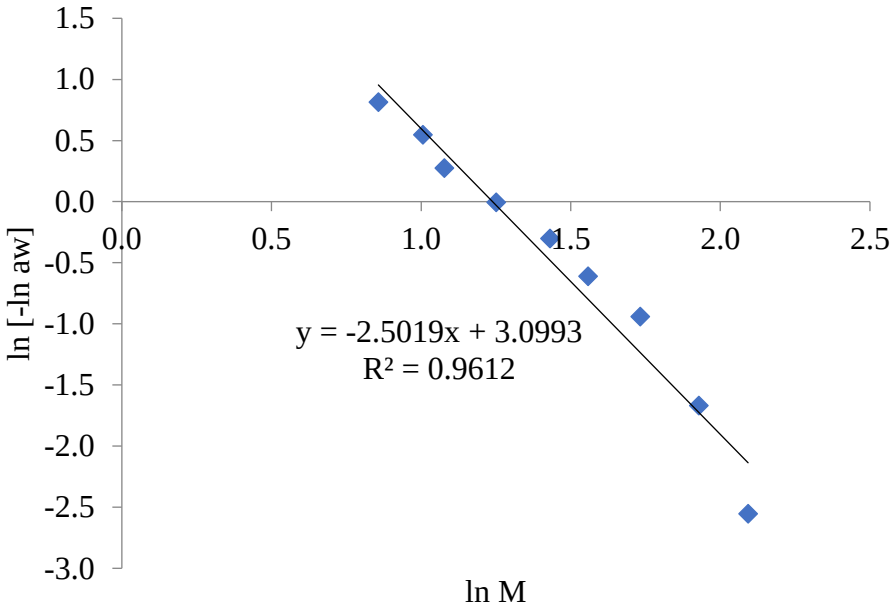

Figure E4: Moringa grits adsorption with modified Hasley model at 35°C

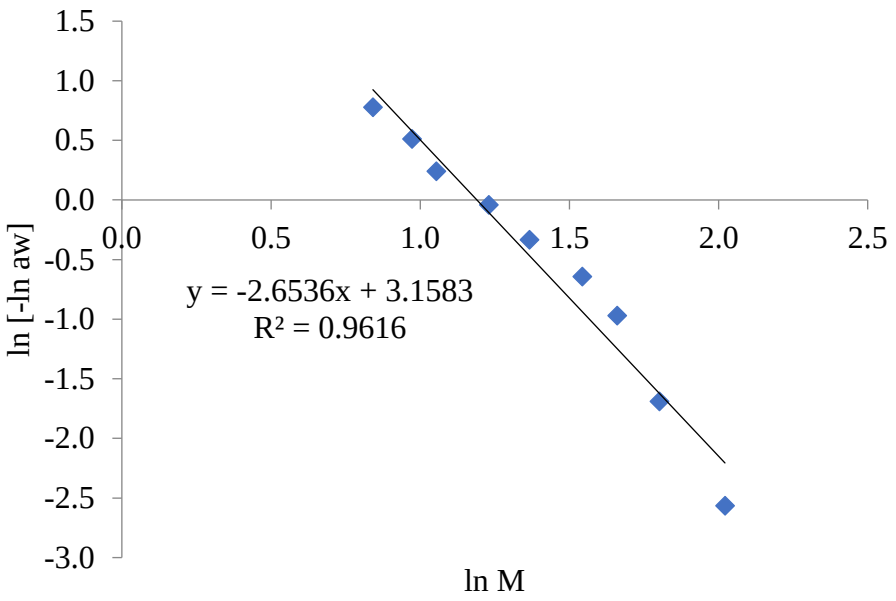

Figure E5: Moringa grits adsorption with modified Hasley model at 40^{o}C

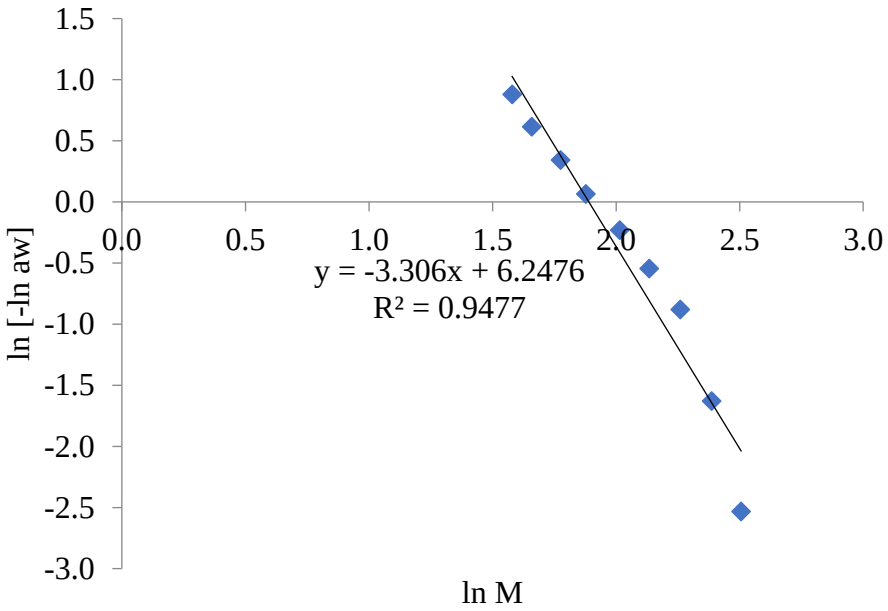

Figure E6: Moringa seed adsorption with modified Hasley model at 20^{o}C

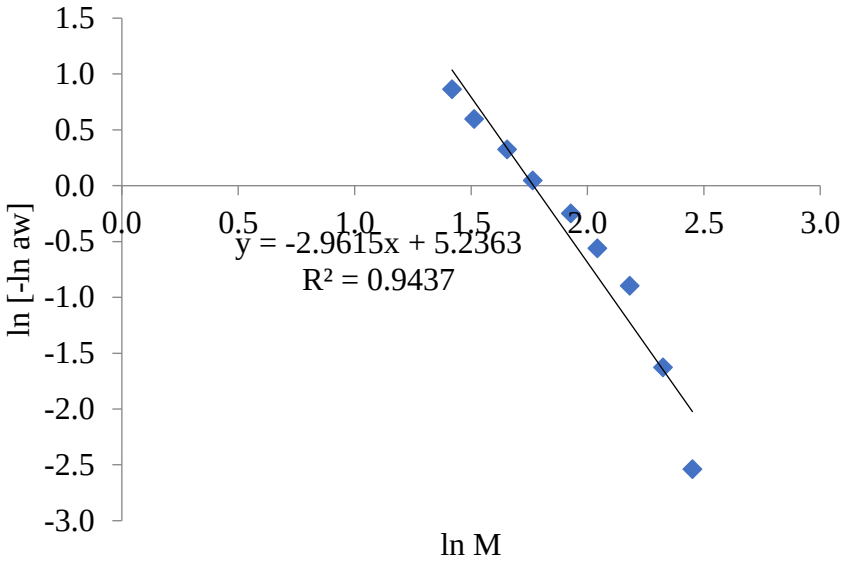

Figure E7: Moringa seed adsorption with modified Hasley model at 25^{o}C

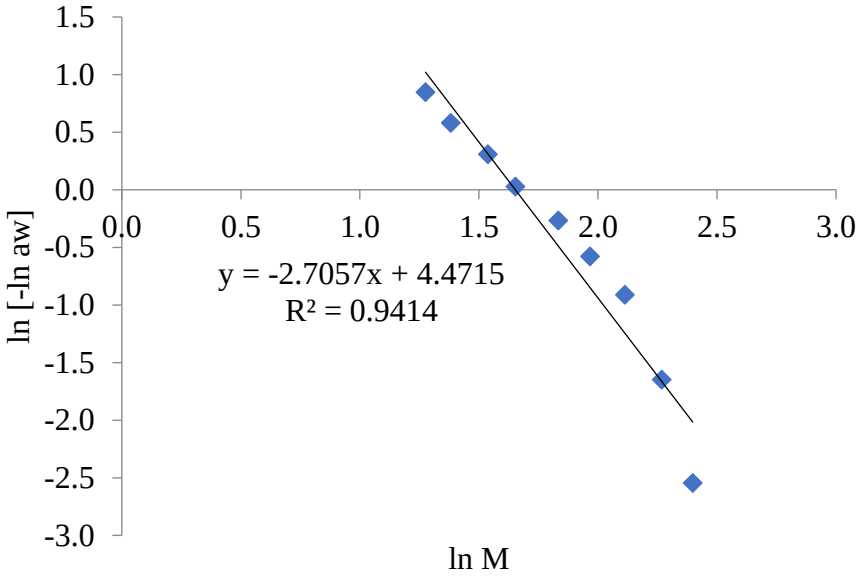

Figure E8: Moringa seed adsorption with modified Hasley model at 30^{o}C

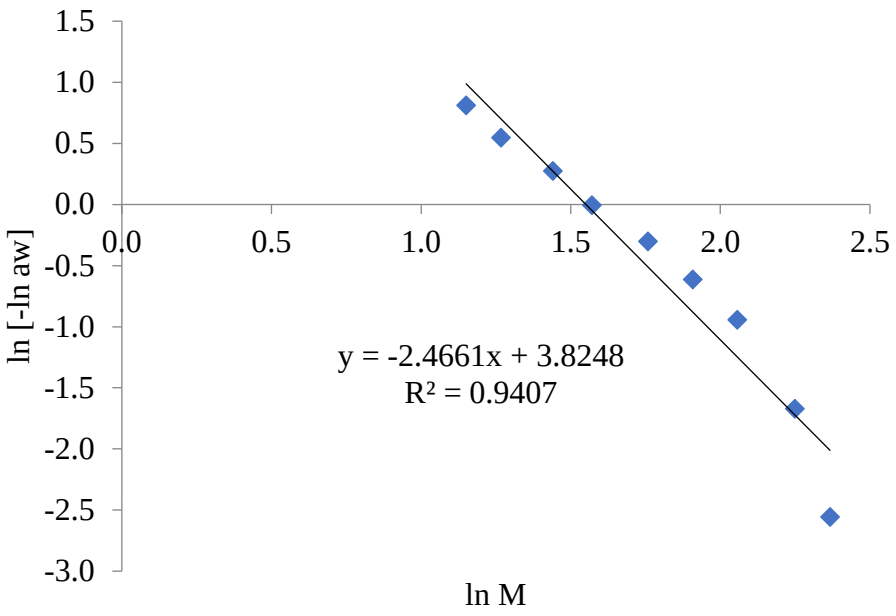

Figure E9: Moringa seed adsorption with modified Hasley model at 35°C

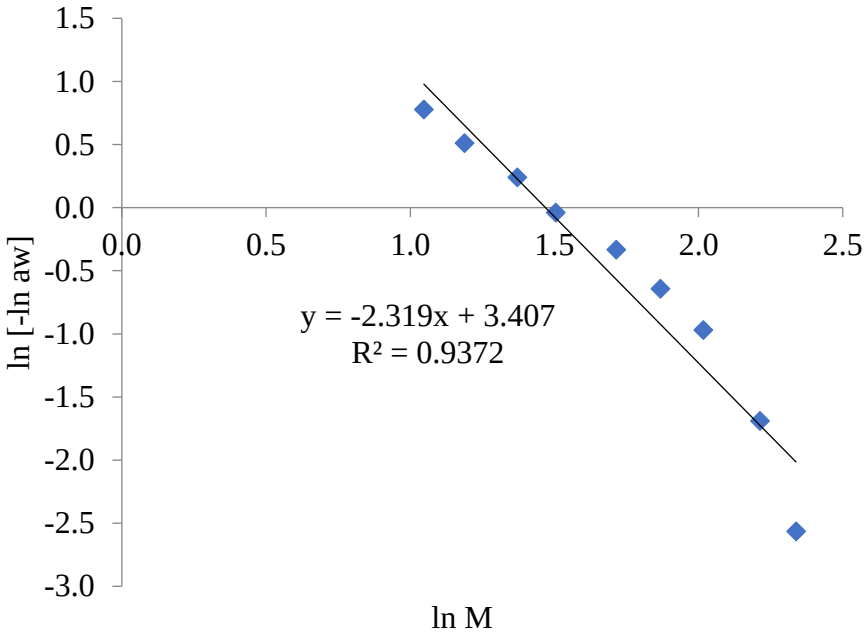

Figure E10: Moringa seed adsorption with modified Hasley model at 40°C

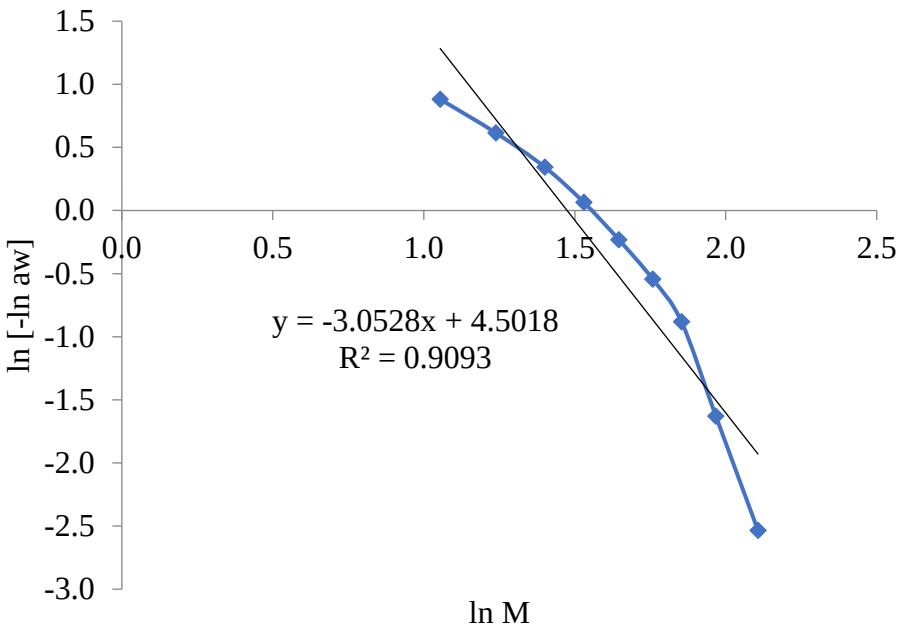

Figure E11: Moringa grits desorption with modified Hasley model at 20^{o}C

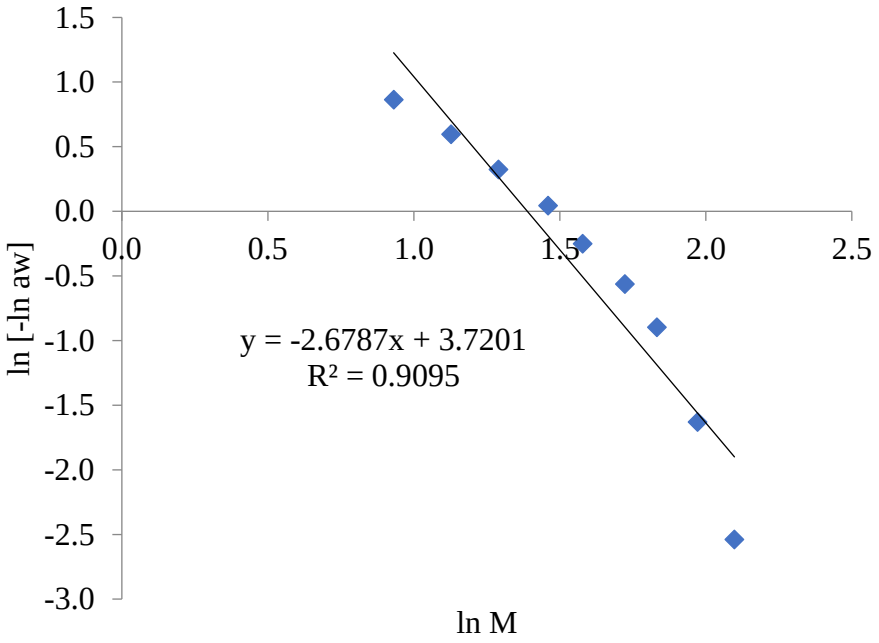

Figure E12: Moringa grits desorption with modified Hasley model at 25^{o}C

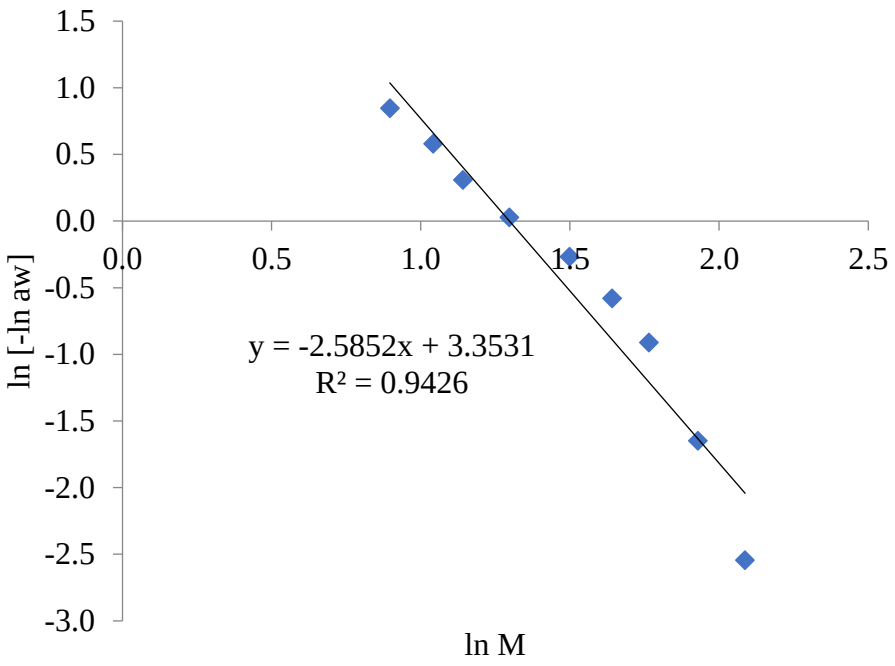

Figure E13: Moringa grits desorption with modified Hasley model at 30°C

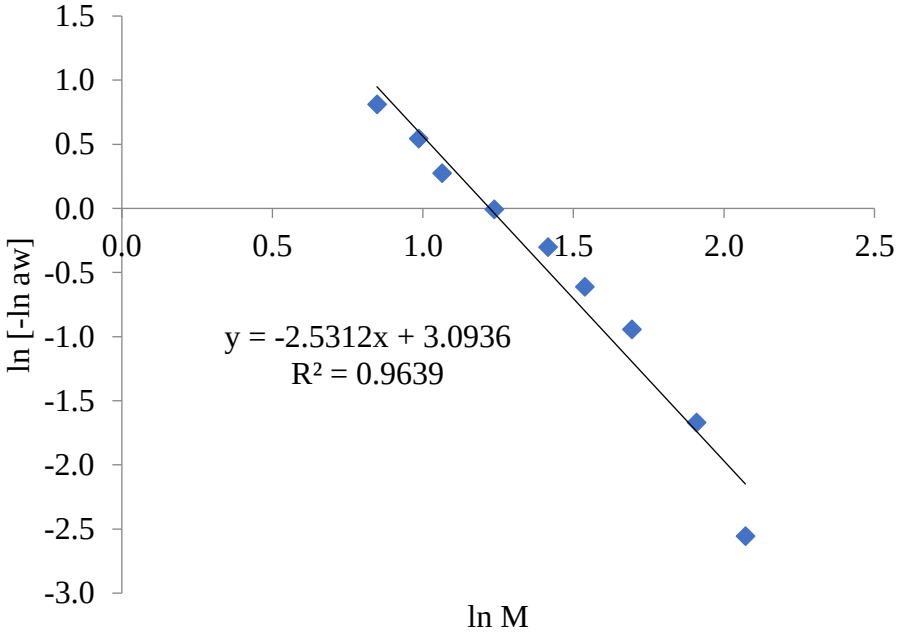

Figure E14: Moringa grits desorption with modified Hasley model at 35°C

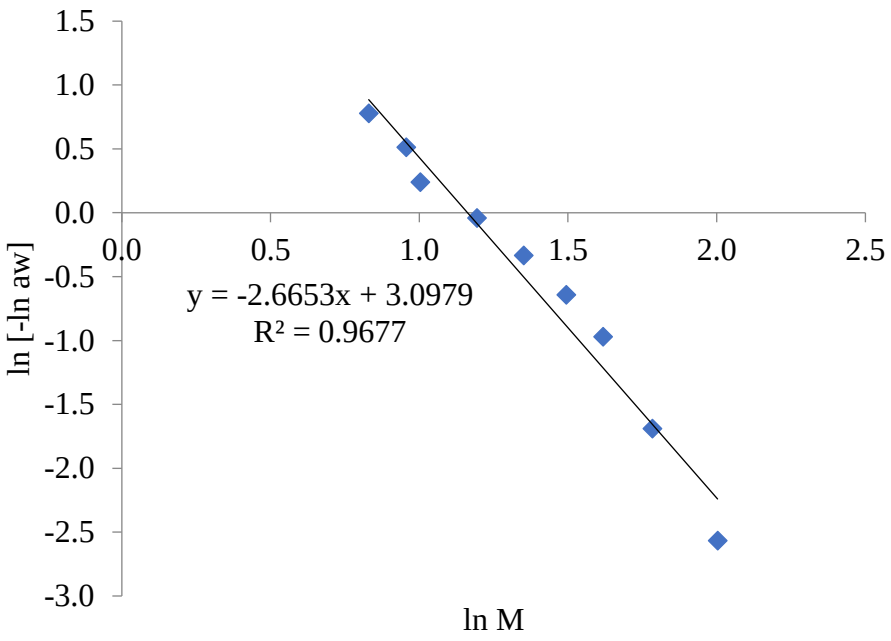

Figure E15: Moringa grits desorption with modified Hasley model at 40^{o}C

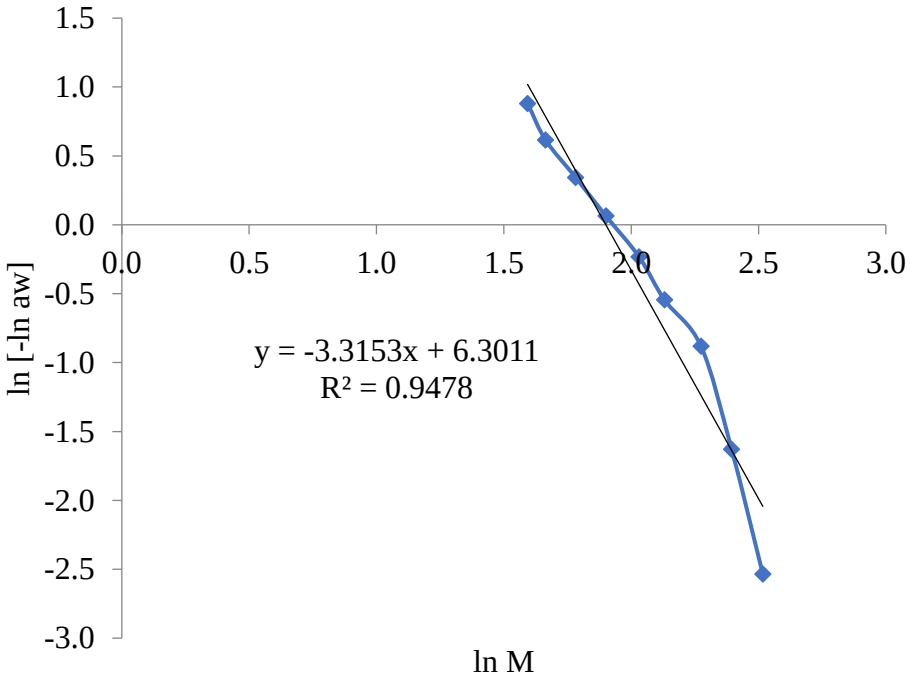

Figure E16: Moringa seed desorption with modified Hasley model at 20^{o}C

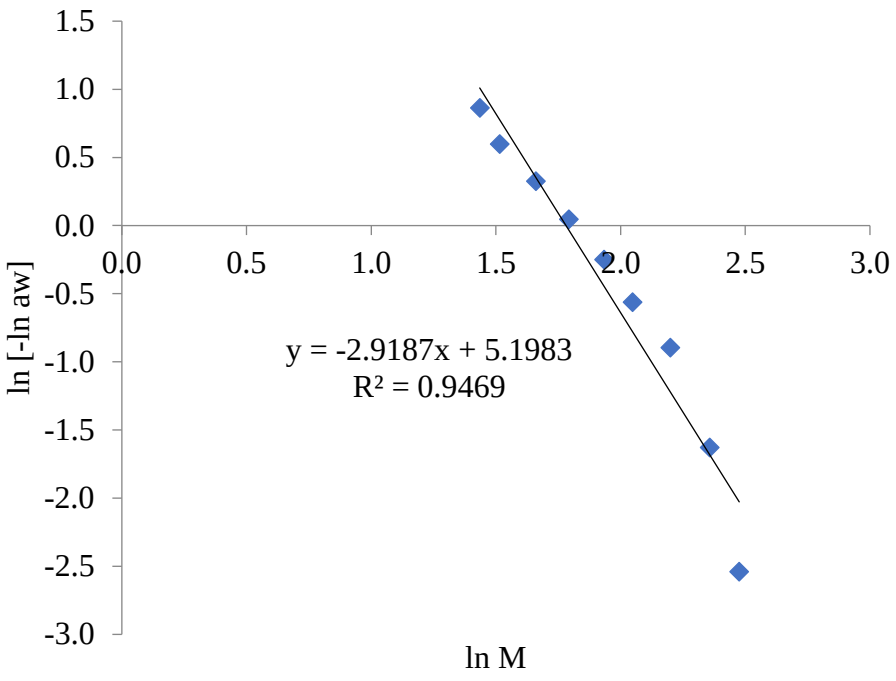

Figure E17: Moringa seed desorption with modified Hasley model at 25^{o}C

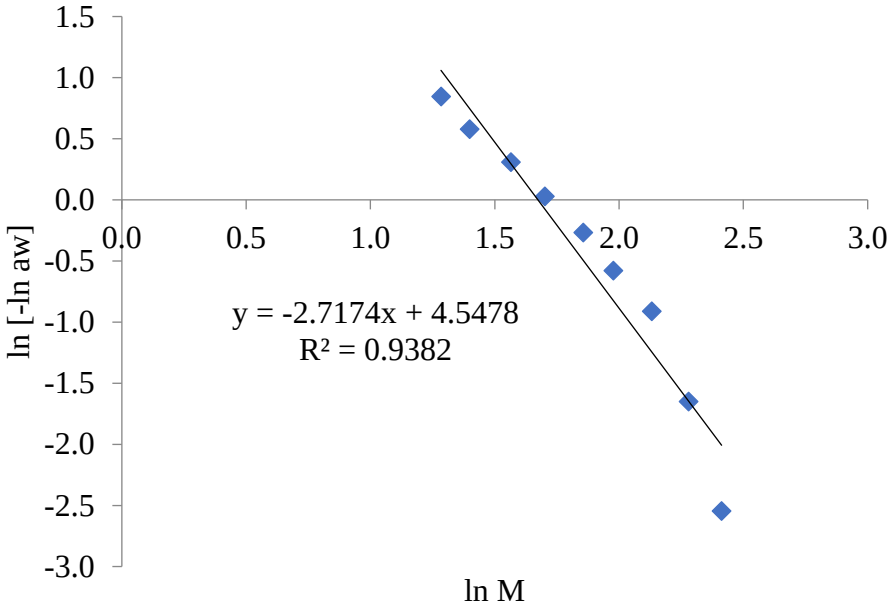

Figure E18: Moringa seed desorption with modified Hasley model at 30^{o}C

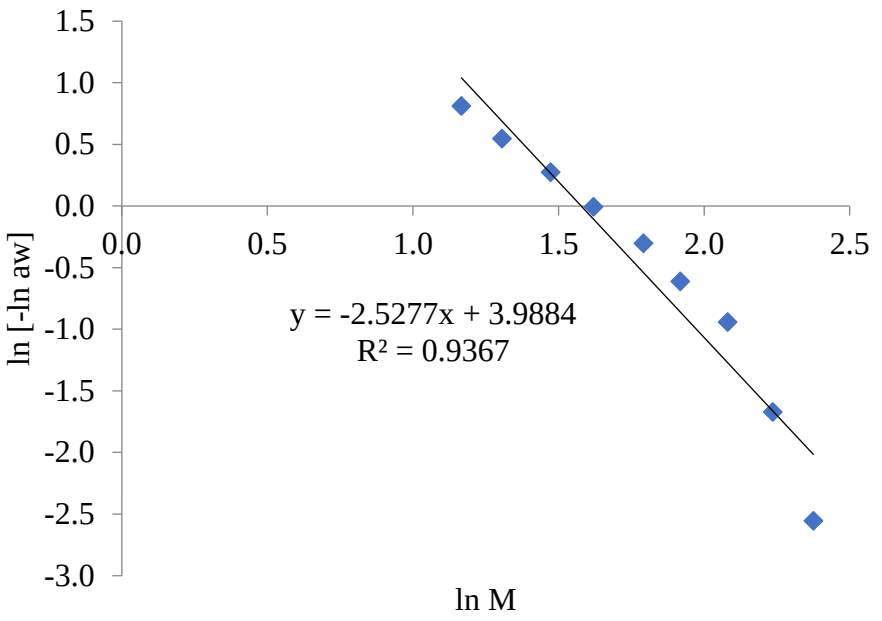

Figure E19: Moringa seed desorption with modified Hasley model at 35°C

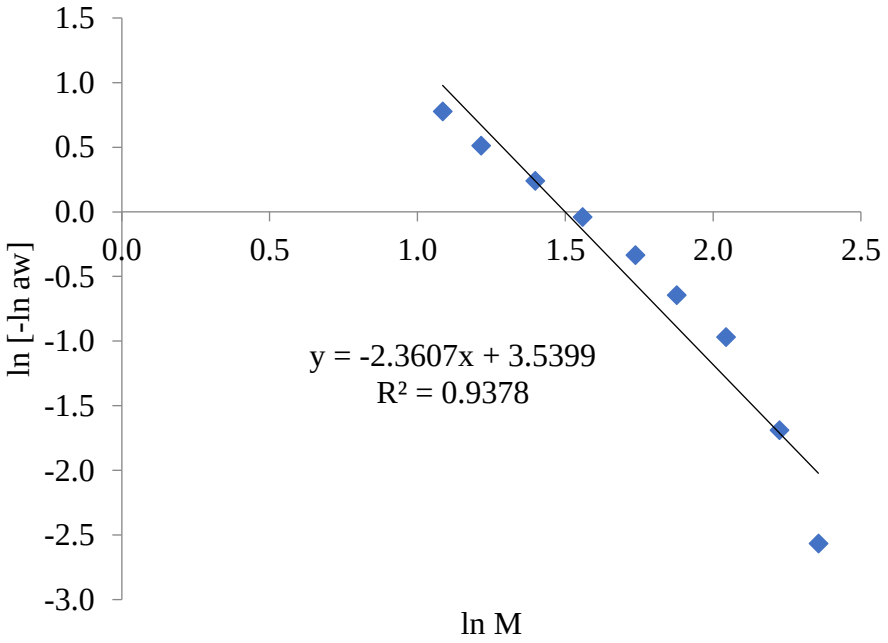

Figure E20: Moringa seed desorption with modified Hasley model at 40°C

APPENDIX F: Caurie model fittings

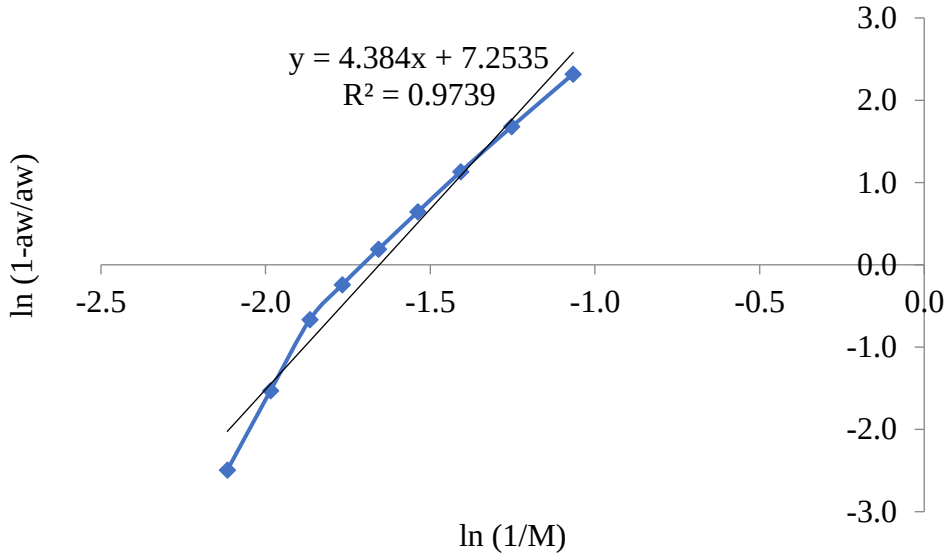

Figure F1: Moringa grits adsorption with Caurie model at 20^{o}C

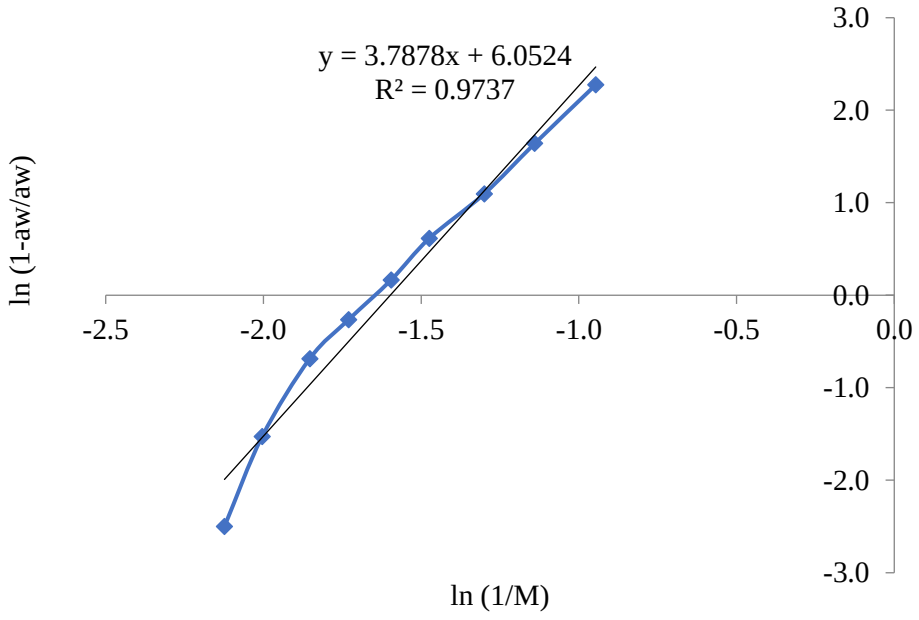

Figure F2: Moringa grits adsorption with Caurie model at 25^{o}C

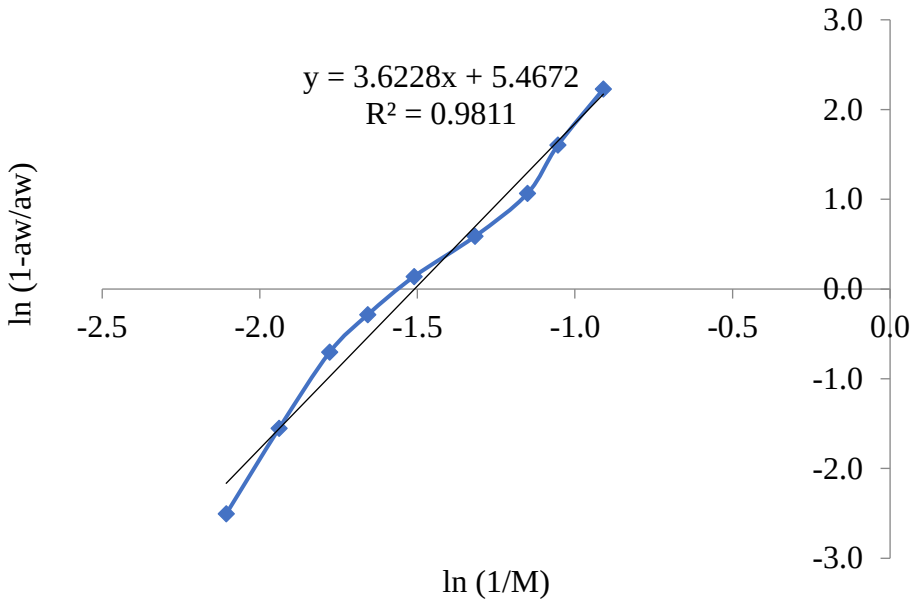

Figure F3: Moringa grits adsorption with Caurie model at 30^{o}C

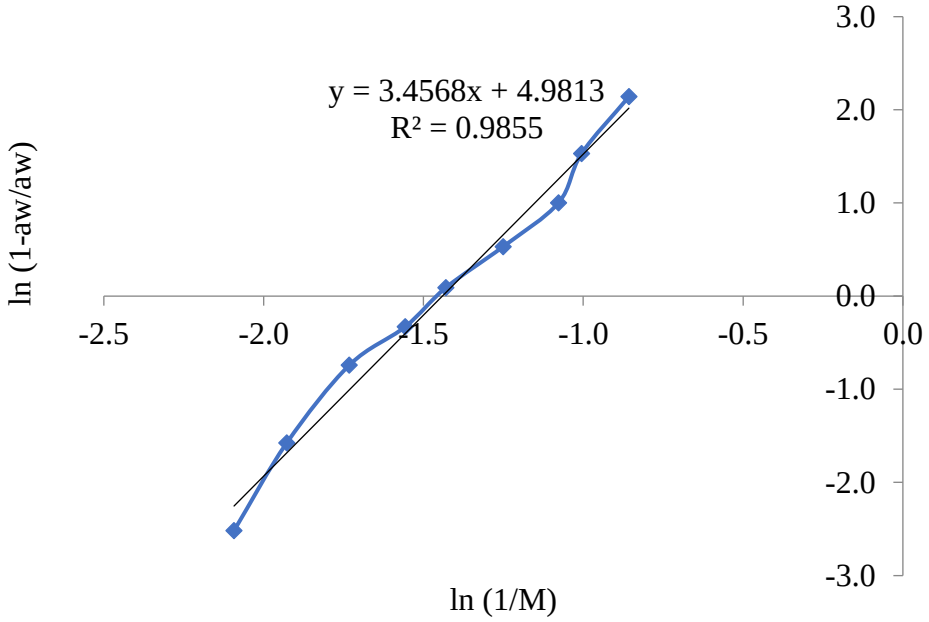

Figure F4: Moringa grits adsorption with Caurie model at 35^{o}C

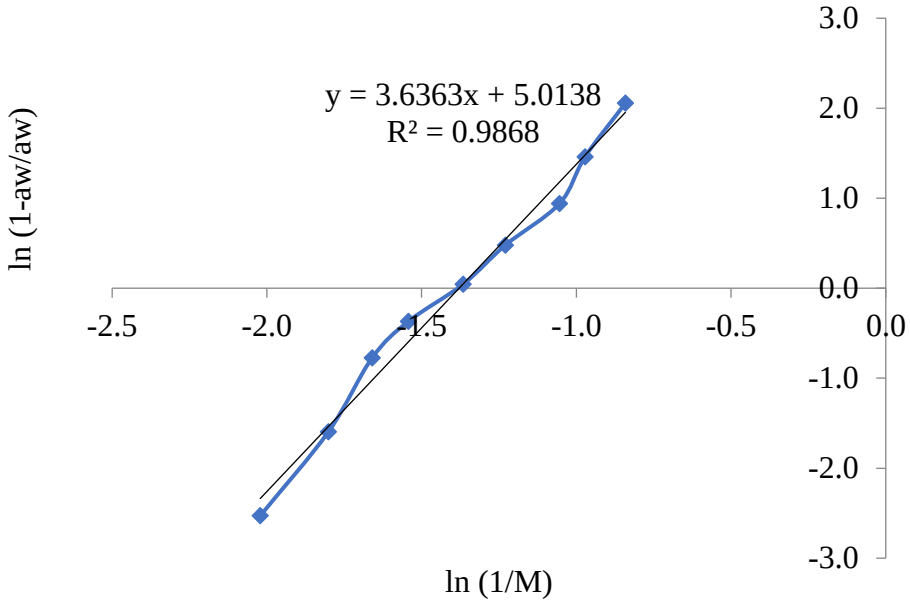

Figure F5: Moringa grits adsorption with Caurie model at 40^{o}C

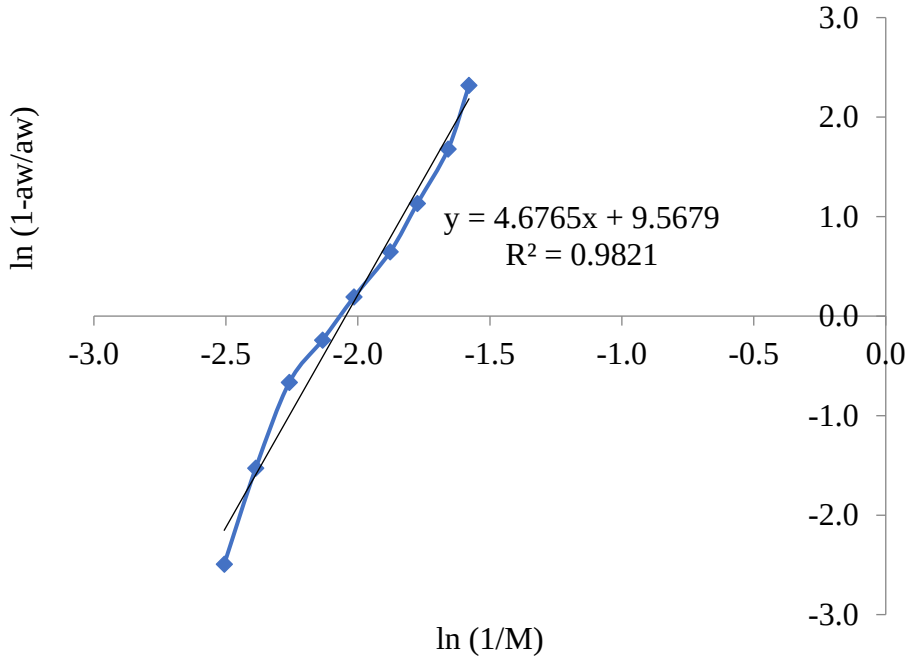

Figure F6: Moringa seed adsorption with Caurie model at 20^{o}C

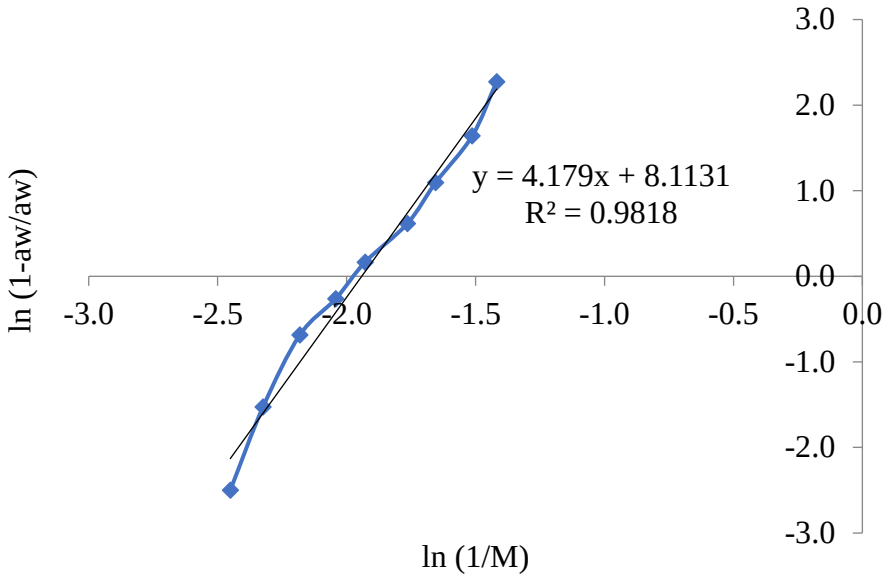

Figure F7: Moringa seed adsorption with Caurie model at 25^{o}C

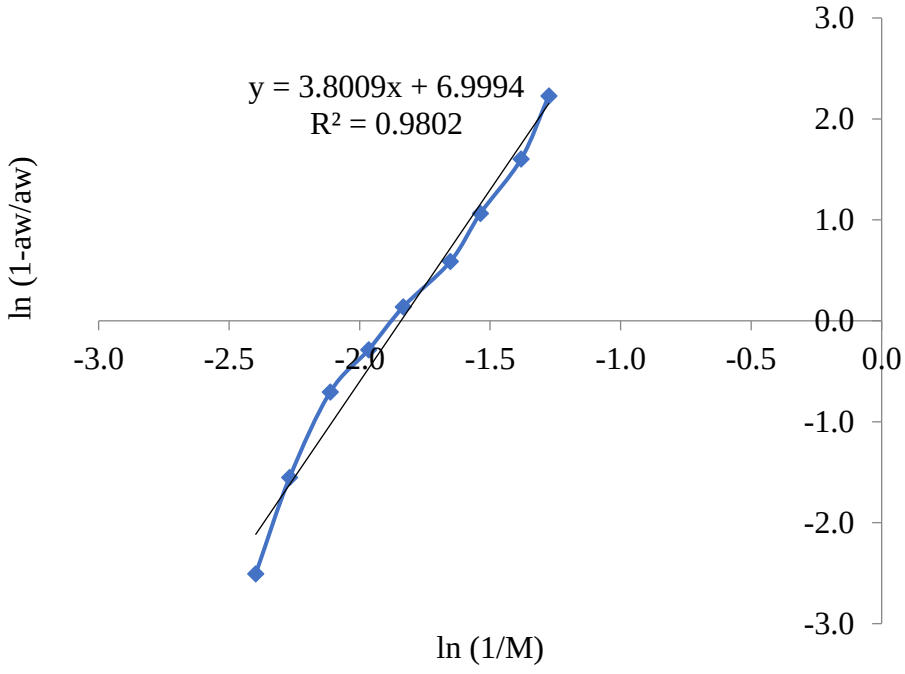

Figure F8: Moringa seed adsorption with Caurie model at 30^{o}C

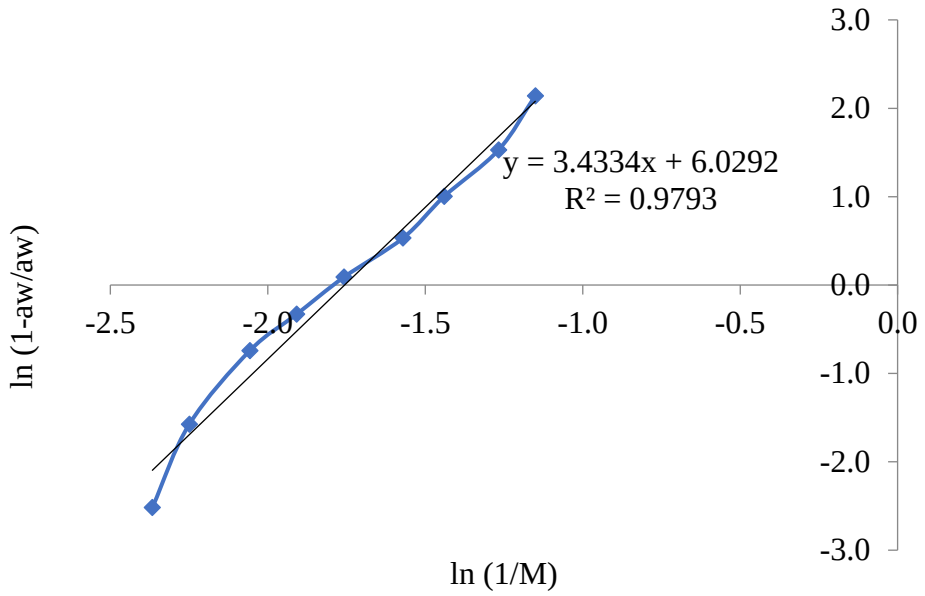

Figure F9: Moringa seed adsorption with Caurie model at 35°C

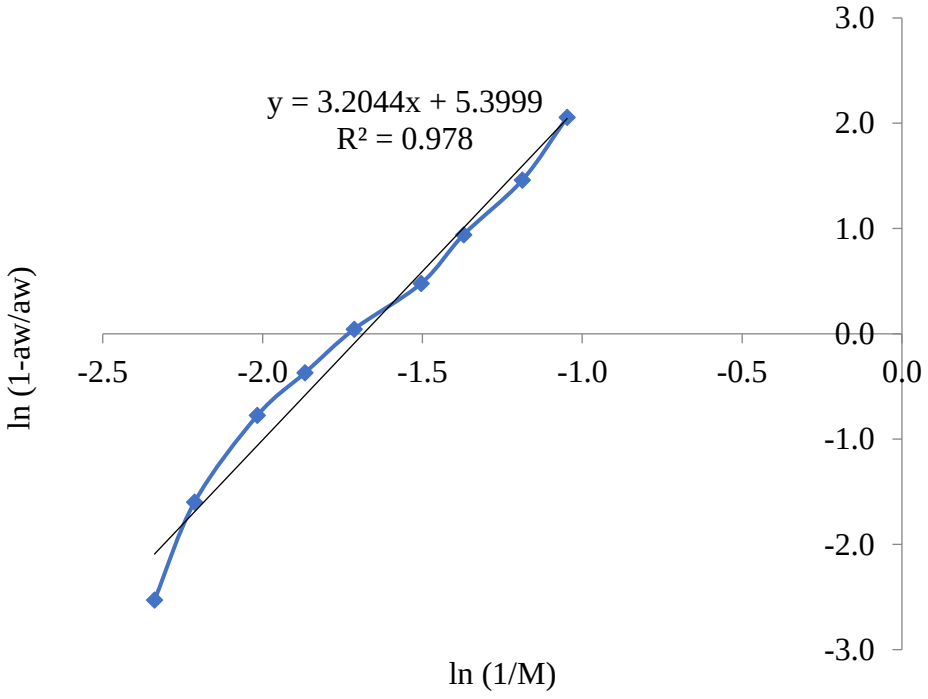

Figure F10: Moringa seed adsorption with Caurie model at 40°C

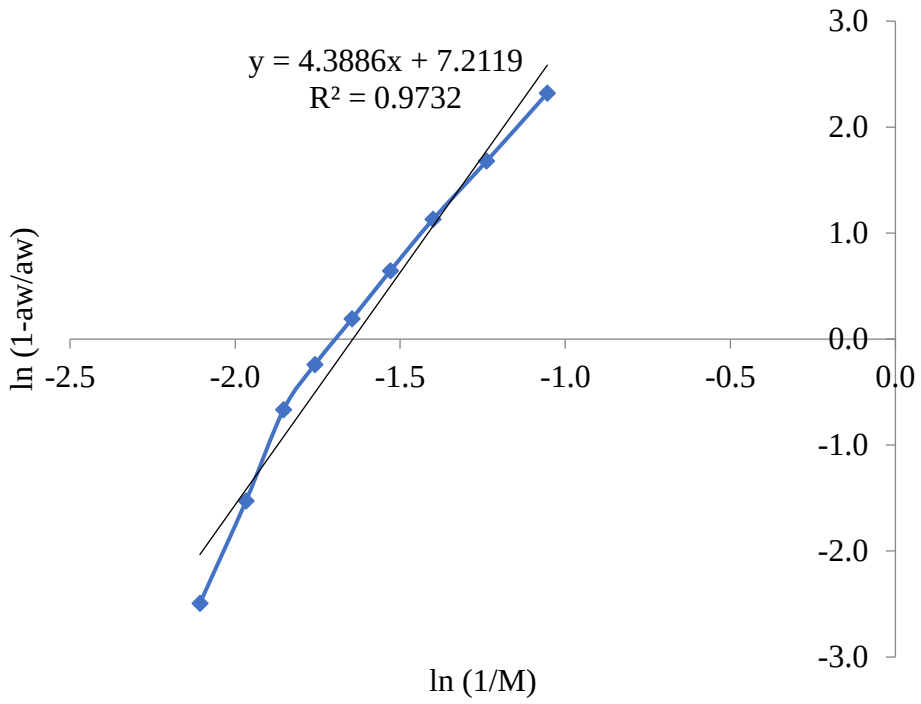

Figure F11: Moringa grits desorption with Caurie model at 20ºC

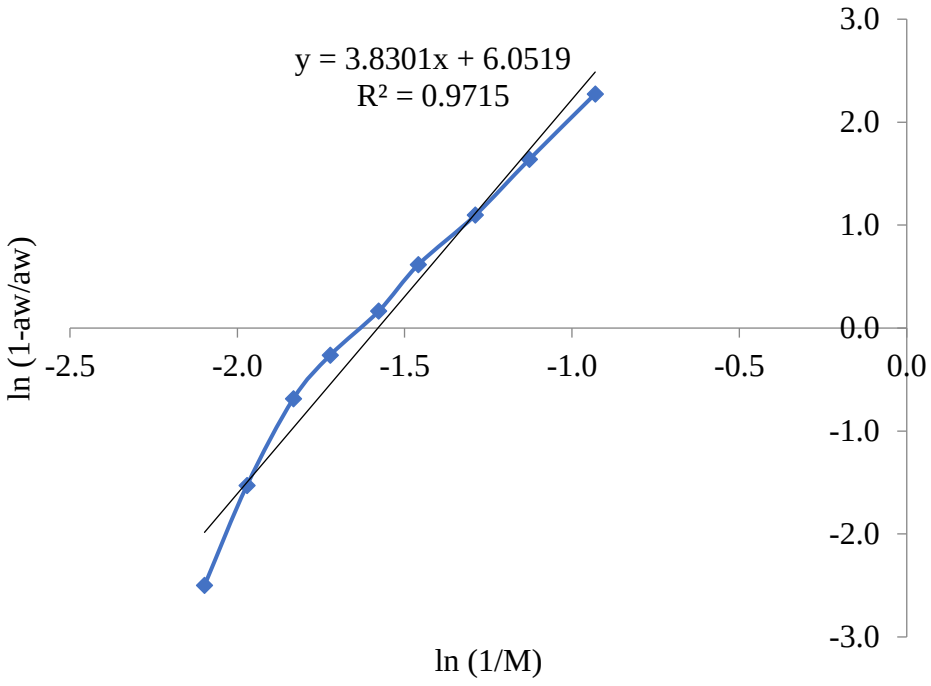

Figure F12: Moringa grits desorption with Caurie model at 25ºC

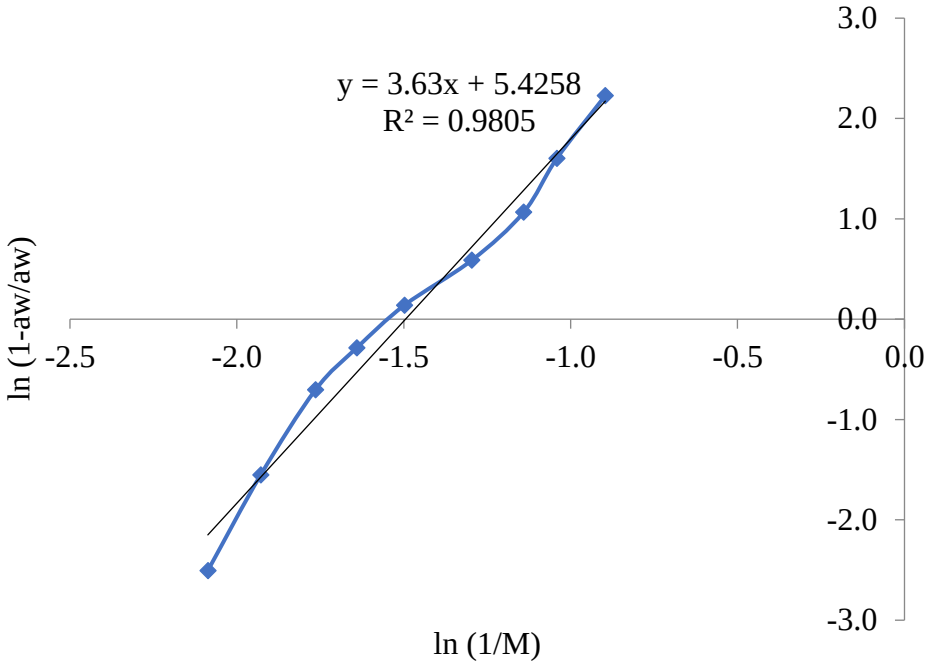

Figure F13: Moringa grits desorption with Caurie model at 30°C

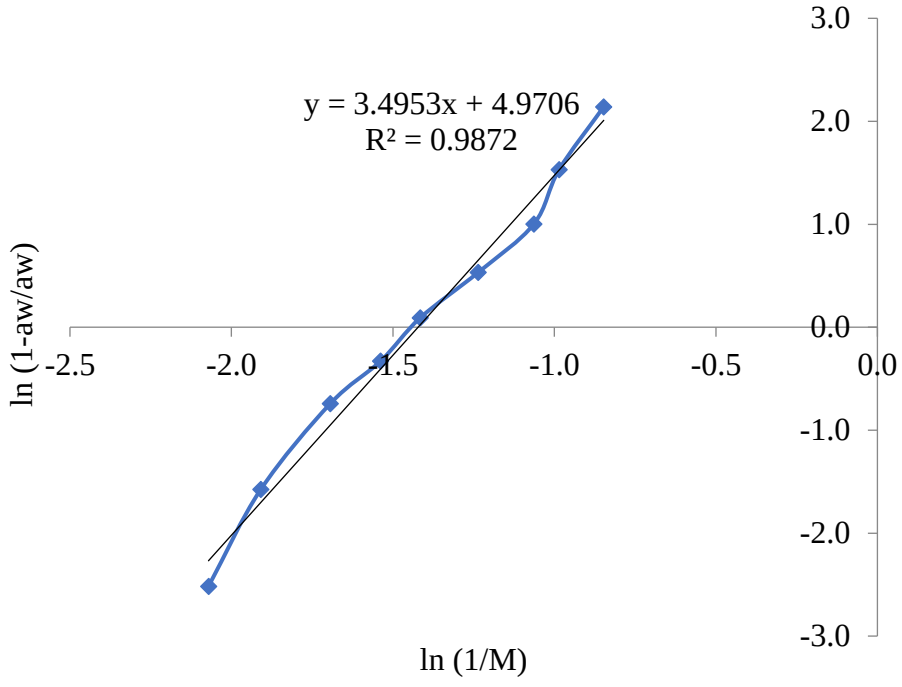

Figure F14: Moringa grits desorption with Caurie model at 35°C

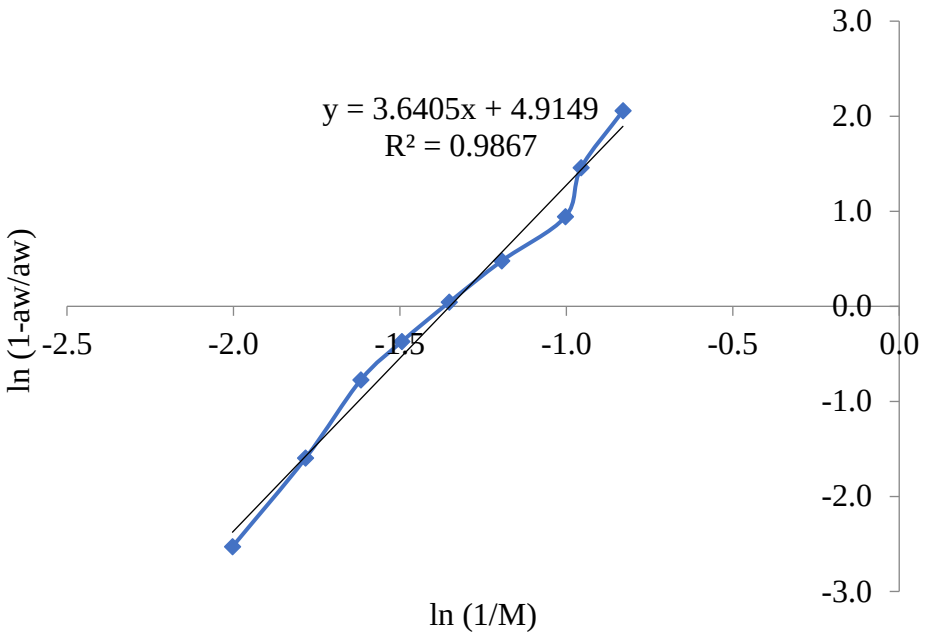

Figure F15: Moringa grits desorption with Caurie model at 40°C

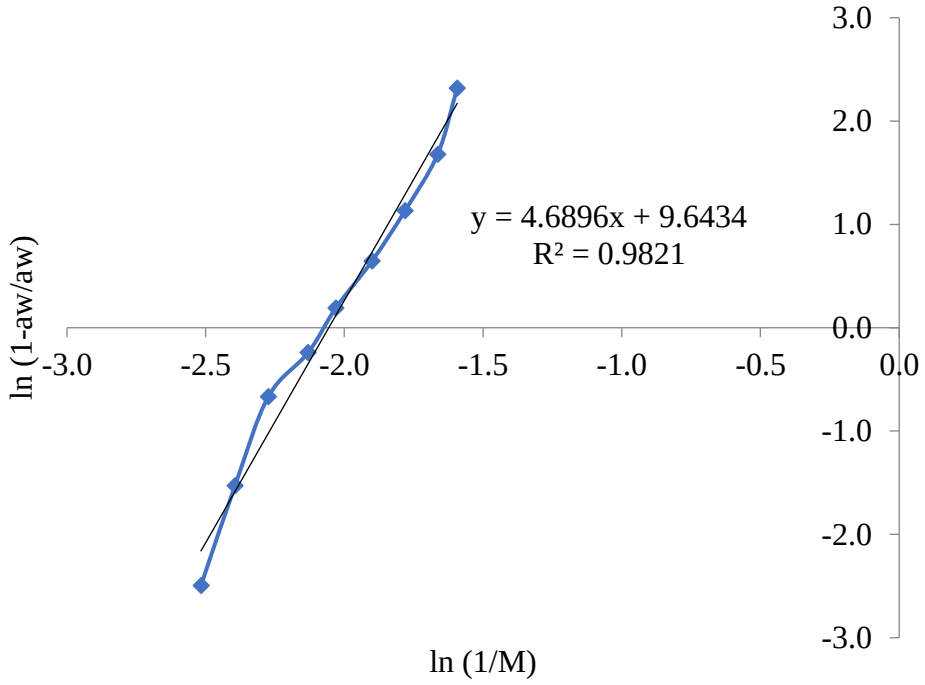

Figure F16: Moringa seed desorption with Caurie model at 20°C

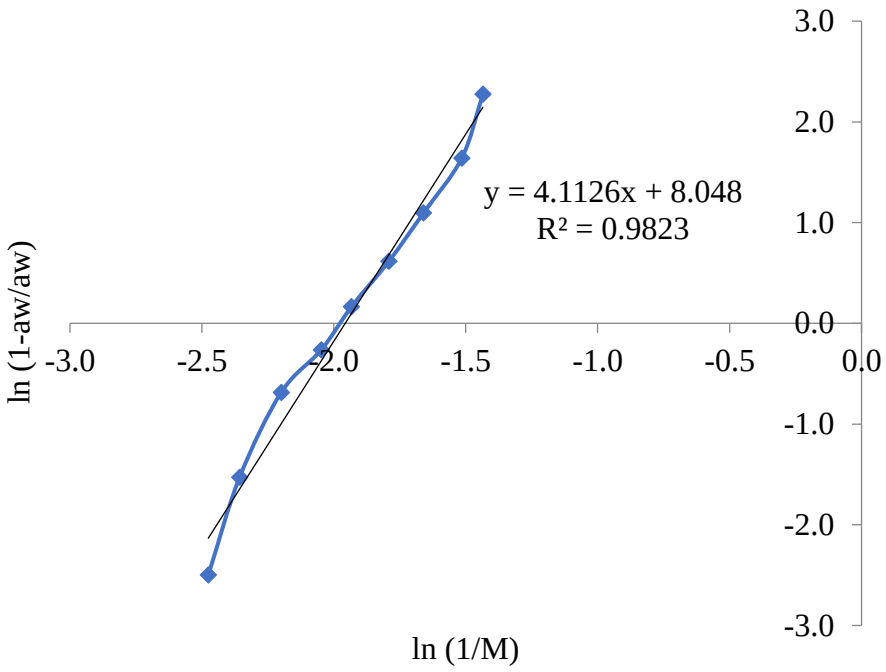

Figure F17: Moringa seed desorption with Caurie model at 25^{o}C

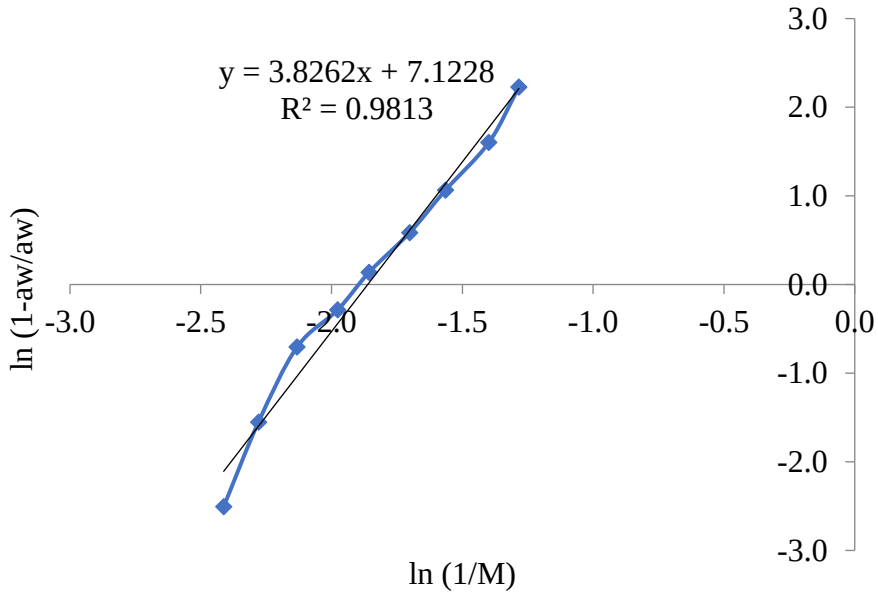

Figure F18: Moringa seed desorption with Caurie model at 30^{o}C

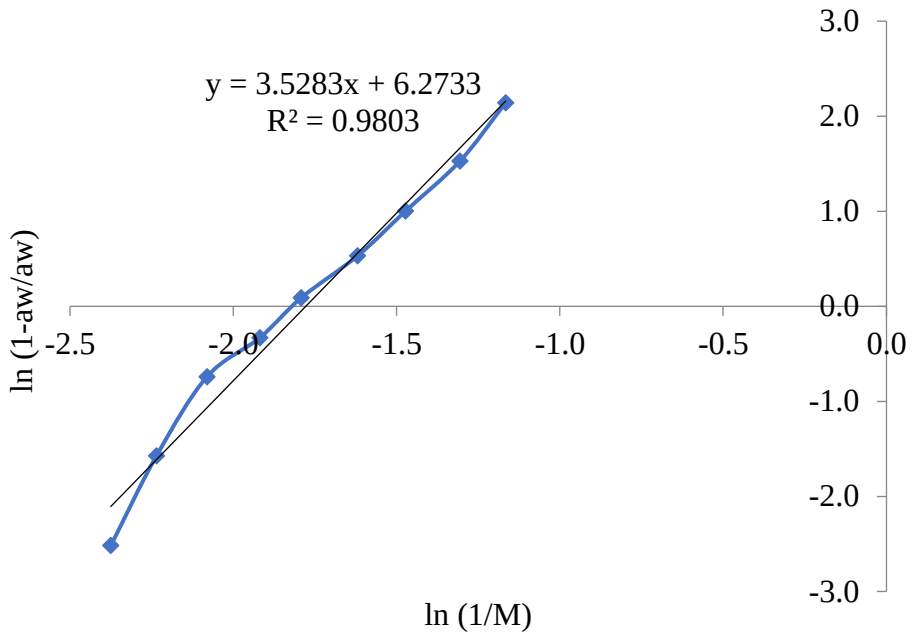

Figure F19: Moringa seed desorption with Caurie model at 35ºC

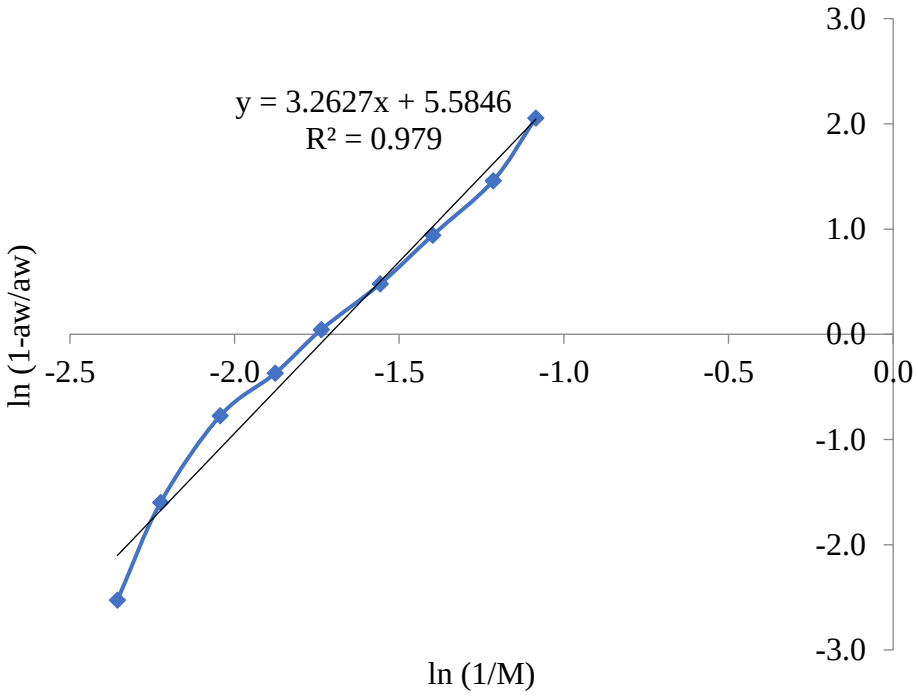

Figure F20: Moringa seed desorption with Caurie model at 40ºC

APPENDIX G: Experimental and predicted EMC

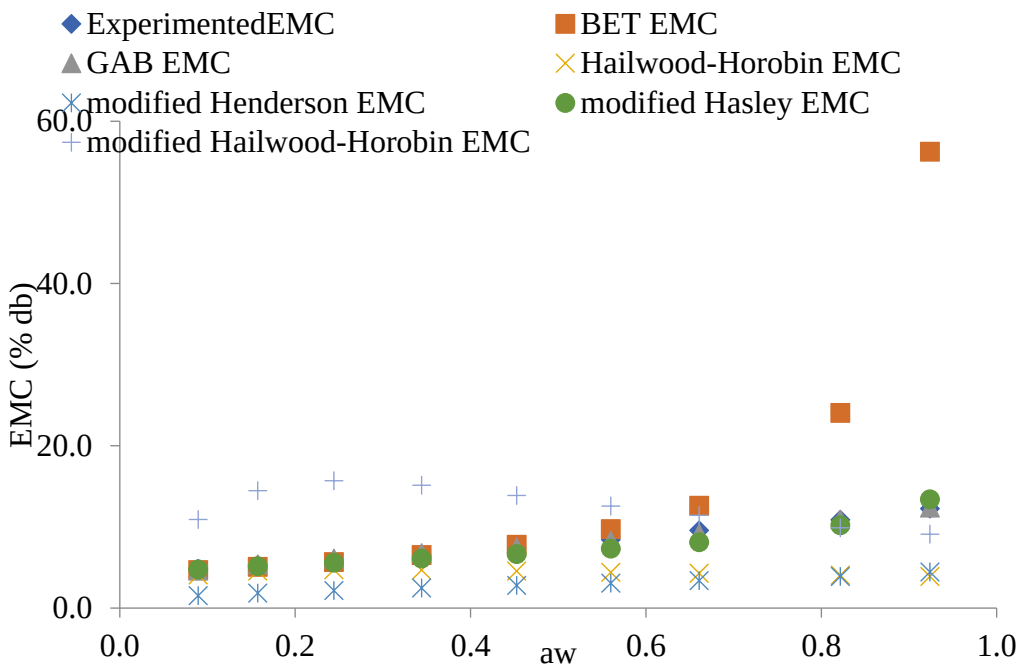

Figure G1: Experimental and predicted adsorption EMC for moringa seed at 20°C

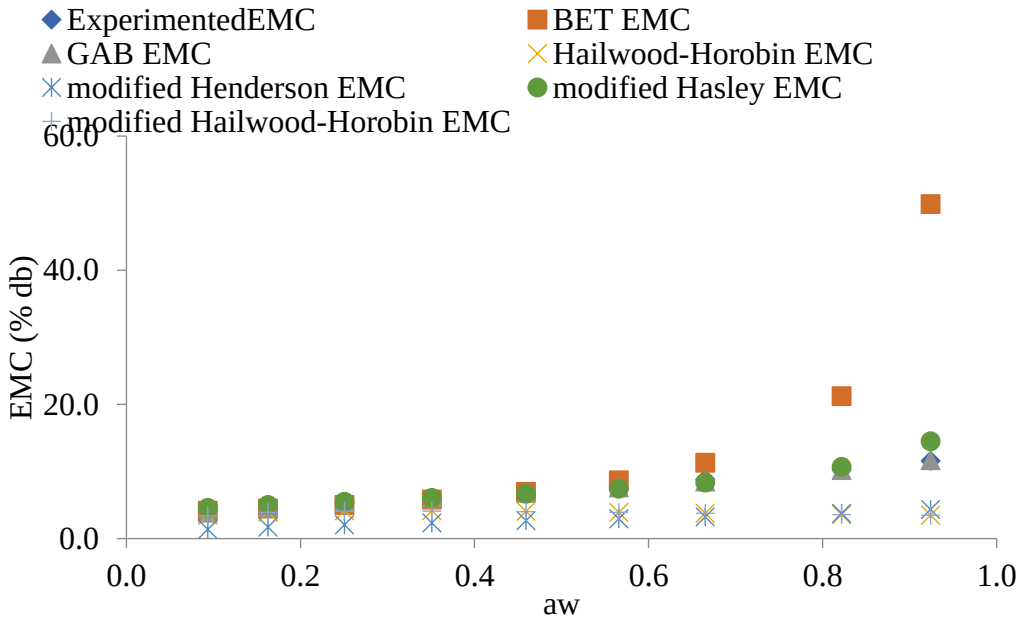

Figure G2: Experimental and predicted adsorption EMC for moringa seed at 25°C

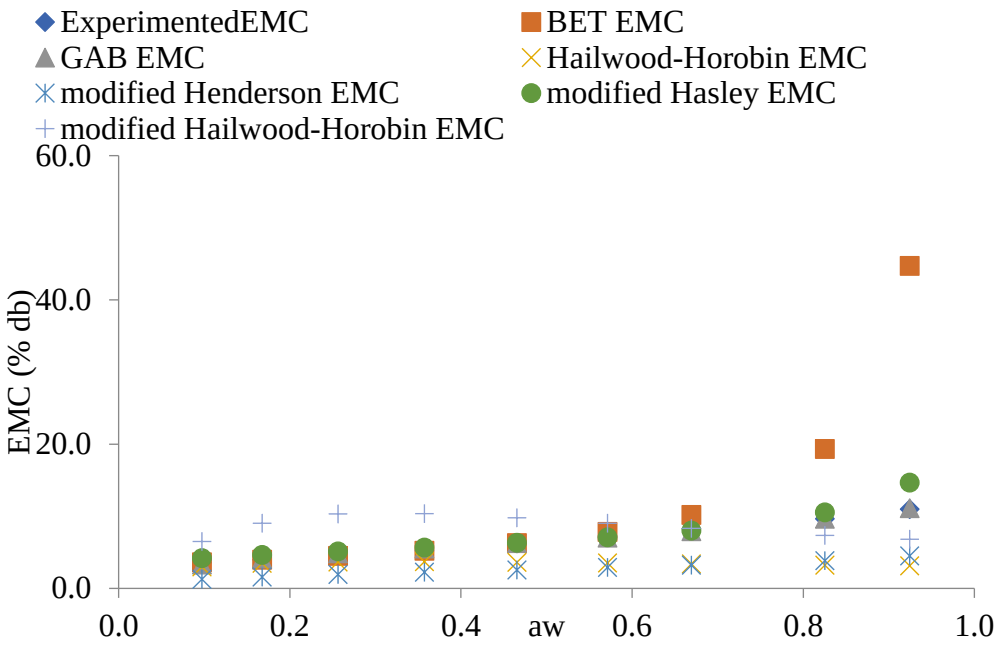

Figure G3: Experimental and predicted adsorption EMC for moringa seed at 30°C

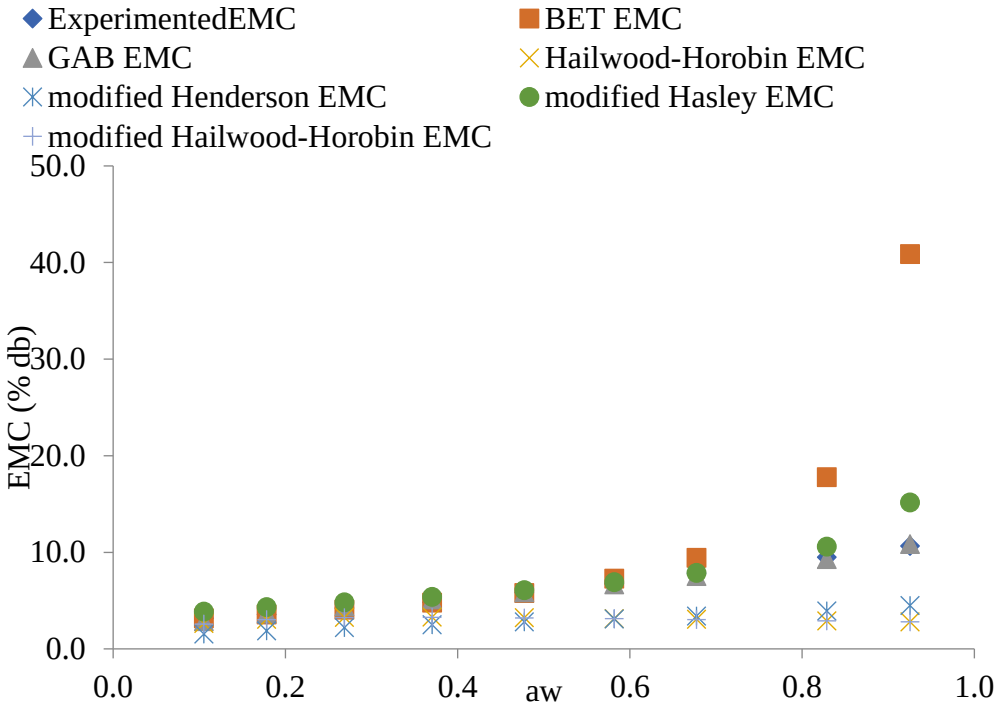

Figure G4: Experimental and predicted adsorption EMC for moringa seed at 35°C

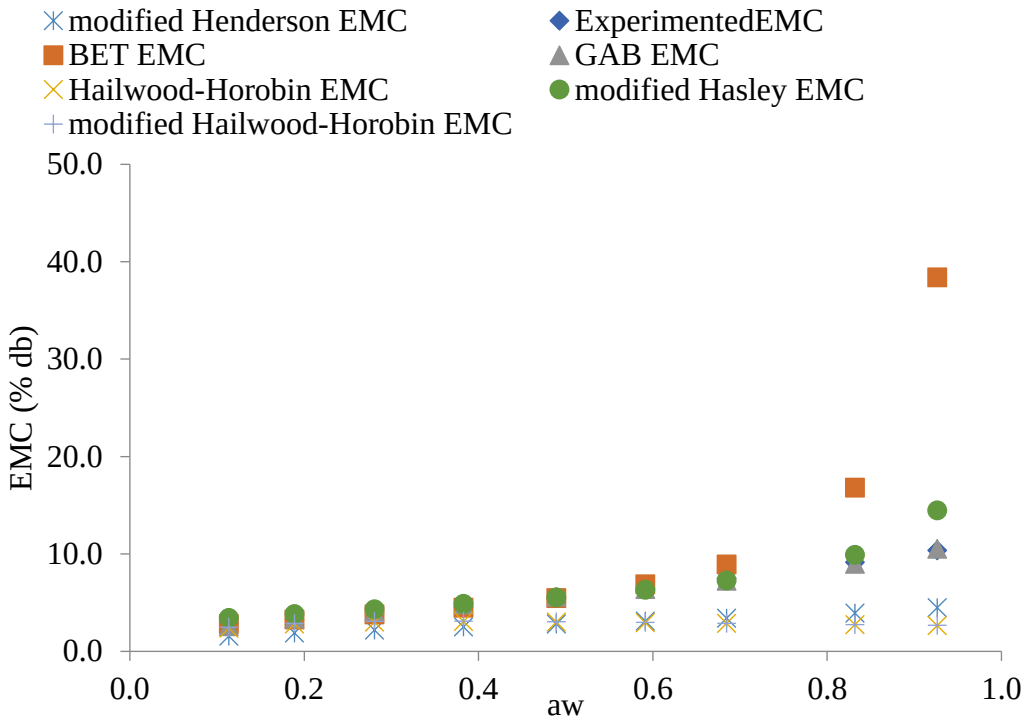

Figure G5: Experimental and predicted adsorption EMC for moringa seed at 40°C

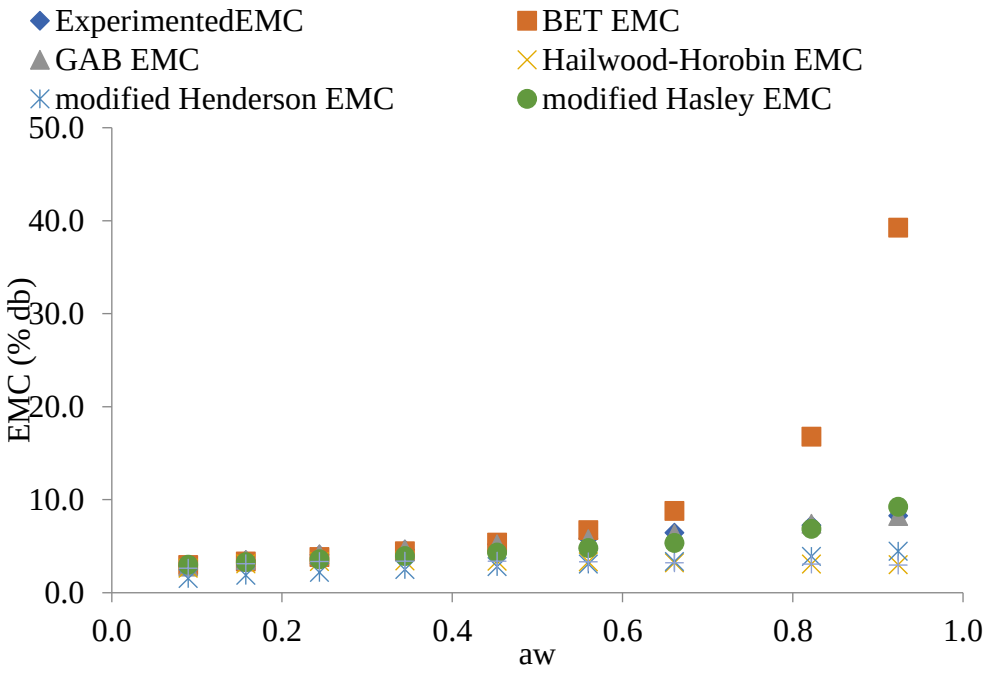

Figure G6: Experimental and predicted adsorption EMC for moringa seed grits at 20°C

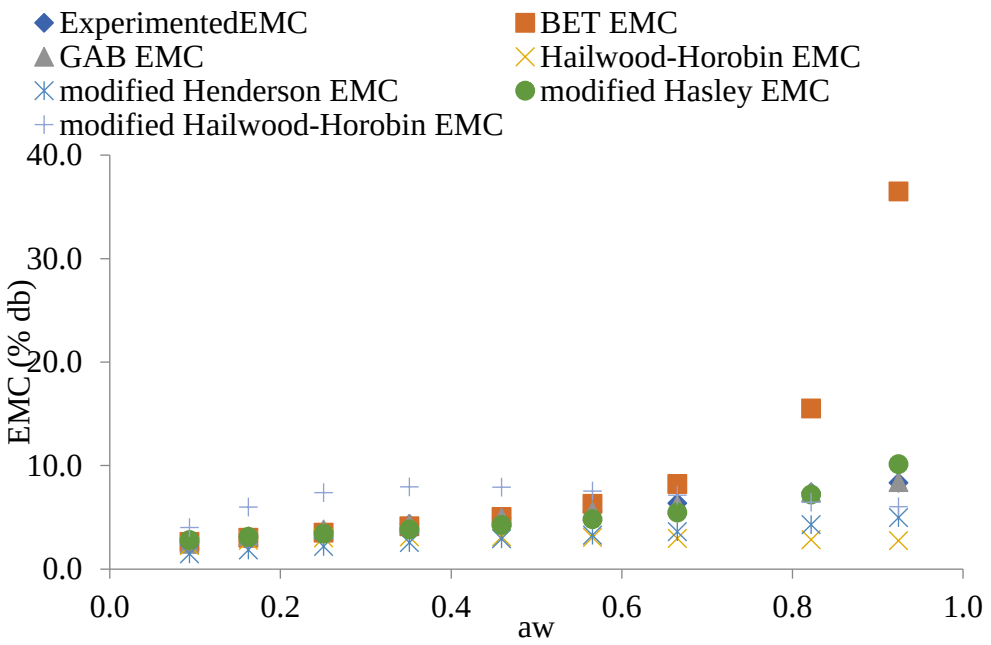

Figure G7: Experimental and predicted adsorption EMC for moringa seed grits at 25ºC

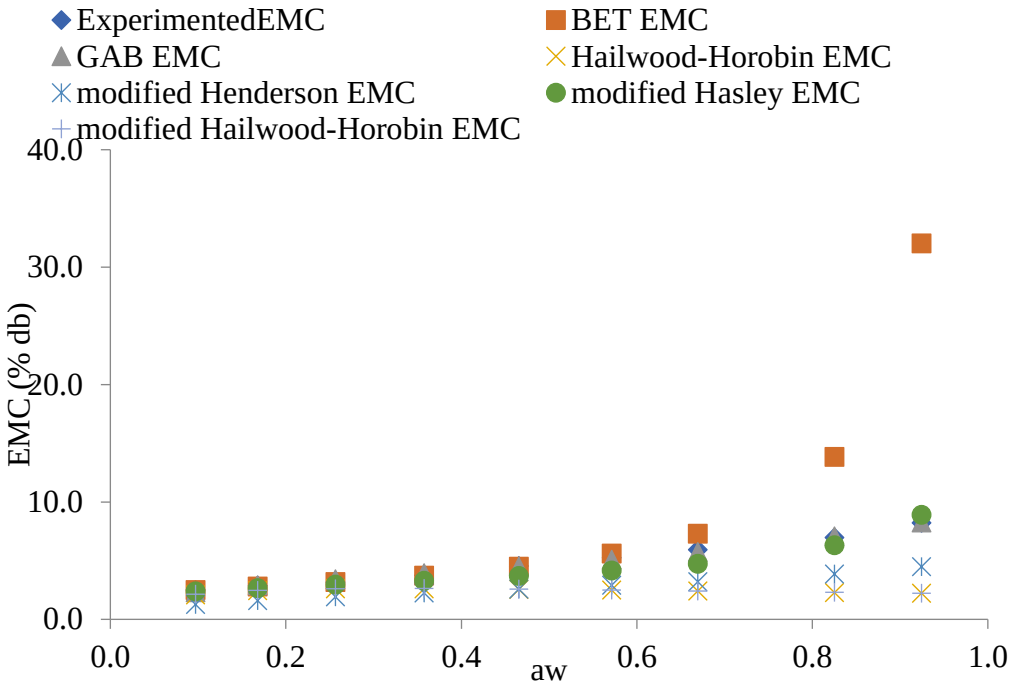

Figure G8: Experimental and predicted adsorption EMC for moringa seed grits at 30ºC

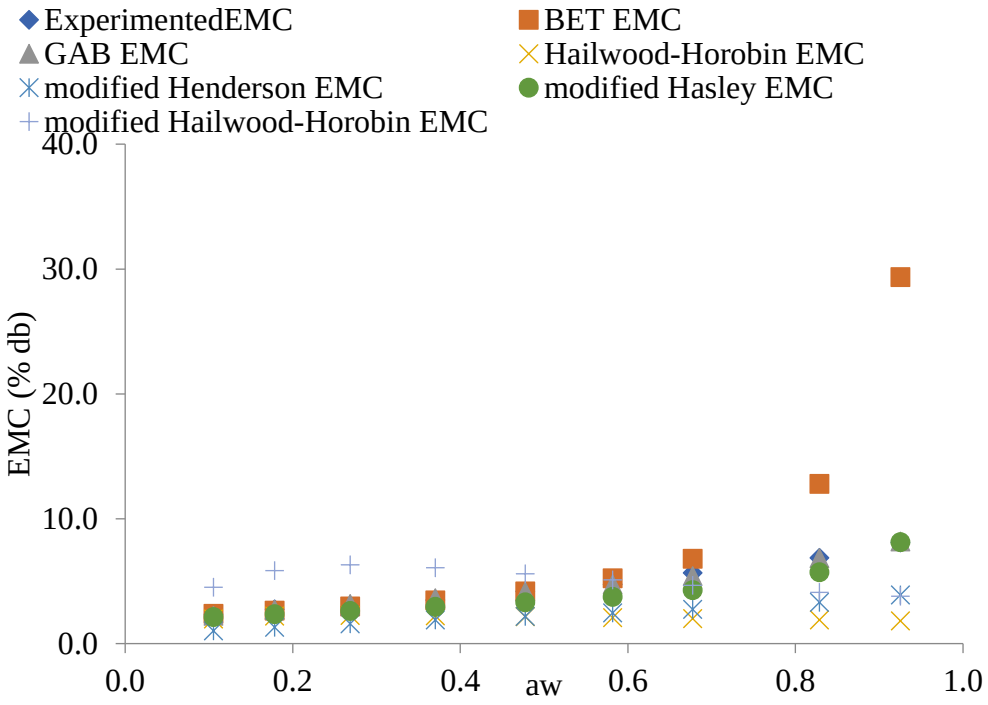

Figure G9: Experimental and predicted adsorption EMC for moringa seed grits at 35^{o}C

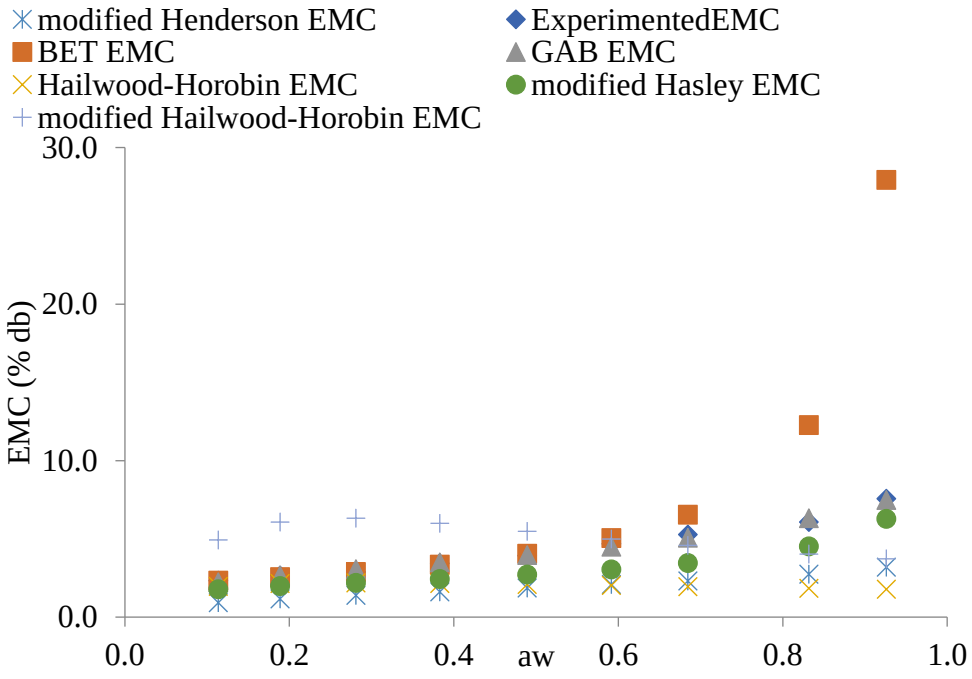

Figure G10: Experimental and predicted adsorption EMC for moringa seed grits at 40^{o}C

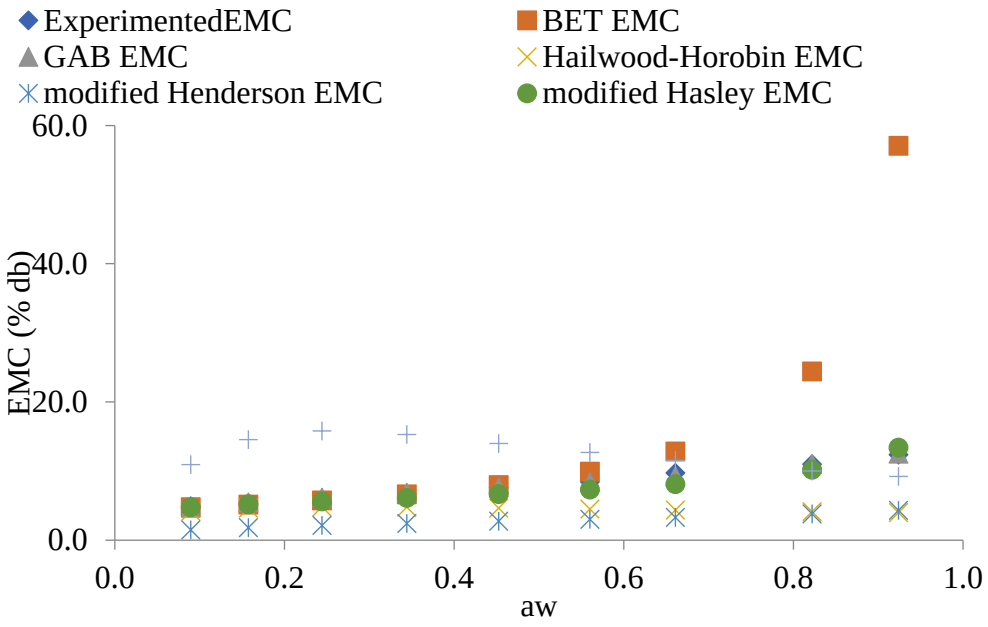

Figure G11: Experimental and predicted desorption EMC for moringa seed at 20°C

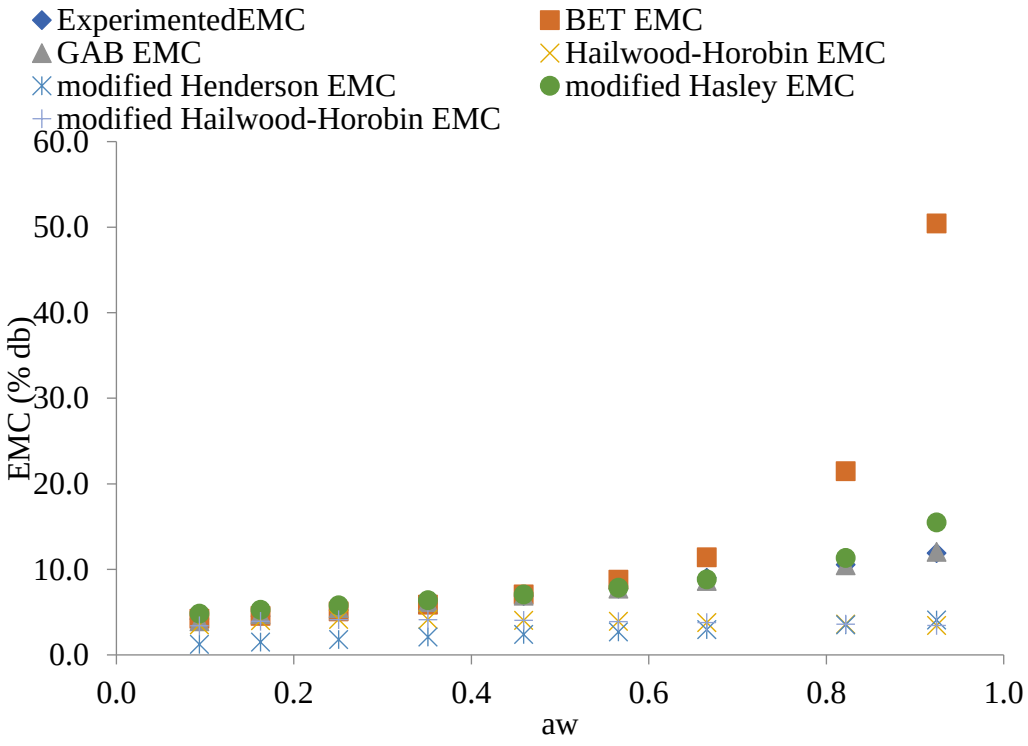

Figure G12: Experimental and predicted desorption EMC for moringa seed at 20°C

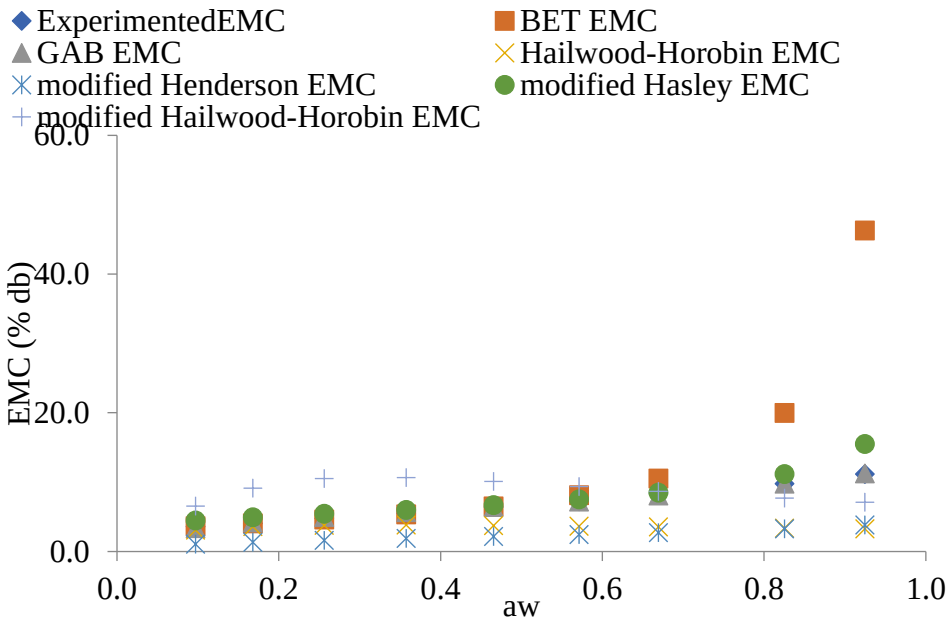

Figure G13: Experimental and predicted desorption EMC for moringa seed at 30°C

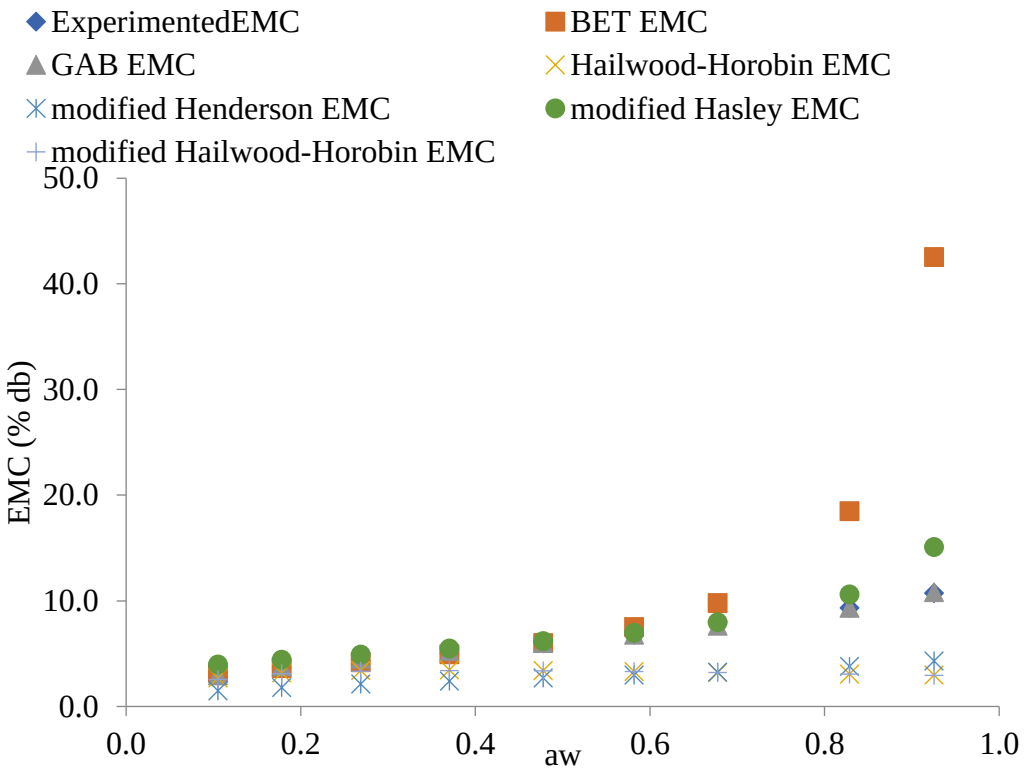

Figure G14: Experimental and predicted desorption EMC for moringa seed at 35°C

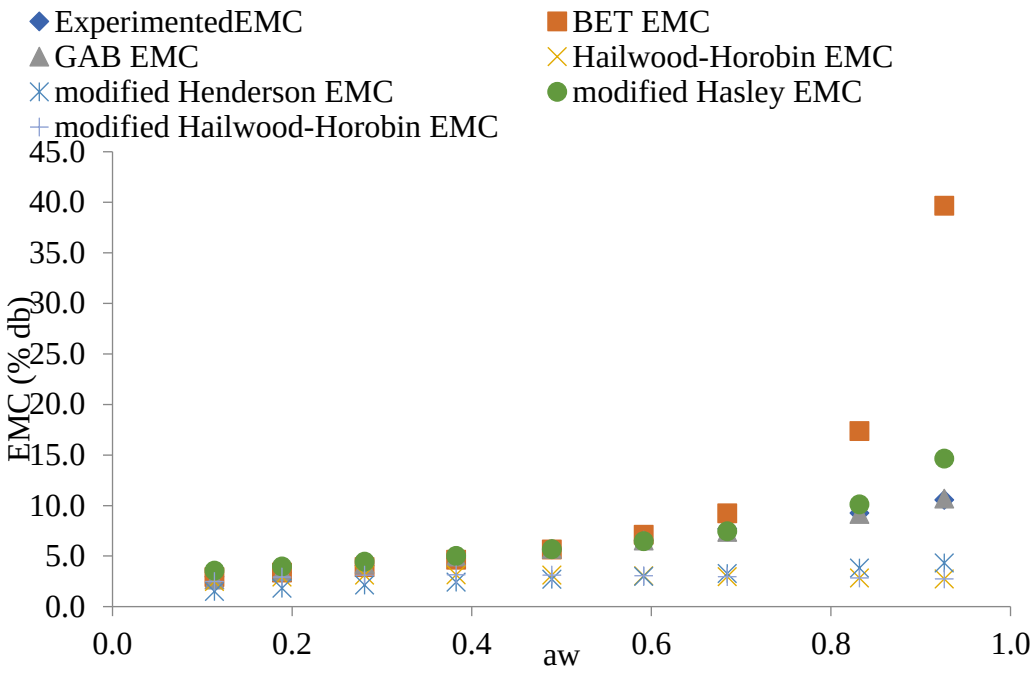

Figure G15: Experimental and predicted desorption EMC for moringa seed at 40^{o}C

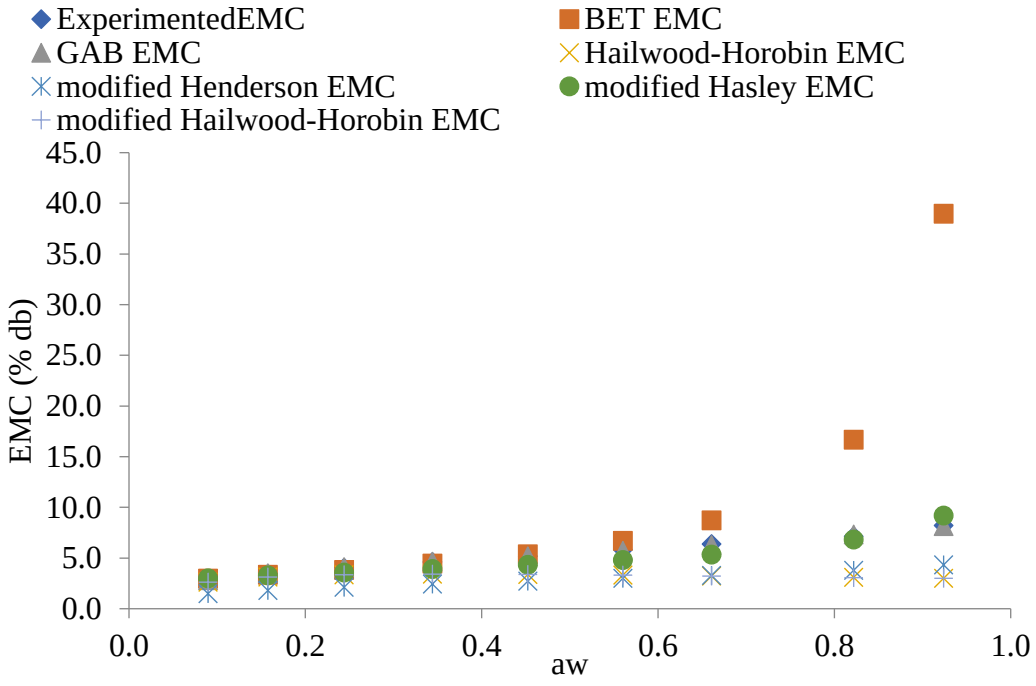

Figure G16: Experimental and predicted desorption EMC for moringa seed grits at 20^{o}C

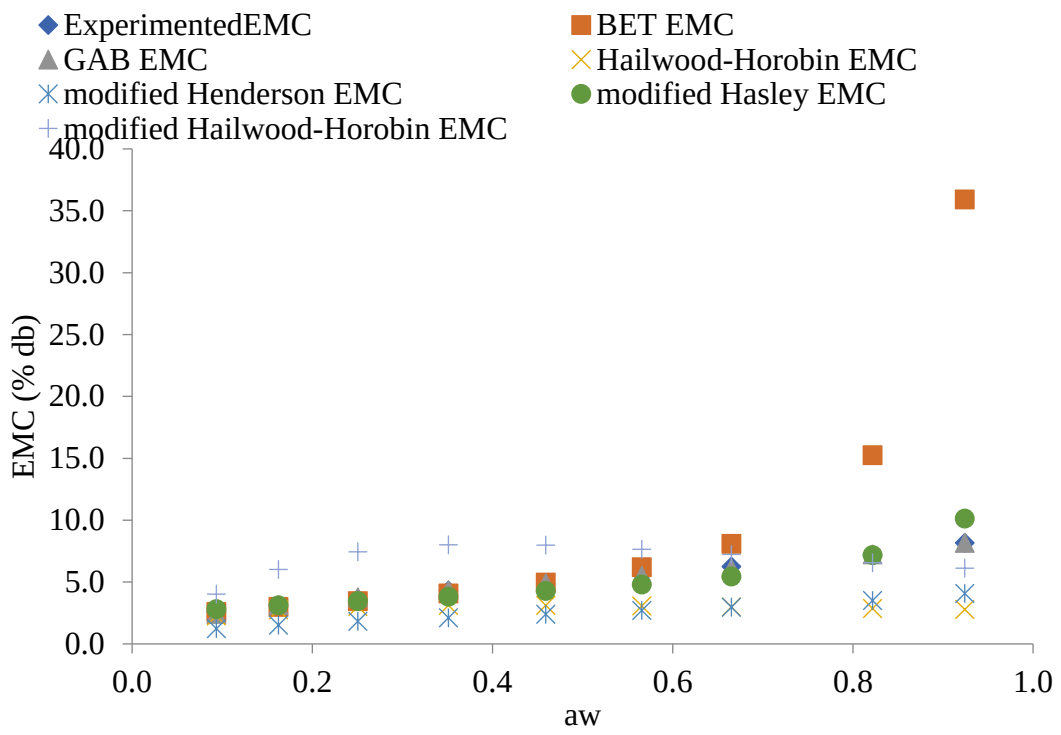

Figure G17: Experimental and predicted desorption EMC for moringa seed grits at 25ºC

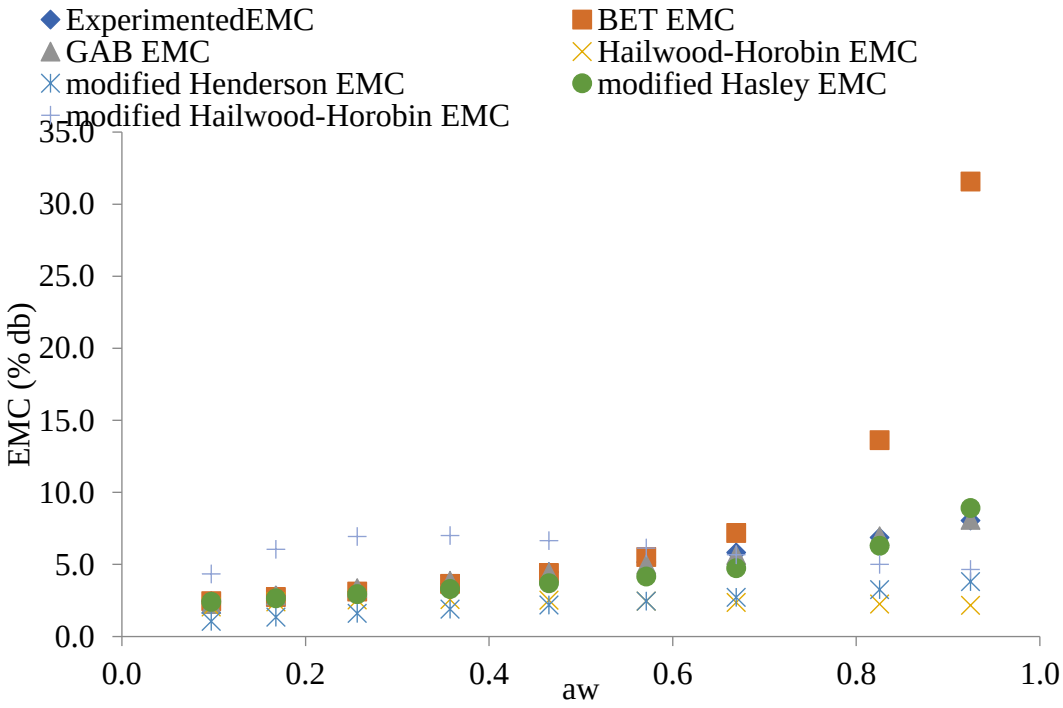

Figure G18: Experimental and predicted desorption EMC for moringa seed grits at 30ºC

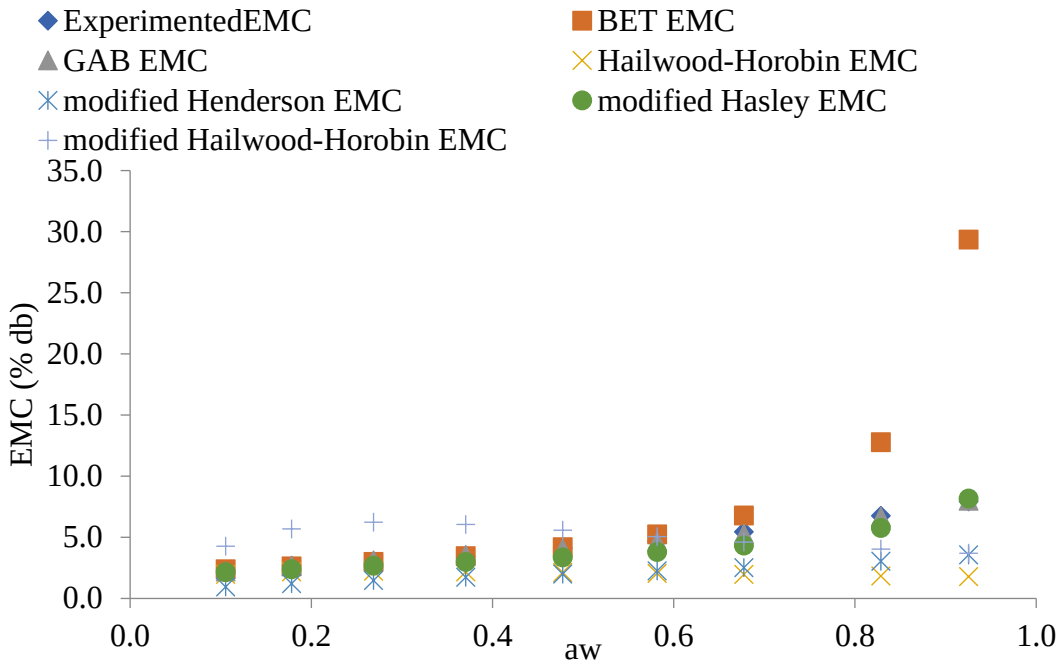

Figure G19: Experimental and predicted desorption EMC for moringa seed grits at 35ºC

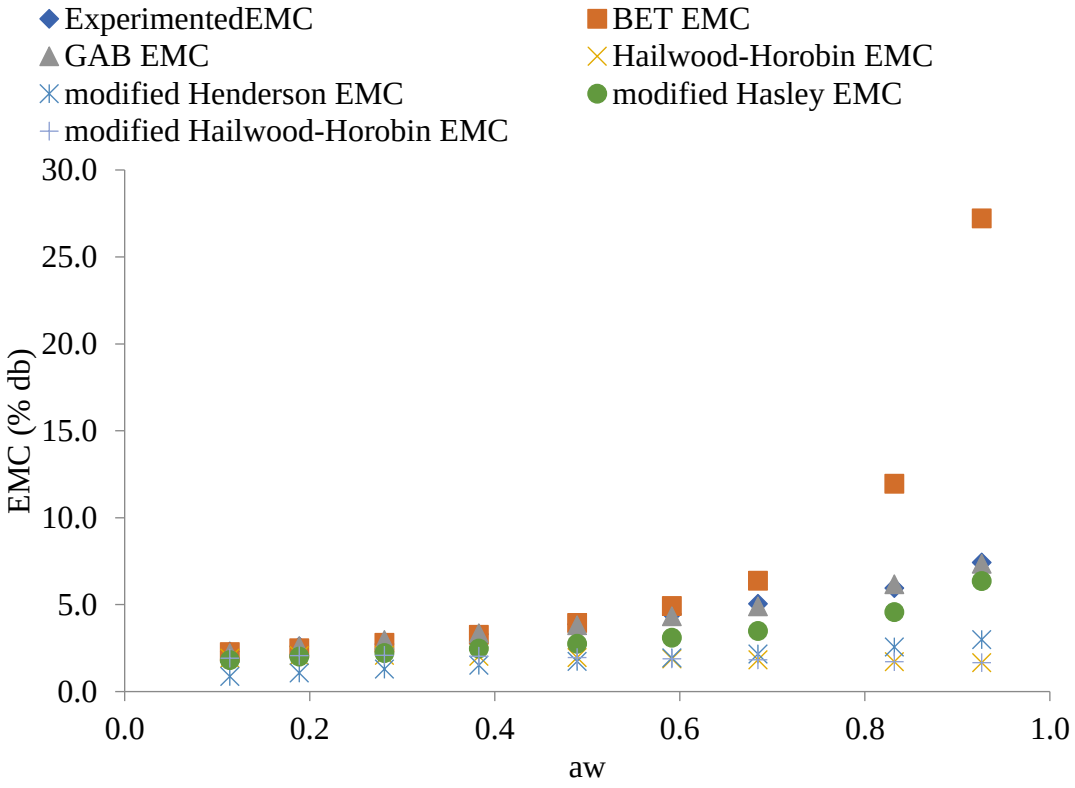

Figure G20: Experimental and predicted desorption EMC for moringa seed grits at 40ºC

APPENDIX H

Table H1: One-way ANOVA for BET Monolayer Moisture Content

Source	SS	df	MS	F	Prob > F
Between groups	0.02134439	1	0.02134439	0.07	0.7967
Within groups	2.40592042	8	0.300740053		
Total	2.42726481	9	0.26969609		

Bartlett's test for equal variances: chi-square (1) = 0.0085; Prob>chi^2 = 0.926

Table H2: One-way ANOVA for GAB Monolayer Moisture Content

Source	SS	df	MS	F	Prob > F
Between groups	0.024206457	1	0.024206457	0.07	0.7960
Within groups	2.71001195	8	0.338751494		
Total	2.73421841	9	0.303802046		

Bartlett's test for equal variances: chi-square (1) = 0.0127; Prob>chi^2 = 0.910

Table H3: One-way ANOVA for Caurie's Monolayer Moisture Content

Source	SS	Df	MS	F	Prob > F
Between groups	0.012959975	1	0.012959975	0.04	0.8536
Within groups	2.85433304	8	0.35679163		
Total	2.86729301	9	0.318588113		

Bartlett's test for equal variances: chi-square (1) = 0.0007; Prob>chi^2 = 0.979

Table H4: One-way Analysis of Variance for BET Monolayer Moisture Content

Source	SS	df	MS	F	Prob > F
Between groups	.014516067	1	.014516067	0.03	0.8717
Within groups	4.17385402	8	.521731753		
Total	4.18837009	9	.465374455		

Bartlett's test for equal variances: chi-square (1) = 0.0003; Prob>chi^2 = 0.985

Table H5: One-way Analysis of Variance for GAB Monolayer Moisture Content

Source	SS	Df	MS	F	Prob > F
Between groups	0.003648099	1	0.003648099	0.02	0.8870
Within groups	1.35619048	8	0.16952381		
Total	1.35983858	9	0.151093176		

Bartlett's test for equal variances: chi-square (1) = 0.0008; Prob>chi^2 = 0.978

Table H6: One-way Analysis of Variance for Caurie's Monolayer Moisture Content

Source	SS	Df	MS	F	Prob > F
Between groups	0.012040908	1	0.012040908	0.02	0.8834
Within groups	4.20210591	8	0.525263238		
Total	4.21414682	9	0.468238535		

Bartlett's test for equal variances: chi-square (1) = 0.0161; Prob>chi^2 = 0.899